Enhancement of Death Receptor-Mediated Apoptosis in Multiple Myeloma Cells

Amal Ali Arhoma

A thesis submitted in partial fulfilment of the requirements of Sheffield Hallam University for the degree of Doctor of Philosophy

June 2017

Dedication

For Mum and Dad

Everything I am or hope to be, I owe to you.

Abstract

Background: Multiple Myeloma (MM) is currently incurable despite many novel therapies. Tumour Necrosis Factor-Related Apoptosis-Inducing Ligand (TRAIL) is a potential anti-tumour agent although the effects as a single agent are limited. This investigation determined whether the Histone Deacetylase (HDAC) inhibitor SAHA, or inhibitors of the histone methyltransferases G9a and EZH2 (BIX 01294 and GSK343) and Nuclear export inhibitor (NEI) LMB, enhance TRAIL-induced apoptosis and overcome TRAIL resistance in both suspension culture, and 3D cell culture as a model of solid disseminated MM lesions that form in bone.

Methods: The effects of TRAIL sensitizers and/or TRAIL treatment were investigated in both suspension cultures and in an alginate-based 3D culture model. Apoptosis was detected by assessment of nuclear morphology using Hoechst 33342/PI staining. TRAIL-resistant cells were generated by acute exposure of TRAIL sensitive cells to TRAIL followed by the selection of TRAIL-resistant cells (TRAIL^R). Apoptotic effects in quiescent cells (labelled as PKH26^{Hi}) were also determined. Subsequently, an investigation was undertaken to identify potential mechanisms of action of these agents when used alone and in combination with TRAIL.

Results: TRAIL significantly induced apoptosis in a dose-dependent manner in OPM2, RPMI 8226, NCI-H 929, U266, JJN3 human MM cell lines and ADC-1 plasma cell leukaemia cells. All epigenetic modifiers and NEI synergistically enhanced TRAIL responses in several lines and responses were potentiated in 3D culture. Interestingly, TRAIL^R cells were sensitive to BIX 01294 and LMB; however, TRAIL responses in cells that had been selected for TRAIL^R were not further enhanced by SAHA and GSK343. Quiescent PKH26^{Hi} cells were resistant to dual therapy. Mechanistically, TRAIL and TRAIL sensitizers induced apoptosis via both extrinsic and intrinsic pathways in addition to decreasing the expression of oxidative enzyme catalase.

Conclusions: Inhibitors of HDAC, EZH2 and G9a and NEI are potent sensitisers of TRAIL responses both in suspension, and crucially in 3D cell culture, which may mimic physiological aspects of bone metastases. These agents may be a therapeutic option in combination with TRAIL and may increase TRAIL sensitivity in insensitive cells, but not in cells that have specifically been selected for acquired TRAIL-resistance, and not in quiescent cells.

Table of Contents

List of Figures

List of Tables

Publications, Conferences attended and Presented works

Publications:

Manuscripts Submitted:

Arhoma, A, Chantry, AD, Haywood-Small, SL, Cross, NA (2017). SAHA-induced TRAIL-sensitisation of Multiple Myeloma cells is enhanced in 3D cell culture. (Submitted to Experimental Cell Research. Accepted).

Manuscripts in Preparation:

Arhoma, A, Chantry, AD, Haywood-Small, SL, Cross, NA (2017). Nuclear Export Inhibitor (NEI) Leptomycin B enhances response to TRAIL in Multiple Myeloma. Biochemical and Biophysical Research Communications

Arhoma, A, Chantry, AD, Haywood-Small, SL, Cross, NA (2017). Inhibitors of EZH2 and G9a are potent TRAIL sensitisers in multiple myeloma cells, and responses are potentiated in 3D cell culture. Biochemical and Biophysical Research Communications.

Arhoma, A, Chantry, AD, Haywood-Small, SL, Cross, NA (2017). Selection of PKH26HI quiescent populations selects for cells with insensitivity to TRAIL**.** Biochemical and Biophysical Research Communications.

Poster Presentations:

The British Association for Cancer Research (BACR) (2017). Abstract title: Inhibitors of HDACs, EZH2 and G9a are potent TRAIL sensitisers in multiple myeloma cells, and responses are potentiated in 3D cell culture. Nottingham, UK.

Cancer research day (Sheffield University): 8 March (1017). Abstract title: Inhibitors of HDACs, EZH2 and G9a are potent TRAIL sensitisers in multiple myeloma cells, and responses are potentiated in 3D cell culture. Sheffield, UK.

BMRC Winter Poster Session: 5th December (2016). Abstract title: HDAC-inhibitor SAHA Act Synergistically with TRAIL in Multiple Myeloma cell lines 3D TRAIL - resistance. Sheffield, UK.

National Cancer Research institute (NCRI): 6-9 November (2016) Abstract title: Selection of PKH26HI quiescent populations selects for cells with insensitivity to TRAIL. Liverpool, UK.

National Cancer Research institute (NCRI): 6-9 November (2016) Abstract title: SAHA-induced TRAIL-sensitisation is enhanced in 3D cell culture. Liverpool, UK.

SciFest: 26th March (2016). Abstract title: Enhancement of Death Receptor-mediated apoptosis in Multiple Myeloma using the Nuclear Export Inhibitor Leptomycin B, Sheffield Hallam University. *Poster prize was Award.*

BMRC Winter Poster Session: 15th December (2016). SAHA-induced TRAIL-sensitisation is enhanced in 3D cell culture. Sheffield, UK.

The HWB Faculty Research Day: 1st July (2016). Abstract title: The effect of anti-tumour agents on non-proliferating cells isolated by using PKH26 red flouncing label. Sheffield, UK.

BMRC Winter Poster Session: 7th December (2015). Abstract title: Three dimensional culture sensitizes Multiple Myeloma cells to Histone methyltransferases (HMTases) inhibitor. Sheffield, UK.

National Cancer Research institute (NCRI): 1-4 November (2015) Abstract title: Three dimensional culture sensitizes Multiple Myeloma cells to Histone methyltransferases (HMTases) inhibitor. Liverpool, UK.

The North East Postgraduate Conference (NEPG): 12th October (2015). Abstract title: Three dimensional culture sensitizes Multiple Myeloma cells to Histone methyltransferases (HMTases) inhibitor. Newcastle, UK.

The HWB Faculty Research Day: 17th June (2015). Abstract title: Three dimensional culture sensitizes Multiple Myeloma cells to Histone methyltransferases (HMTases) inhibitor. Sheffield, UK.

BMRC Winter Poster Session: 11th December (2014). Abstract title: Enhancement of Death Receptor-mediated apoptosis in Multiple Myeloma using the Nuclear Export Inhibitor Leptomycin B. Sheffield, UK.

Libya higher education forum (2014) Abstract title: The Nuclear Export Inhibitor (NEI) Leptomycin B enhances response to TRAIL in Multiple Myeloma. London, UK.

National Cancer Research institute (NCRI): 2-5 November (2014) Abstract title: Enhancement of Death Receptor-mediated apoptosis in Multiple Myeloma using the Nuclear Export Inhibitor Leptomycin B. Liverpool, UK.

The HWB Faculty Research Day: 4th June (2014). Abstract title: Enhancement of Death Receptor-mediated apoptosis in Multiple Myeloma using the Nuclear Export Inhibitor Leptomycin B. Sheffield, UK.

BMRC Winter Poster Session: 17th December (2013). Abstract title: Nuclear Export Inhibitor (NEI) Leptomycin B enhances response to TRAIL in Multiple Myeloma. Sheffield, UK.

Relevant Courses and Workshops

3D models workshop, Nottingham Conference Centre, Nottingham **(2017)**.

Leadership Development Programme, Sheffield Hallam University **(2016)**.

'Researchers Who Teach' Course, Sheffield Hallam University **(2015)**.

Cancer research day, Sheffield University **(2014)**.

Faculty of Health & Wellbeing PhD workshop series, Sheffield Hallam University **(2013-2014).**

Abbreviations

2D	Two-dimensional
3D	Three-dimensional
AIF	Apoptosis-inducing factor
ALDH	Aldehyde Dehydrogenase
AML	Acute Myeloid Leukaemia
Apaf-1	Apoptotic Protease Activating Factor-1
AR	Antigen Retrieval
ASCT	Autologous Stem Cell Transplantation
ATLL	Adult T-cell Leukaemia/Lymphoma
ATP	Adenosine-5'-Triphosphate
Bad	Bcl-2-Associated Death Promoter
Bak	Bcl-2-Analgised/Killer
Bax	Bcl-2- Associated X Protein
Bcl-2	B-Cell Lymphoma 2
Bcl-xL	B-cell lymphoma-extra large
BH-3	Bcl-2 Homology Domain3
Bid	BH3-Interacting-Domain Death Agonist
Bik	Bik, Bcl-2-interacting killer
BIX 01294	diazepin-quinazolinamine
BM	Bone Marrow
BMSCs	bone marrow stromal cells
BrdU	5-bromo-2-deoxyuridine
BSA	Bovine Serum Albumin
CAD	Caspase-Activated Deoxyribonuclease
CARD	Caspase Recritument Domain
Caspase	Cysteinyl-Aspartate-Specific Protease
CD4	Cluster of differentiation 4
CD5	Cluster of differentiation 5
CDKs	CDK Dependent Kinase
CDKIs	CDK Dependent Kinase Inhibitors
CCND	Cyclin D
cDNA	Complementary DNA
c-flip	Cellular FLICE-Like Inhibiting Protein
CISs	Cancer Initiating Cells
CO$_2$	Carbon Dioxide
COX-2	Cyclooxygenase-2
CRMI	Chromosome region maintenance protein 1
CSCs	Cancer Stem Cells
CSR	Class switch recombination
CV	Co-efficient of Variation
CXCR4	C-X-C chemokine receptor type 4
DAB	3-3'-Diaminobenzidine Tetrahydrochloride
DcR	Decoy Receptor
DD	Death Domain
DED	Death Effector Domain
Diablo	Direct IAP Binding Protein
DISC	Death-Inducing Signalling Complex
DKK1	Dickkopf-related protein 1

DNA	Deoxyribonucleic Acid
DR	Death Reseptor
DSBs	DNA Double Strand Breaks
DZNep	3-Deazaneplanocin A
ECM	Extracellular Matrix
EDTA	Ethylene Diaminetra-Acetic Acid
EGFR	Epidermal Growth Factor Receptor
EZH2	Enhancer of Zeste Homologue 2
FACS	Fluorescent Activated Cell Sorting
FADD	Fas-Associating Death Domain Protein
Fas	First Apoptosis Signal
FBS	Fetal Bovine Serum
FSC	Forward Scatter
G_1	Gap 1
G_2	Gap 2
GSH	Glutathione
GDP	Guanosine Diphosphate
GTP	Guanosine Triphosphate
H_2O_2	hydrogen peroxide
HAT	Histone acetyltransferase
HDAC	Histone Deacetylase
HDAC[i]	Histone Deacetylase Inhibitor
HDAT	Histone acetyltransferases
HIF	Hypoxia-Inducible Factor
HIF-1	Hypoxia-Inducible Factor-1
HMTase	histone methyltransferases
HMTase[i]	histone methyltransferases Inhibitor
HO-2	Heme Oxygenase isoforms
HOX	Homeobox Gene
HRD	Hyperdiploid myeloma
HRK	Harakiri, BCL2 Interacting Protein
HRP	Horseradish Peroxidase
HSCs	Hematopoietic Stem Cells
HSP27	Heat Shock Protein 27
HSP60	Heat Shock Protein 60
HSP70	Heat Shock Protein 70
IAPs	Inhibitor of Apoptosis Proteins
IC_{50}	Inhibitory Concentration of 50%
IG	Immunoglobulin
ICAMs	intercellular adhesion molecules
IGF	Insulin-like growth factor
IHC	Immunohistochemistry
IKK	IkB Kinase
IL	Interleukin
ID2	DNA binding 2
INF-α	Interferon-alpha
JAK	Janus Kinase
JIRF4	Interferon Regulatory Factor 4
JUNB	transcription factor jun-B
KDMs	Histone lysine demethylase
KMTs	Histone lysine methyltransferase
LMB	Leptomycine B

M	Mitotic
MAPK	Mitogen-Activated Protein Kinase
MAPKs	Mitogen Activated Protein Kinases
MCL-1	Induced myeloid leukemia cell differentiation protein
MDM2	Mouse double minute 2 homolog
MIP 1 α	Macrophage Inflammatory Protein 1 α
MGUS	Monoclonal Gammopathy of Unknown Significance
MM	Multiple Myeloma
MMPs	Matrix Metalloproteinases
MMSET	Multiple Myeloma SET domain
MOMP	Mitochondrial Outer Membrane Permeabilisation
mRNA	Messenger RNA
MYC	Myelocytomatosis
NEI	Nuclear Export Inhibitor
NES	Nuclear Export Signal
NF-Kb	Nuclear Growth-Kb
NHRD	Non-Hyperdiploid myeloma
NKCs	Natural Killer Cells
NLS	Nuclear Localization Signal
NPC	Nuclear pore complex
OPG	Osteoprotegerin
PARP	Poly (ADP-ribose) Polymerase
PBS	Phosphate Buffered Saline
PCR	Polymerase Chain Reaction
PGE2	Prostaglandin E2
PI	Propidium Iodide
PI3K	Phosphoinositol-3-Kinase
PKB	Protein Kinase B
PKH^{Hi}	PKH High stain
PKH^{Lo}	PKH Lpw stain
PON2	Oxidative Protein Paraoxonase-2
PRb	Retinoblastoma Protein
PRC2	Polycomb Repressive Complex 2
PS	Phosphatidylserin
PUMA	p53 Up-regulated Modulator of Apoptosis
qRT-PCR	Quantitative Real Time Polymerase Chain Reaction
RANKL	Receptor Activated of NF-kB Ligand
RAS	Rat of Sarcoma
RNA	Ribonucleic Acid
RNase	Ribonuclease
ROS	Reactive Oxygen Species
RPMI 1640	Roswell Park Memorial Institute medium 1640
rRNA	Ribosomal RNA
RT	Reverse transcription
(Runx3)	Runt-related transcription factor 3
S	DNA Synthesis Phase
SCID	Severe combined immunodeficiency
SHM	Somatic hypermutation
SIAH1	seven in absentia homolog
SSC	Side Scatter
STD	Standard Deviations
TBS	Trise-Buffered Saline

TGF-α	Transforming Growth Factor-alpha
TGF-β	Transforming Growth Factor-beta
TNFR	Tumour Necrosis Factor Receptor
TRAIL	TNF-Related Apoptosis-Inducing Ligand
TRAIL^R	TRAIL-Resistant cells
VCAMs	vascular cell adhesion molecule
VEGF	Vascular endothelial growth factor
Wt	Wild type
XBP1	X-box binding protein 1
XIAP	X-linked Inhibitor of Apoptosis Protein

Acknowledgments

1. General Introduction

1.1   An Overview of Cancer

The term cancer is derived from the Greek word referred to a crab or crayfish because of the resemblance of the finger-like dissemination bulges from cancer to the legs of a crab (Hecht., 1987). Cancer is a disease characterised by an uncontrolled division and spread of abnormal cells into surrounding body tissues (American Cancer Society., 2014; Cancer Research UK., 2014; National Cancer institute., 2015). Cancer is a most important public health problem worldwide and is the second-leading cause of death in the USA (Siegel *et al*., 2016). According to American Cancer Society and Cancer Research UK (2014) approximately 4.7 million and 3.5 million cases of deaths were estimated in male and female respectively (American Cancer Society., 2014; Cancer Research UK., 2014). In the UK, more than 331,000 people are diagnosed with cancer each year and the most common cancers are prostate, colorectal, and melanoma among males, and breast and colorectal among females (Cancer Research UK., 2014).

Cancer caused by multiple changes and mutations in genes that control the cell function and division result in disrupts the normal cell processes (Hanahan and Weinburg., 2011). These genetic changes can be either inherited (germline) or arise during the lifetime (somatic) as a result of environmental exposure to chemicals or radiation. These internal and external are many factors which may act together in order to initiate and support the development of cancer by trigger the cells to undergo unrestricted proliferation and invasion (American Cancer Society., 2014).

Malignant solid tumours have the ability to spread into, or invade adjacent tissues or metastasis by travel to distant places in the body through the blood or the lymphatic system and give rise new secondary tumours far from the original primary cancerous tumour. In contrast, benign tumours do not spread into, or invade, adjacent tissues. Benign tumours are usually not threating human life if it is excised, and they usually don't undergo local recurrence grow back, however, in some cases, they can be life

threatening due to pressing on surrounding tissues such as benign brain tumours (American Cancer Society., 2014; Cancer Research UK., 2014). Most cancers form masses of solid tumour tissue, however, many blood cancer, such as leukemias, commonly do not form solid mass tumours (American Cancer Society., 2014; Cancer Research UK, .2014), but multiple myeloma (MM) and lymphoma do form solid masses (Teo and Peh., 2004).

1.2   Normal Haematopoiesis

Haematopoiesis is the processes of formation of blood cellular components from common haematopoietic stem cells (HSCs) reside in bone marrow (Kondo., 2010; Jagannathan-Bogdan and Zon., 2013). Haematopoietic stem cells are self-renewing cells with the capability to produce at least some of their daughter cells with identical characteristics of HSCs for developmental and proliferative potential. These cells have the unique ability to differentiate to all of the different classes of mature blood cell types and tissues (Passegue *et al*., 2003; Kondo., 2010; Jagannathan-Bogdan and Zon., 2013). During haematopoiesis, HSCs give rise myeloid and lymphoid progenitor lineage, which further differentiate into more specific blood cell types (Passegue *et al*., 2003; Kondo., 2010; Jagannathan-Bogdan and Zon., 2013).

The lymphoid progenitors produce immune T- and B-cell lymphocytes and natural killer cells (NKCs). Whilst the myeloid progenitor lineage produce, erythrocytes and granulocytes which include: eosinophils, basophils, neutrophils, and monocytes which differentiate into the macrophage (Orkin and Zon., 2008). T-cells play an important role in cell mediate immunity and their proliferation and differentiation requires the detection of specific antigen, which is also essential to help other immune response cell types such as B-cells and NKCs cells. The activation of T-cells by detection of specific antigen by T-cell receptor (TCR) in addition to activation by co-stimulatory signals

delivered by accessory surface molecules on T-cells (Alegre *et al*., 2001). Moreover, B-cells activated in response to foreign antigen, which recognized by membrane-bound immunoglobulin (IgM) and turns into antibody producing plasma cells. B-cells originate in the bone marrow and released into blood or lymph as B-cells prior to their final differentiation into antibody producing plasma cells (Figure 1.1) (Calame., 2001; Bernasconi *et al*., 2002).

Haematopoiesis is a highly organized cellular process that regulates cellular proliferation and differentiation capacity as well as bone marrow release of cells in order to ensure there is a compliment of each type of blood cells and optimal haematopoiesis status is maintained (Sachs., 1996). Therefore, impaired haematopoiesis is a feature of malignant disorders such as multiple myeloma (MM) (Bommert *et al*., 2006) and studying the process of hematopoiesis can help to clear understand the underlying mechanisms behind blood disease and cancers (Jagannathan-Bogdan and Zon., 2013).

Figure 1.1: Illustration of the development of different blood cells from HSCs
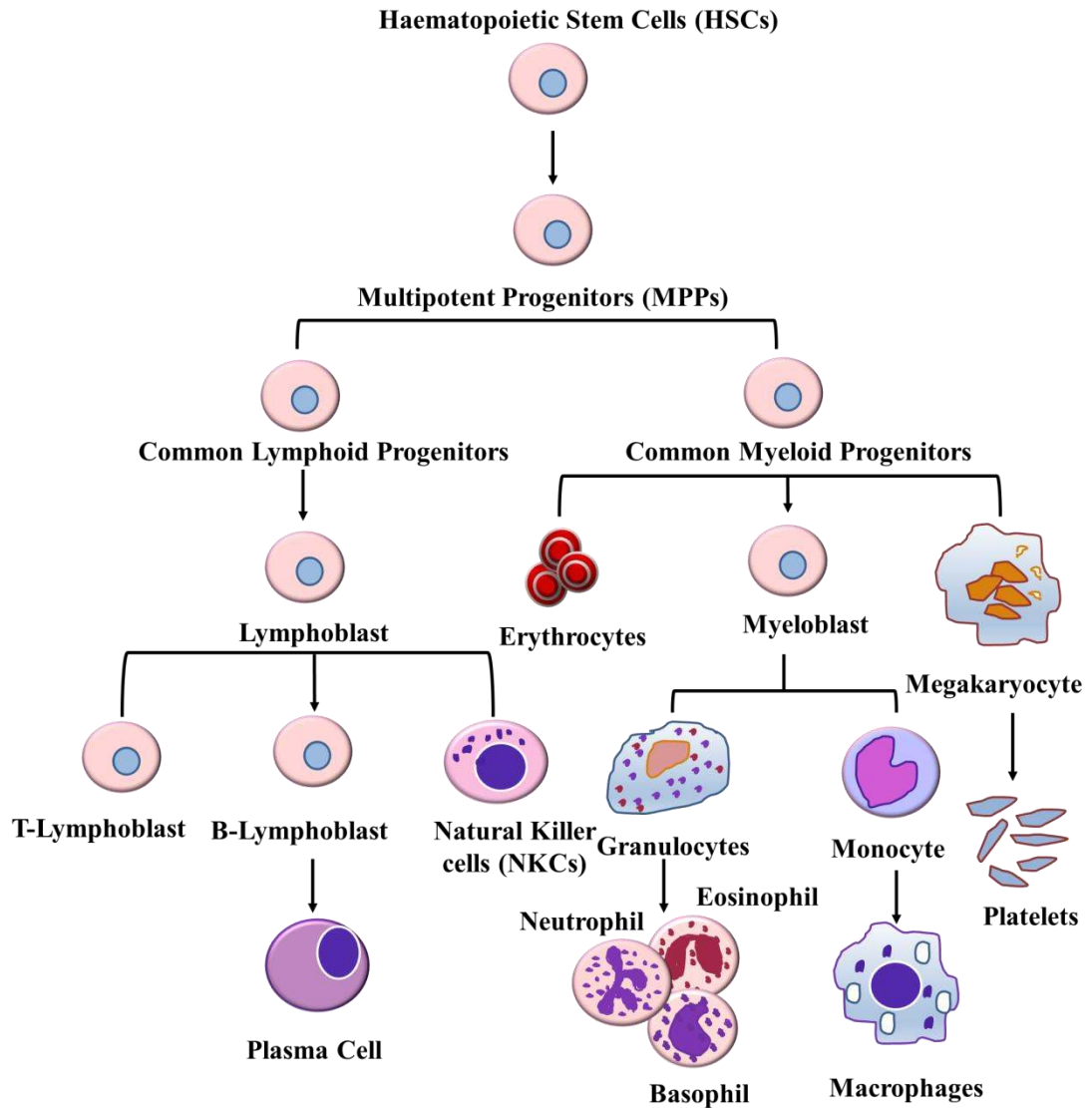
Figure 1.1: Illustration of the development of different blood cells HSCs. *During haematopoiesis, HSCs give rise lymphoid and myeloid progenitors which in turn differentiate into more specific cell types including all white blood cells, red blood cells, and platelet. Modified from Passegue et al., 2003.*

1.3   Multiple Myeloma Overview

Multiple myeloma (MM) is a clonal plasma cell malignancy characterised by a proliferation of antibody secreting plasma cells in the bone marrow (Lemancewicz *et al.*, 2013) and subsequently by an increase of monoclonal para-protein (Cook and Macdonald., 2007). The bone marrow accumulation of B-cells interferes with the production of other blood cells, which may result in the formation of soft-tissue masses (plasmacytomas) and osteolytic bone lesions (Ciolli., 2012). Multiple myeloma accounts for 1% of the malignant diseases and approximately 10% of all hematological cancers (Jemal *et al*., 2009). It is considered the most common blood malignancy in the USA, after non-Hodgkin lymphoma (Zaravinos *et al*., 2014). Furthermore, it is mainly a disease of the elderly with a median age at diagnosis is 66 years (Salameh *et al*., 2013). The common clinical manifestations of multiple myeloma are the bone lesion that appears as painful osteolytic bone lesions caused by tumour cells disrupting normal bone turnover, with long-lasting pain or vertebral crush fractures, renal impairment and hematologic abnormalities including anemia and hypercalcemia. In addition, the reduction of humoral immunity may lead to recurrent infection (Laubach *et al*., 2011).

1.3.1   Molecular Pathogenesis of Multiple Myeloma

In recent years, significant efforts have been exerted to identify the underlying cellular and molecular changes in the multiple myeloma pathogenesis (Piazza *et al*., 2013). The myeloma cells are developed from premalignant maturation of monoclonal plasma cells that originate at the post-germinal center B-cells. Furthermore, increasing evidence indicates that multi-step genetic impairments and micro-environmental changes play a key role in the transformation of these premalignant cells into malignant neoplasms.

Multiple myeloma represents the final evolution of a premalignant precursor phase, known as monoclonal gammopathy of unknown significance (MGUS) that progresses

to smoldering myeloma and finally to intra-medullary and extra-medullary symptomatic myeloma (Figure 1.3). (Palumbo and Anderson., 2011). Monoclonal gammopathy of unknown significance (MGUS) has an age-dependent prevalence of 3% of individuals > 50 years old and the sporadic progression of MGUS to MM has an average rate of 1% per year (Zaravinos *et al*., 2014). Similar to multiple myeloma, MGUS produces a monoclonal immunolglobin (Ig) (mostly non-IgM) and it is distinguished clinically from multiple myeloma by <10% of mononuclear cells in bone marrow with no secondary end-organ damage (Paszekova *et al*., 2014). The progress of MGUS to smoldering and symptomatic multiple myeloma respectively is related to acquisition or suseguent oncogenic mutation. Despite the recent advances to understand the pathogenesis of multiple myeloma, it remains unclear which patient with MGUS will progress to multiple myeloma, and which one will not (Chesi and Bergsage, 2013).

Multiple myeloma plasma cells have low proliferation rate and dependent on bone marrow microenvironment regulation for growth (Menu *et al*., 2004). The interaction of myeloma plasma cells with the other extracellular matrix (ECM) cells in the bone marrow environment represents the key requirements for the pathogenesis of MM, migration, growth and survival of myeloma cell (Piazza *et al*., 2013). Moreover, the secretion of growth factors and cytokines by multiple myeloma cells and by other cells in the bone marrow microenvironment such as bone marrow stromal cells (BMSCs) (Valentin-Opran *et al*., 1982), which is regulated by cell–cell adhesion activates signalling cascades including the NFκB-pathway (Chauhan *et al*., 1996), the Ras/Raf/MEK/MAPK-pathway (Leow *et al.,* 2013), the PI3K/Akt-pathway (Li *et al*., 2013; Mao *et al*., 2011), the Wnt-pathway (Dutta-Simmons *et al*., 2009; Qiang *et al.,* 2003), and the JAK/Stat3-pathway (Kawano *et al*., 1988) that have provided promising targets approach for novel multiple myeloma therapies (Figure 1.2) (Podar *et al.*, 2009).

1.3.1.1   Interaction of Multiple Myeloma with Bone Marrow Environment

The bone marrow (BM) milieu consists of mesenchymal stem cell-derived bone marrow stromal cells, osteoblast and adipocytes among other haemopoietic cells together with vascular endothelial cells and the extracellular matrix (Gooding and Edwards., 2016). The interaction of myeloma plasma cells with stromal cells via the adhesion molecules including intercellular adhesion molecules (ICAMs), vascular cell adhesion molecules (VCAMs) and very late antigen-4 (VLA-4) results in up-regulating the expression of tyrosine kinase receptors and chemokine receptors (Raab *et al*, 2009). This binding, in turn, stimulates the secretion of a wide range of cytokines/growth factors and chemotactic agents such as IL-6 (Figure 1.4) (Raab *et al*, 2009). In addition, the internal signals and external stimuli such as hypoxia promote the secretion of Hypoxia-inducible factor-1 (HIF-1) and angiogenic cytokine vascular endothelial cell growth factor (VEGF) (Kuehl1 and Bergsagel., 2012). The pro-angiogenic molecule VEGF enhances the bone marrow microvascular density and accounts for the abnormal myeloma tumour vessels structure (Figure 1.2).

Moreover, the complex interaction among these varieties of cells leads to an imbalance in the osteoblasts and osteoclasts function. As a result suppression in the activity of osteoblast which is mediated by Dickkopf-related protein 1 (DKK1). Dickkopf-related protein 1 (DKK1) produced by MM prevents Wnt signalling, preventing osteoblast differentiation (Qiang *et al*, 2008) and promoting adipocyte differentiation (Ruan *et al*., 2013). Whereas the action of Macrophage Inflammatory Protein 1 α (MIP1α) enhances the osteoclast function (Palumbo, and Anderson., 2011) (Figure 1.4). In addition, dysregulation of Receptor Activator of NF-κB Ligand (RANKL) and osteoprotegerin (OPG) has been shown be play a crucial role in the pathogenesis of MM bone disease (Shipman and Croucher., 2003). Receptor Activated of NF-kB Ligand (RANKL), is expressed by stromal cells and osteoblasts in the BM microenvironment (Anderson *et*

al., 1997; Lacey *et al.*, 1998) and bind to its receptor RANK, on the surface of osteoclast precursors in order to promote osteoclast differentiation and bone resorption (Burgess *et al.,* 1999). A soluble decoy receptor, OPG, has also been identified that can bind to RANKL and inhibiting its interaction with RANK, thus preventing bone osteoclastic bone resorption (Simonet *et al.*, 1997). Myeloma cells may increase expression of RANKL, activating RANK on pre-osteoclasts. In addition, decrease expression of OPG has been reported in bone marrow of MM patients (Shipman and Croucher., 2003). This results in bone lytic disease, immunodeficiency and stimulates the growth and the survival of multiple myeloma cells (Kyrtsonis *et al.*, 2010).

Figure 1.2: The role of the bone marrow microenvironment in multiple myeloma pathogenesis
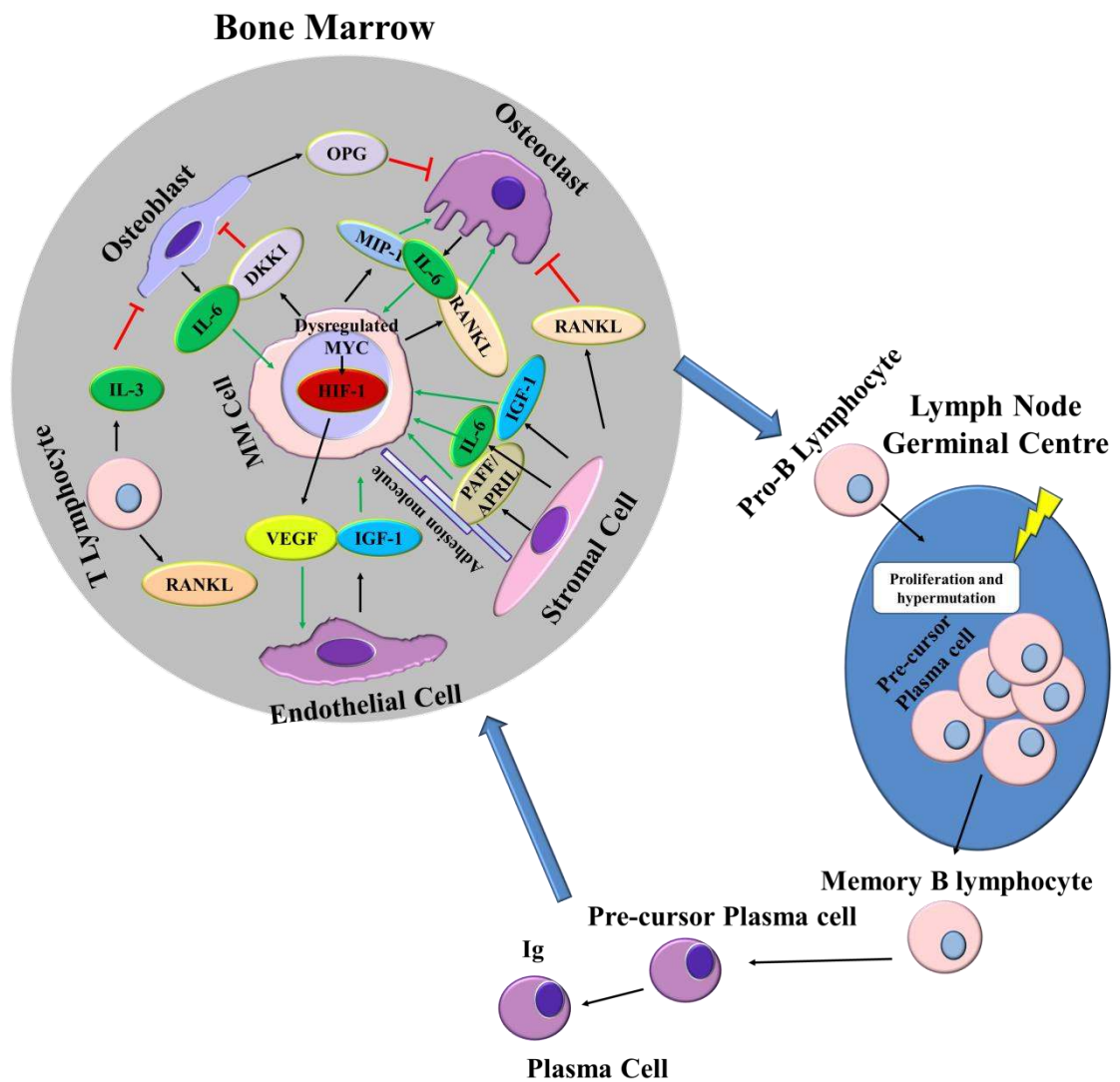
Figure 1.2: The role of the bone marrow microenvironment in multiple myeloma pathogenesis. Complex Interactions of MM tumour cells with the BM cells via the adhesion molecules resulting in the release of survival and growth factors e.g. IL-6. Moreover, they promote the secretion of angiogenic factor including HIF-1 and VEGF, and decreases the activity of osteoblast by DKK1 produced by myeloma prevents Wnt signalling and preventing osteoblast differentiation, Whereas the increased RANKL and decrease in OPG (a negative regulator of RANKL) enhances the osteoclast activity and ultimately stimulates the survival and growth of MM cells. Modified from Kuehl and Bergsagel., 2012, and Kyrtsonis et al., 2010.

1.3.2 Genetic Alteration of Multiple Myeloma

At the molecular level, multiple myeloma is associated with considerable heterogeneity and chromosomal abnormalities suggesting two distinct categories: Hyperdiploid myeloma (HRD) and non-hyperdiploid myeloma (NHD) (Herve *et al.*, 2011). Hyperdiploid myeloma is characterized by multiple trisomies of chromosomes 3, 5, 7, 9 11, 15, 19 and 21 and primary IgH translocations in ~10% of cases, while non-hyperdiploid myeloma is associated with primary IgH translocations in ~ 70% of cases (Fonseca *et al.,* 2003). Hyperdiploid tumour patients have a better prognosis than non-hyperdiploid tumour patients (Kumar *et al*., 2012) (Figure 1.3).

1.3.2.1 *Primary IgH Translocations as an Early Genetic Event in Multiple Myeloma*

During the development of B-cells, the rearrangement of immunoglobulin heavy chain (IgH) locus on chromosome 14 and immunoglobulin light chain (IgL) locus on chromosomes 2 and 22 takes place in about half the cases of MM. There are three Primary IgH translocation groups identified by fluorescent *in situ* hybridization (FISH). These IgH translocations target three genes, including the cyclin D (CCND) family (11q13-CYCLIN D1: 15 %; 6p25-CYCLIN D3: 2 %; 12p13-CYCLIN D2: 1 %), Wolf-Hirschhorn syndrome candidate 1/FGFR3 (MMSET/FGFR3) genes (4p16-FGFR3 /MMSET: 15 %) and the MAF family (16q23-MAF: 5 %; 20q12-MAFB: 2 %; 8q24.3-MAFA: 1 %) (Chesi and Bergsage., 2013). Breakpoints usually happen in the region near, or within IgH switch regions as related to error in somatic hypermutation (SHM) or isotype class switch recombination (CSR) (Kuehl and Bergsagel., 2002), hence being selected to recognize a certain antigen, they sometimes occur near V(D)J sequences of IgH on chromosome 14q32. It is supposed that these chromosomal translocations represent the initiating oncogenic events involved in developing normal B-cells (Bergsagel and Kuehl., 2001).

1.3.2.2 *Cyclin D and MAF Genes Dysregulation in Multiple Myeloma Tumours*

Almost in all cases of MGUS and multiple myeloma tumours, there is an increase in the expression of the cyclin D (CCND) genes that results from cis-dysregulation and trans-dysregulation of cyclin D and MAF gene translocation respectively. Moreover, it has been found that the level of expression of CCND1 mRNA in MM and MGUS tumour is high compared to the lack of expression by normal B-cells and the majority of hyperdiploid myeloma tumours express CCND1 bi-allelically, which may be due to trisomy of chromosome 11. A few percent of multiple myeloma tumours (<5%) that do not express high CCND gene level have a inactivated retinoblastoma gene (pRb1) (Figure 1.3) (Kuehl and Bergsagel., 2012; Chesi and Bergsage., 2013).

Additionally, it is thought that translocations of CCND dysregulate only CCND gene expression while MAF translocations dysregulate MAF transcription factor expression which in turn up-regulates the expression of many genes such as CCND2 and adhesion molecules, the key factor in the interaction of MM tumour cells with the BM microenvironment (Kuehl and Bergsagel., 2012; Chesi and Bergsage., 2013).

1.3.2.3 *Multiple Myeloma Su(var) 3-9, Enhancer-of-zest, Trithorax (SET domain) (MMSET)*

Multiple myeloma Su(var) 3-9, Enhancer-of-zest, Trithorax (SET domain) (MMSET) is a major epigenetic regulator in MM patients with t(4;14) translocation that harbours the worst prognosis (Asangani *et al.*, 2013) and it is thought to be the driving factor in MM pathogenesis of this specific subtype (Popovic *et al*., 2014). MMSET is a nuclear protein with multiple domains important for the regulation of genes including the function SET domain, which codes histone methyltransferase (HMTase) activity (Licht *et al*., 2011). HMTases are chromatin modifiers that control the transcriptiomic landscape in normal and development of disease including tumour progression and formation (Asangani *et al*, 2013). HMTases catalyse the binding of 1-3 methyl groups at

a specific lysine or arginine residues on H3 and H4 histones, altering the transcriptional activity of chromatin (Wood and Shilatifard., 2004).

It has been found that MMSET over-expression enhances the global increase in the dimethylation of H3K36 which is associated with actively transcribed genes in addition to the genome-wide loss of H3K27 trimethylation (Popovic *et al*., 2014) and re-expression of developmental gene Hox (Wang *et al.,* 2007). Moreover, this effect is associated with the significant change in DNA methylation (Xiao *et al*., 2013). The effects of over-expression of MMSET include increased cell cycle, altered/reduced response to DNA damage and reduced apoptosis (Licht *et al*., 2011). Matinez-Garcia., (2011) established that the knock-down of MMSET expression inhibits growth, modifies cell adhesion properties and consequently triggers apoptosis in the MM cell lines (Martinez-Garcia., 2011).

Additional oncogenic events in the pathogenesis of multiple myeloma tumours are chromosome 13 deletions disrupting RB1 which are often an early event in both hyperdiploid myeloma and non-hyperdiploid myeloma pathways (Chiecchio *et al.,* 2009), mutations of BRAF and RAS and increased c-MYC expression (Chng *et al.*, 2011), deletions of TP53 and loss of chromosome 17p (Lode *et al*., 2010). Moreover, the translation of MGUS to MM is associated with secondary Ig translocations including mostly IgK and IgL (Gabrea *et al*., 2008). In addition, mutations in genes involving in protein translation, homeostasis and RNA regulating metabolism are recognized in MM patients (Figure 1.3) (Chapman *et al*., 2011).

Figure 1.3: Molecular pathogenesis and genetic alteration of Multiple Myeloma
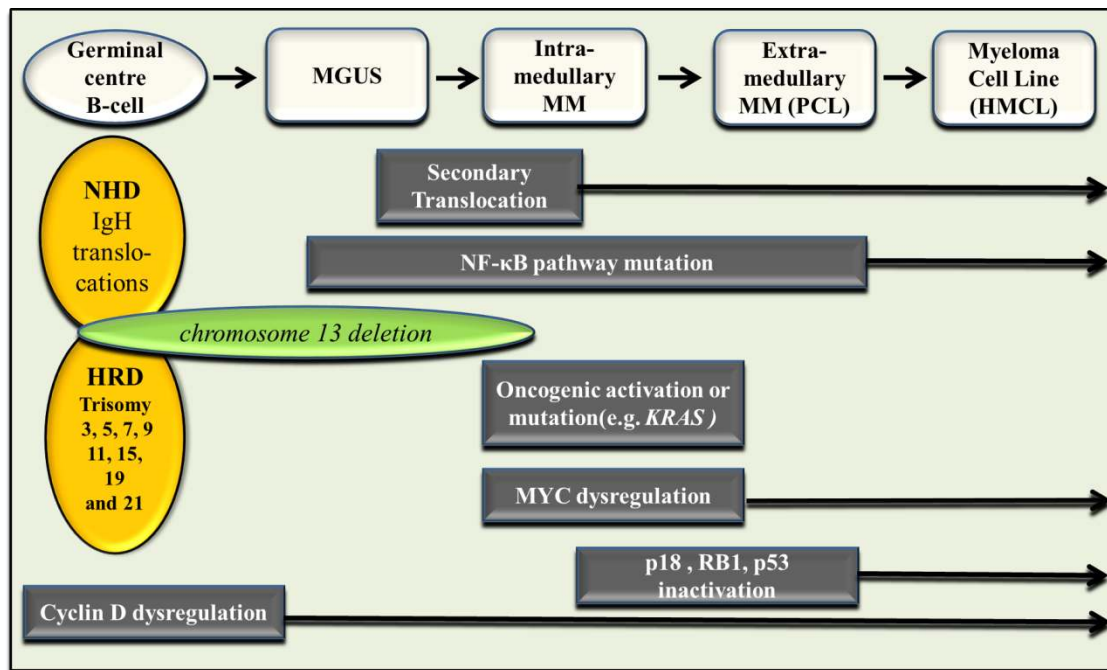
Figure 1.3: Molecular pathogenesis and genetic alteration of Multiple Myeloma. The primary transition is shared by plasma cells in MM and in MGUS; they involve partially overlapping genetic events include primary IgH translocations, multiple trisomies, and deletion of chromosome 13 associated with CCND gene dysregulation. The progression from MGUS to MM is associated with the increase in the expression of MYC and sometimes the mutation of KRAS in addition to chromosome 13 deletion. Further progression of multiple myeloma is associated with MYC rearrangements at Ig locus, NF-κB pathway mutations, p53 mutation or deletion as well as p18INK4c and RB1 inactivation. Modified from Kuehl and Bergsagel., 2012, and Palumbo and Anderson., 2011.

1.4   Cell Cycle

The cell cycle process is a sequence of firmly integrated events that allow the cell growth division, and DNA duplication to give two daughter cells (Alison., 2011; Garrett., 2001; Schwartz and Shah., 2005). This process occurs in two major phases: interphase and mitosis. During interphase, the cell grows and DNA replication occurs and cell prepared to enter mitotic phase by amplifying it organelles, cellular contents, and proteins. While the mitotic phase (M) is a relatively short period during which the cell undergoes division to generate two new cells (Alison., 2011; Garrett., 2001; Schwartz and Shah., 2005). Interphase is subdivided into further distinct phases G_1, S (DNA synthesis), G_2 and G_0 (Figure 1.4) (Nurse., 2000).

1.4.1   Regulation of Cell Cycle Process

The cell cycle is controlled by a family of protein dependent kinase holoenzymes which are activated by cyclins.

1.4.1.1   Cyclin-Dependent Kinases (CDKs)

Cyclin dependent kinases (CDK) is serine/threonine kinases family which have a crucial role in regulating cell division cycle (Garrett., 2001). Progression through the cell division cycle requires coordinated activation of the CDK by association with the regulatory cyclin subunit. Specific cyclin-CDK complexes activate during different cell cycle phases and these activated cyclin-CDK complexes, in turn, phosphorylate target substrates such as Retinoblastoma (pRb) (Carnero., 2002).

Cellular entry into G_1 phase of cell cycle controlled by binding of cyclin D1, D2 and D3 to cyclin D-dependent kinases CDK4 and CDK6. Progression from G_1 to synthesis phase (S) is regulated by cyclin E-CDK2 complex in order to commit the cell to synthesis DNA. In addition, the progression into S-phase regulated by complexed of cyclin A with CDK2. Progression the cell from G_2 phase into mitosis requires the

binding of the CDK1 with cyclin A as well as cyclin B which has a role in protein phosphorylation during mitosis (Figure 1.4) (Garrett., 2001; Schwartz and Shah., 2005; Malumbers and Barbacid., 2007).

1.4.1.2 Cyclin Dependent Kinase Inhibitor (CDK^i)

CDK activity is regulated by inhibitory proteins, named Cyclin Dependent Kinase Inhibitor (CDK^i) which can bind either to CDK alone or to the complex of CDK and cyclin partner and cause cell cycle arrest at different cell cycle phases (Garrett., 2001; Schwartz and Shah., 2005; Malumbers and Barbacid., 2007). There are two families of CDK^i regulatory proteins: the inhibitor of CDK4 (INK4) family which include different protein member, including p16^{INK4a}, p15^{INK4b}, p18^{INK4c} and p19^{INK4d}. These specifically inhibits the activity of CDK4 and CDK6 resulting in G$_1$ arrest. The other CDK^i inhibitor families are the CDK interacting protein or kinase inhibitory protein CIP/KIP family, comprising of p21$^{cip1/waf1,}$ p27^{kip1} and p57^{kip2}, which lead to cell cycle arrest specifically in G/S boundary, S and G$_2$/M (Figure 1.4) (Carnero., 2002).

Progression of the cell through the cell division cycle can be inhibited by modulating of specific mechanisms involved in different phases of cell cycle. Arrest in G$_1$ phase is triggered by inhibition of Cyclin D-CDK4 and Cyclin D-CDK6 complex. While S phase arrest stimulated by DNA damage as well as the reduction in Cyclin A-CDK2 and Cyclin E-CDK2 complex expression (Figure 1.2). In response to DNA damage or stress, the tumour suppressor gene p53 is activated which in turn upregulates the expression of p21^{CIP} and p27^{KIP1} inhibiting Cyclin A-CDK2 and Cyclin E-CDK2 complexes resulting in S-phase arrest (Figure 1.5). Moreover, arrest in G$_2$/M phase is triggered by inhibition of Cyclin B-CDK1 complex via p53 activation (Garrett., 2001; Schwartz and Shah., 2005; Malumbers and Barbacid., 2007; Turner *et al*., 2012). Dis-regulation of cell cycle regulatory molecules play an essential role in cancer progression (Dai and Grant., 2003)

and altered CDK activity has been showed in most human cancer cells (Fischer and Gianella-Borradori., 2003).

1.4.1.3   Cell Cycle Checkpoints

Regulation of CDK activity is crucial for the ordered control of cell growth, DNA duplication and mitotic chromosome distribution to new daughter cells. In order to ensure this, surveillance processes operate as checkpoints to regulate cell cycle progression (Carnero., 2002). These sensor processes ensure that cell completing each phase of cell cycle prior to the start of the next phase by ensuring that proper controlling growth stimulating and inhibiting signals transmit their influences on the progression of the cell cycle (Garrett., 2001; Schwartz and Shah., 2005; Malumbers and Barbacid., 2007). For example, DNA damage activates the checkpoints mechanism by transmitting a signal to the cell cycle progression apparatus resulting in a slowing the cell cycle progression until the risk has been either removed or repaired. Failure to restore the DNA damage stimulate the cell cycle arrest at this phase (Vermeulen *et al*., 2003; Schwartz and Shah., 2005) (Figure 1.4). The cell cycle checkpoints are regulated by two main tumour suppressor proteins p53 (Golias *et al.,* 2004) as well as pRb (Burkhart and Sage., 2008).

1.4.1.4   Irreversible Cell Cycle Arrest: Cell Senescence

Cell senescence or replicative senescence is a phenomenon by which cells undergo irreversible growth arrest in order to prevent unlimited cellular proliferation (Campisi., 2000). Besides aging, senescence may be activated by DNA double strand breaks and premature telomere shorting or in response to oxidative stress. Senescence is essential in order to avoid continuous cell proliferation which could lead to DNA damage due to telomere shorting as a result of incomplete replication of telomeric end of the chromosome (Blasco., 2005; Collado and Serrano., 2010). However, senescence cells contribute to many diseases and aging (Collado *et al.,* 2007). Telomeres are the caps at

the end of chromosomes, containing a repetitive nucleotide sequences, which protects the chromosome. Over time, the telomere ends become shorter and loss of telomeres result in loss of genes in chromosome cap and ultimately DNA damage and stimulating of p53 and pRb signaling pathways (Ferbeyre *et al*., 2002).

Figure 1.4: A schematic representation phases of cell cycle and regulation
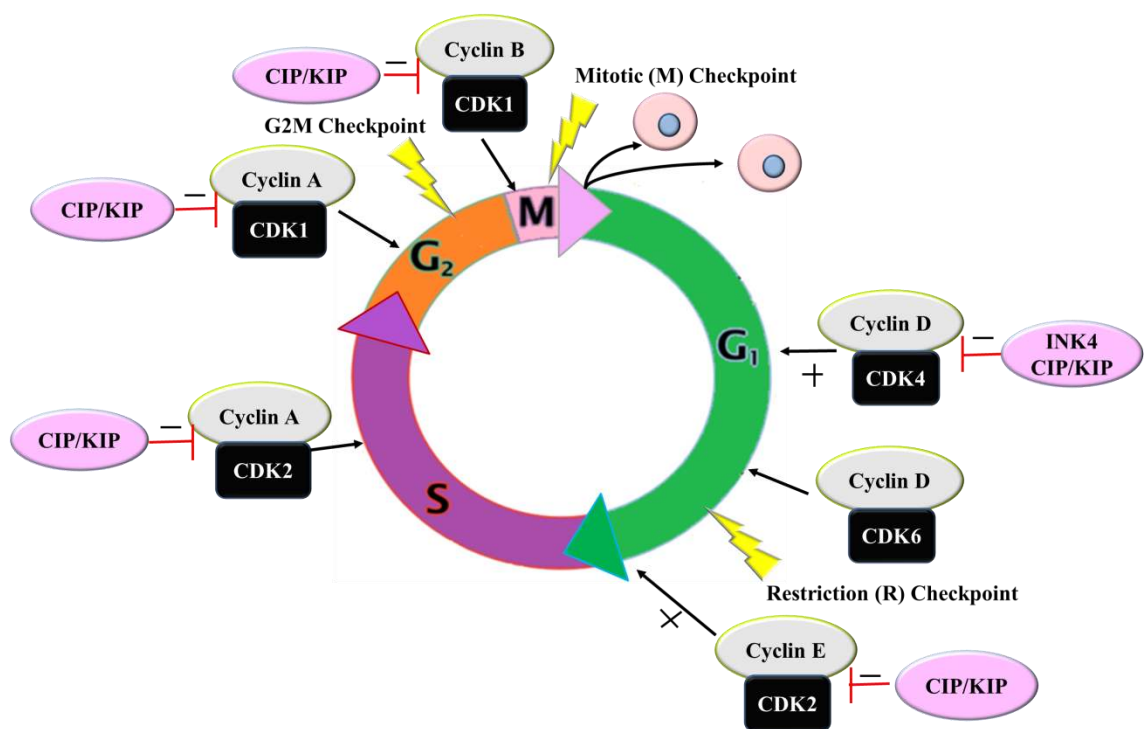
Figure1.4: A schematic representation phases of cell cycle and regulation. Cell cycle has four phases: G_1 phase, S-phase, G_2 phase and M phase and the progress through the cycle is regulated by the activity of numerous CDK–cyclin complexes (CDK) and cyclin dependent kinase inhibitor (CDK^i). Modified from Vermeulen et al., 2003; and Malumbers and Barbacid., 2007.

Figure 1.5: A schematic representation the role of p53 in regulation of cell cycle
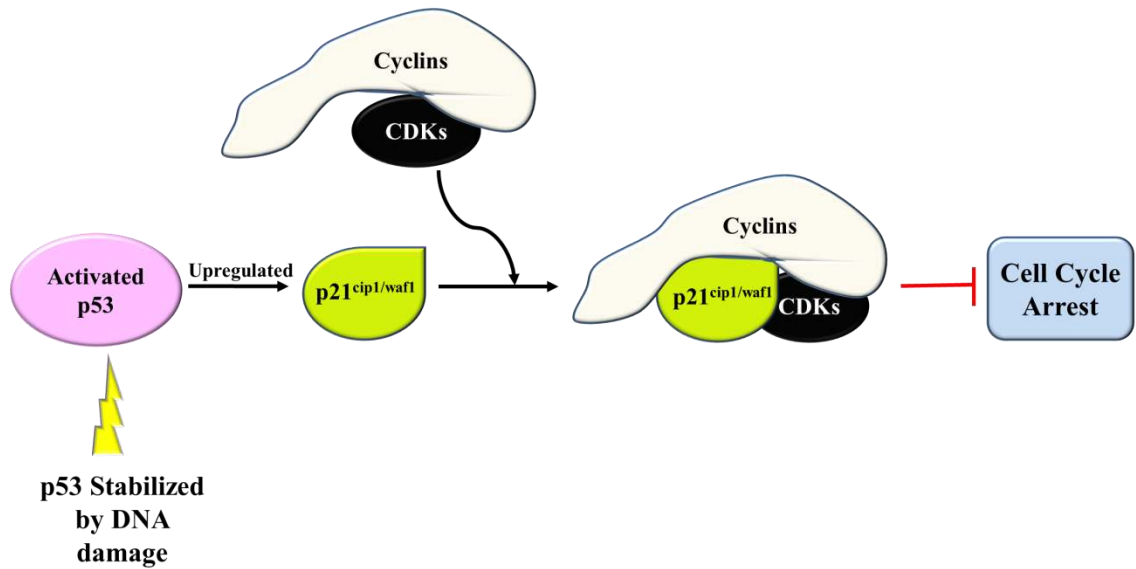
Figure 1.5: A schematic representation the role of p53 in the regulation of cell cycle.
In response to DNA damage or stress, p53 is activated and up-regulates the expression
of $p21^{CIP/WAF1}$ and CDK–cyclin complexes, resulting in cell cycle arrest. Modified from
Golias et al., 2004, and Zilfou and Lowe., 2009.

1.4.2   Cancer Initiating Cells (CICs)

All tissues are originated from the organ-specific stem cells that are defined by their ability to undergo self-renewal and differentiate into cell types of a particular organ (Wicha, *et al.,* 2006). Through the self-renewal processes and differentiation, stem cells able to maintain tissue homeostasis by asymmetric cell divisions (Mitalipov and Wolf., 2009). Self-renewal is tightly regulated process by which stem cells produce progeny identical to themselves. In addition, stem cells produce differentiated cells of multipotent progenitors, which generate more committed progenitors as well as differentiated cells via asymmetrical division (Ginestier *et al*., 2007).

Numbers of molecular markers have been used for detections of stem cell subpopulations, including, enzyme activity such as aldehyde dehydrogenase (ALDH1), expression of specific cell surface antigen and transcription factors (Uchida *et al*., 2000; Richardson *et al*., 2004; Barker *et al*., 2007). These biomarkers are restricted to stem cell population and distinguish them from more differentiated cells. The common methods of identification and isolation of stem cell subpopulation is by utilization of function assays in combination with the expression of tissue specific biomarker which deficient in more differentiated cells (Reya., 2001). In addition to expression of these markers in both embryonic and adult stem cells, have been shown to be expressed in many cancer types, including breast and prostate cancer (Al-Hajj *et al*., 2003; Alison *et al*., 2011; Wang and Dick., 2005; Collins *et al*., 2005). These cancer cells sub-population are proposed to play a role in cancer progression, metastasis, self-renewal, relapse and drug resistant in many types of cancer and therefore may represent cancer stem cells (CSCs) (Yang *et al*., 2015). Examples of CSC markers in some types of human cancers used in CSC detection are shown in Table 1.1.

Representative Cell Surface Markers Used in CSCs Detection		
Cancer type	Positive	Negative
Breast adenocarcinoma	CD44, ALDH	CD24
Acute myeloid leukemia	CD34, ALDH	CD38
Colon adenocarcinoma	CD133, CD44	N/A
Prostate adenocarcinoma	CD44, CD133, α2 β1	CD24
Pancreatic adenocarcinoma	CD44, CD133	CD24
Hepatocellular carcinoma	CD133, EpCAM, CD90	N/A
Multiple Myeloma	CD45, CD19, CD20, and CD22	CD138

Table 1.1: Examples of CSC markers in some human cancers types used CSCs detection

(adapted from Al-Hajj et al., 2003; Bae et al., 2010; Bhatia et al., 1997; Brychtova et al., 2007; Collins et al., 2005; Corti et al., 2006; Corbin et al., 2011; Dean ., 2009; Du et al., 2008; Ginestier et al., 2007; Hart et al., 2005; Huang et al., 2009; Jeter et al., 2011; Johansson et al., 1999; Kim et al.,2002; Lin et al., 2006; Liu et al., 2011; Looijenga et al., 2003; Matsuo and Drexler., 1998; Podberezin et al., 2013; Quinatana et al., 2008; Richardson et al., 2004; Santagata et al., 2007; Singh and Topham., 2003; Uchida et al., 2000; Wang et al., 2012; Yin et al., 1997).

1.4.2.1 *Multiple Myeloma Initiating Cells*

The determination of cells responsible for the initiation, maintenance and progression of multiple myeloma is not fully understood due to the difficulty of growing of MM cells *in vivo* and *in vitro*. Multiple myeloma is characterized by the clonal expansion of neoplastic plasma cells that appear to be quiescent due to the low cloning efficiency and proliferative index of the patient's bone marrow samples (Drewinko *et al*., 1981; Hamburger and Salmon., 1977). As a result, it is still unclear whether plasma cells of MM have the proliferative capability needed for the initiation and maintenance of

disease. On the other hand, plasma cells are phenotypically similar to mature B-cells as well as expressing the identical idiotype and sequences of immunoglobulin gene have been seen in the peripheral blood and bone marrow of multiple myeloma patients (Matsui *et al.*, 2004). A number of studies pointed out those clonal B-cells represent the MM proliferating compartment or progenitor cells (Mitterer *et al.,* 1999; Davies *et al.,* 2000).

Most of the myeloma cell lines as well as the patient specimens of multiple myeloma are characterized by neoplastic plasma cells that expressed the Syndecan-1 (CD138) cell surface antigen (Kuehl and Bergsagel., 2002). During the development of B-cells, the expression of CD138 is limited to terminally differentiated normal plasma cells due to the absence of highly proliferative normal plasmablasts and all earlier stages of B-cell. Furthermore, it has been shown that human cell lines of MM are composed of a small percentage (<5%) CD138^{-Ve} cells these have greater clonogenic potential than the corresponding CD138^{+Ve} plasma cells *in vitro*. In addition, the CD138^{-Ve} cells from the multiple myeloma patient sample are clonogenically similar both *in vivo* and *in vitro* while CD138^{+Ve} cells are not. CD138^{-Ve} cells phenotypically resemble post-germinal center B-cells, and their clonogenic growth is repressed by the anti-CD20 monoclonal antibody Rituximab. These observations suggested that CD138^{-Ve} B-cells serve as myeloma progenitor stem cells that have an ability to replicate and consequently differentiate into malignant cells (Matsui *et al*., 2004; Peacock *et al*., 2007). Clinical studies suggest that most cancer cells are eradicated by chemotherapy but the cells with the clonogenic potential features are responsible for tumour regrowth and are relatively drug resistant (Matsui *et al.,* 2008).

It has been documented that Syndecan1/CD138^{-Ve} cells, which represents clonogenic progenitor myeloma cells are more resistant to TRAIL-mediated apoptosis than CD138^{+Ve} cells due to the lower expression levels of TRAIL receptors (R1 and R2)

(Vitovski *et al*., 2012). Moreover, isolated quiescent PKH26^{Hi} MM cell using PKH dye exhibited enriched stem-like properties and more resistant to anti-myeloma therapeutic agents including cyclophosphamide, bortezomib, vincristine, prednisone, and rituximab *in vitro* compared with PKH^{Lo} cell populations (Chen *et al*., 2014).

1.4.3 Current Multiple Myeloma Therapy

In the last decade, major advances in multiple myeloma treatment have improved the outcome of myeloma patients. The introduction of anti-tumour drugs Thalidomide, the proteasome inhibitor Bortezomib, and Lenalidomide caused a paradigm shift in myeloma therapy. The combination of these novel agents with traditional cytotoxic drugs has also increased response rates. In addition, chemotherapy followed by autologous stem cell transplantation (ASCT) has established an improved response rate and survival benefit compared with traditional chemotherapy (Attal *et al*., 2006; Barlogie *et al*., 2004). ASCT is a preferred treatment strategy for young MM patients either as part of the initial course therapy or at the time of progression of disease (Mohty and Harousseau., 2014). Recently, the use of this novel approach for elderly patients has also resulted in an improved outcome (Mateos *et al.*, 2015).

1.4.3.1 *Autologous Stem-Cell Transplantation (ASCT)*

Autologous stem-cell transplantation (ASCT) has become a standard treatment strategy for young patients of (Mateos *et al*., 2015). Although this option is not curative, ASCT advances response rates and extends median overall survival by around one year in MM (Attal *et al*., 1996; Child *et al*., 2003). The most widely used regimen is Melphalan, 200 mg/m^2 (Kyle and Rajkumar., 2007). Randomized trials demonstrated that overall survival is almost the same whether ASCT is done immediately after the induction therapy or delayed at the time of relapse. Therefore, the decision on ASCT timing is depend on both patient and physician preference (Blade *et al*., 2005).

In some cases, Multiple Myeloma patients receive a second course of ASCT next to recovery from the first procedure. This approch is called tandem (double) ASCT (Attal *et al*., 2003; Cavo *et al*., 2005). On the other hand, allogeneic transplantation is the only treatment option to a limited number of multiple myeloma patients because of age and histocompatibility. The high treatment-related mortality mainly liked to severe graft-versus-host disease (GVHD) and opportunistic infections has made this transplants approach intolerable for most of MM patients (Barlogie *et al*., 2004; Kyle and Rajkumar., 2007). Unfortunately, the median duration of response among myeloma patients after receiving the course of chemotherapeutic agents and ASCT does not exceed 3 years as well as almost all myeloma patients experience relapse progress (Attal *et al*., 2006).

1.4.3.2   *Thalidomide Analogues*

The discovery of thalidomide represented a key milestone in the myeloma therapy (Barlogie *et al*., 2004). However, several thalidomide analogs were developed in an attempt to enhance efficacy and reduce the toxicity of anti-myeloma therapy especially after thalidomide was established to be a teratogen. Lenalidomide is immunomodulatory agent belongs to a class of thalidomide analogs display occasionally neurotoxicity (Kyle and Rajkumar., 2007). 91% of newly diagnosed myeloma patients in a phase II trial attained a good response with lenalidomide in combination with dexamethasone (Rajkumar *et al.,* 2005). In June 2006, Lenalidomide and dexamethasone treatment regimen was approved by the FDA for the treatment of MM patients who have failed one prior treatment (Kyle and Rajkumar., 2007).

1.4.3.3   *Bortezomib*

A new class of anti-myeloma agents includes the proteasome inhibitor Bortezomib or Velcade with remarkable activity in a patient who relapses to standard therapy such as

thalidomide (Barlogie *et al*., 2004). Patients with relapsed refractory myeloma in a phase II clinical trial confirmed that approximately one-third of patients respond to Bortezomib treatment (Richardson et al., 2003). In a subsequent randomized trial, time to disease progression was found to be greater with bortezomib compared with dexamethasone alone in relapsed myeloma patients (Kyle and Rajkumar., 2007). Bortezomib is effectively combined with DNA-damaging cytotoxic agents such as melphalan and doxorubicin (Barlogie *et al.*, 2004). In addition, a number of combination therapy regimens containing bortezomib, e.g. bortezomib, thalidomide and dexamethasone (VTD) regimen, Bortezomib plus cyclophosphamide (VD) regimen have been examined in randomised phase III trials pre ASCT with some encouraging results (Mateos *et al*., 2015).

1.5   Targeted Cancer Therapies

Targeted anti-cancer therapies are designed to have the ability to modulate a particular pathway or molecular signal important for tumour progression and development (Signore *et al*., 2013). The identification of appropriate target depends on understanding the underlying tumour molecular changes (Niemoeller and Belka., 2013). These approaches trigger the generation of therapeutic agents that modulate the cell cycle pathways, stimulate cancer cell death, and hinder tumour angiogenesis. This includes apoptotic therapeutics, immune-therapeutics and the hormonal therapy that are applied in cancers treatment (Queirolo and Acquati., 2006; Gray-Schopfer *et al*., 2007).

1.5.1   Apoptosis as a Target Cancer Therapy

The major goal of targeted anti-cancer therapy aims to selectively eradicate the malignant cells via triggering the apoptotic pathways. Increasing evidence points to the loss of the apoptotic process playing a key role in establishing tumour formation and resistance to chemotherapy (Pore *et al*., 2013; Vitovski *et al*., 2012). Therefore,

elucidating the apoptotic signals and the underlying mechanistic changes in the cancer cell may result in the development of novel therapeutic approaches (Niemoeller and Belka, 2013).

Apoptosis or programmatic cell death is an essential regulatory mechanism for maintaining tissue homeostasis and development (Stuckey and Shah., 2013). A number of caspases are instrumental for both initiation and execution of apoptotic signals (Alnemri *et al.*, 1996). These caspase proteases usually originate in an inactive form (pro-caspase) and its activation takes place by proteolysis at certain Asp-amino acid residues via the participation of other caspases (Green and Reed., 1998; Wolf and Green., 1999). Two main forms of initiator caspase exist depending on the presence and lack of particular regulatory amino-terminal domain motifs that facilitate homotypic interactions, the Death Effector Domain (DED) present in caspase-8/10 and the Caspase Recruitment Domain (CARD) present in caspase-9. The human apoptotic signal cascade contains initiator caspases (2, 8, 9, and 10) and effector caspases (3, 6 and 7) (Henderson and Brancolini., 2003; Philchenkov., 2012).

1.5.2   Apoptotic Cascade Signals

Though there are various numbers of signals that activate apoptotic pathways, the induction of upstream caspases is produced mainly by a restricted number of signaling pathways (Adrian and Martin, 2001; Adams and Cory, 2002). Two primary caspase activating pathways are extrinsic, or the death receptor pathway, and intrinsic, or the mitochondrial pathway (Krammer, 1998; Suliman *et al.*, 2001). Moreover, additional apoptotic cascades have been identified including caspase-2 genotoxic stress-dependent stimulation through p53 (Lassus *et al.,* 2002) and p53-Induced Death Domain protein (PIDD) (Berube *et al.*, 2005).

1.5.2.1 Extrinsic Pathways

The extrinsic signalling pathway is stimulated by binding specific ligands such as the Tumour Necrosis Factor (TNF) to specific death cell surface receptors such as TNFR. These receptors are type I transmembrane proteins characterised by the existence of 80 residue length death domain (DD) within the cytoplasmium (Philchenkov., 2012). Additionally, FasL binds to Fas and TRAIL binds to Death Receptor-4 and -5 (Ashkenazi., 2002)

Ligand binding stimulates the recruitment of many cytosolic proteins resulting in the formation of the death inducing signaling complex (DISC) leading to the recruitment of the adaptor molecule Fas Associated protein with death domain (FADD) which has a death effector domain (DED). FADD interacts with the activated death receptors allowing the binding of FADD with procaspases-8 and -10 which then become activated. Once procaspase is activated by cleavage, it stimulates the downstream effector caspases-3, -6 and -7 and the apoptotic signals in turn are activated (Figure 1.6) (Fox *et al*., 2010; Pennarun *et al*., 2010).

1.5.2.2 Intrinsic Pathways

In some cells (Type I cells), caspase -8 and -10 stimulation is adequate for the initiation of apoptotic cascade, however, in other cells (Type II cells), the involvement of the mitochondrial pathways is essential (Philchenkov., 2012). The latter is triggered in response to hypoxia and DNA damage and results in the outer-mitochondrial membrane pore formation and thus promotes pro-apoptotic factor release such as cytochrome c into the cytosol (Green and Reed., 1998; Kraemer., 1998). The mitochondrial membrane disruption depends on the Bcl-2 protein family (Desagher and Martinou., 2000) that contains anti-apoptotic proteins including Mcl-1, Bcl-XL, Bcl-2, and the pro-apoptotic

protein including Bax, Bak, Bad and Bid in addition to the stress sensors BH3-proteins such as NOXA and PUMA (Pore *et al*., 2013).

The release of mitochondrial pro-apoptogenic cytochrome c results in the formation of a functional signal complex called apoptosome that consists of procaspase-9 along with Apaf-1. This leads to activating caspase-9 by cleavage and consequently activation of the executioner caspases-3 and -7 (Figure 1.6) (Wu., 2009).

These signals are regulated on numerous levels. For instance, c-flip is a negative caspase stimulation regulator in the DISC which catalytically inactivates caspase-8 and -10. Another class of negative regulators is the inhibitors of apoptosis proteins (IAPs) which directly inhibit the caspase activity or induce caspase degradation and their action is linked to Smac/DIABLO, a pro-apoptotic factor released from mitochondria (Figure 1.6) (Niemoeller and Belka., 2013).

1.5.3   Apoptotic Mediated Anti-Cancer Drugs

1.5.3.1   TRAIL as a Target in Anti-cancer therapy

Since it was discovered, the tumour necrosis factor-related apoptosis inducing ligand (TRAIL) obtained extensive interest for its potent anti-cancer killing activity by triggering tumour cells to undergo apoptosis in a variety of tumour cell types and producing a negligible effect on the normal cells (Stuckey and Shah., 2013). This ability has led to an investigation of the therapeutic potential of TRAIL as a promising apoptotic anti-cancer drug (Kruyt., 2008; Siegelin *et al*., 2009).

TRAIL belongs to the TNF cytokine superfamily that induces the apoptotic cascades (Liu *et al*., 2013). It is type II transmembrane protein inserted into the membrane of the cells by exposing carboxyl terminus that contains the death receptor binding domain. By the action of metalloproteases enzyme, the membrane-bound form of TRAIL can be cleaved to a soluble TRAIL form. Both the membrane-bound as well as the soluble

TRAIL form form trimers that trigger apoptosis via their interaction with the DR4/5. In contrast, the TRAIL receptor is mainly transmembrane type I with N-terminus binding domains extra-cellularly (Kimberley and Screaton., 2004; LeBlanc and Ashkenazi., 2003).

Four different membrane-bound TRAIL receptors have been identified. They are TRAIL-R1 (DR4), TRAIL-R2 (DR5), TRAIL-R3 (LIT, Decoy Receptor (DcR1), TRAIL-R4 (TRUNDD and DcR2) (Ashkenazi *et al*., 2002) in addition to the circulating soluble decoy receptor Osteoprotegerin (OPG) (Emery *et al*., 1998). DR4 and DR5 characterized by the existence of cytoplasmic functional tail Death Domain (DD) that is able to recruit apoptosis signalling molecules and stimulate cell death. On the other hand, DcR1 and DcR2 are decoy receptors that do not have the function DD in their intracellular part, while OPG has no intracellular domain, but has the ability to bind with TRAIL but with a low affinity in comparison to DR4 and DR5, attenuating downstream death signaling (Holen *et al*., 2002; Kimberley and Screaton., 2004).

1.5.3.2 *TRAIL-Based Therapy and Apoptotic Signaling*

The interaction of TRAIL with its membrane receptors DR4 and DR5 leads to the induction of receptor cross-linking, caspase cascade and subsequently to apoptosis via two different irreversible apoptotic signals (Liu *et al*., 2013). This binding facilitates and activates the initiator pro-caspase-8 that induces apoptosis signals either directly via the activation of effector caspases-3 and -7 in the extrinsic pathway (Pan *et al.,* 1997) or by stimulating the intrinsic, mitochondrial death cascade indirectly through the cleavage of Bid to its active form (t-Bid) in the intrinsic pathway. As a consequence of these events, cleaved Bid stimulates Bax/Bak oligomerization resulting in the release of the pro-apoptotic factors cytochrome c which in turn activates caspase-9 followed by the activation of downstream executioner caspases (Figure 1.6) (Yamada *et al*., 1999).

Executioner caspases, such as caspase-3, -6 and -7, have only a small prodomain and cleave diverse cellular substrates including ICAD/ DFF45, gelsolin, fodrin, poly (ADP ribose) polymerase (PARP), and others (Engels *et al.*, 2000).

Figure 1.6: A schematic representation the apoptotic pathways
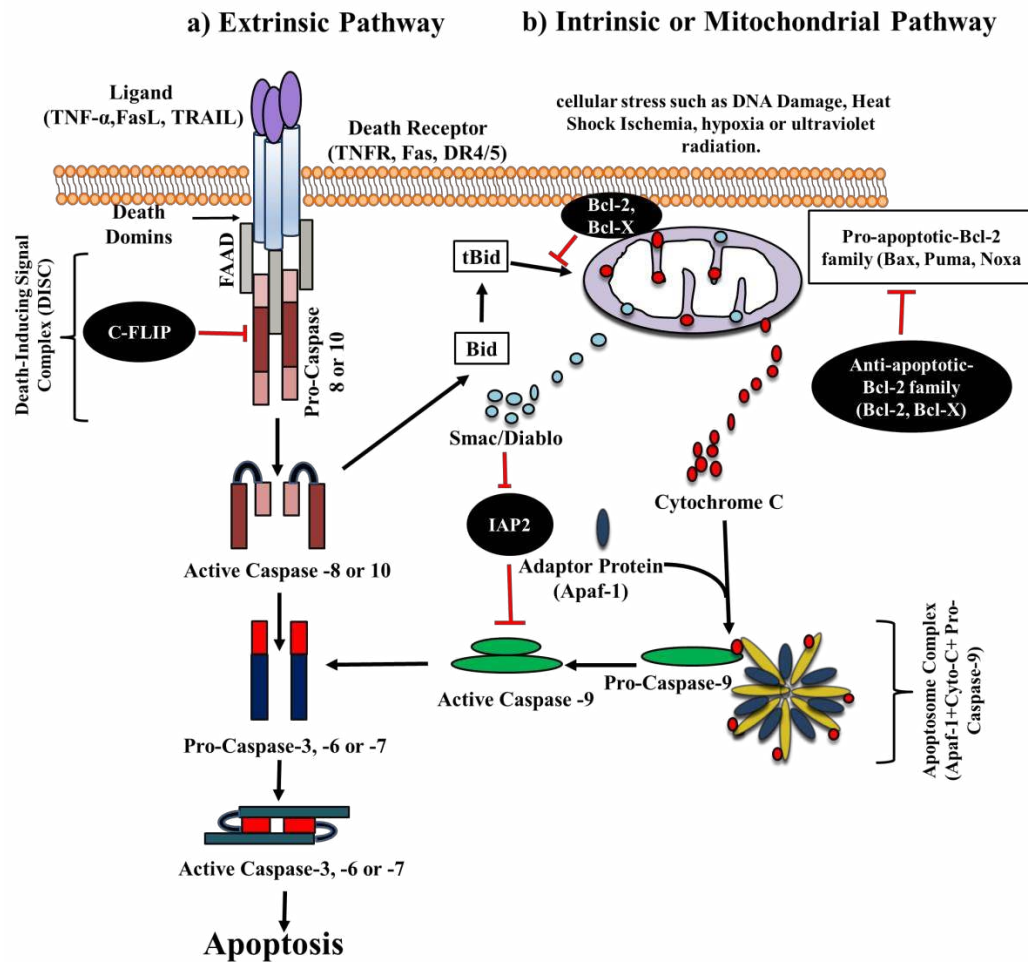
Figure1.6: A schematic representation the apoptotic pathways. a) The extrinsic pathway is stimulated by binding of ligands to a death receptor. This binding facilitates and activates the initiator pro-caspase 8 that induces the apoptosis via the activation of effector caspases-3, -6 and -7. b) The intrinsic pathways of apoptosis activated by cellular stress such as DNA damage or hypoxia. This cellular stress promotes the release of mitochondrial pro-apoptotic factors such as cytochrome c into the cytosol and in turn activating the caspase-9 by cleavage and consequently the executioner caspases-3, -6 and -7 activations. Modified from Fox et al., 2010, and Hersey and Zhang., 2001.

1.5.3.3   TRAIL Based Therapy (TRAIL Mimetic)

A number of agonistic antibodies and novel variants of recombinant human (rh) TRAIL have been generated (De Wilt., 2013). Number of clinical phase I studies have revealed that the soluble TRAIL (AMG951, Dulanermin) exerts a partial anti-cancerous response in hematologic malignancies and solid tumour displaying a short half-life without any adverse events related to its administration (Herbst *et al*., 2006; Ling *et al*., 2006; Pan *et al*., 2007). In addition, the combination of TRAIL AMG951 with rituximab in other clinical trial study appears safe and shows evidence of activity in patients with low-grade non-Hodgkin lymphoma (Yee *et al*., 2007).

Similar to soluble TRAIL, the agonistic monoclonal antibodies (mAbs) have been used both as an anti-tumour agent to stimulate TRAIL-mediated apoptotic response (Lee *et al*., 2011). A number of agonistic anti-TRAIL-R mAbs has been generated and introduced into clinical trail, including Mapatumumab (anti-TRAIL-R1, Human Genome Science) (Hotte *et al.,* 2005; Younes *et al*., 2005), Lexatumumab (anti-TRAIL-R2, Human Genome Sciences) (Patnaik *et al*., 2006; Plummer *et al*., 2007) as well as APOMAB (anti-TRAIL-R2, Genentech) (Camidge *et al.,* 2007). These agonistic anti-TRAIL-R1/-R2 mAbs activate the DR4 and DR5 TRAIL via agonist-mediated oligomerization resulting in clustering of intra-cellular DD, subsequently inducing the apoptotic pathway (Lee *et al*., 2011; Testa., 2010). Notably, these agents bypass decoy receptors and OPG (Locklin *et al*., 2007).

1.5.3.4   The Role of TRAIL-Based Therapies in Multiple Myeloma

Gene expression studies provided an interesting observation that TRAIL and its receptors DR4/5 are highly expressed in myeloma cells compared to plasma cells, and this could stimulate an autocrine apoptotic signaling mechanism (Jourdan *et al*., 2009). However, in multiple myeloma the apoptotic cascades are depressed by the over-

expression of TRAIL decoy receptors especially DcR2 as well as OPG which act as a paracrine survival factor for myeloma cells by inhibiting TRAIL-induced apoptotic cell death (Shipman and Croucher., 2003). It has been found that the TRAIL-base therapies induce the apoptosis of MM cell lines as well as the primary myeloma cells both *in vitro* and *in vivo* (Gazitt., 1999; Mitsiades *et al*., 2001; Vitovski *et al.*, 2012). Studies suggest that agonistic DR4/5 mAbs might have an advantage over recombinant soluble TRAIL in the stimulation of apoptosis of myeloma cells due to its ability to bypass the inhibition of TRAIL-mediated apoptosis by the decoy receptors (Menoret *et al*., 2006; Locklin *et al*., 2007). TRAIL resistance in myeloma is developed not only due to the effect of the decoy receptors but it is also associated with c-flip over-expression even though this observation was not supported by other studies (Mitsiades *et al*., 2002). In addition, it was reported that the secretion of the survival factor IL-6 by bone marrow stroma plays an important role in the TRAIL resistance of myeloma cells by stimulating the signalling pathways in addition to the increased level of c-flip (Perez *et a*l., 2008).

1.5.4   TRAIL Sensitizers

In order to restore or enhance the TRAIL-mediated apoptosis signaling combined therapy of TRAIL and other agents have demonstrated promising results (Sayers and Cross., 2014; Booth *et al*., 2009; Henrich *et al*., 2012). *In vitro* studies have displayed that several classes of anti-tumour agents were shown to sensitize to TRAIL-induced apoptosis in leukemia, multiple myeloma and solid tumours (De Wilt., 2013). These agents used in combination with TRAIL either induce the expression of TRAIL-R1/-R2 or reduce the expression of anti-apoptotic proteins expression such as c-flip, Bcl-2 and XIAP (Testa., 2010). Amongst those are the proteasome inhibitors bortezomib (Balsas *et al*., 2009; Sayers *et al.*, 2006), doxorubicin (Vitovski *et al.*, 2012) and HDAC[i] (Fandy *et al*, 2005). Moreover, unpublished studies have documented Nuclear Export Inhibitors as highly effective TRAIL sensitisers (Figure 1.7).
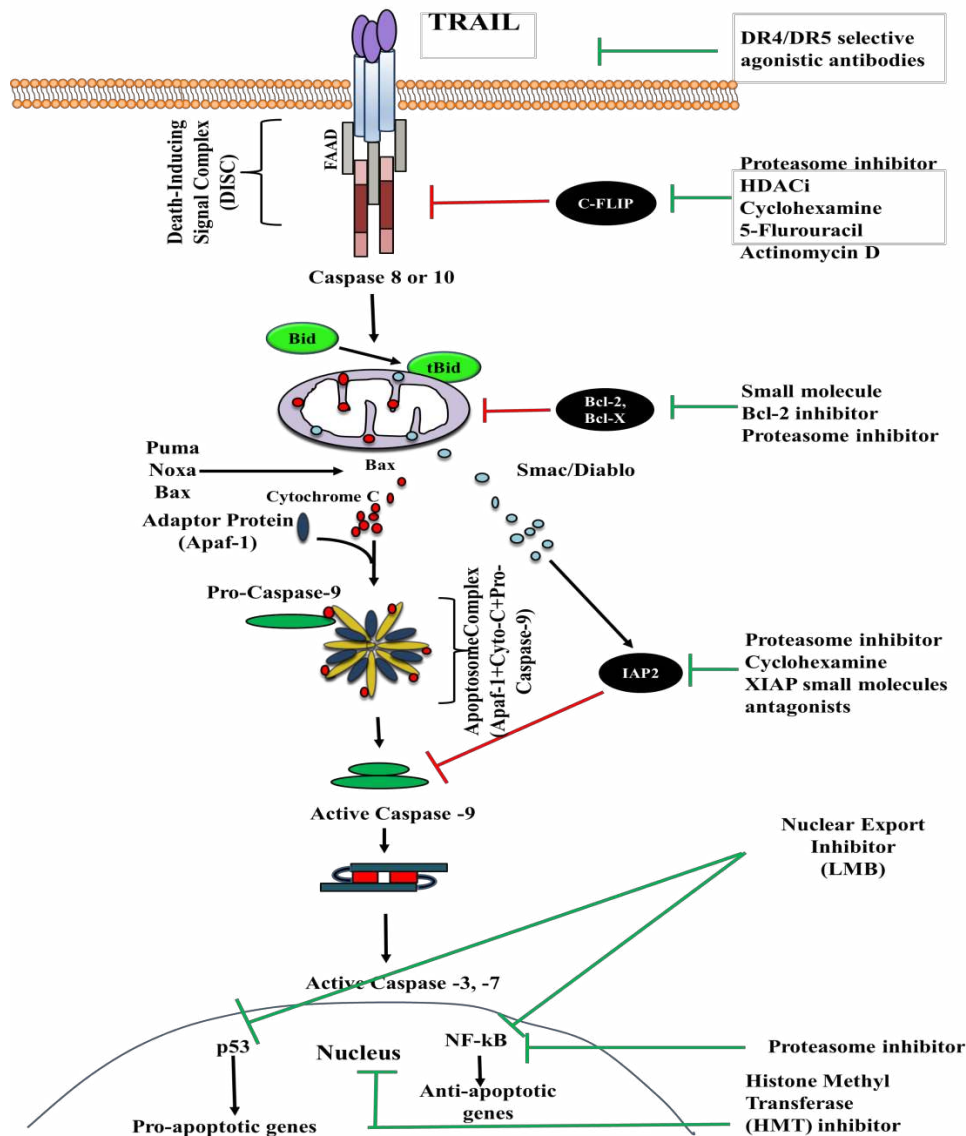
Figure 1.7: Re-sensitization of cancer cells to TRAIL-mediated apoptosis.

Triggers of Death Receptors by TRAIL can be blocked by decoy receptors and agonist antibodies to DR4 and DR5 can bypass this inhibition. TRAIL signalling can be inhibited by a number of negative regulators on various levels such as c-FLIP, anti-apoptotic Bcl-2 family members and inhibitors of apoptosis proteins (IAPs). Most standard chemotherapy DNA-damaging agents and radiotherapy cause up-regulation of DR4 or DR5 and pro-apoptotic Bcl-2 family members such as Bax, Puma, and Noxa possibly through the stimulation of p53. Newer anti-cancer agents that target cell processes such as proteasome inhibitors or histone modification and changes in gene expression (HDACi) Histone Methyltransferase (HMTase) inhibitor may allow the bypass of multiple anti-apoptotic pathways as shown. Additionally, Nuclear Export Inhibitor (NEI) Leptomycin B may also enhance apoptosis signalling by inhibiting the export of CRM1-mediated protein from the nucleus causing entrapment of nuclear p53. Modified from Sayers and Cross., 2014.

33

1.6   General Hypothesis

The general hypotheses of this investigation are: (1) TRAIL responses in multiple myeloma can be enhanced by small molecules inhibitor to enhance apoptotic cell death. (2) Generation of TRAIL^R cells will inhibit NEI/HMT^i/HDAC^i-induced TRAIL-sensitization. (3) TRAIL insensitive cells represent CD138^{-ve} PKH-26^{Hi} quiescent CSC populations.

The specific aims ofthis study were to:

1. Investigate the efficacy of TRAIL to induce apoptotic cell death either alone or in combination with potential TRAIL sensitizers in term of induction of apoptosis and cell cycle arrest.

2. Screen the effect of TRAIL either alone or in combination with TRAIL senstizers on established colonies of multi-cellular alginate spheroid model of human multiple myeloma cell lines and compare the effect of these drugs in both suspension and 3D cultures models.

3. Develop TRAIL^R cell lines and test for sensitization with small moleculues inhibitors.

4. Isolate PKH26^{Hi} quiescent multiple myeloma populations and assessed for sensitivity to TRAIL/TRAIL sensitizers vs. parental cells.

5. Identify the potential mechanistic pathways for the TRAIL sensitizers.

2. Effect of NEI, HDAC^i, and HMTase^i on TRAIL Response in Multiple Myeloma Cells

2.1 Introduction

Clinical trials to assess the safety and anti-cancer activity of Tumour Necrosis Factor-Related Apoptosis-Inducing Ligand (TRAIL) and agonistic Death Receptor antibodies have been completed in several tumour types (Doi *et al* 2011; Herbst *et al*., 2010, Von Pawel *et al*., 2014) including multiple myeloma (Matthews *et al*., 2013). Unfortunately, TRAIL resistance develops *in vitro* (Jian *et al*., 2016) and in clinical trials, TRAIL insensitivity may be present in most tumours (Abdulghani *et al.*, 2013). Consequently combined therapy of TRAIL with other anti-tumour agents is required to restore the TRAIL sensitivity (Deleu *et al*., 2009; Sayers and Cross., 2014; Booth *et al*., 2009; Henrich *et al*., 2012).

2.1.1 Nuclear Export Inhibitors (NEIs) as an Inhibition of Nuclear Cytoplasmic Trafficking

NEIs are potential anti-tumour agents that inhibit the transport of proteins containing a nuclear export signal (NES) from the nucleus to the cytoplasm resulting in the alteration of the cell cycle and the induction of apoptosis (Figure 2.1) (Turner *et al*., 2012). One of the first NEI discovered was Leptomycin B (LMB) which as an anti-fungal antibiotic unsaturated branched-chain fatty acid is isolated from Streptomyces bacteria (Fan *et al*., 2013).

The nuclear envelope is a selective physical barrier that plays an important role in cell cycle regulation and transcription. The nuclear-cytoplasmic transport of RNA, the essential regulators of cell cycle suppression, transcription or specific therapeutic agent (Turner *et al*., 2012) are tightly controlled by pores embedded in the nuclear envelop membranes known as the nuclear pore complex (NPC). The small molecules and proteins are passively diffused through the NPC while the movement of large molecules (>5 kDa) through NPS needs the assistance of particular nuclear-cytoplasmic transport

receptors protein (karyopherins). Most of these transport proteins belong to the karyopherin-β protein family (Cook *et al*., 2007) and each of the karyopherin-β transport signals recognition of specific cargo protein or RNA. The movement of intracellular protein is regulated by unique amino acids or signaling sequences present within each cargo protein called a nuclear localization signal (NLS). These are required for the movement of cargo out of the nucleus and nuclear export signals (NES) for the exporting of nucleus cargo to the cytoplasm (Figure 2.1) (Lange *et al*., 2007).

The ubiquitous transport receptor chromosome region maintenance protein 1 (CRM1/exportin 1) plays a role in binding and exporting proteins as well as RNA. In humans, 19 transport receptor molecules karyopherin have been recognized. Among those are importins, exportins, and transportins (Das *et al*., 2015). However, the specific recognition signals (NLS/NES) for most of these transport molecules have not been identified yet. For CRM1, the NES contains hydrophobic amino acids sequences such as leucine, isoleucine, methionine, valine and phenylalanine (Turner *et al*., 2014). The NES consensus motif is HX2–3HX2–3HXH, where H is a hydrophobic amino acid and X is any amino acid. This sequence could be present in a more complex structure of proteins e.g. α-helical proteins (Figure 2.1) (Turner *et al*., 2012).

For nuclear import, the NLSs of cargo protein is recognized by Importin of the Importin α/β heterodimer, and is nucleus docking and translocation via the nuclear pore complex is facilitated by Importin β subunit that is bounded to a small GTPase molecule, known as RAs-related Nuclear protein (RAN-GTP) which in turn displaces the Importin α subunit to mediate cargo release. In the export route from the nucleus, NES on the cargo protein or the export substrate is recognized and bound to the RAN-GTPase-dependent export mediators or Exportin such as CRM1. These complexes are produced in the nucleus binding together with the high affinity. Once the CRM1-RAN-GTP-cargo protein complex is synthesized in the nucleus, it is exported to the cytoplasm via NPC.

By the action of RAN-GTPase, RAN-GTP is hydrolyzed to RAN-GDP that facilitates the dissociation of the export complex into its separate components releasing export substrate into the cytoplasm and recycling the CRM1 receptor proteins and RAN-GTP back into the nucleus to undergo another nuclear export cycle (Figure 2.1) (Leprêtre, *et al*., 2008; Wagstaff and Jans., 2009).

2.1.1.1 Leptomycin B as exportin1/CRM1-dependent Nuclear Export Inhibitor

Leptomycin B (LMB) is a highly specific and potent CRM1 inhibitor that has the ability to bind and inhibit CRM1 Exportin by a Michael-type covalent addition at cysteine 528. The alkylation of the reactive site cysteine 528 residue blocks the binding of CRM1 to the cargo protein leucine-rich nuclear export sequence and prevents the CRM1-cargo-RAN-GTP export complex formation; thus, it obstructs the nuclear export of CRM1-mediated protein into the cytoplasm. Most inhibitors of CRM1 function by modifying the reactive site cysteine 528 either permanently or reversibly. Thus, LMB is a potent CRM1 inhibitor that mediates the inhibition of the nuclear protein export and the existence of leucine-rich nuclear export signals that are used as standards to label whether a protein is exported via CRM1 (Figure 2.1) (Wagstaff and Jans., 2009).

Figure 2.1: The Nuclear-cytoplasmic transport and LMB mechanism of action
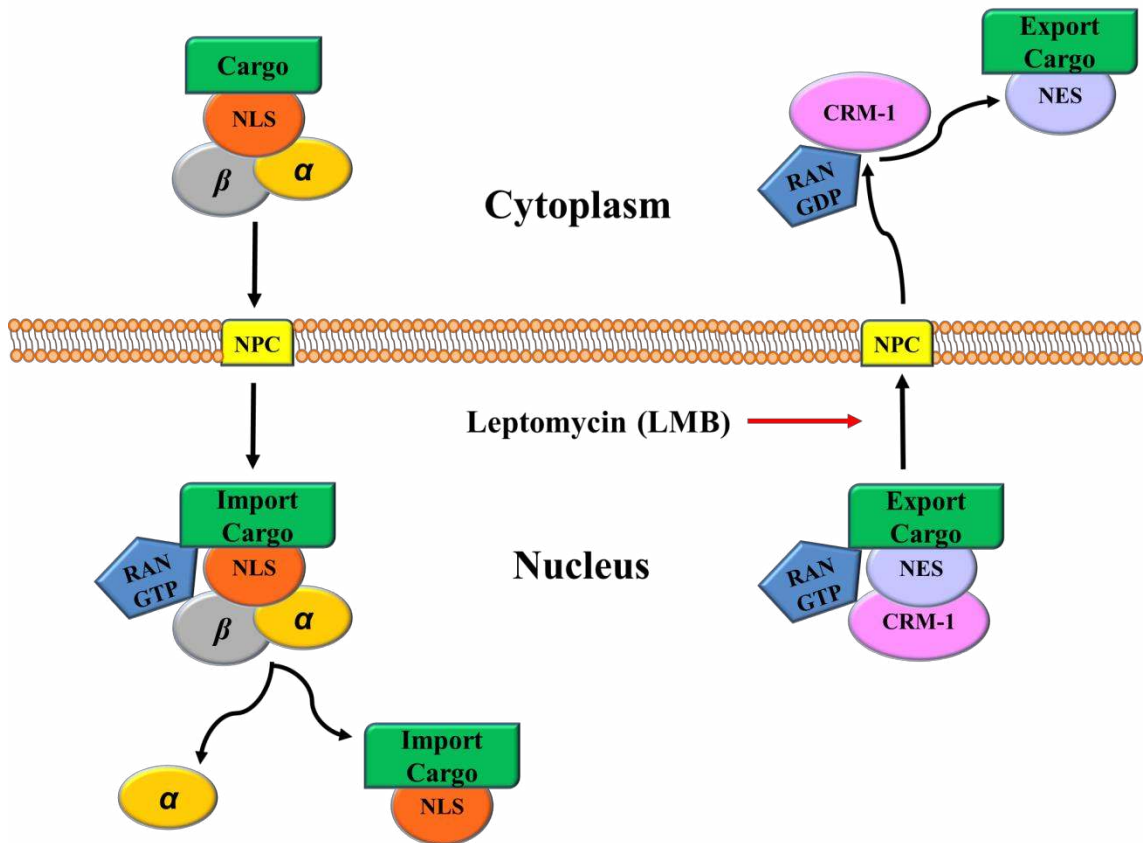
Figure 2.1: The Nuclear-cytoplasmic transport and LMB mechanism of action*. NLS of cargo protein is recognized by α Importin of the Importin α/β heterodimer. Docking and translocation into the nucleus facilitated by β Importin binding to RAN-GTP which displaces the Importin α to mediate the release of the cargo. For export, NES on cargo protein is recognized and bound to Exportin/CRM-1 bound with RAN-GTP and translocation into the cytoplasm occurs. Hydrolysis of RAN-GTP into RAN-GDP facilitates cargo dissociation. The site of action of LMB is indicated by the red arrow. Modified from Wagstaff and Jans., 2009.*

2.1.1.2 *Leptomycin B and Apoptosis*

Leptomycin B is a highly specific and potent CRM1 inhibitor that triggers the apoptosis and cell cycle arrest at the G_1 and G_2 phases in a certain cancerous cell. As a result, the nuclear accumulation of CRM1-dependent export proteins occurs including the tumour suppressor protein p53, $p21^{CIP}$, $p27^{KIP1}$, APC, BRAC1, FOXO proteins, N-WASP/FAK, galectin-3, INI1/hSNF5, Bok, nucleophosmin, RASSF2, Merlin (Turner *et al.*, 2012) and NFκB transcription factors (Miskolci *et al*., 2006).

p53 is a tumour suppressor protein which is produced in the cytoplasm in response to stresses, DNA damage and oncogene activation (Green and Kroemer., 2009). As a nuclear transcription factor, it controls the expression of genes involved in some cell processes such as the cell cycle, apoptosis and autophagy. The tumour suppressor protein p53 possesses sequences of both nuclear localization signal and nuclear export signal. Moreover, it is nuclear localization depending on its import in α/β binding while the nuclear export of p53 requires binding to CRM1.

Nuclear p53 versus cytoplasmic localization is controlled by a number of post-translational modifications. Basal levels of p53 in normal healthy cells are maintained by Mouse double minute 2 homolog (MDM2) -stimulated proteasomal polyubiquitination and degradation. MDM2 mediated p53 C-terminus monoubiquitination, and sumoylation and this monoubiquitination exposes the NES, allowing nuclear export via a CRM1-dependent manner (Lindenboim *et al.*, 2011; Shao *et al.*, 2011).

LMB significantly induces the activation of p53 resulting in apoptosis stimulation and growth arrest (Mutka *et al*., 2009). Although LMB toxicity at concentrations <5 nM for 1h has limited it is clinical usefulness as a single agent (Fan *et al.*, 2013). Treatment with LMB has proved to induce cell death in lung adenocarcinoma cell lines and in

esophageal cancer (Shao *et al.*, 2011). Moreover, the p53 wild type in adenocarcinoma cell line was more LMB resistant than the null or mutant p53. Besides, LMB treatment sensitized the drug-resistant cancer cells to chemotherapeutic agents (Lu *et al*, 2012). As a TRAIL sensitizer, preliminary work from our laboratory showed that LMB/TRAIL co-treatment enhanced the apoptotic responses of PC3 prostate cancer cells to TRAIL (Haywood-Small *et al.*, 2011). The underlying molecular mechanisms of how LMB induces apoptosis is not clearly understood, however, as it has been shown that the apoptotic effect of LMB is associated with cytochrome c-mediated caspases-3 activation as well as the selective XIAP and Mcl-1 down-expression (Jang *et al.*, 2004).

2.1.2 Epigenetic Modifiers as Anti-Cancer Agents

2.1.2.1 *Histone Deacetylase Inhibitors (HDAC[i])*

Recently, growing evidence has suggested that not only gene impairment, e. g. deletions, structural chromosomal abnormalities, and point mutations are responsible for initiation and progression of malignancies, but also the epigenetic alterations play an essential role in tumour suppressor gene down-regulation and oncogene up-regulation (Baylin and Ohm., 2006; Lund and Lohuizen., 2004). Remodeling of chromatin is one of the major epigenetic regulations processes (Baylin and Ohm., 2006; Lund and Lohuizen., 2004).

Modifications either on the histone level or the DNA level result in altering the chromatin state into an open or closed configuration. The core histone post-translational modifications are mainly on the amino-terminal tail, which is rich in lysine. These modifications include methylation, acetylation, and deimination which are important for the alteration of gene expression as they facilitate the DNA accessibility and binding with other complexes of non-histone protein that could include transcriptionally co-activating or co-repressing factors (Deleu *et al.*, 2009).

The chromatin acetylation is controlled by two main enzymes, histone acetyltransferases (HAT) and histone deacetylases (HDAC) (Peterson and Laniel., 2004). The HAT acetylates core histones lead to more relaxed and transcriptionally active chromatin structure, whereas HDAC catalyses the removal of the acetyl group leading to a more compact, transcriptionally inactive chromatin form. Histone hyperacetylation permits the occurrence of transcription; while histone deacetylation prevents transcription; therefore, HDAC inhibitors (HDAC^i) induce transcription of epigenetically silenced genes (Figure 2.2) (Bradner *et al*., 2010). Deimination allows decondensation of chromatin and induces a stem-like phenotype. Specifically, deimination of histones has recently been associated with haematopoietic stem cell behavior (Nakashima *et al*., 2013), and targeting this pathway has been showing to enhance TRAIL responses (Khalid., 2016).

2.1.2.2 *The Role of HDAC^i in Controlling Gene Expression*

The non-selective HDAC^i suberoylanilide hydroxamic acid (SAHA) or Vorinostat inhibits HDAC I and II class activity and its anti-cancer action has been widely investigated in many cancer types. SAHA directly binds to HDACs catalytic site and inhibits their activity (Figure 2.2). Blocking the activity of HDAC by SAHA leads to gene expression modification in a wide range of tumour cell lines such as multiple myeloma and it inhibits the activity of HDAC with IC50s of high nM to low µM range *in vitro* in many cancer cells (Hideshima and Anderson., 2013).

Figure 2.2: The role of HDAC^i SAHA in the regulation of gene expression
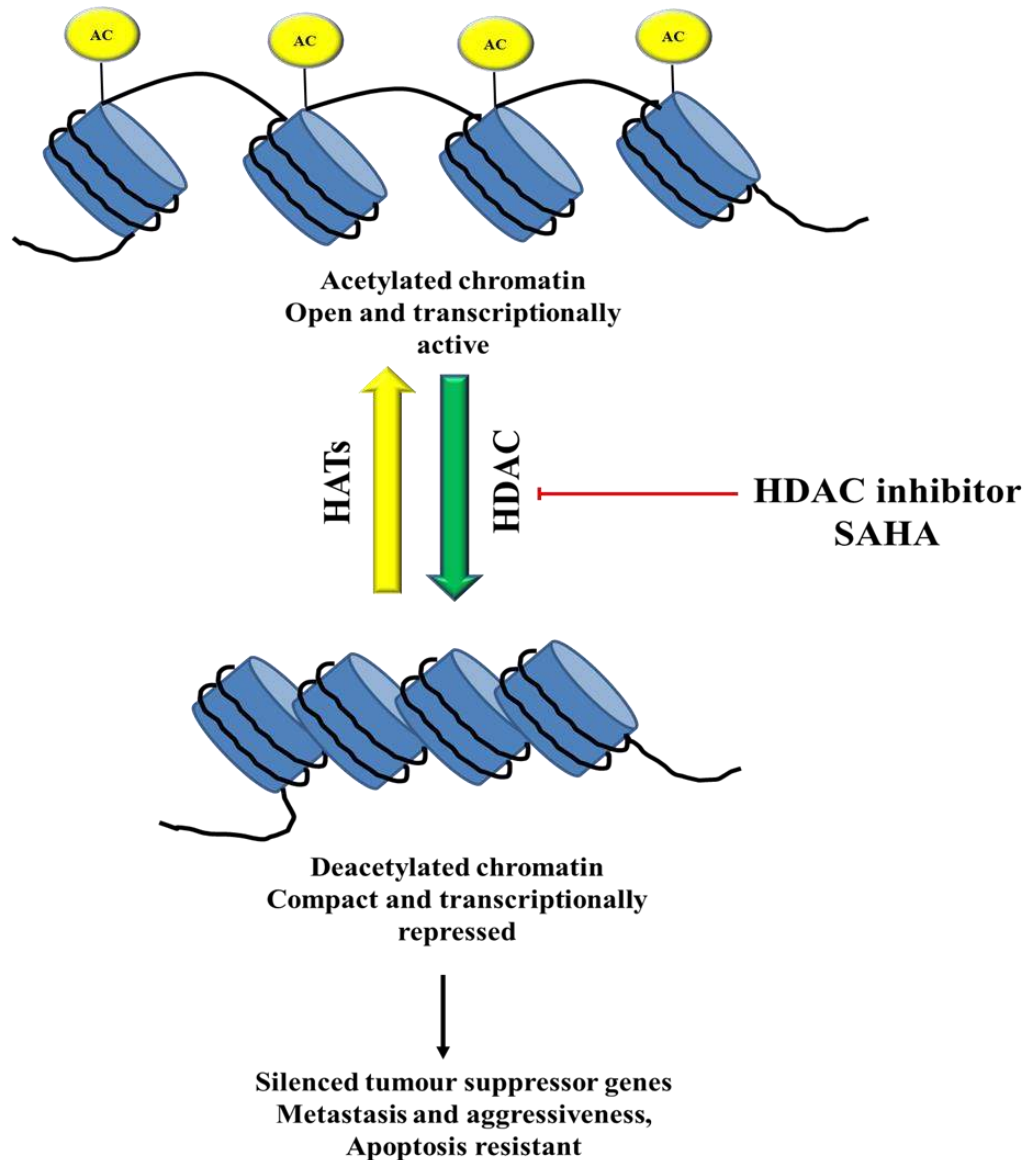
Figure 2.2: The role of HDAC^i SAHA in the regulation of gene expression. The chromatin acetylation is controlled by two main enzymes, histone acetyltransferases (HAT) and histone deacetylases (HDAC). The HAT catalyses the acetylation of core histones lead to open and transcriptionally active chromatin structure, whereas HDAC catalyses the removal of the acetyl group leading to closed and transcriptionally inactive chromatin form. Inhibition of HDAC by HDAC^i SAHA re-expressed the tumour suppression genes and activating apoptosis and promotes growth inhibition. Modified from Pons et al., 2009.

The mechanisms of action of HDAC[i] as an anti-myeloma agent in preclinical studies have not yet been fully understood. Inhibition of histone deacetylation mainly induces gene transcription and as a result, HDAC[i] trigger transcription. Therefore, HDAC[i] triggers the transcription of positive and negative regulators of proliferation and/or the survival of the cell and growth inhibition or cytotoxicity (Hideshima and Anderson., 2013).

In multiple myeloma, the non-selective HDAC inhibitors vorinostat or SAHA trigger p21[CIP/WAF1] up-regulation, and induce the expression of p53 protein and, pRb dephosphorylation and subsequently triggers apoptosis. It has been found that p21 [CIP/WAF1] up-regulation occurs before the induction of p53, therefore, the up-regulation of p21 [CIP/WAF1] by SAHA may be p53 independent (Mitsiades *et al*., 2003). Moreover, the regulation of the anti-apoptotic proteins Bcl-2 plays a key role in SAHA-mediated apoptosis in multiple myeloma cells via a caspase-independent pathway in addition to caspase-dependent cascade via cleaving of PARP (Mitsiades *et al*., 2003). Furthermore, SAHA activity suppresses the growth factors such as IL-6, IGF-1, blocks angiogenesis, inhibits the activity of proteasome and inhibits osteoclastogenesis (Mitsiades *et al.*, 2004).

SAHA augments the anti-MM effect of other therapeutic agents. Among these are dexamethasone, proteasome inhibitors and immunomodulatory therapy (Mitsiades *et al.*, 2004). In addition, SAHA enhances TRAIL-induced cytotoxicity due to the pro-apoptotic proteins up-regulation including Bak, Bim, Bax, PUMA and Noxa and anti-apoptotic proteins down-regulation such as Bcl-2 and Bcl-xL (Fandy *et al*., 2005).

2.1.2.3   *Histone Methyltransferase Inhibitors (HMTase[i])*

In addition to the histone acetylation, another epigenetic modification that is play an important role in the regulation gene expression and identified in oncogenesis is the

histone methylation status of histones. This post-transcriptional modification can target either lysine or arginine residues of histone tail (Nebbioso *et al*., 2012). The histone lysine methylation is catalyzed by two classes of enzymes: histone lysine methyltransferases (KMTs) and demethylases (KDMs) (Ding *et al*., 2013). Histone methylation has been normally associated with silencing of gene, however, some lysine methylation patterns can link to active genes (Figure 2.3). For example, methylation of histones residues H3K4, H3K36, and H3K79 is correlated with gene activation, while methylation on H3K9 or H3K27 linked to transcriptional suppression and methylation of H4, K20 is a known mark of gene silencing (Cho *et al*., 2011; Casciello *et al*., 2015). Moreover, histone lysine methylation controls the transcription according to the methylation status. For example, trimethylation of H3K9 has served as a transcriptional repressive mark. H3K9 monomethylation has been associated with active promoters (Cho *et al*., 2011; Casciello *et al*., 2015).

2.1.2.4 *The role of G9a as a Histone Methyltransferase in Controlling Gene Expression*

G9a, also known as a nuclear histone lysine methyltransferase (HMT), mainly catalyzes monomethylation and dimethylation of H3 lysine 9 in euchromatin. It is vital for early embryonic development and associated with transcriptional silencing of tumour suppressor genes (Figure 2.3) (Casciello *et al*., 2015; Ding *et al*., 2013; Nebbioso *et al*., 2012). G9a is comprised of a catalytic SET domain, ankyrin repeats which identify mono- and -dimethyl histone by SET domain and an automethylation site the N-terminal end (Casciello *et al*., 2015).

High G9a levels have been reported in several types of human cancers such as lung cancer cells (Chen *et al*., 2010), bladder carcinomas (Cho *et al*., 2011), ovarian cancer (Hua *et al*., 2014) and haematological malignancy (Lehnertz *et al*., 2014) and knockdown of G9a has been presented to suppress the growth of tumour cells (Chen *et*

al., 2010; Cho *et al*., 2011; Kondo *et al*., 2008). However, the underlying molecular basis of G9a role in sustaining tumour cell survival is not fully understood.

In addition, G9a has tumour growth and survival advantages through control the amino acid metabolism and transcriptional triggering of genes involved in a serine-glycine biosynthetic pathway (Ding *et al*., 2013). This finding suggesting the key role of G9a in the tumour development and progression and targeting this enzyme might represent a new approach for cancer therapy.

2.1.2.5   G9a Inhibitor BIX 01294

BIX 01294 or a diazepin-quinazolinamine derivative is a specific G9a inhibitor by suppression the H3K9Me2 level (Figure 2.3) (Kim *et al*., 2013). Moreover, BIX 01294 stimulates apoptosis in human neuroblastoma cells by increasing caspase-8 and -3 activity (Lu *et al*., 2013) as well as decrease the growth of bladder cancer cells (Cho *et al*., 2011). In addition, knockdown of G9a or treatment with BIX 01294 suppressed the growth of bladder, breast, lung and prostate tumour cells (Chen *et al.*, 2010; Ding *et al.*, 2013; Kubicek *et al*., 2007).

Figure 2.3: The role of HMTase[i] in the regulation of gene expression
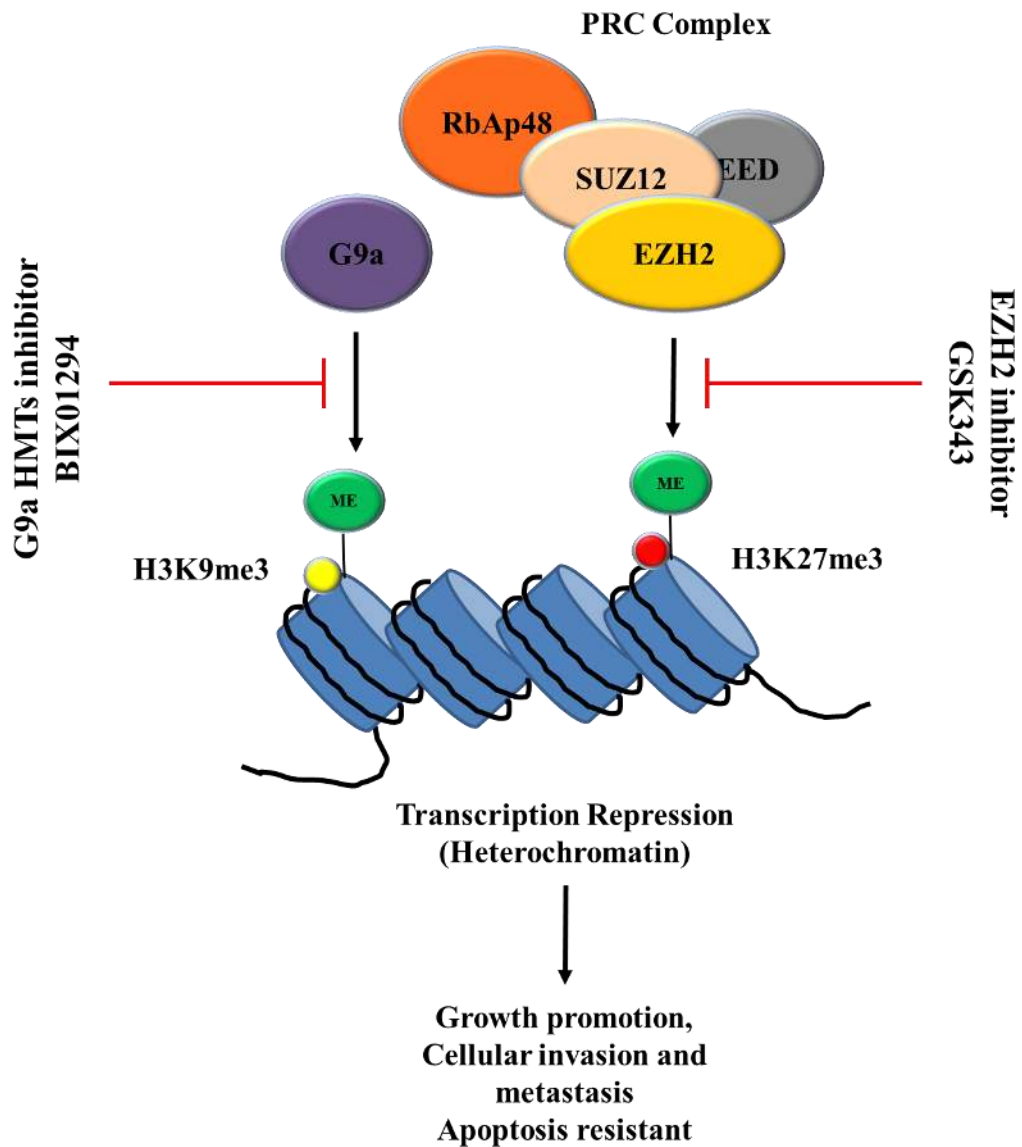
Figure 2.3: The role of HMTase[i] in the regulation of gene expression. G9a, a nuclear histone lysine methyltransferase (HMT), mainly catalyzes monomethylation and dimethylation of H3K9 and EZH2 catalyzes trimethylation of H3K27. Inhibition of G9a and EZH2 HMTase by BIX 01294 and GSK343 respectively associated with silences TSGs, inhibits proliferation and induces apoptosis. Modified from Yoo and Hennighausen., 2012.

2.1.2.6 EZH2 Inhibitor GSK343

Similar to G9a, Enhancer of Zeste Homologue 2 or EZH2 is a member of HMTase family which transcriptional silencing the expression of target genes (Figure 2.3). EZH2 is the catalytic subunit of the Polycomb Repressive Complex 2 (PRC2), which has been involved in cancer progression (Verma *et al*., 2012). EZH2 catalyzes trimethylation of lysine 27 (Lys 27) on histone H3 (H3K27) (Figure 2.3) (Popovic *et al*., 2014). Over-expression of EZH2 is found in many types of solid tumours such as breast cancer (Kleer *et al*., 2006), prostate cancer (Varambally *et al*., 2002) and gastric cancer (Matsukawa *et al*., 2006) as well as multiple myeloma (Croonquist and Van Ness., 2005; Kalushkova *et al*., 2010). High levels of EZH2 are correlated with cancer growth, metastasis, as well as the poor outcome (Yamaguchi1 and Hung., 2014). EZH2 inhibits apoptosis in a number of tumours, including bladder cancer (Wang *et al*., 2014), prostate cancer (Li *et al*., 2013), and leukemia (Zhou *et al*., 2011). Therefore, targeting EZH2 in cancer cells is an effective therapeutic approach (Zhang *et al*., 2014).

However, the exact mechanisms of apoptosis inhibition by EZH2 still poorly understood. It has been found that EZH2 mediate apoptosis resistance in prostate cancer by epigenetic silencing of two pro-apoptotic microRNAs (miRNA), miR-205 (target Bcl-2) and miR-31 target E2F transcription factor 6 (E2F6) encoding (Zhang *et al*., 2014). A number of small molecule EZH2 inhibitors have been identified and demonstrated potent anti-cancer activity (Van Aller *et al*., 2013; Garapaty-Rao *et al*., 2013). Recently, highly potent and selective EZH2 inhibitors, GSK126 and GSK343 (Figure 2.3) (Amatangelo *et al*., 2013; Verma *et al*., 2012) inhibited the proliferation of breast and prostate cancer cell lines (Verma *et al*., 2012) and hepatocellular carcinoma (Liu *et al*., 2016).

Inhibition of EZH2 by GSK343 and UNC1999 decreased myeloma cells viability and induced apoptotic cell death and UNC1999 up-regulated the expression of genes in

signaling pathways related to apoptosis, Wnt, MAPK, ID and cellular differentiation such as DNA binding 2 (ID2) (Agarwal *et al*., 2016). Moreover, down-regulation of the expression of a number of oncogenes involved in myeloma most notably CD69, transcription factor jun-B (JUNB) and X-box binding protein 1 (XBP1) (Agarwal *et al*., 2016) which have been shown to stimulate cell growth, survival and therapy resistance in MM (Fan *et al*., 2014). Furthermore, GSK343 inhibits growth, induced cell cycle arrest as well as induced cell death of osteosarcoma by targeting on EZH2-c-Myc and fuse binding protein 1 (FBP1)-c-Myc signal pathways (Xiong *et al*., 2016). Co-treatment with the Euchromatic Histone Lysine Methyltransferase 2 (EHMT2) inhibitor UNC0638 significantly inhibited the growth of breast cancer cells (Brown *et al*., 2014), suggesting that EZH2 inhibitors GSK343 could be a potential therapeutic option for cancer (Xiong *et al*., 2016).

Figure 2.4: The role of epigenetic modifiers agents HDAC[i] and HMTase[i] in the regulation gene expression
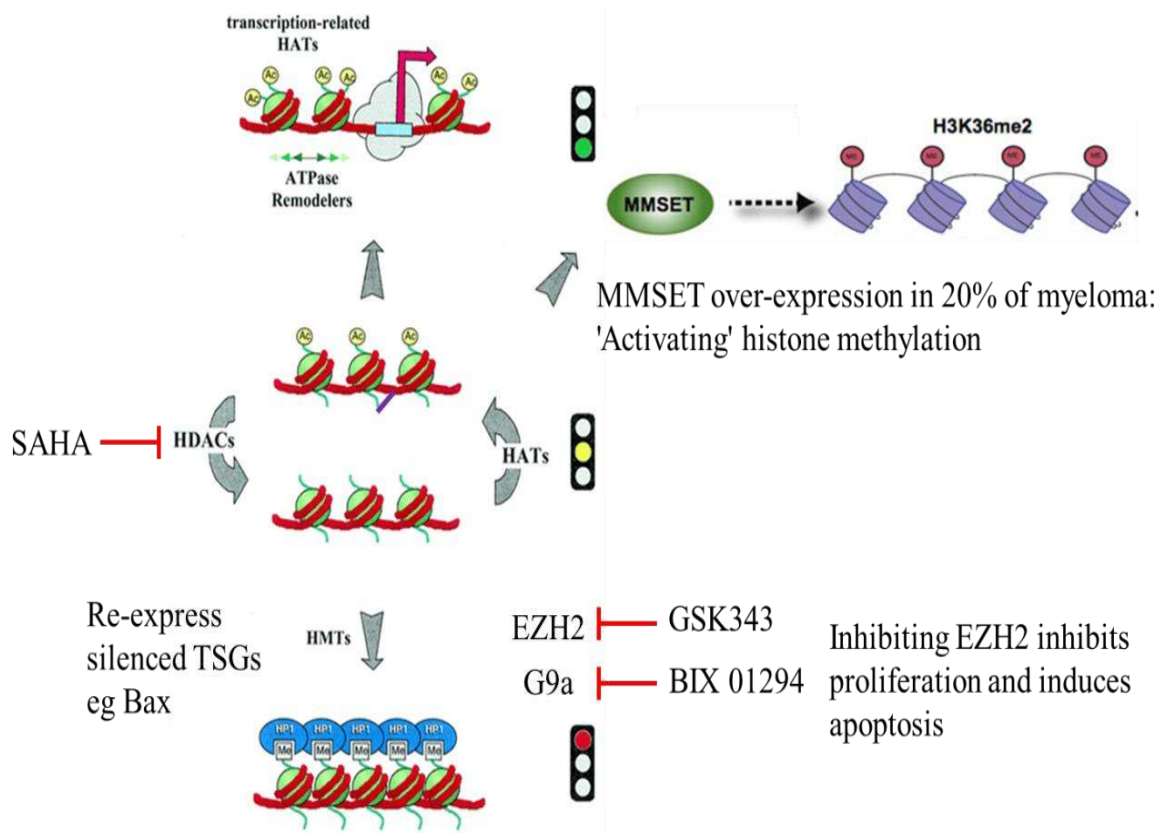
Figure 2.4: Summary of the role of epigenetic modifiers agents HDAC[i] and HMTase[i] in the regulation gene expression and inhibits proliferation inhibition and induces apoptosis. Modified from Asangani et al., 2013, and Pons et al., 2009, and Yoo and Hennighausen., 2012.

2.1.3   Hypothesis

The current investigation has focused on the hypothesis that Nuclear export inhibitor (NEI), epigenetic modifiers Histone Deacetylase (HDAC) inhibitor and inhibitors of the histone methyltransferases G9a and EZH2 enhance TRAIL sensitivity in multiple myeloma cells.

2.1.4   Aims

The aim of this study to assess the efficacy of TRAIL to induce apoptotic cell death either alone or in combination with the TRAIL sensitizers in order to overcome intrinsic resistance and render tumour cells more sensitive to TRAIL.

2.2   Materials and Methods

2.2.1   Cell Lines

Five human Multiple Myeloma cell lines (NCI-H 929, RPMI 8226, OPM2, JJN3, and U266) and one primary cell culture generated from a case of plasma cell leukaemia (ADC-1); together with non-tumour $CD34^+$ and $CD133^+$ (Stem Cell Technology) positive haematopoietic progenitor stem cells (HSC) and a primary Human Renal Epithelial Cells (HREC) (Innoprot) were used. All the MM cell lines were tested regularly for Mycoplasma infections throughout the study using MycoAlert™ mycoplasma detection kit and were all tested negative (Lonza).

2.2.1.1   *Multiple Myeloma Cell Lines*

NCI-H 929, source − obtained from the pleural fluid of a 67-year-old caucasian female with an IgA-producing plasmacytoma (Euorpean Collection of Cell Cultures (ECACC), Salisbury, UK; cat no 95050415)

RPMI 8226, source − obtained from the peripheral blood of a 61year old man with multiple myeloma at diagnosis (ECACC, Salisbury, UK; cat no 87012702)

OPM2, source − obtained from the peripheral blood of a 56-year-old woman with multiple myeloma in terminal leukaemic phase (Deutsche Sammlung von Mikroorganismen und Zellkulturen GmbH (DSMZ), Braunschweig, Germany; DSMZ no ACC 50)

JJN3, source − plasma cell leukaemia (kind gift from Professor I Franklin, University of Glasgow, UK)

U266 cells (derived from the peripheral blood of a 53-year-old man with MM) were purchased from LGC Standards (UK)

ADC-1 − *ex vivo* cell line taken from the peripheral blood of a patient with plasma cell leukaemia presenting to the Dept of Haematology, Sheffield Teaching Hospitals.Patient

cells were acquired with appropriate ethical permission (REC reference: 05/Q2305/96). All participants provided written consent. Original consent forms are stored in a secure location and patient demographics and disease feature entered into an encrypted database governed by the Research and Development Service Sheffield Teaching Hospitals, NHS Foundation Trust UK. This consent procedure was approved by the South Sheffield Research Ethics Committee in August 2005 and subsequently ratified by the NHS Health Research Authority, National Research Ethics Committee Yorkshire and the Humber - Sheffield in November 2012.

2.2.1.2 *Non-tumour Cell Lines*

CD34$^+$ and CD133$^+$ cells are haematopoietic stem cells and can be isolated from human cord blood. These stem cells are capable of self–renewal and high proliferative capacity into multiple haematopoietic lineages.

Human Renal Epithelial Cells (HREC) are isolated from human kidney. Renal Epithelial cells play a key role in renal function. Similar to most other epithelial cells, renal epithelial cells show a polarized morphology which is vital for their function. They are also a major site of injury in a variety of congenital, metabolic, and inflammatory diseases.

2.2.2 Cell Culture Medium

Multiple myeloma cell lines and haematopoietic progenitor stem cells (CD133$^+$ and CD34$^+$) were cultured in RPMI-1640 media (Invitrogen) supplement with L-Glutamine supplemented with 10% fetal calf serum, 1% penicillin/streptomycin and 1% non-essential amino acid. The non-tumour primary human renal cells HREC were cultured in special Epithelial Cell Medium (EpiCM) supplemented with 10 ml of fetal Bovine Serum (FBS), 5 ml of Epithelial Cell Growth, Supplement (EpiCGS), and 5 ml of penicillin/streptomycin.

2.2.3 Cell Sub-Culture

For suspension cells: multiple myeloma and HSC (CD133^{+} and CD34^{+}) cells were seeded into T75 cm^2 flask (Invitrogen) containing complete RPMI-1640 media. Cultures were maintained at 37ºC with 5% CO2 in humidified incubator. Cell typically split at a 1:5 split ratio twice a week.

For the adherent cells (HREC), cells were maintained up to 80% confluence before passaging: culture media was removed and 10 ml of Phosphate Buffered Saline (PBS; Gibco) was used to wash the cells and 3 ml of Trypsin (0.05%) - EDTA (0.02%) (Gibco) was added and incubated at 37ºC until detachment of cells was achieved. Then, cells were incubated in 10 ml of complete special Epithelial Cell Medium (EpiCM). The resulting cell suspension was seeded at a 1:5 split ratio twice a week. The cells then incubated under standard cell culture conditions at 37ºC with 5% CO_2 atmosphere.

2.2.4 Seeding Cells into 96 Well Plate

Suspension cells were centrifugation at 400 g for 5 minutes, then the cell re-suspend in complete media and the cells counted by the Countless system (Invitrogen) using trypan blue staining (Invitrogen) and the number of cells/ml was determined. After that, 200 µl of the cells at a density of 350,000 cells/ml is passed into 96-well plate and settled in the incubator at 37 ºC for 2-3 h before drugs were added.

Adherent cells were centrifugation after trypsinisation and the cells counted as above (Section 2.2.4) 200 µl of the cells at a density of 250,000 cells/ml is passed into 96-well plate and incubated at 37 ºC for 24 before drugs were added.

2.2.5 Treatment of MM and Non-Tumour Cells with Cytotoxic Agents

TRAIL (Pepro Tech EC Ltd) was dissolved in media (10 µg/ml), Leptomycin B (Nuclear export Inhibitor) (Enzo Life Science) was dissolved in absolute ethanol (10 µM), SAHA (Sigma) was dissolved in DMSO (10 mM), BIX01924 (Sigma) was

dissolved in media (10 mM); and finally GSK343 (Sigma) was dissolved in DMSO (10 mM). A stock solution of 10 µg/ml of TRAIL, 10 nM of LMB, 10 mM of SAHA, BIX 01294 and GSK343 were prepared to generate desired treatment concentrations and aliquoted into 10 µl/aliquot and stored at -20 ºC.

In order to induce apoptosis, TRAIL at 50 ng/ml, 25 ng/ml, 10 ng/ml and 2 ng/ml were added to the cells in a 96-well plate in triplicate, three wells for each concentration. The cells were treated with escalating the concentrations of LMB (10 nM) at a dose from 0-5 nM, SAHA at 0-10 µM, BIX 01294 at 0-20 µM and GSK343 at 0-20 µM. In addition, these drugs used either alone or in combination with TRAIL in order to determine the synergistic response. Control cells were dilution in 1/1000 DMSO or Ethanol, so control and treated cells treated with the same concentration of vehicle control. Table 2.1 illustrates the drug dilutions used in this work. After stimulation, the cells were incubated for 24 hours in the humidified incubator.

Drugs	Investigated concentration	1ml drug concentration prepared (enough for 5x wells of 96 well plates)
TRAIL (10 mg/ml)	50ng/ml	50 µl of 1/10 diluted stock (10 µg/ml)
	25 ng/ml	25 µl of 1/10 diluted stock (10 µg/ml)
	10 ng/ml	10 µl of 1/10 diluted stock (10 µg/ml)
	2 ng/ml	20 µl of 1/100 (a further 1/10 dilution)
LMB (10µM)	5nM	5 µl of 1/10-diluted stock (1µM)
	2nM	20 µl of 1/100-diluted stock (0.1µM)
	1nM	10 µl of 1/100-diluted stock (0.1µM)
	0.5nM	5 µl of 1/100-diluted stock (0.1µM)
	0.25nM	2.5 µl of 1/100-diluted stock (0.1µM)
SAHA (10mM)	10µl	10 µl of 1/10-diluted stock (1mM)
	5µl	5 µl of 1/10-diluted stock
	1µl	1 µl of 1/100-diluted stock
BIX-01294 (10mM)	20µl	20 µl of 1/10-diluted stock (1uM)
	15µl	1.5 µl stock/well or 15µl of 1/10-diluted stock (1µM)
	10µl	1 µl stock/well or 10µl of 1/10-diluted stock (1µM)
	5µl	5 µl of 1/10-diluted stock (1µM)
	1µl	10 µl of 1/100-diluted stock (0.1µM)
	0.5µl	5 µl of 1/100-diluted stock (0.1µM)
GSK343 (10mM)	20µl	20 µl of 1/10-diluted stock (1µM)
	15µl	1.5 µl stock/well or 15µl of 1/10-diluted stock (1µM)
	10µl	1 µl stock/well or 10µl of 1/10-diluted stock (1µM)
	5µl	5 µl of 1/10-diluted stock (1µM)
	1µl	10 µl of 1/100-diluted stock (0.1µM)

Table 2.1: Illustrated the drugs dilution used in this work

Technique	Cell line	Investigated concentration
Hoechst 33342 PI stain	All six MM cell lines: OPM2, NCI-H 929, RPMI 8226, U266, JJN3 and ADC-1 Non-tumour cell lines: HSC cells (CD133$^+$ and CD34$^+$) and PHRC	LMB: 0.5, 1, 2, 5 nM SAHA: 1,5, 10 µM BIX 01294: 1, 5, 10, 15, 20 µM GSK343: 1, 5, 10, 15, 20 µM Either alone and in combination with lower significant dose of TRAIL (LSD)
Caspase-3 substrate	MM cell lines: NCI-H 929, RPMI 8226, U266, and ADC-1	Combination treatment doses which synergistically enhanced apoptosis as determined by Hoechst 33342/PI staining
CellTiter-Glo	All six MM cell lines: OPM2, NCI-H 929, RPMI 8226, U266, JJN3 and ADC-1 Non-tumour cell lines: HSC cells (CD34$^+$) and PHRC	LMB: 0.5, 1, 2, 5 nM SAHA: 1,5, 10 µM BIX 01294: 1, 5, 10, 15, 20 µM GSK343: 1, 5, 10, 15, 20 µM Either alone and in combination with LSD of TRAIL
Cell cycle analysis	MM cell lines: NCI-H 929, RPMI 8226, U266, JJN3 and ADC-1	Combination treatment doses which synergistically enhanced apoptosis as determined by Hoechst 33342/PI staining

Table 2.2: The cell lines and the investigated drug concentration used for different techniques

2.2.5.1 MycoAlert™ Mycoplasma Detection

One of the most contaminants of cells in continuous cultures is Mycoplasma infections, which can lead to serious alteration in cell proliferation, morphology, metabolism and cellular responses including gene expression. (Uphoff and Drexler., 2005; Volokhov *et al.,* 2011; Young *et al.*, 2010). Moreover, their presence in cell culture go undetected for months thus frequent testing is essential (Uphoff and Drexler., 2005; Volokhov *et al.,* 2010; Young *et al.*, 2010). The MycoAlert™ Mycoplasma Detection assay (Lonza) was used and cultures tested negative throughout the project.

2.2.6 Assessment of Apoptosis

2.2.6.1 Hoechst 33342 and Propidium Iodide (PI) of Nuclear Morphology by Fluorescence Microscopy

Following treatment with drugs, induction of apoptosis was assessed using Hoechst 33342 and Propidium Iodide (PI) staining (Sigma-Aldrich, Dorset, England). Cells were stained with 10 µg/ml Hoechst 33342 and 10µg/ml PI for 30 min at 37ºC and examined using fluorescence microscope (Olympus, IX81, UK) and images captured using Cell-F software. Apoptotic cells were counted manually and percent apoptosis calculated based on duplicate representative fields of view each containing at least 100 cells for three independent experiments.

2.2.6.2 NucView Caspase 3 Activity Assay by Flow Cytometry

NucView caspase 3 activities assay which allows assessing caspase-3 activity within intact cells in the real-time assay without inhibiting the process of apoptosis. The caspase-3 substrate is composed of a fluorogenic DNA dye and a DEVD moiety substrate specific for caspase-3. In apoptosis, the substrate (non-fluorescent) rapidly crosses the membranes of the cell to the cytoplasm, where it is cleaved to form a high-affinity DNA dye by caspase-3 that stains the nucleus with bright green. Thus, the

NucView™ 488 caspase-3 substrate is bi-functional, allowing detection of activity of intracellular caspase-3 as well as visualization of nuclear morphology changes during apoptosis (Cen *et al*., 2008; Skommer *et al*., 2010; Smith *et al*., 2012).

To confirm apoptosis at doses that exhibited synergistic induction of apoptosis with Hoechst 33342/Propidium Iodide staining, NucView Caspase-3 activity assay (Biotium) was used. Selected doses of LMB, SAHA, BIX 01294 and GSK343 in the presence or absence of TRAIL were added as above (Table 2.2). As a negative control, 1µL of the irreversible Caspase-3 Inhibitor Z-DEVD-FMK (R&D systems Cat # FMK004) was added to inhibitor wells (~100µM final concentration). Following treatment 200µl of each cell suspension was transferred to a flow cytometry tube and 2.5µL of NucView™ 488 Caspase-3 substrate (0.2 mM) (Cambridge Bioscience, Cambridge, UK) was added to the sample (including inhibitor sample) except 'unstained control' and incubates cells at room temperature for 20 minutes. Finally, the samples were analyzed on the flow cytometer using a Beckman Coulter Gallios flow cytometer. Ten thousand events were acquired per sample.

2.2.7 CellTiter-Glo® Luminescent Cell Viability Assay

For ATP level measurement to quantify viable cells, MM Cells were plated at 350,000 cells/ml in a 96-well plate and treated with cytotoxic agents for 24h. Following incubation, 50 µl of CellTiter-Glo® Reagent were added to each well and incubated for 10 minutes at room temperature luminescence was measured using Wallac Victor 2 1420 luminometer. All treatments were performed in triplicate, in three independent experiments.

2.2.8 Flow Cytometry for Analysis of Cell Cycle using Propidium Iodide (PI)

Analysis of cell cycle was performed by seeding the cell at 0.5×10^6 cells per well and treated with TRAIL at the lowest dose that induced a statistically significant apoptotic

response as a single treatment, combined with the anti-tumour agents (LMB, SAHA, BIX 01294 and GSK343) and incubated at 37°C for 24 h. Following treatment, cells were harvested and centrifuged for 5 minutes at 400g prior to wash twice with 100 µl cold phosphate buffered saline. Subsequently, cells were fixed with 80% ethanol *(v/v)* and stored at -20°C overnight. Then, cells were centrifuged and washed twice prior to the addition of 300 µl of 50 µg/mL PI (Sigma) and 50 µl of 0.1 unit/mL DNase-free RNase A (Sigma) and stored overnight at 4ºC. Cellular DNA content was analysed using the flow cytometer with BD FACSCalibur™ (BD Biosciences) instrument. Ten thousand events were acquired per sample and data analysed with FlowJo software. Data quantified using the Waston (pragmatic) equation that assessed the proportion of diploid cells in G_0/G_1, S and G_2/M phases of cell cycles in addition to the the quality control parameter such as Co-efficient of Variation (CV) and the debrise associated with each sample.

2.2.9   Generation of TRAIL-resistant Multiple Myeloma Cells *in vitro*

In order to generate TRAIL-insensitive cells NCI-H 929, RPMI 8226, and OPM2 were seeded into T25cm flasks and grown in escalating doses of TRAIL (2 ng/ml-50 ng/ml) for 1 year. Cell viability in response to TRAIL was checked every week and the dose of TRAIL is increased depending on cell viability. Also, TRAIL-resistant cells were generated by acute exposure of the TRAIL-sensitive cells with a high/lethal dose of TRAIL (50ng/ml) followed by the selection of TRAIL-resistant cells. The cytotoxic activity of TRAIL was determined on NCI-H 929, RPMI 8226, and OPM2 and compared to cell isolated from parental TRAIL-sensitive cells. Live cells were counted using the Cell Countless system (Invitrogen) and cell viability was determined using trypan blue staining. Cell death response to anti-tumour agents for the cell exposure to the acute toxic dose was assessed and apoptosis was assessed using Hoechst 33342/PI staining of nuclear morphology as described previously (Section 2.2.6.1).

2.2.10 Statistical Analysis

Data was expressed as the median with range. Shapiro-Wilke test using Stats Direct software (Stats Direct Ltd, England) was used for analysis whether data followed a normal distribution. Data which did not follow a normal distribution, Kruskal–Wallis and Connover-Inman post hoc was using to investigate significant differences. $p < 0.05$ was considered statistically significant. The TRAIL sensitizer-mediated potentiation of TRAIL-induced apoptosis was determined by showing that apoptosis was induced by a combined treatment which was significantly greater than additive (i.e., apoptosis resulting from co-treatment with TRAIL and TRAIL sensitizer was significantly greater than the sum of apoptosis induced by TRAIL alone along with apoptosis induced by TRAIL sensitizer alone).

2.2.10.1 Analysis of Effect of Anti-Tumour Agents in combination with TRAIL on Cell Cycle

Cell cycle progression was analyzed using FlowJo software and the statistical significant was determined by comparison the percentage of treated cells in each phase to the vehicle control in addition to the comparison of combined treatment to both the vehicle control and individual treatment. This effect was classified as:

Interactive Effect when the combination treatment of anti-tumours agents with TRAIL induces a highly significant cellular accumulation in cell cycle phase when compared to both the vehicle control and individual treatment ($p < 0.05$).

Antagonistic Effect when the combination therapy showed no significant difference compared to control, but there was significantly decreased of cell cellular accumulation compared to phases arrested by individual agents alone ($p < 0.05$).

2.3 Results

2.3.1 Effect of TRAIL Treatments on Apoptosis using Hoechst 33342 and PI Nuclear Staining on Multiple Myeloma Cell Lines

Multiple myeloma cell lines (NCI H 929, RPMI 8226, OPM2, JJN3, U266 and ADC-1) were treated with TRAIL (0–50 ng/ml) for 24 h. OPM2 MM cell was sensitive to TRAIL followed by RPMI 8226, NCI-H 929, and ADC-1 cell lines showed also significant apoptotic responses. In contrast, U266 and JJN3 were less sensitive to TRAIL but showed significant induction of apoptosis at 50 ng/ml ($p<0.05$) (Figure 2.5). Furthermore, the majority of MM cell lines showed greater sensitivity than the non-tumour cell; HSC (CD133$^+$) and the normal human renal cell line (HREC) there was no significant induction of apoptosis. However, TRAIL induces apoptosis in the HSC CD34$^+$.

Figure 2.5*: Effect of TRAIL treatment on apoptosis of multiple myeloma and non-tumour cells*
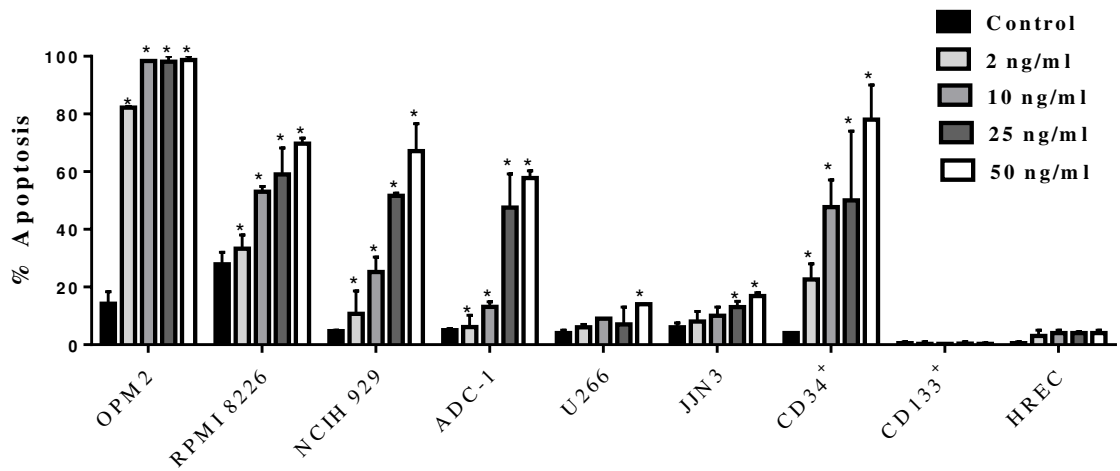
Figure 2.5: Effect of TRAIL treatment on apoptosis of multiple myeloma and non-tumour cells. Cells were treated with 0-50 ng/ml TRAIL for 24 h. The treatment with TRAIL potently induces apoptosis of MM cells in a dose-dependent manner. U266, JJN3, non-tumour cells CD133+ and HREC were less sensitive to TRAIL treatment compared to other MM cell lines. The columns represent the mean of 3 independent experiments. Data are expressed as the median with range. The statistical significance was determined by comparison treatment with the control, statistical significance was set at p<0.05=* and determined by Kruskal–Wallis test.

2.3.2 Effect of TRAIL Sensitizers in Combination with TRAIL on Apoptosis in Multiple Myeloma Cell Lines

2.3.2.1 *Effect of Leptomycin B (NEI) in Combination with TRAIL on Apoptosis in Multiple Myeloma*

Multiple Myeloma cells were treated with TRAIL at the lowest dose that induced significant apoptosis as a single treatment, and combined with LMB. LMB was found significantly to induce apoptosis in a dose-dependent manner in a panel of myeloma cell lines, OPM2, NCI- H 929, RPMI 8226, JJN3, U266 and ADC-1, although with varying potency following treatment with 0-5 nM LMB for 24 h ($p < 0.0001$) (Figure 2.6 a) and the combination with TRAIL synergistically enhanced TRAIL responses in all cell lines. The co-treatment of 2ng/ml TRAIL in ADC-1 cells in this study with sub-lethal doses of LMB (0-5 nM) significantly potentiated apoptosis to levels greater than those induced by either the agent alone or by their additive effect (Figure 2.6 a). In ADC-1 cells, an apoptotic response of 84.3±4.1% ($p < 0.0001$) was measured following treatment with combined dose of 5 nM LMB and 2 ng/ml TRAIL for 24 h. Whereas, the apoptotic response for 5 nM LMB alone and 10 ng/ml TRAIL was 46.4±3.5% and 22.6 ±4.5% respectively (Figure 2.6 a, b). The synergistic effect of TRAIL and LMB varied on other MM cells line depending on the drug concentration. However, no synergistic response was observed following the treatment with LMB combined with a high dose of TRAIL in non-tumour cell line HSC CD133^{+} and human renal cell line HREC. On the other hand, CD34^{+} stem cells significantly responded to LMB either alone or in combination with TRAIL (Figure 2.6). An example of morphological assessment of apoptosis using Hoechst 33342/PI nuclear staining in ADC-1 cells after treatment with different concentration for LMB either alone or in combination with TRAIL is shown in Figure 2.6 b.

Figure 2.6: Effect of apoptosis on the multiple myeloma cell lines and non-tumour cells after the treatment with LMB +/-TRAIL for 24 h

a)

b)
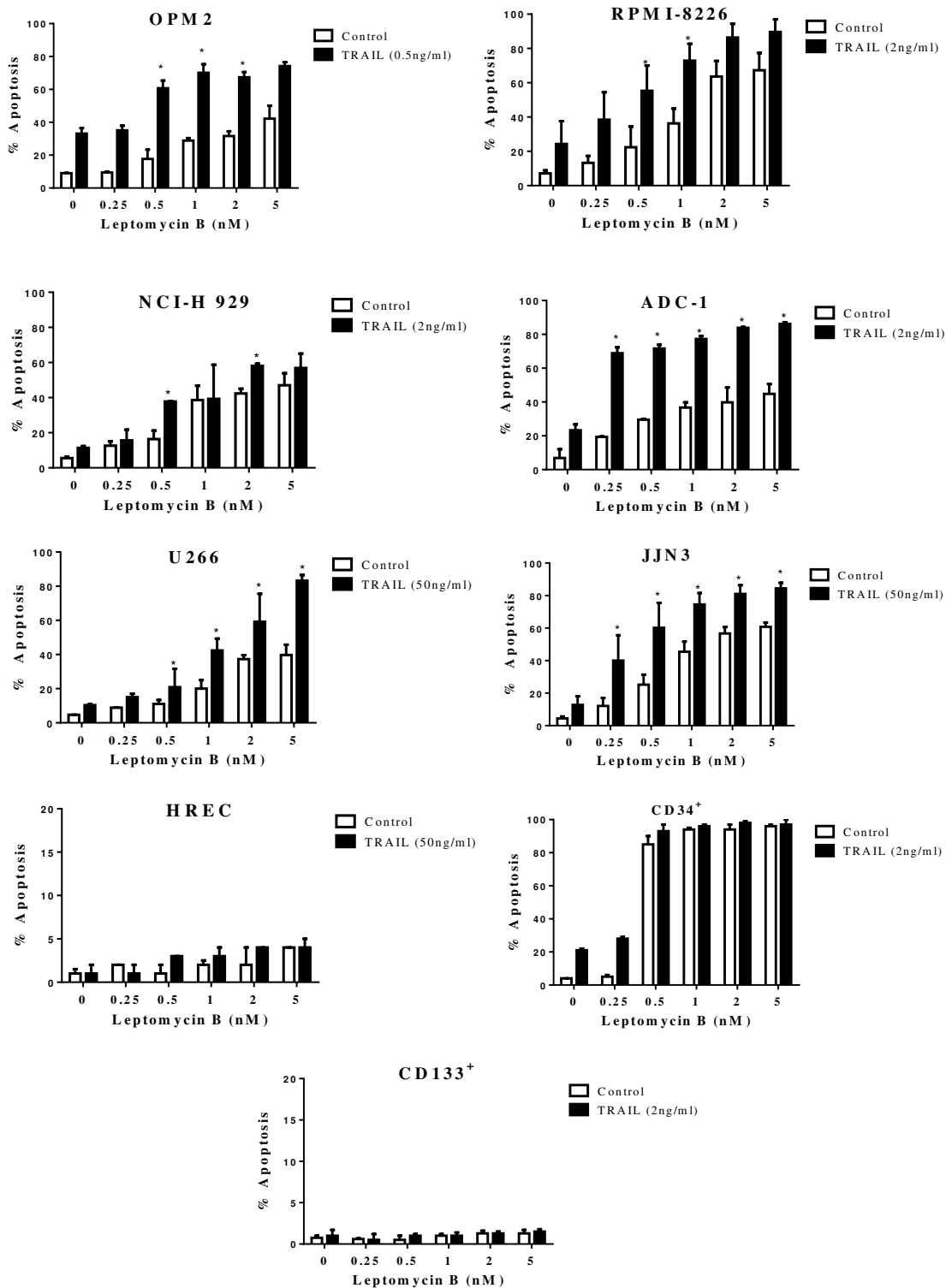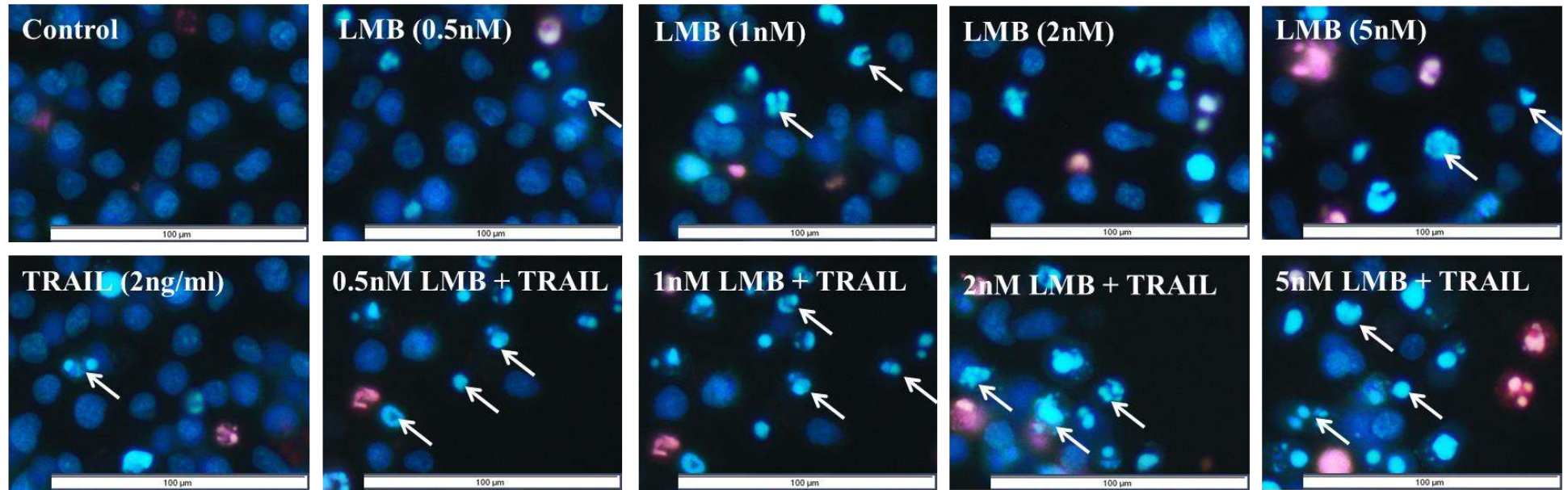
Figure 2.6: Effect of apoptosis on the multiple myeloma cell lines and non-tumour cells after the treatment with LMB +/-TRAIL for 24 h. a*) The percentage of apoptotic Multiple Myeloma cells treatment with LMB for 24h was increased in a concentration-dependent manner. The synergistic response was defined as a comparison of combination treatment group with the sum of the effects of TRAIL alone + LMB alone and significance determined by using by the Kruskal–Wallis test (p<0.05). (*) showing that apoptosis was induced by a combined treatment which was significantly greater than additive. **b)** Morphological assessment of apoptosis using Hoechst 33342/PI nuclear staining, after treatment shows LMB synergistically enhances TRAIL apoptosis in ADC-1 cell line. Apoptotic cells were identified by condensation and or fragmentation of the nucleus and intense staining while live cells were clear-edged, round, regular and uniformly stained nuclei. The red cells are permeabilised (necrotic or late apoptotic).*

2.3.2.2 *Effect of SAHA (HDAC[i]) in Combination with TRAIL on Apoptosis in Multiple Myeloma Cell Lines*

Multiple myeloma cells were treated with TRAIL at the lowest dose that induced significant apoptosis as a single treatment, and combined with SAHA. Hoechst 33342 and PI staining of nuclear morphology indicate that SAHA induces apoptotic activities in MM cell lines (Figure 2.8). SAHA induced apoptosis of myeloma cells in a dose-dependent manner in all multiple myeloma cell lines athough effect sizes were smallest in NCI-H 929, JJN3 and OPM2 (Figure 2.7). SAHA combined with TRAIL synergistically inducing apoptosis in all myeloma cell lines ($p < 0.001$, Kruskal–Wallis) except OPM2 (Figure 2.7). There was no significant induction of apoptosis with TRAIL in non-tumour HSC CD133^{+}and HREC. However, SAHA induced apoptosis in the HSC CD34^{+} with a synergistic response with TRAIL. An example of morphological assessment of apoptosis using Hoechst 33342/PI nuclear staining in U266 cells after treatment with different concentration for SAHA either alone or in combination with TRAIL is shown in Figure 2.7 b.

Figure 2.7: Effect of apoptosis on the multiple myeloma cell lines and non-tumour cells after the treatment with SAHA +/-TRAIL for 24 h

a)

b)
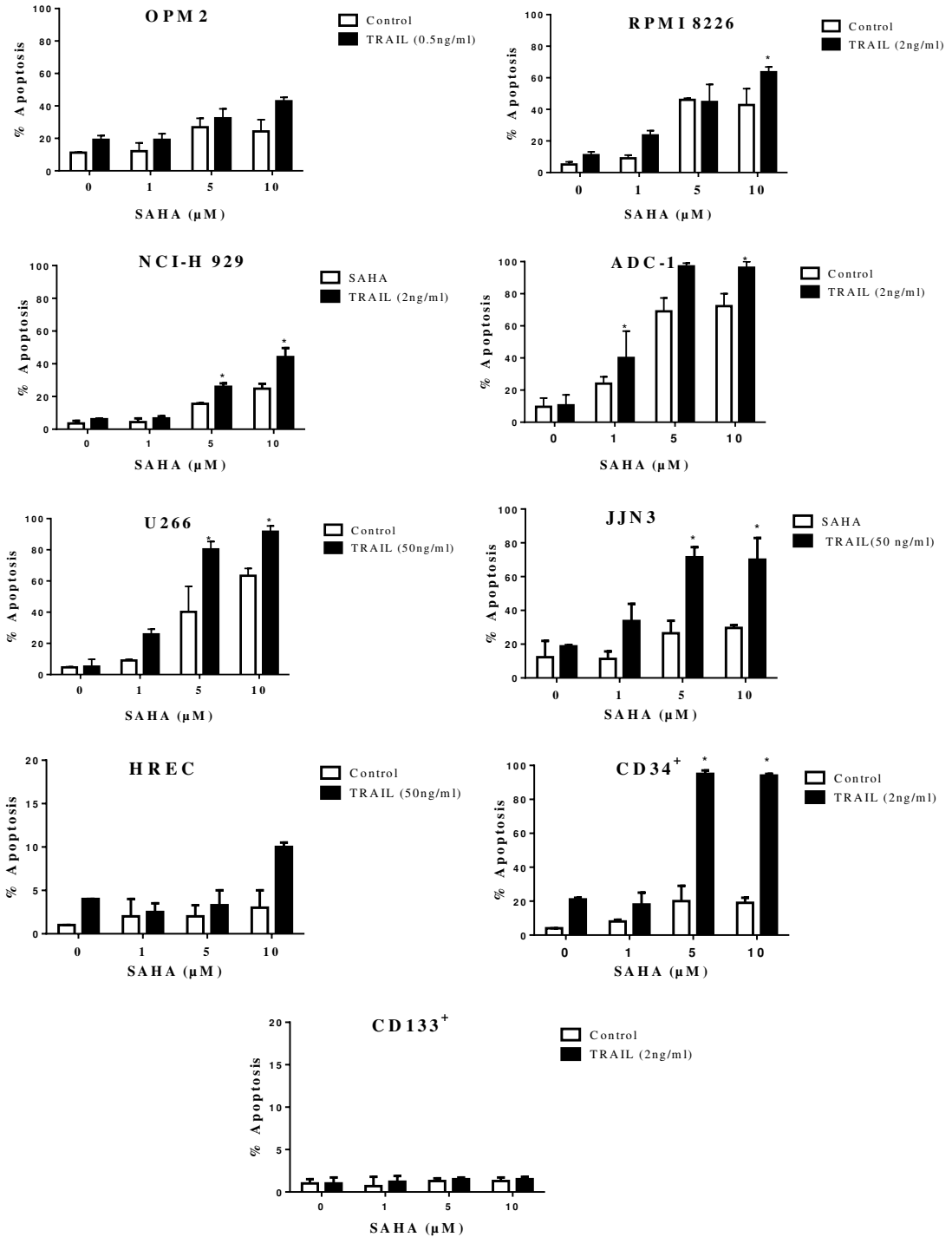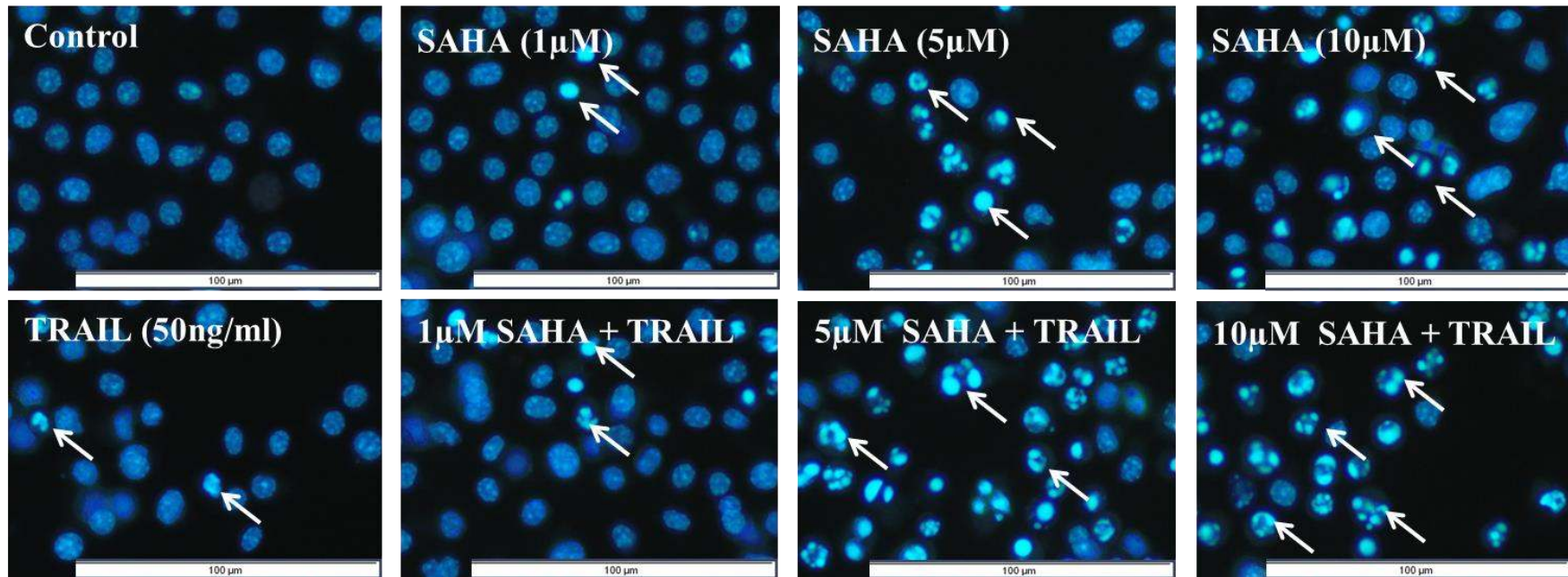
***Figure 2.8: Effect of apoptosis on the multiple myeloma cell lines and non-tumour cells after the treatment with SAHA +/-TRAIL for 24 h. a)** The percentage of apoptotic multiple myeloma cells treatment with SAHA for 24h was increased in a concentration-dependent manner (p<0.05, Kruskal–Wallis). The synergistic response was defined as a comparison of combination treatment group with the sum of the effects of TRAIL alone + SAHA alone and significance determined by using by the Kruskal–Wallis test (*=p<0.05). **b)** Morphological assessment of apoptosis using Hoechst 33342/PI nuclear staining, after treatment shows SAHA synergistically enhances TRAIL apoptosis in U266 cell line. Apoptotic cells were identified by condensation and or fragmentation of the nucleus and intense staining while live cells were clear-edged, round, regular and uniformly stained nuclei. The white arrow indicated the apoptotic cells. The red cells are permeabilised (necrotic or late apoptotic).*

2.3.2.3 Effect of the G9a HMTase[i] BIX 01294 Treatment in Combination with TRAIL on Apoptosis in Multiple Myeloma Cell Lines

MM cells were treated with BIX 01294 alone and in combination with TRAIL at the lowest dose that induced significant apoptosis as a single treatment to investigate their effect on induction of apoptosis following 24 hours (Figure 2.8 a). The data are illustrated in Figure 2.8 which demonstrates that MMSET positive cells (NCI-H 929, OPM2 and ADC-1) uniquely sensitive to BIX 01294 alone ($p < 0.001$). However, BIX 01294 synergistically significant enhanced TRAIL responses in MMSET-negative cell lines (RPMI 8226, U266 and JJN3) ($p < 0.001$) (Figure 2.8). In addition, there was no significant induction of apoptosis with TRAIL in non-tumour HSC CD133^{+} and renal cell line HREC and no synergistic response was seen when BIX 01294 was combined with a high dose of TRAIL for 24 h. However, BIX 01294 induced apoptosis in the haematopoietic stem cell CD34^{+} with synergistic response with TRAIL. An example of morphological assessment of apoptosis using Hoechst 33342/PI nuclear staining in U266 cells after treatment with different concentration for BIX 01294 either alone or in combination with TRAIL is shown in Figure 2.8 b.

Figure 2.8: Effect of apoptosis on the multiple myeloma cell lines and non-tumour cells after the treatment with BIX 01294 +/-TRAIL for 24 h

a)

b)
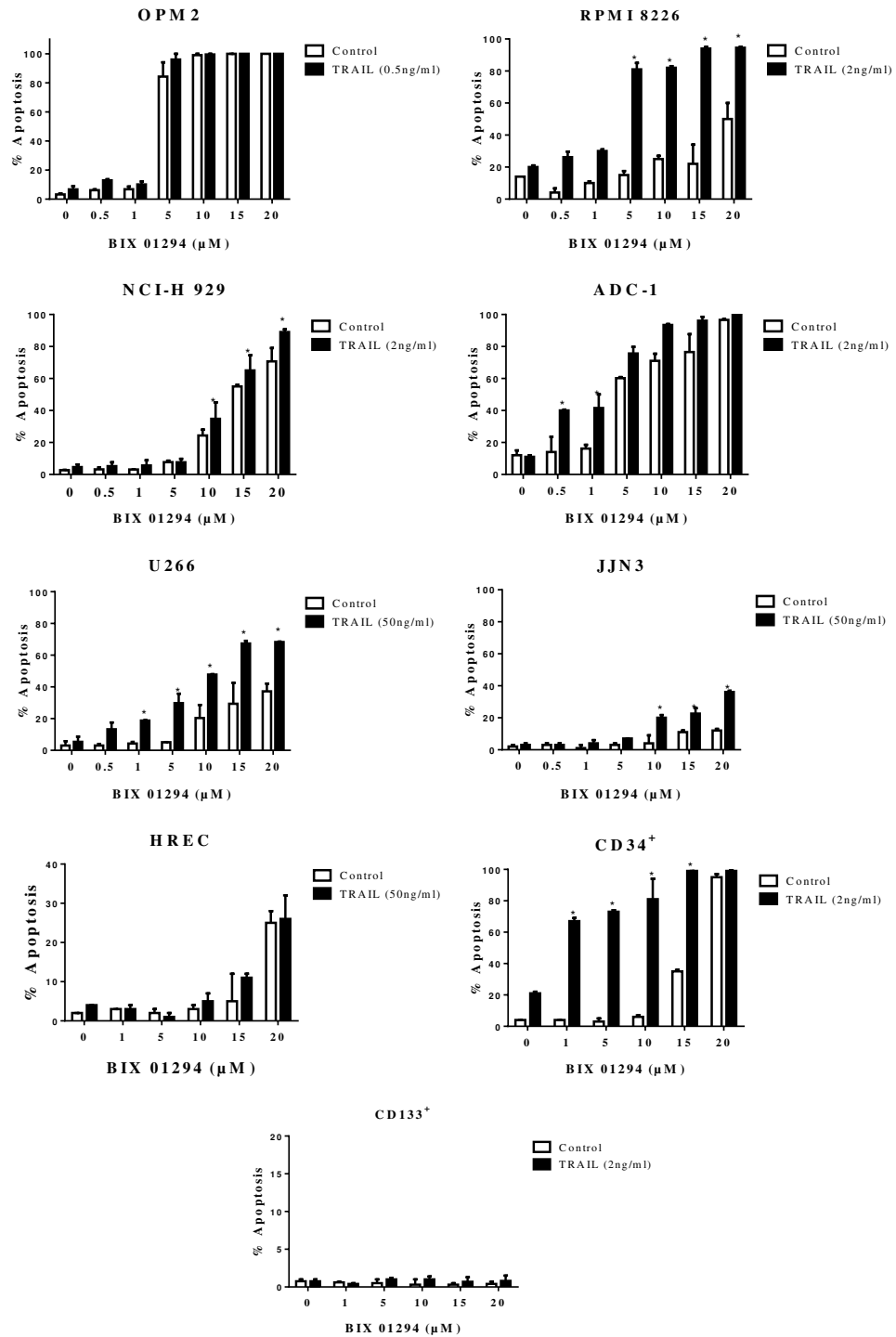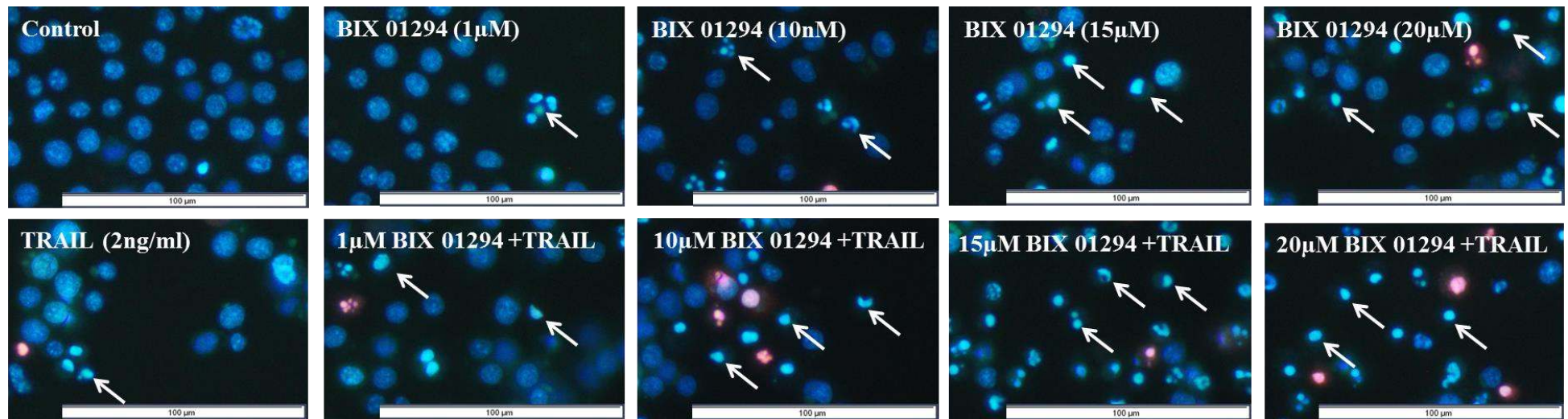
Figure 2.8: Effect of apoptosis on the multiple myeloma cell lines and non-tumour cells after the treatment with BIX 01294 +/-TRAIL for 24 h. a) The percentage of apoptotic multiple myeloma cells treatment with BIX 01294 for 24h was increased in a concentration-dependent manner (p < 0.05, Kruskal–Wallis). The synergistic response was defined as a comparison of combination treatment group with the sum of the effects of TRAIL alone + BIX 01294 alone and significance determined by using by the Kruskal–Wallis test (p<0.05). (*) showing that apoptosis was induced by a combined treatment which was significantly greater than additive. b) Morphological assessment of apoptosis using Hoechst 33342/PI nuclear staining after treatment shows BIX 01294 synergistically enhances TRAIL apoptosis in U266 cell line.

2.3.2.4 Effect of the HMTase^i GSK343 (EZH2^i) in Combination with TRAIL on Apoptosis in Multiple Myeloma Cells

Cells were treated with GSK343 alone and in combination with TRAIL at the lowest dose that induced significant apoptosis as a single treatment to investigate their effect on induction of apoptosis following 24 h (Figure 2.9). GSK343 alone potently induced apoptosis in U266 and synergistic enhancement of TRAIL responses seen in all cells. The synergy effect of TRAIL and GSK343 varied on multiple myeloma cells line depending on the drug concentration. For example, NCI-H 929 cell line showed a significant increase in apoptotic cells following the individual treatment with 17.5% with 10 µM GSK343 alone and 4.9% with 2 ng/ml TRAIL alone, whilst the combination treatment showed 46.9% when assessed following 24 h ($p<0.001$) (Figure 2.9). In contrast, no synergistic response was observed when GSK343 used in combination with TRAIL in non-tumour cell line CD133$^+$ and renal cell line HREC. However, the haematopoietic stem cell CD34$^+$ was less sensitive to GSK343 than MM cells with a synergistic response with TRAIL. An example of morphological assessment of apoptosis using Hoechst 33342/PI nuclear staining in RPMI 8226 cells after treatment with different concentration for GSK343 either alone or in combination with TRAIL is shown in Figure 2.9 b.

Figure 2.9: Effect of apoptosis on the multiple myeloma cell lines and non-tumour cell after the treatment with GSK343 +/-TRAIL for 24 h

a)

b)
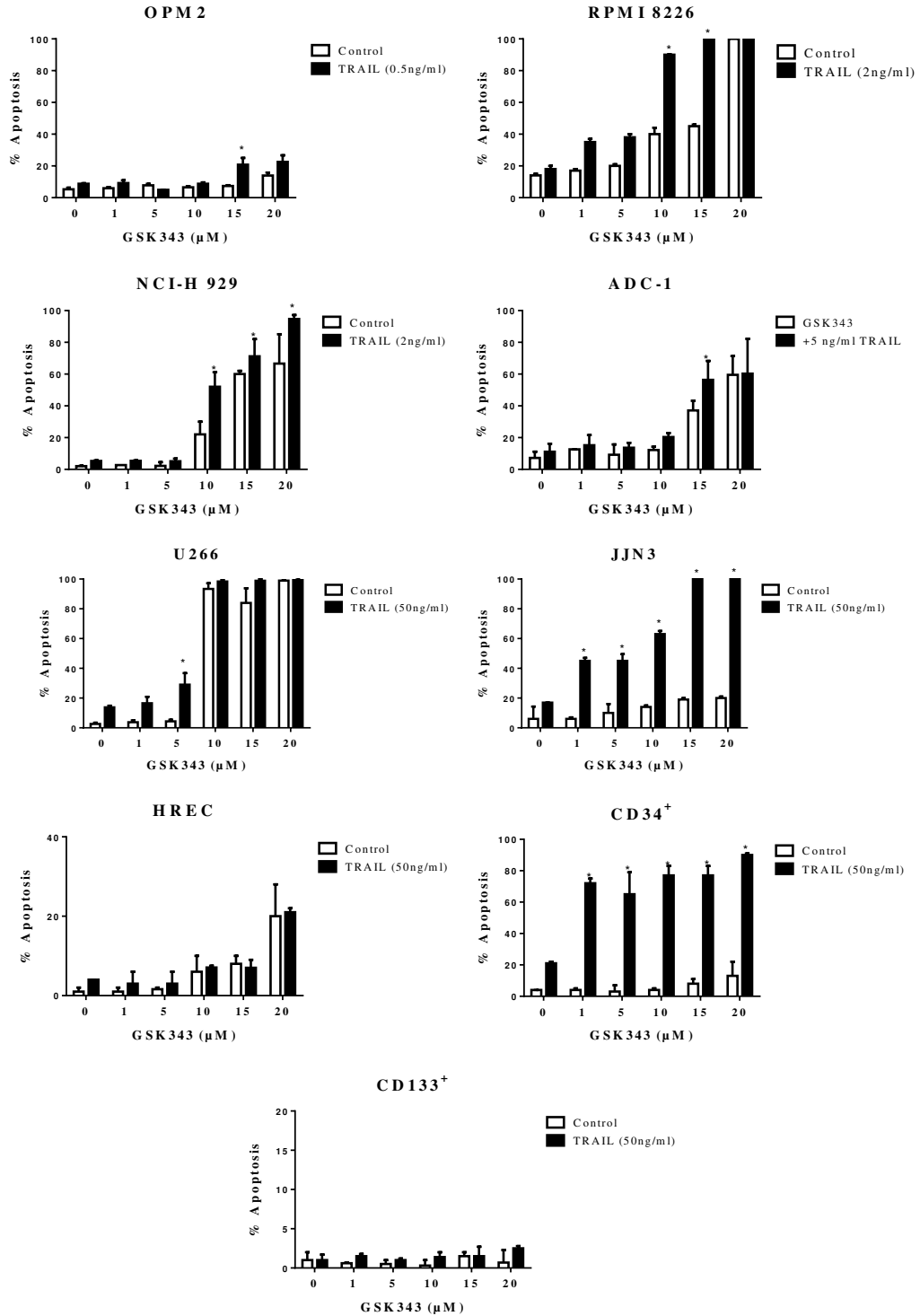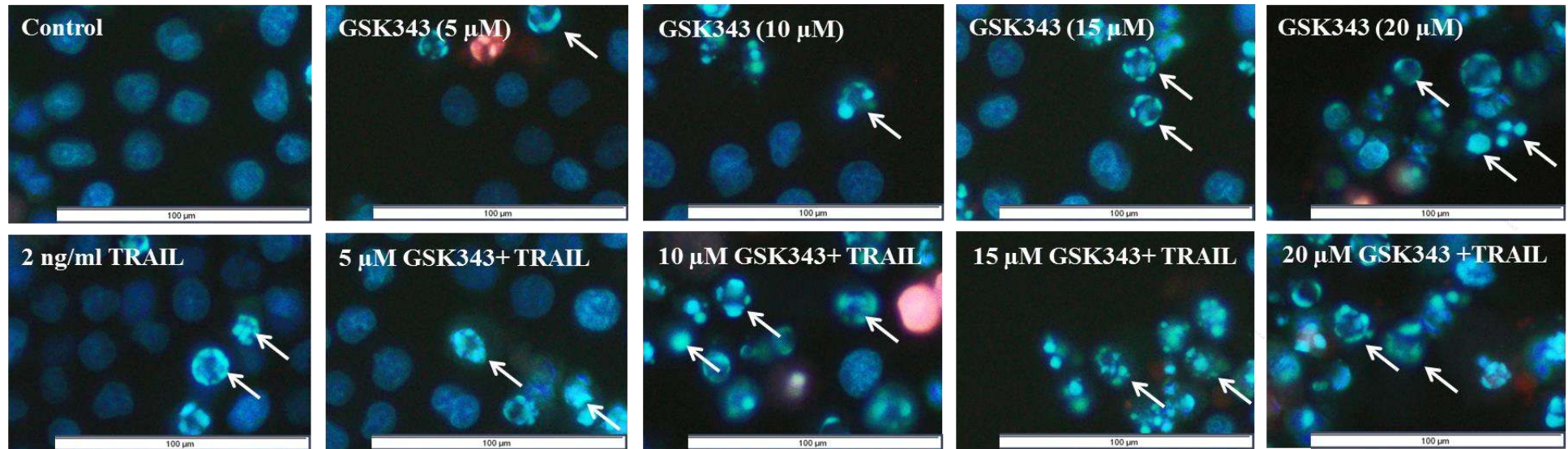
Figure 2.9: Effect of apoptosis on the multiple myeloma cell lines and non-tumour cell after the treatment with GSK343 +/-TRAIL for 24 h. (a *Morphological assessment of apoptosis using Hoechst 33342/PI nuclear staining after treatment shows GSK343 synergistically enhances TRAIL apoptosis in RPMI 8226 cell line. The percentage of apoptotic multiple myeloma cells treatment with GSK343 for 24h was increased in a concentration-dependent manner (p < 0.05, Kruskal–Wallis). The synergistic response was defined as a comparison of combination treatment group with the sum of the effects of TRAIL alone + GSK343 alone and significance determined by using by the Kruskal–Wallis test (p<0.05). (*) showing that apoptosis was induced by a combined treatment which was significantly greater than additive.* **b)** *Morphological assessment of apoptosis using Hoechst 33342/PI nuclear staining after treatment shows GSK343 synergistically enhances TRAIL apoptosis in RPMI 8226 cell line.*

2.3.3 Effect of TRAIL Sensitizers on Proliferation in Multiple Myeloma Cell Lines

2.3.3.1 *Effect of Leptomycin B (NEI) in Combination with TRAIL on Proliferation in Multiple Myeloma Cell Lines*

To examine the effect of LMB, both alone and in combination with TRAIL on cell proliferation, the CellTiter-Glo® Luminescent Cell Viability Assay was performed. The data are illustrated in Figure 2.10 which demonstrates that LMB significantly inhibited the proliferation of multiple myeloma. Furthermore, the co-treatment of LMB with TRAIL reduced cell proliferation. When LMB was combined with TRAIL in NCI-H 929, U266, RPMI 8226, JJN3 and ADC-1 were more effective than individual drug in order to cause a significant inhibition in ATP level, used as a marker of cellular proliferation (p<0.05) (Figure 2.10). However, the non-tumour cell line HREC was the least sensitive to LMB alone compared to the multiple myeloma cells lines and the synergistic effect was seen in combination with TRAIL. On the other hand, LMB significantly inhibited the proliferation of CD34^{+} and the co-treatment of LMB with TRAIL further reduction cell proliferation (Figure 2.10).

Figure 2.10: Effect of LMB on ATP levels
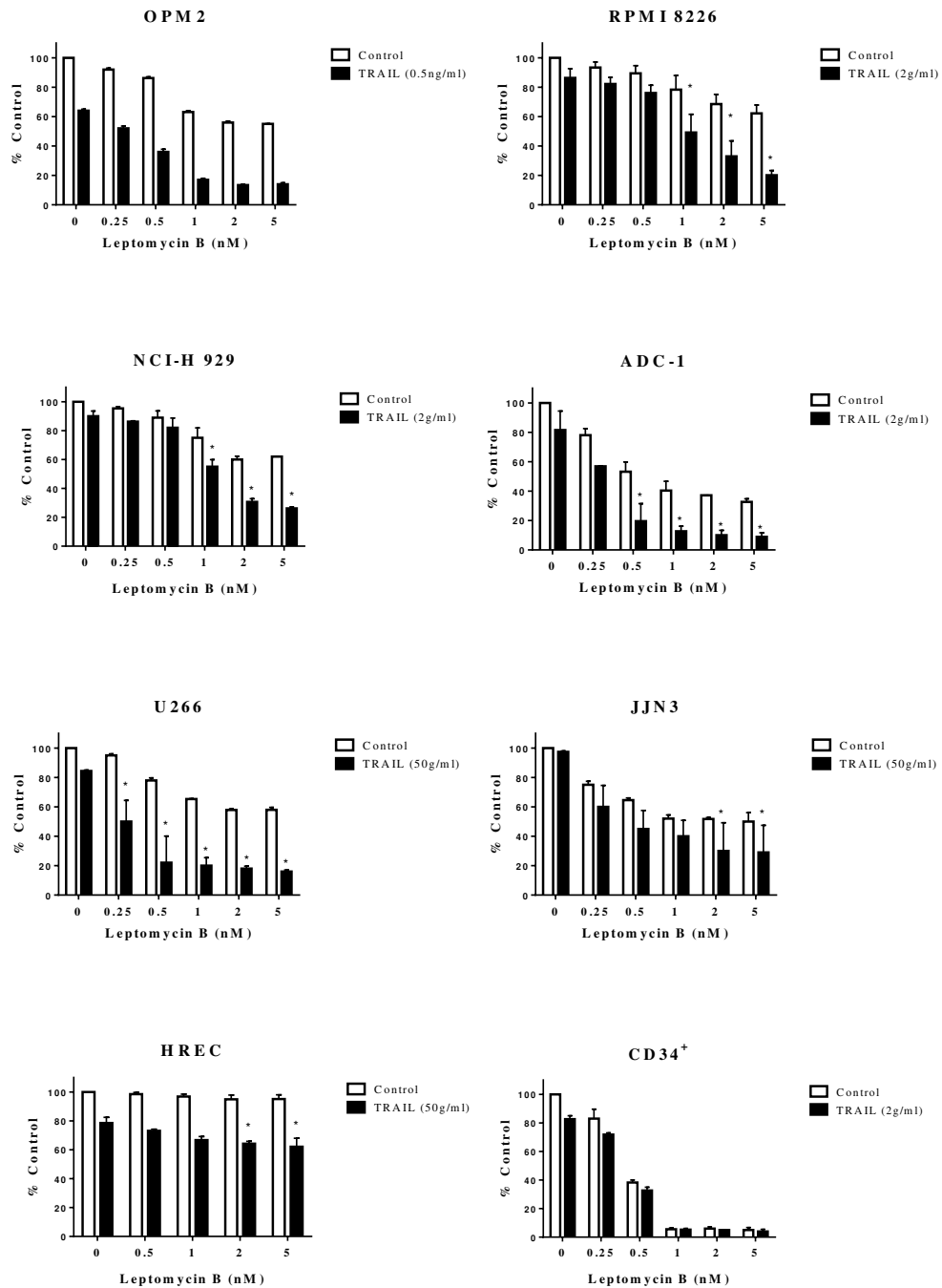
Figure 2.10: Effect of LMB on ATP levels, as evaluated by CellTiter-Glo® assay. The cells were treated as indicated for 24 hours. *Data was normalized to the vehicle control which was assigned 100% cell viability. The data is expressed as median with range (three independent experiments, each in triplicate). The statistical significance was determined by comparison with the vehicle control, statistical significance was set at p<0.05 by the Kruskal–Wallis test. Synergistic reduction in viable cell numbers is denoted by (*).*

2.3.3.2 *Effect of SAHA (HDAC^i) in Combination with TRAIL on Proliferation in Multiple Myeloma Cell Lines*

The cytotoxic effects of SAHA on myeloma cell lines NCI-H 929, RPMI 8226, OPM2, JJN3, U266 and ADC-1 cells following treating with increasing concentrations of SAHA for 24 h were studied using CellTiter-Glo® Luminescent Cell Viability Assay. Viability assays identified that treatment with SAHA for 24h resulted in reduced viable cells in multiple myeloma cell lines in a dose dependent manner (Figure 2.11). SAHA alone significantly reduced cell numbers in all cell lines ($p<0.05$) (Figure 2.11). TRAIL was used at the lowest dose that resulted in significant apoptosis by Hoechst 33342/PI staining, and as such, weak effects seen with TRAIL alone are expected. Combination treatment with SAHA + TRAIL resulted in synergistic reduction in ATP levels in OPM2, RPMI 8226, NCI-H 929, U266, ADC-1 and JJN-3, however, effect sizes in the latter two cell lines were smaller. However, the non-tumour cell lines HREC did not show any significant reduction in ATP level following treatment with SAHA and the synergistic effect was seen in when SAHA was combined with TRAIL. On the other hand, high dose of SAHA significantly inhibited the proliferation of CD34$^+$ and the co-treatment of SAHA with TRAIL induced more reduction in cell proliferation (Figure 2.11).

Figure 2.11: Effect of SAHA on ATP levels
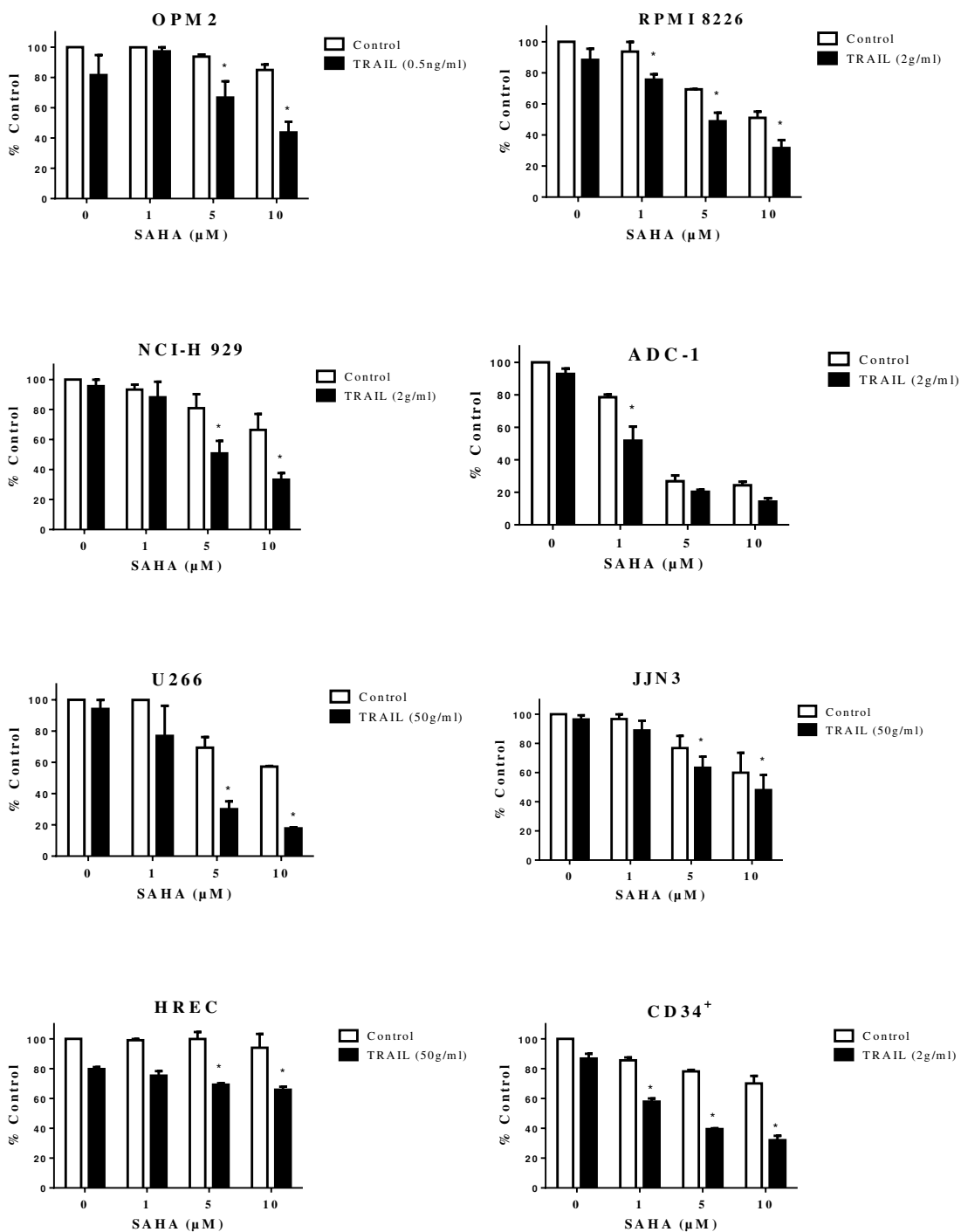
Figure 2.11: Effect of SAHA on ATP levels, as evaluated by CellTiter-Glo® assay. The cells were treated as indicated for 24 hours. Data was normalized to the vehicle control which was assigned 100% cell viability. The data is expressed as median with range (three independent experiments, each in triplicate). The statistical significance was determined by comparison with the vehicle control, statistical significance was set at $p < 0.05$ by the Kruskal–Wallis test. Synergistic reduction in viable cell numbers is denoted by (*).

2.3.3.3 Effect of the G9a HMTase[i] BIX 01294 Treatment in Combination with TRAIL on Proliferation in Multiple Myeloma Cell Lines

Cells were treated with BIX 01294 alone and in combination with TRAIL at the lowest dose that induced significant apoptosis as a single treatment to investigate their effect on inhibition of ATP levels after 24 h ($p<0.001$) (Figure 2.12). MMSET-positive cells (NCI-H 929 and, OPM2) demonstrated a significant decrease in the percent of ATP following treatment with BIX 01294 alone for 24 h ($p<0.001$) (Figure 2.12). BIX 01294 synergistically enhanced TRAIL responses in MMSET-negative cell lines (U266 and JJN3) (Figure 2.12). A neglible effect on cell proliferation was observed in the non-tumour cell line HREC with BIX 01294 treatments alone. In contrast, a synergistic effect was observed with a high dose of BIX 01294 in combination with a high dose of TRAIL. On the other hand, high dose of BIX 01294 significantly inhibited the proliferation of CD34^{+} and the co-treatment of BIX 01294 with TRAIL induced more reduction in cell proliferation (Figure 2.12).

Figure 2.12: Effect of BIX 01294 on ATP levels
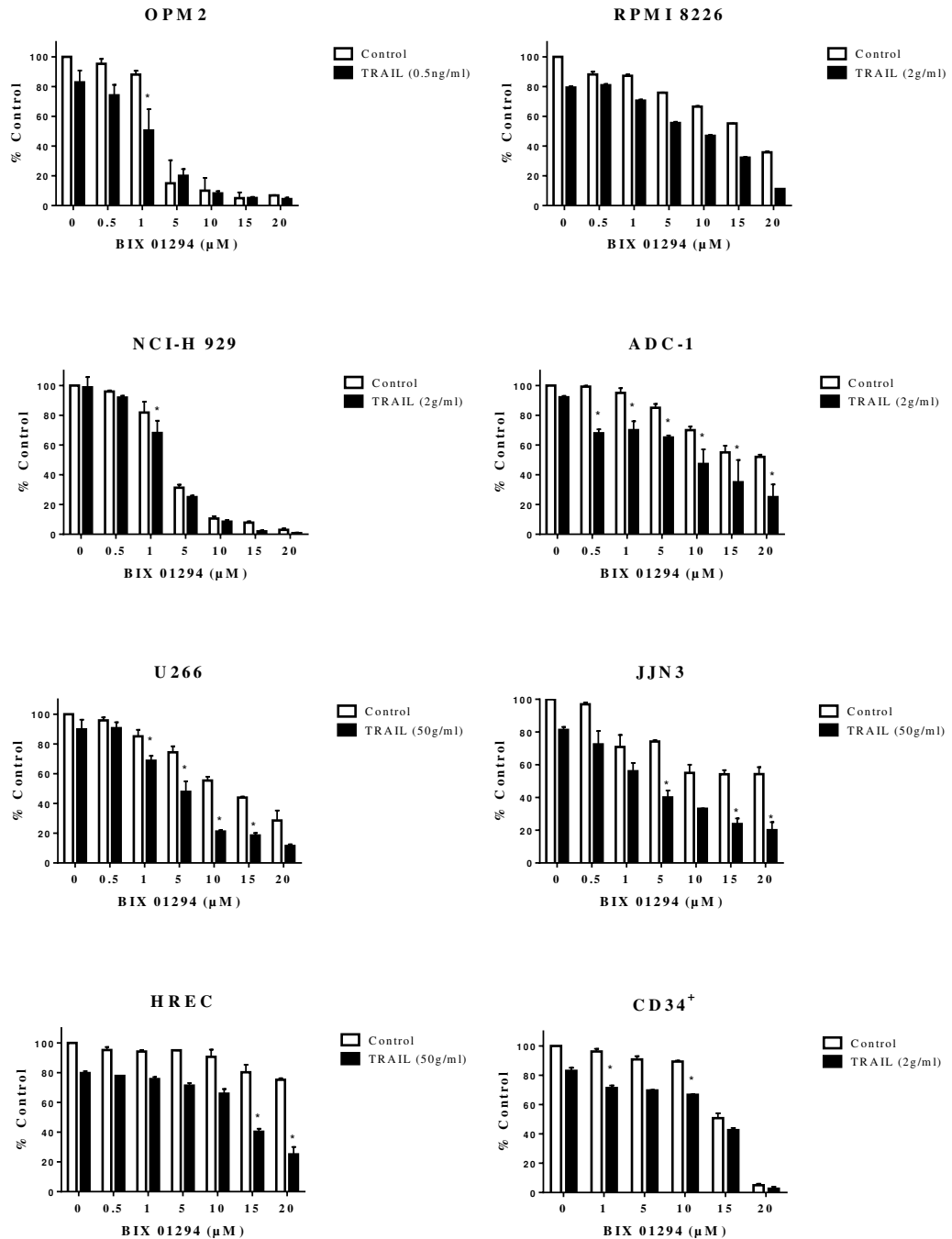
Figure 2.12: Effects of BIX 01294 on ATP levels, as evaluated by CellTiter-Glo® assay. The cells were treated as indicated for 24 hours. Data was normalized to the vehicle control which was assigned 100% cell viability. The data is expressed as median with range (three independent experiments, each in triplicate). The statistical significance was determined by comparison with the vehicle control, statistical significance was set at $p<0.05$ by the Kruskal–Wallis test. Synergistic reduction in viable cell numbers is denoted by (*).

2.3.3.4 Effect of the HMTase[i] GSK343 (EZH2[i]) Treatment in Combination with TRAIL on Proliferation in Multiple Myeloma Cell Lines

The effect HMTase[i] GSK343 on cell proliferation following treatment with GSK343 at 0-20 µM for 24 h showed a significant decrease in ATP level in MM cell lines in dose dependent manner ($p < 0.05$) (Figure 2.13). However, within the multiple myeloma cell lines different response to GSK343 treatment was observed, where JJN3 and U266 were the most affected and demonstrated a significant decrease in ATP level ($p < 0.05$) (Figure 2.13). Combination treatment with TRAIL resulted in synergistic reduction of ATP levels in U266, NCI-H 929, RPMI 8226, and OPM2. In contrast, JJN3 and ADC-1, cell lines failed to show any synergistic response to GSK343 treatment when combined with TRAIL. A neglible effect on cell proliferation was observed in the non-tumour cell lines CD34^{+} and HREC GSK343 treatments alone. In contrast, a synergistic effect was observed with a high dose of GSK343 in combination with a high dose of TRAIL (Figure 2.13).

Figure 2.13: Effect of GSK343 on ATP levels
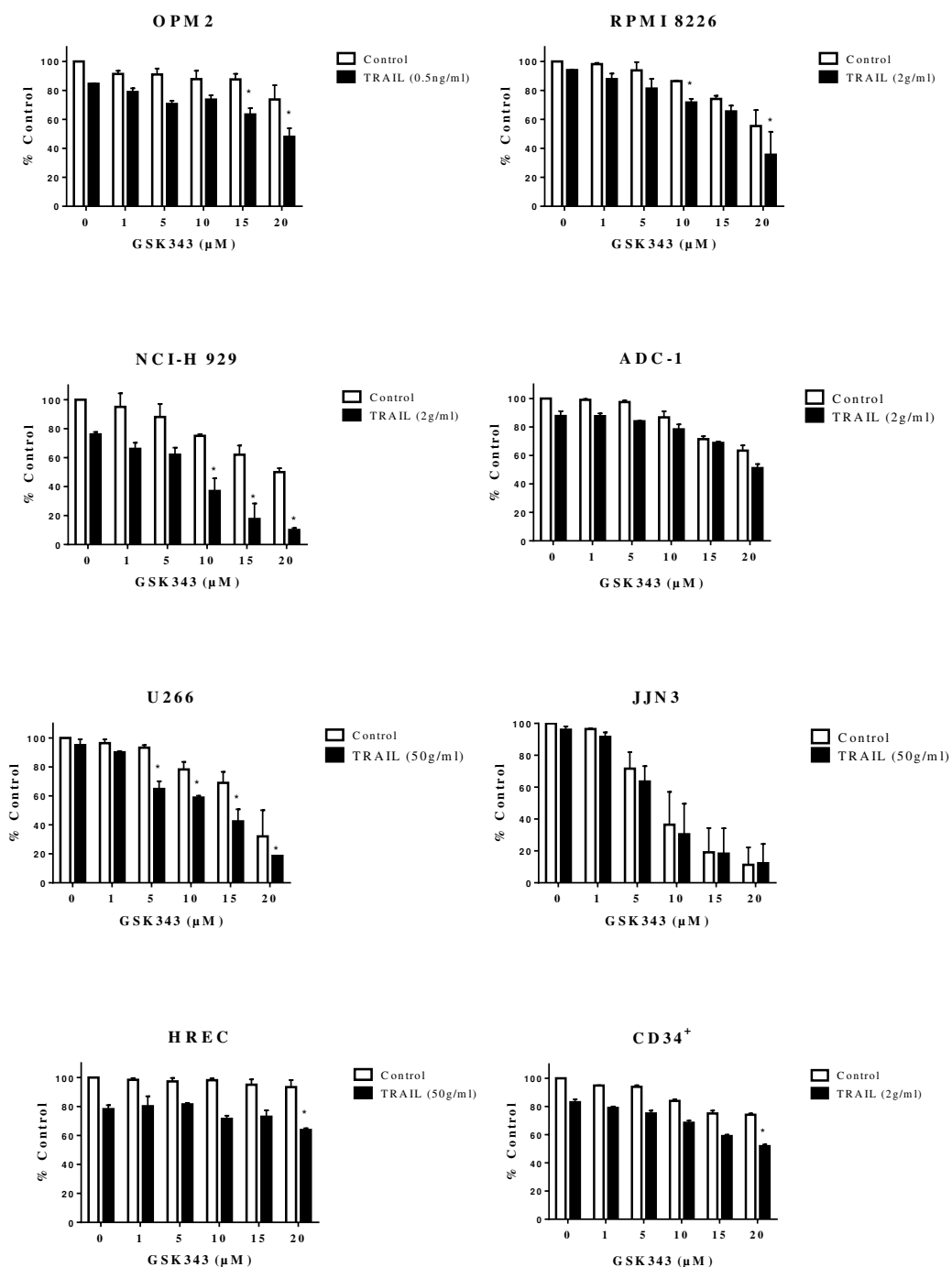
Figure 2.13: Effect of GSK343 on ATP levels, as evaluated by CellTiter-Glo® assay. The cells were treated as indicated for 24 hours. *Data was normalized to the vehicle control which was assigned 100% cell viability. The data is expressed as median with range (three independent experiments, each in triplicate). The statistical significance was determined by comparison with the vehicle control, statistical significance was set at p<0.05 by the Kruskal–Wallis test. Synergistic reduction in viable cell numbers is denoted by (*).*

2.3.4   Effect of TRAIL Sensitizers on Caspase Activity in Multiple Myeloma Cells

2.3.4.1   Effect of LMB (NEI) in Combination with TRAIL on Caspase-3 Activity in Multiple Myeloma Cells

To confirm the morphological assessment of apoptosis by Hoechst 33342/PI staining, caspase-3 activity assays using flow cytometry was used. Combination treatment doses which synergistically enhanced apoptosis as determined by Hoechst 33342/PI staining showed significant induction of apoptosis following caspase-3 activation assay in NCI-H 929, RPMI 8226, ADC-1 and U266 ($p<0.05$) (Figure 2.14).

Figure 2.14: Effects of LMB in combination with TRAIL on caspase-3 activity in multiple myeloma cells
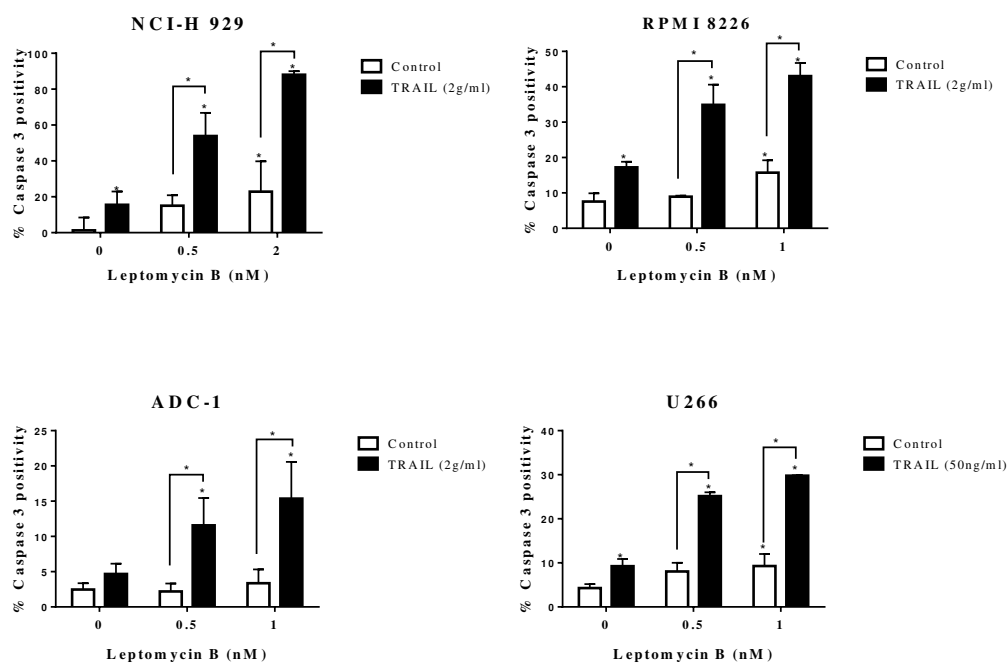
Figure 2.14: Effects of LMB in combination with TRAIL on caspase-3 activity in multiple myeloma cells. The cells were treated with LMB and TRAIL alone and in combined for 24 h. The data is expressed as median with range. The statistical significance was determined by comparison with the vehicle control, statistical significance was set at $p<0.05$ by the Kruskal–Wallis test.

2.3.4.2 Effect of SAHA (HDAC[i]) in Combination with TRAIL Caspase-3 Activity in Multiple Myeloma Cells

The effectiveness of SAHA in inducing apoptosis was conforming by caspase-3 activity assays using flow cytometry. Multiple myeloma cell lines were treated with combination treatment doses which synergistically enhanced apoptosis as determined by Hoechst 33342/PI staining. SAHA induced significantly higher levels of apoptosis determined by caspase-3 activity in NCI-H 929, U266 and RPMI 8226 ($p < 0.05$) (Figure 2.15).

Figure 2.15: Effects of SAHA in combination with TRAIL on caspase-3 activity in Multiple Myeloma cells
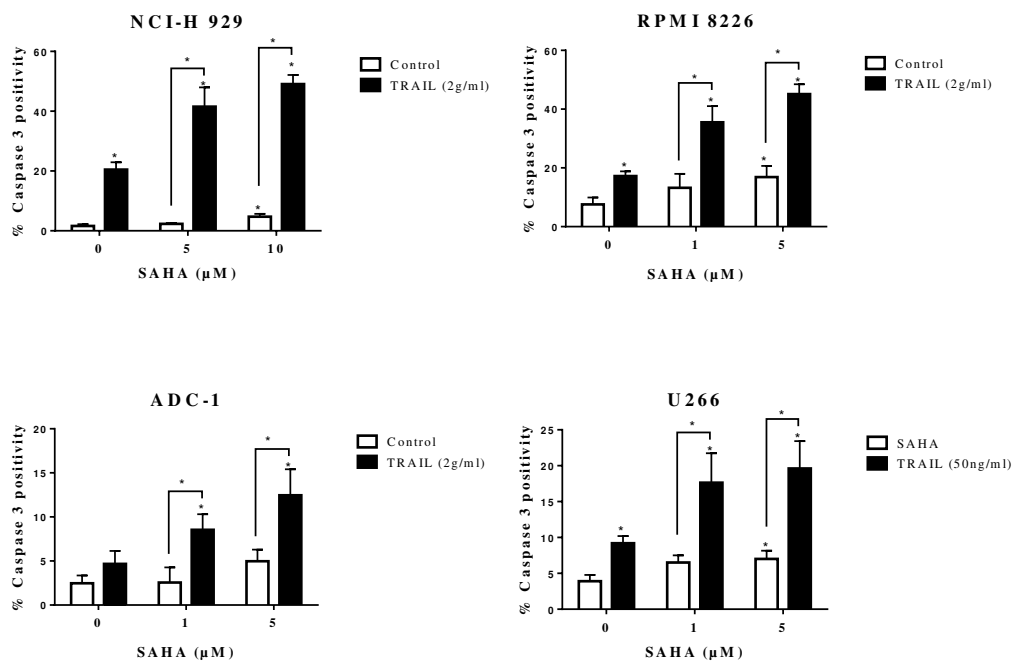
Figure 2.15: Effects of SAHA in combination with TRAIL on caspase-3 activity in multiple myeloma cells. The cells were treated with SAHA and TRAIL alone and in combined for 24 h. The data is expressed as median with range. The statistical significance was determined by comparison with the vehicle control, statistical significance was set at $p < 0.05$ by the Kruskal–Wallis test.

2.3.4.3 Effect of the G9a HMTase[i] BIX 01294 in Combination with TRAIL on Caspase-3 Activity in Multiple Myeloma Cells

NCIH 929, U266, RPMI 8226 and ADC-1 cells showed significant induction of apoptosis as shown by increased caspase-3 activation following 24 h incubation when treated with BIX 01294 alone and after the combination treatment of BIX 01294 and TRAIL (Figure 2.16) ($p < 0.05$).

Figure 2.16: Effects of BIX 01294 in combination with TRAIL on Caspase-3 activity in Multiple Myeloma cells

Figure 2.16: Effects of BIX 01294 in combination with TRAIL on Caspase-3 activity in multiple myeloma cells. The cells were treated with BIX 01294 and TRAIL alone and in combined for 24 h. The data is expressed as median with range. The statistical significance was determined by comparison with the vehicle control, statistical significance was set at p<0.05 by the Kruskal–Wallis test.

2.3.4.4   Effect of the HMase^i GSK343 (EZH2^i) in Combination with TRAIL on Caspase-3 Activity in Multiple Myeloma Cells

GSK343 and TRAIL induced a significant level of apoptosis. GSK343 interacted with TRAIL producing a synergistic effect that significantly increased the caspase activity in RPMI 8226 and ADC-1 MM cell line (Figure 2.17) ($p < 0.05$). These result confirmed the induction of apoptosis shown by Hoechst 33342/PI staining.

Figure 2.17: Effects of GSK343 in combination with TRAIL on caspase-3 activity in multiple myeloma cells
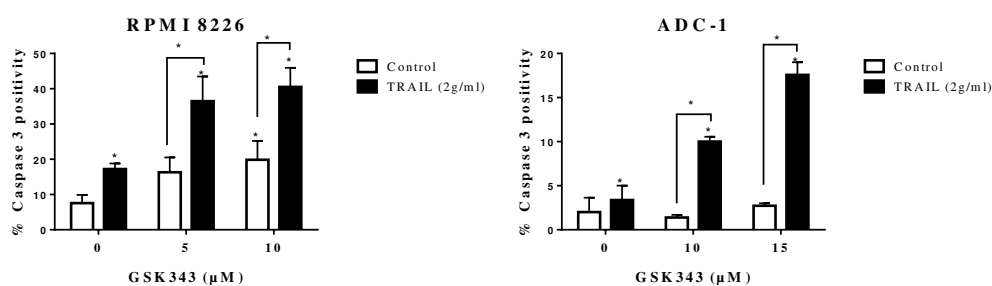
Figure 2.17: Effects of GSK343 in combination with TRAIL on Caspase 3 activity in multiple myeloma cells. The cells were treated with GSK343 and TRAIL alone and in combined for 24 h. The data is expressed as median with range. The statistical significance was determined by comparison with the vehicle control, statistical significance was set at p<0.05 by the Kruskal–Wallis test.

2.3.5 Effect of TRAIL Sensitizers (LMB, SAHA, BIX 01294 and GSK343) on Cell Cycle in Multiple Myeloma Cells

To determine if inhibition of multiple myeloma cell proliferation is due to an increase in the cell cycle arrest, NCI-H 929, RPMI 8266, U266, JJN3 and ADC-1 were treated with LMB, SAHA, BIX 01294 and GSK343 for 24 h and stained with propidium iodide to study the cell cycle progression (Figure 2.18, 2.19, 2.20, 2.21). Multiple myeloma cell lines showed a different response in terms of cell cycle arrest with different concentration of anti-tumour agents. Treatment with LMB showed significant accumulation in S and G_2/M phase in NCI-H 929, G_0/G_1 and S phases in RPMI 8226 and in G_2/M for JJN3 cells ($p < 0.05$) (Figure 2.18). ADC-1 cells showed a significant increase in S and G_2/M phases of the cell cycle when assessed after 24 h following treatment with LMB compared to control cells ($p < 0.05$) (Figure 2.18). Treatment with SAHA caused significant induced cell cycle arrest in G_2/M in ADC-1, S-phase in NCI-H 929 and U266, G_0/G_1 and G_2/M in JJN3 cells ($p < 0.05$) (Figure 2.19). BIX 01294 significantly induced cell cycle arrest in G_0/G, S-phases and G_2/M in RPMI 8226, S-phase in ADC-1 and NCI-H 929 cells ($p < 0.05$) (Figure 2.20). In addition, significant cellular accumulation at G_0/G_1 and G_2/M in ADC-1, S-phase in NCI-H 929, RPMI 8226 and U266, G_0/G_1 in JJN3 following GSK343 treatment alone ($p < 0.05$) (Figure 2.21

Moreover, analysis of combination treatment on cell cycle performed, however, due to increase levels of apoptosis, cell cycle in each phase was unreliable. All data are shown in the appendix (Figure I, II, III, and IV). In addition, some multiple myeloma cells illustrated an increase in sub-G_1 population, which an apoptotic cells indicator when treated combination treatment of anti-tumour agents with TRAIL (Figure 2.22). An example of histograms for the cell cycle phases (G_0/G_1, S, G_2/M) for the U266 multiple myeloma cells after treatment with LMB, SAHA, BIX 01294 and GSK343 either alone or in combination with TRAIL following 24 h is shownin Figure 2.22.

Figure 2.18: Effect of LMB on cell cycle progression in multiple myeloma cells
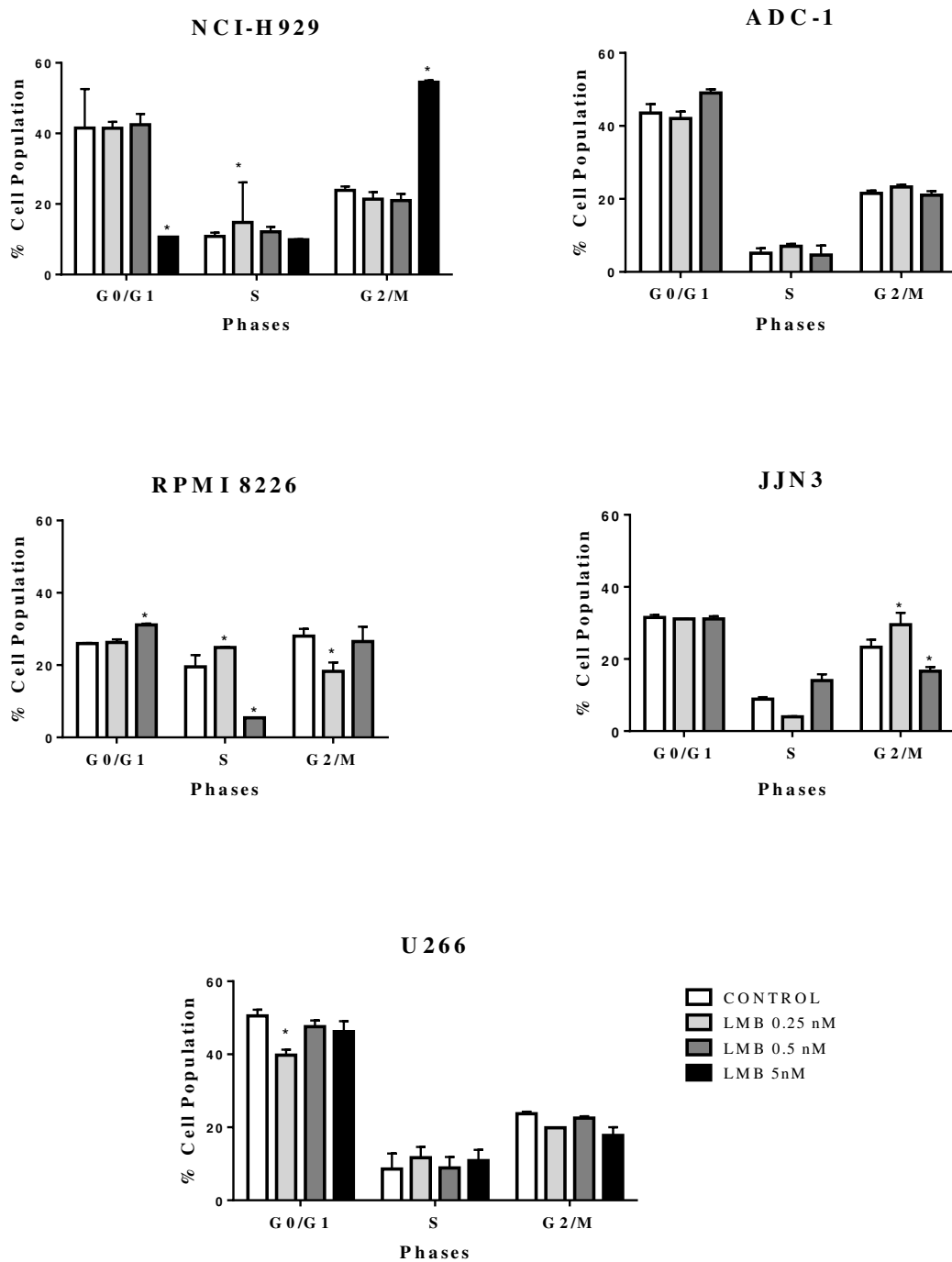
Figure 2.18: Effect of LMB on cell cycle progression in multiple myeloma cells. The cells were treated with selected concentrsations of LMB for 24h. The data is expressed as median with range (three independent experiments). The statistical significance was determined by comparison with the vehicle control (*=p<0.05) (Kruskal–Wallis).

Figure 2.19: The effect of SAHA on cell cycle progression in multiple myeloma cells
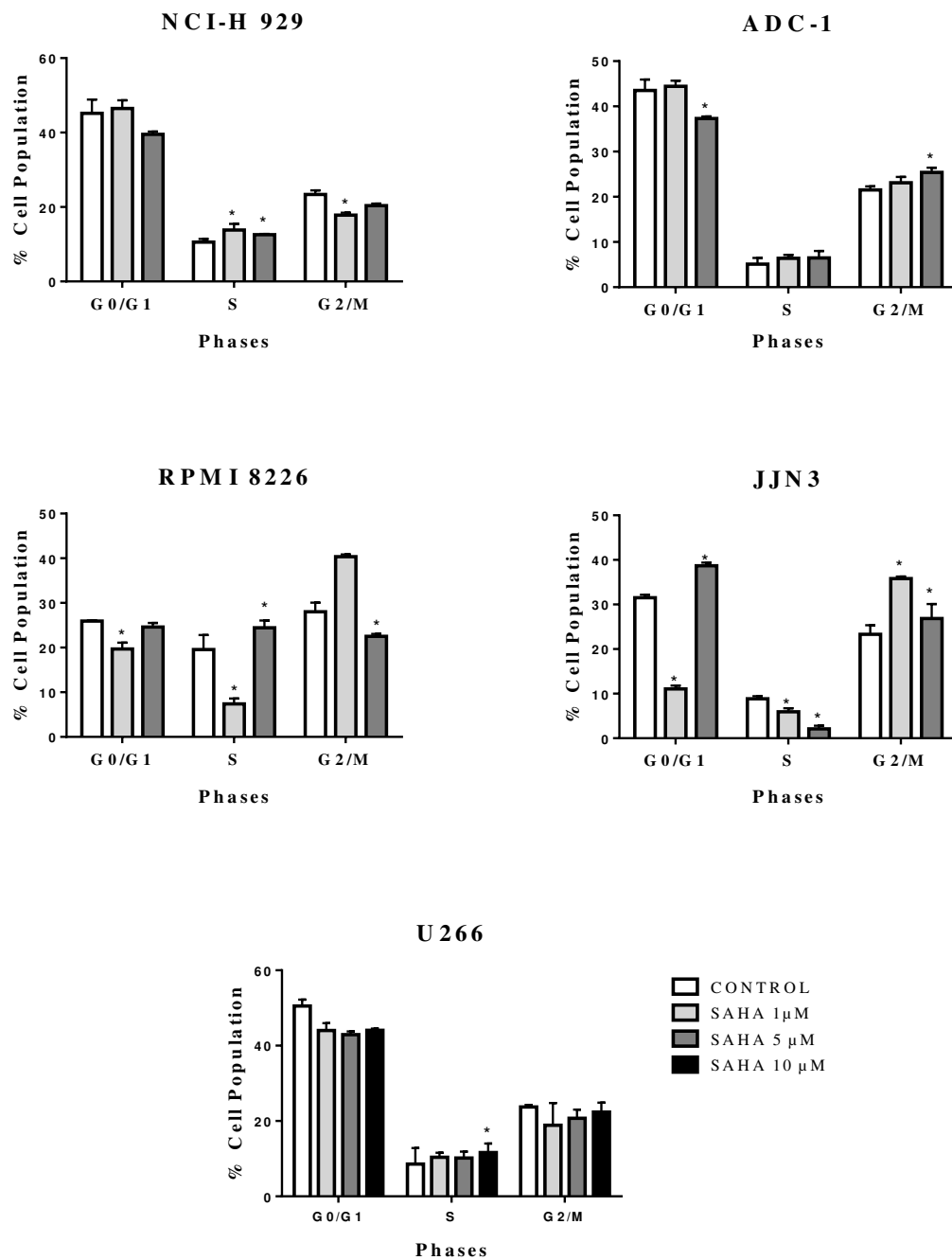
Figure 2.19: Effect of SAHA on cell cycle progression in multiple myeloma cells. The cells were treated with selected concentrsations of SAHA for 24 h. The data is expressed as median with range (three independent experiments). The statistical significance was determined by comparison with the vehicle control (*=p<0.05) (Kruskal–Wallis).

Figure 2.20: Effect of BIX 01294 on cell cycle progression in multiple myeloma cells
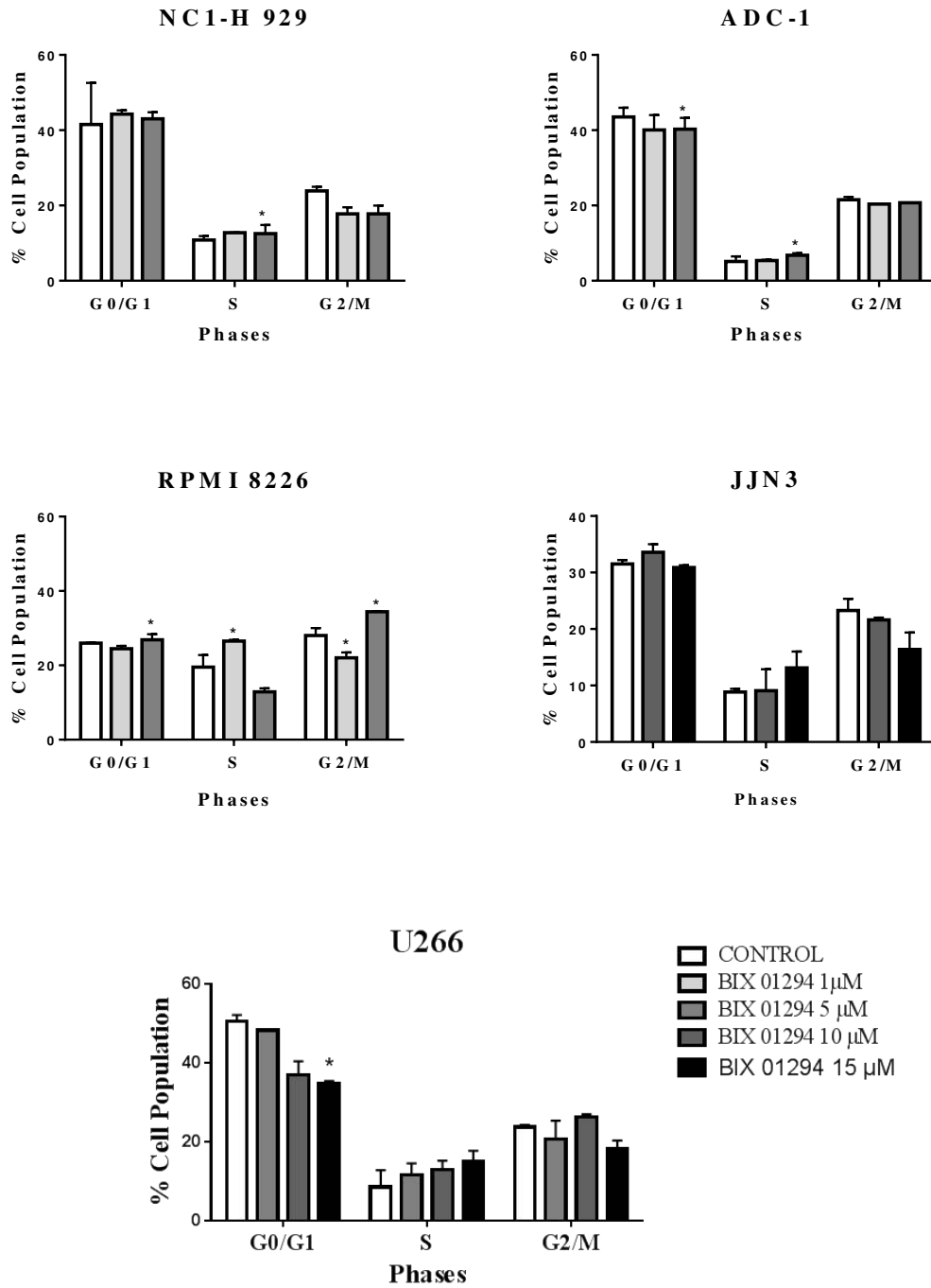
Figure 2.20: Effect of BIX 01294 on cell cycle progression in multiple myeloma cells. The cells were treated with selected concentrsations of BIX 01294 for 24 hours. The data is expressed as median with range (three independent experiments). The statistical significance was determined by comparison with the vehicle control and statistical significance (*=p<0.05) (Kruskal–Wallis).

Figure 2.21: Effect of GSK343 on cell cycle progression in multiple myeloma cells
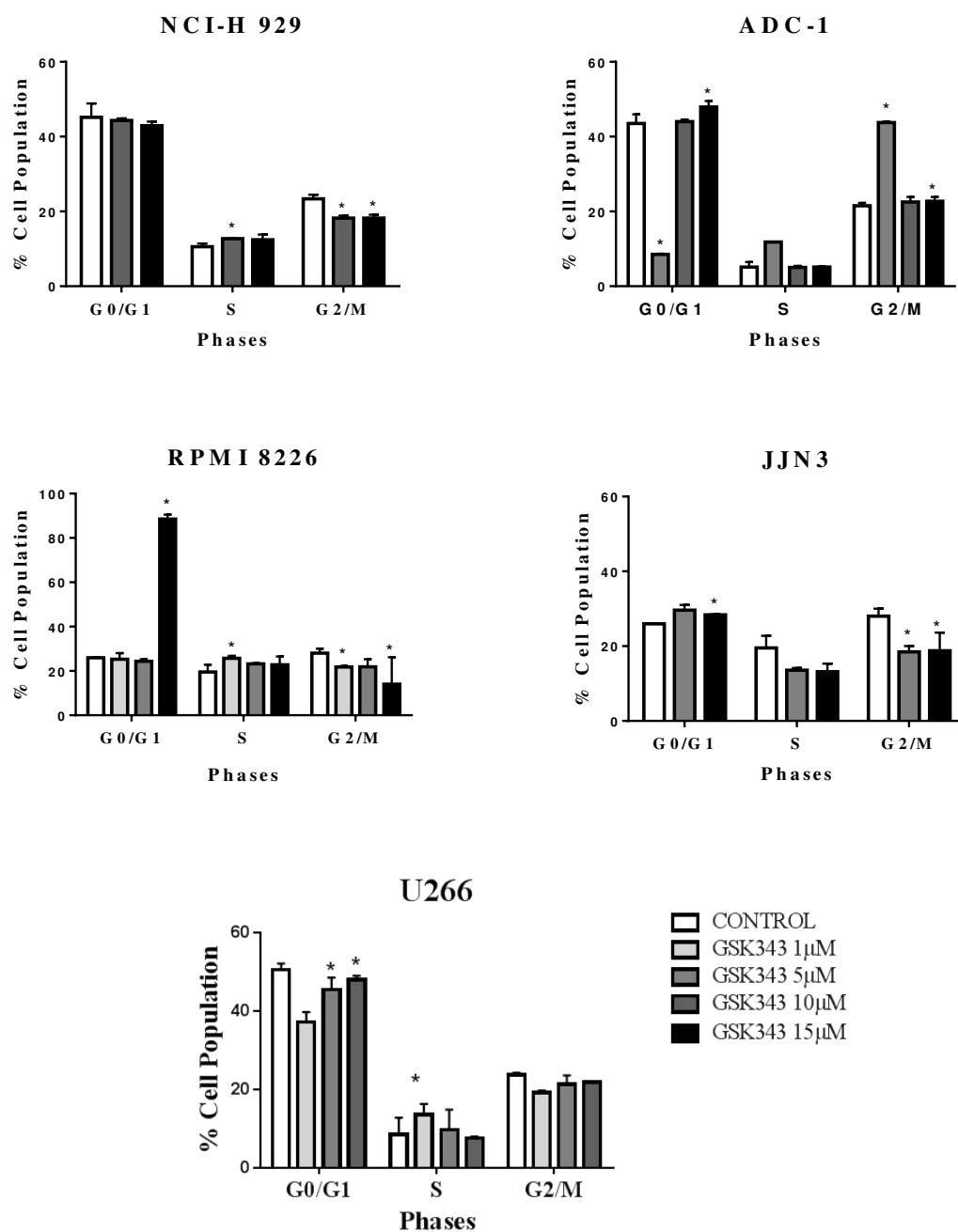
Figure 2.21: Effect of GSK343 on cell cycle progression in multiple myeloma cells. The cells were treated with selected concentrsations of GSK343 for 24 hours. The data is expressed as median with range (three independent experiments). The statistical significance was determined by comparison with the vehicle (*=p<0.05) (Kruskal–Wallis).

Figure 2.22: An example of histograms for the cell cycle phases (G₀/G₁, S, G₂/M) for the U266 multiple myeloma cells after treatment with LMB, SAHA, BIX 01294 either alone or in combination with TRAIL following 24 h
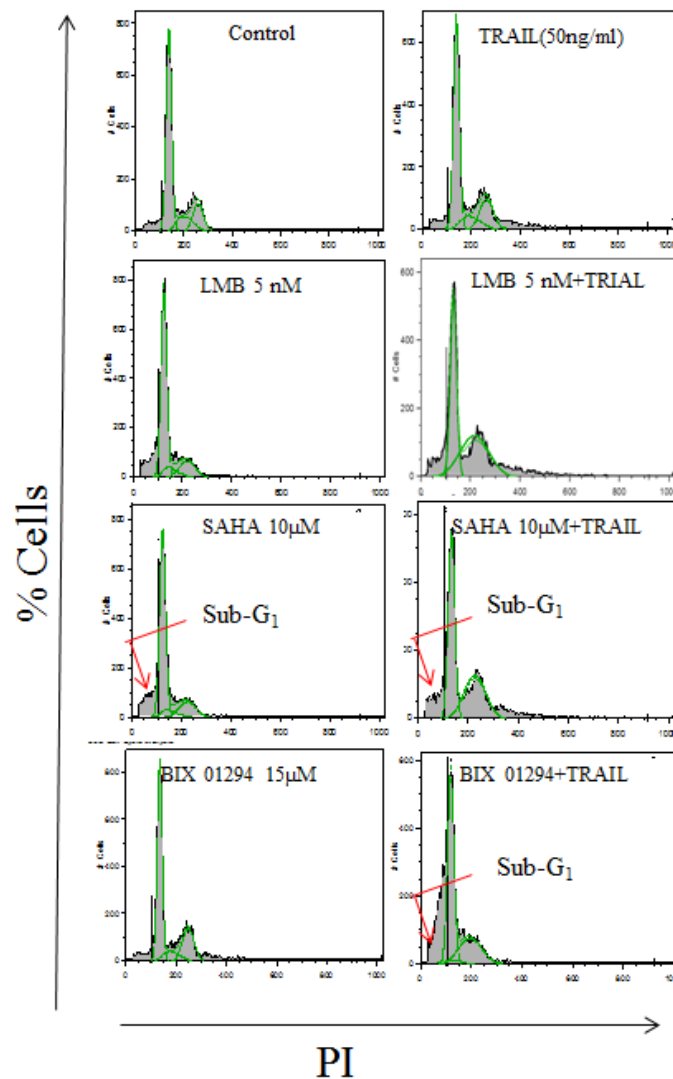
Figure 2.22: An example of histograms for the cell cycle phases (G₀/G₁, S, G₂/M) for the U266 multiple myeloma cells after treatment with LMB, SAHA, BIX 01294 either alone or in combination with TRAIL following 24 h. The percentage of cells in each phase was analyzed with Flow Jo software. In addition, the U266 cells illustrated an increase in sub-G₁ population, which an apoptotic cells indicator when treated with 5 µM SAHA either alone or in combination with TRAIL and co- treatment of BIX 01294 and TRAIL. The statistical significance was determined by comparison with the vehicle ($p < 0.05$) (Kruskal–Wallis).

2.3.6 Prolonged Incubation of TRAIL Sensitive Multiple Myeloma Cells with TRAIL Resulting in the Appearance of TRAIL-Resistant Cells

In order to facilitate the development of TRAIL-resistant culture, this study intentionally chose growth conditions which support the appearance of resistant colonies by prolonged exposure to accelerating dose of TRAIL over 1 year in culture. Measurement of cell number and viability confirmed the TRAIL-insensitive phenotype in NCI-H 929, RPMI 8226 and OPM2 with a highly significant increase of cell viability of TRAIL-resistant cells compared to parental TRAIL sensitive cells in response to high-dose TRAIL ($p < 0.0001$) (Figure 2.23). An alternative method used to generate TRAIL-insensitive population by stimulating the TRAIL sensitive cells with a high/lethal dose of TRAIL (50 ng/ ml) and long term culture of the surviving cells (Figure 2.24). Our data showed that there was an increase in cell viability of TRAIL resistant cells compared to parental TRAIL sensitive cells ($p < 0.0001$) (Figure 2.23 and 24).

Figure 2.23: Generation of TRAIL-resistant population by chronic exposure to escalating TRAIL over 1 year
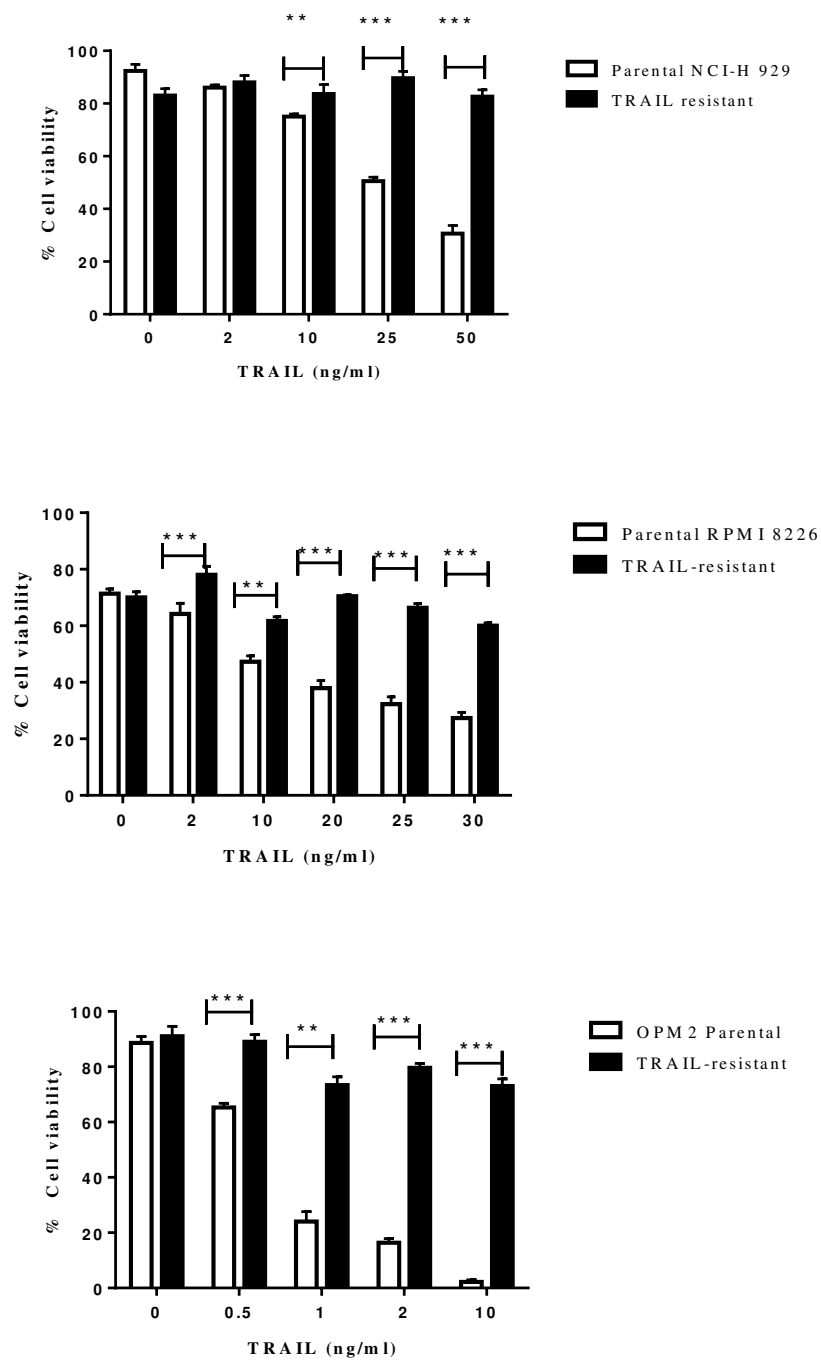
Figure 2.23: Generation of TRAIL-resistant population by incubated TRAIL sensitive cells (NCI-H 929, RPMI 8226, and OPM2) with escalating of TRAIL, result in an increase in cell viability in TRAIL resistant cells compared to parental TRAIL sensitive cells. (*=p<0.01, **=p<0.001, ***=p<0.0001, Kruskal–Wallis test).

Figure 2.24: Generation of TRAIL-resistant population by stimulating the TRAIL sensitive cells with a high/lethal dose of TRAIL
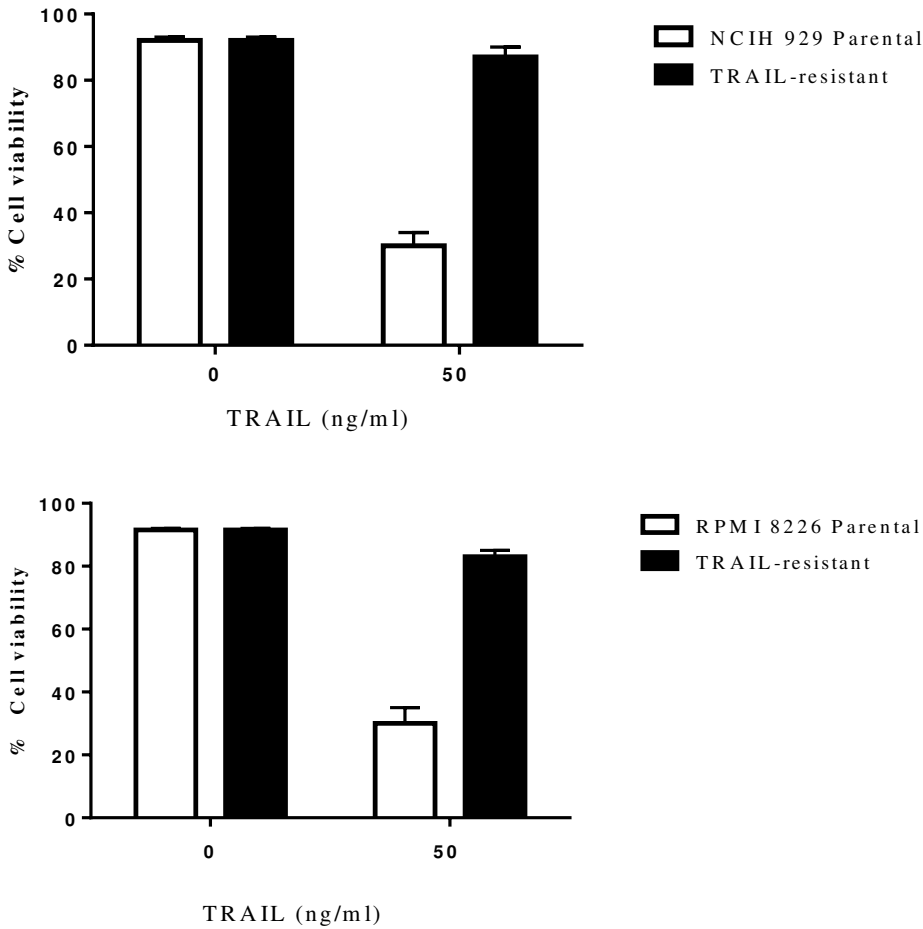
Figure 2.24: Generation of TRAIL-resistant population by stimulating the TRAIL sensitive cells with a high/lethal dose of TRAIL (50 ng/ ml) for one year result in an increase in cell viability in TRAIL resistant cells compared to parental TRAIL sensitive cells. (*=p<0.01,   **=p<0.001, ***=p<0.0001, Kruskal–Wallis test).

2.3.6.1 Effect of TRAIL on Apoptosis in TRAIL-resistant Cell Lines.

Moreover, treatment of the TRAIL-resistant cells with 10 ng/ml and 50 ng/ml TRAIL result in significant reduction of apoptosis in TRAIL resistant cells compared to parental TRAIL sensitive cells or vehicle control (Figure 2.25). An example of morphological assessment of apoptosis using Hoechst 33342 nuclear staining in RPMI 8226 after treatment with different concentration TRAIL is shown in Figure 2.25 a.

Figure 2.25: Effect of TRAIL on apoptosis in TRAIL-*resistant* population

a)

b)

Parental RPMI 8226 cells **TRAIL Resistant**
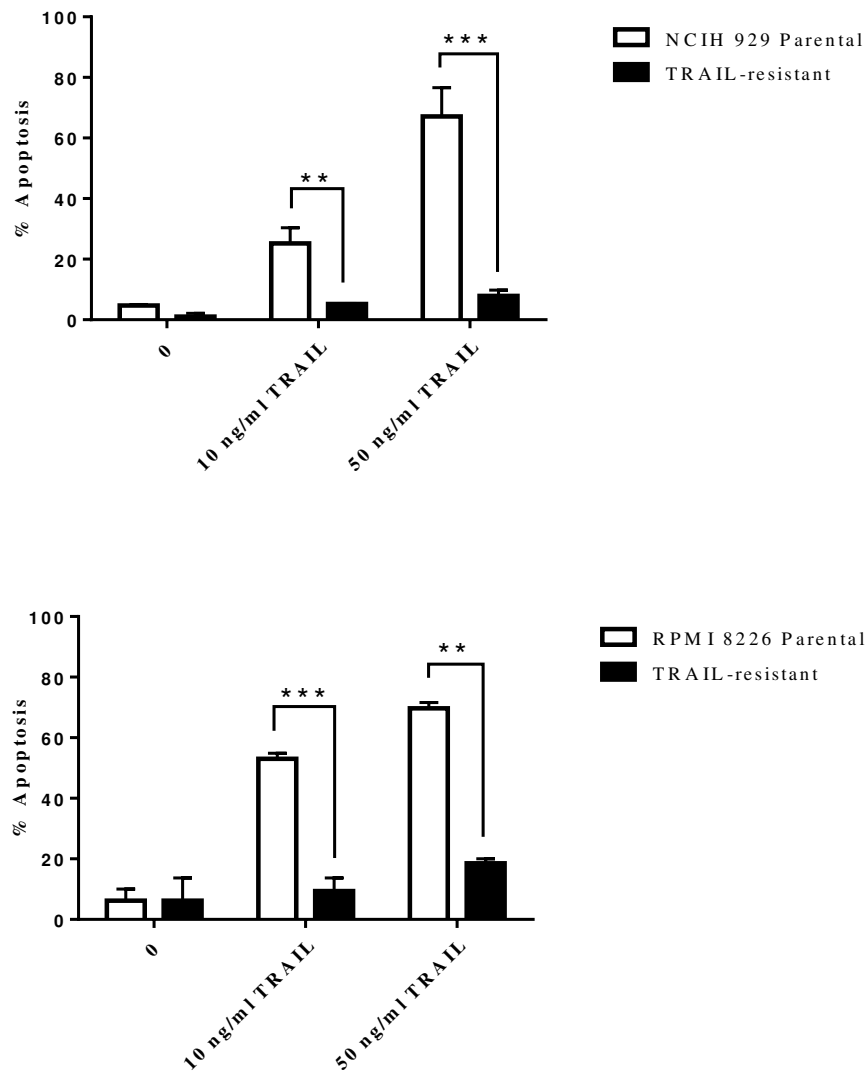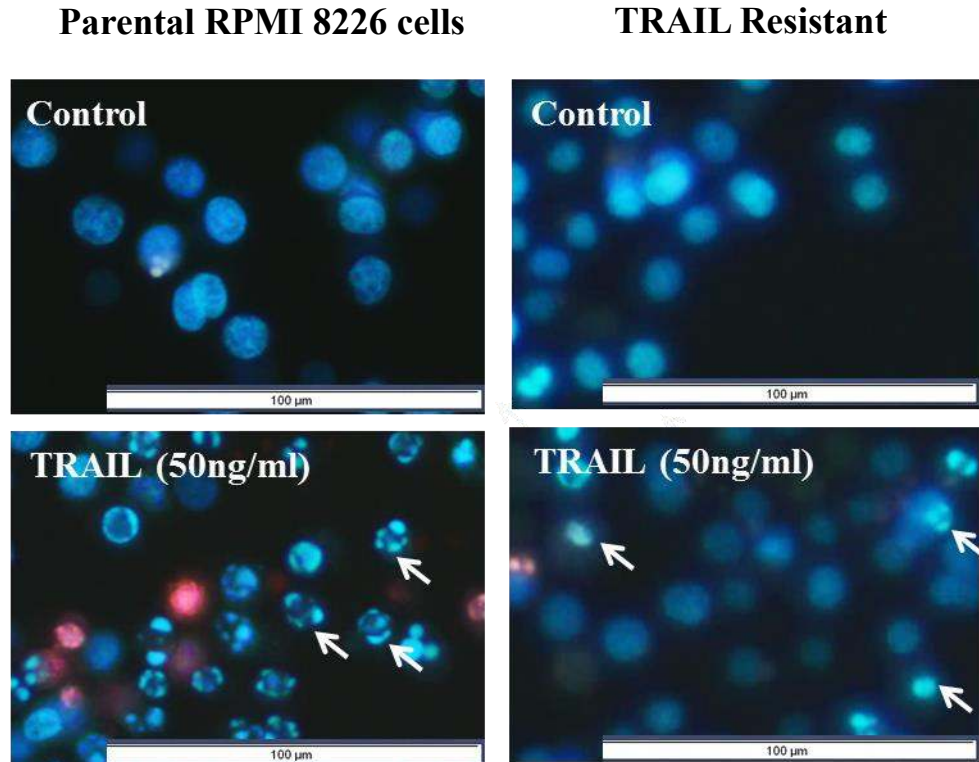
Figure 2.25: Effect of TRAIL on apoptosis in TRAIL-resistant population. a) Stimulation of TRAIL-resistant cells by TRAIL result in significant reduction of the percentage of apoptosis in TRAIL resistant cells compared to parental TRAIL sensitive cells. b) Morphological assessment of apoptosis using Hoechst 33342 /PI nuclear staining, after treatment with TRAIL in parental and TRAIL-resistant RPMI 8226 cell lines. (Kruskal–Wallis test *=p<0.01, **=p<0.001, ***=p<0.0001).

2.3.6.2 *Effect of LMB in Combination with TRAIL in TRAIL-Resistant Multiple Myeloma Cells*

The potential of LMB to induce apoptotic cell death in TRAIL resistant populations was investigated using Hoechst 33342 staining of nuclear morphology. The data are illustrated in Figure 2.26 which demonstrates that TRAIL resistant populations are not sensitized to TRAIL by LMB, whereas there was significant increased sensitivity to LMB and loss of LMB-induced TRAIL-sensitization in TRAIL-resistant RPMI 8226 cells and there was no significant increased sensitivity to LMB in TRAIL^R NCI-H 929 (Figure 2.26). An example of morphological assessment of apoptosis using Hoechst 33342 nuclear staining on parental and TRAIL-resistant RPMI 8826 population after treatment with LMB alone and in combined with TRAIL is shown in Figure 2.26 b.

Figure 2.26: Effect of LMB on apoptosis in TRAIL-resistant population

a)
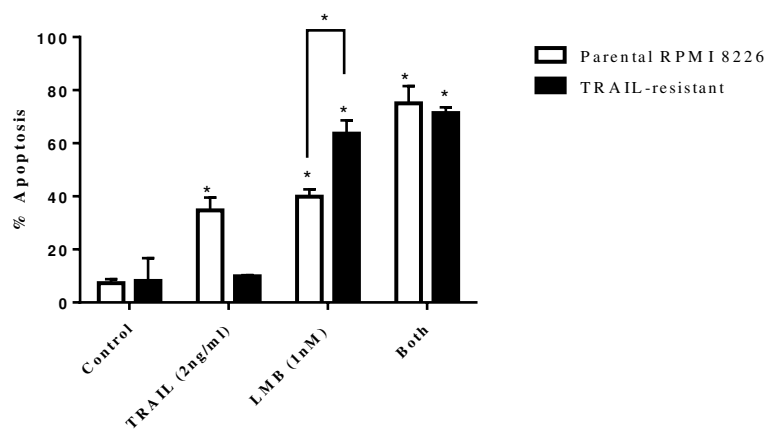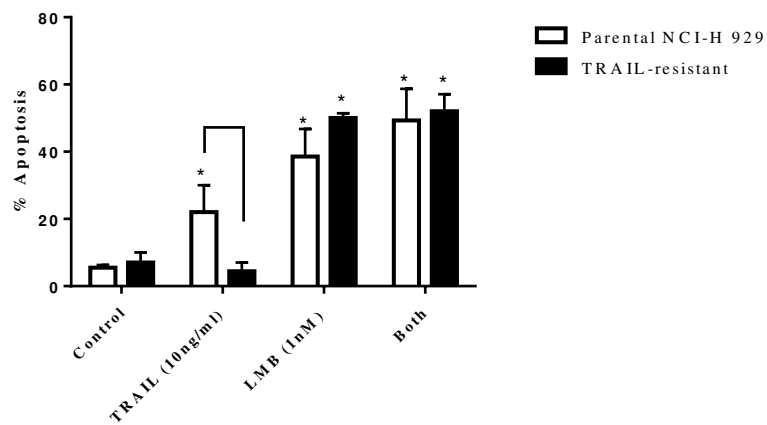
Figure 2.26 b: Morphological assessment of the effect of LMB on apoptosis in

RPMI 8826 TRAIL-resistant population
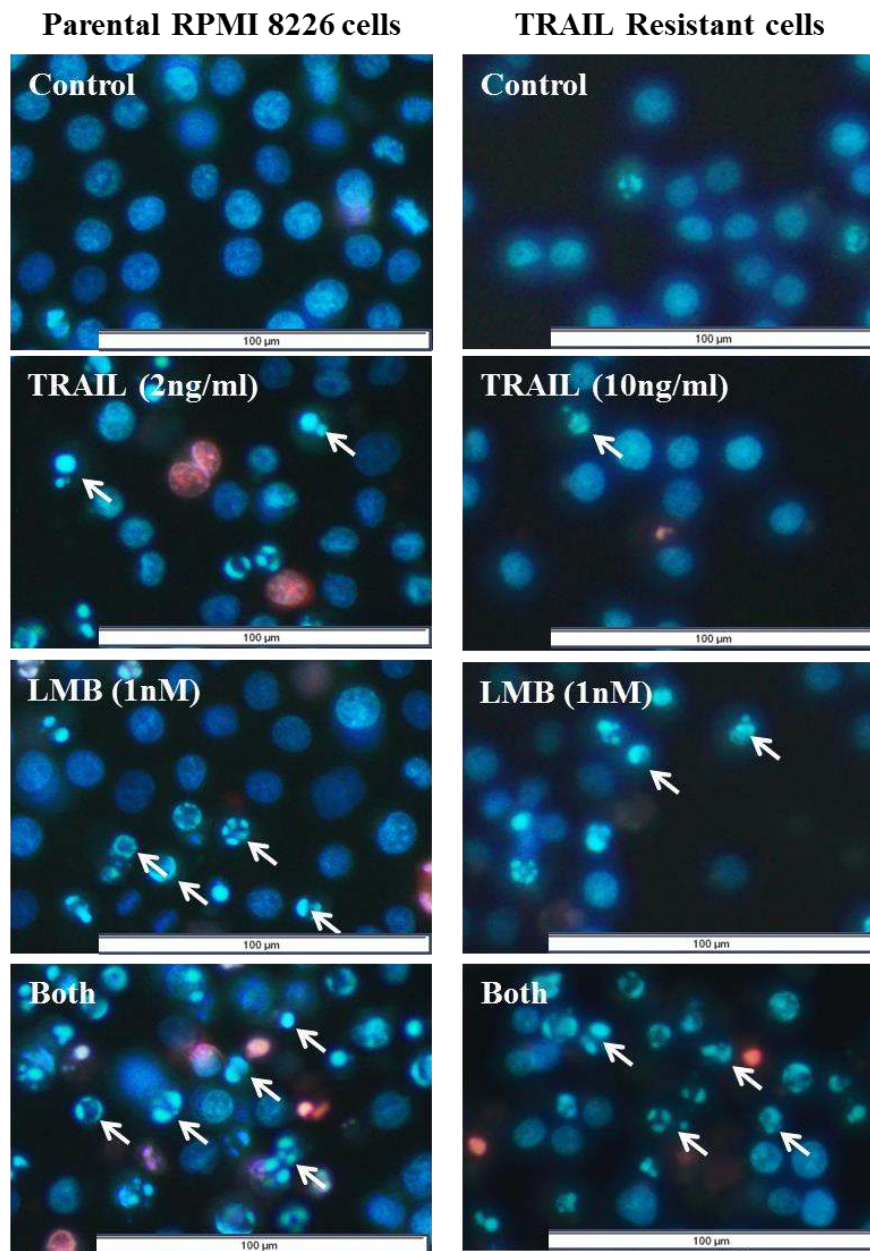
Figure 2.26: a) Effect of LMB on apoptosis in TRAIL-resistant population. Data is expressed as median with range (three independent experiments, each in triplicate). The statistical significance was determined by comparison with the vehicle control, statistical significance was set at p<0.05 by the Kruskal–Wallis test. b) Morphological assessment of apoptosis using Hoechst 33342 /PI nuclear staining, after treatment with LMB in combination with TRAIL in parental and TRAIL-resistant RPMI 8226 cell lines.

2.3.6.3 *Effect of SAHA in Combination with TRAIL in TRAIL-Resistant Multiple Myeloma Cells*

To investigate the effect of SAHA to induce apoptotic cell death in TRAIL resistant populations Hoechst 33342 staining of nuclear morphology was used. The data are illustrated in Figure 2.27 which demonstrates that TRAIL resistant populations are not sensitized to TRAIL by SAHA. Both SAHA and combination responses significantly reduced in TRAIL^R NCI-H 929 cells (p<0.05) and significant loss of SAHA-induced sensitization to TRAIL in TRAIL^R RPMI 8226 cells (p<0.05) (Figure 2.27). An example of morphological assessment of apoptosis using Hoechst 33342 nuclear staining on parental and TRAIL^R NCI-H 929 population after treatment with SAHA alone and in combined with TRAIL is shown in Figure 2.27 b.

Figure 2.27: Effect of SAHA on apoptosis in TRAIL-resistant population

a)
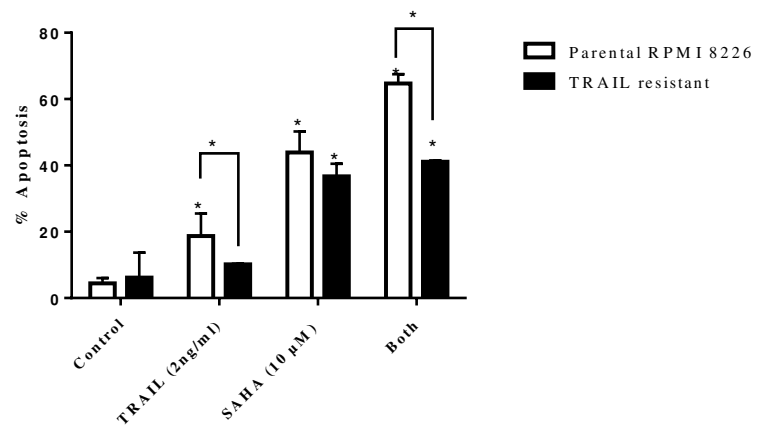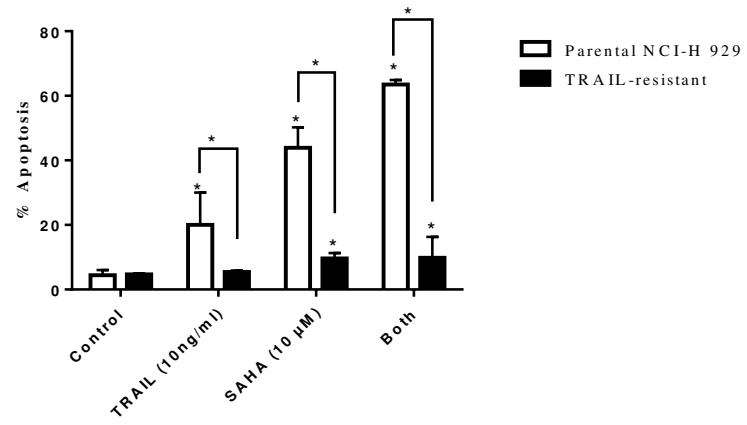
Figure 2.27 b a: Morphological assessment of the effect of SAHA on apoptosis in

NCI-H 929 TRAIL-resistant population
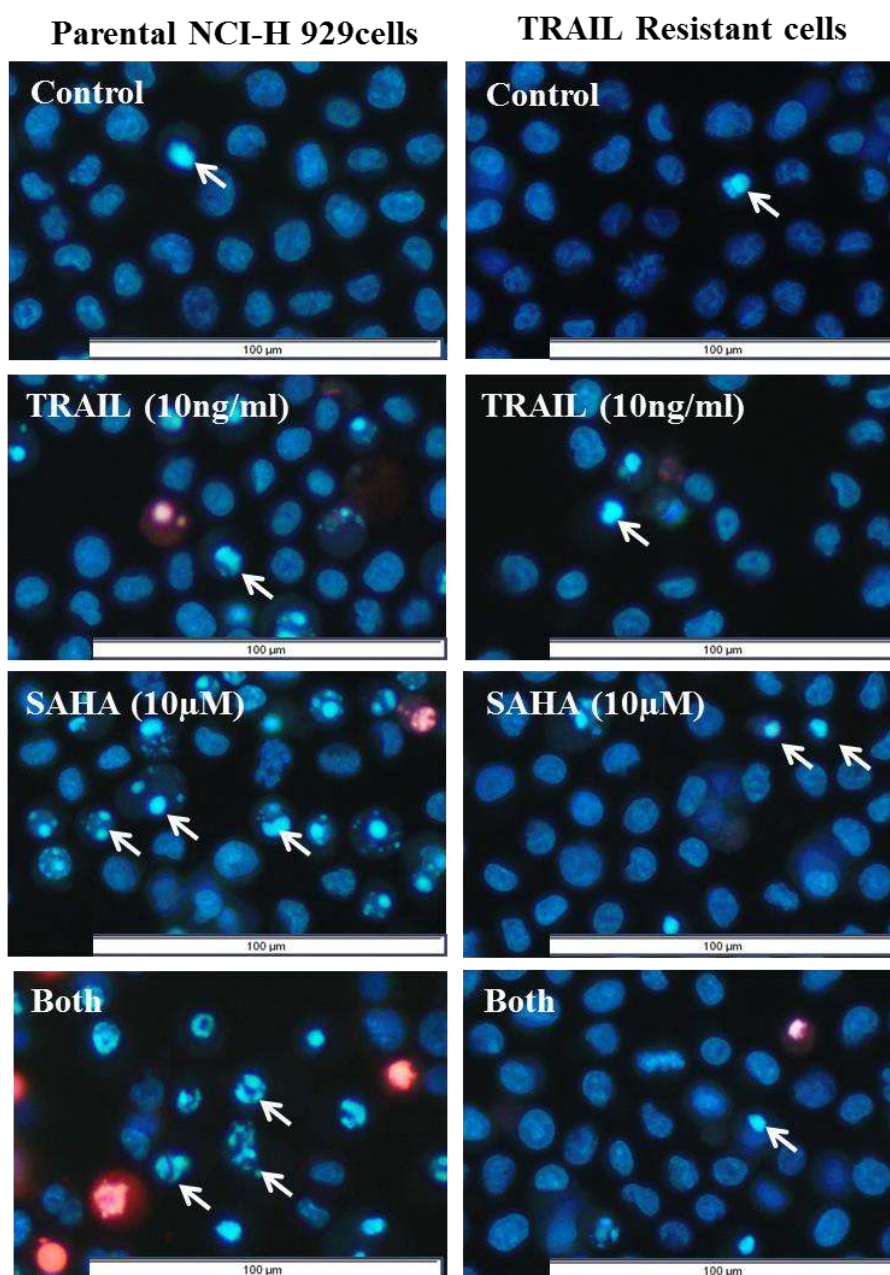
Figure 2.27: a) Effect of SAHA on apoptosis in TRAIL-resistant population. Data is expressed as median with range (three independent experiments, each in triplicate). The statistical significance was determined by comparison with the vehicle control, statistical significance was set at p<0.05 by the Kruskal–Wallis test. b) Morphological assessment of apoptosis using Hoechst 33342 /PI nuclear staining, after treatment with SAHA in combination with TRAIL in parental and TRAIL-resistant NCI-H 929 cell lines.

2.3.6.4 *Effect of the G9a HMTase[i] BIX 01294 in Combination with TRAIL in TRAIL-Resistant Multiple Myeloma Cells*

The effect of BIX 01294 to induce apoptotic cell death in TRAIL resistant populations was investigated using Hoechst 33342 staining of nuclear morphology. The data are illustrated in Figure 2.10 which demonstrates that significant increased BIX 01294 sensitivity on TRAIL-resistant NCI-H 929 cells while significant loss (p<0.05) of TRAIL sensitivity and BIX 01294-enhanced TRAIL responses in TRAIL-resistant RPMI 8226 cells (Figure 2.28). An example of morphological assessment of apoptosis using Hoechst 33342 nuclear staining on parental and TRAIL-resistant RPMI 8226 population after treatment with BIX 01294 alone and in combined with TRAIL is shown in Figure 2.28 b.

Figure 2.28: Effect of BIX 01294 on apoptosis in TRAIL-resistant population

a)
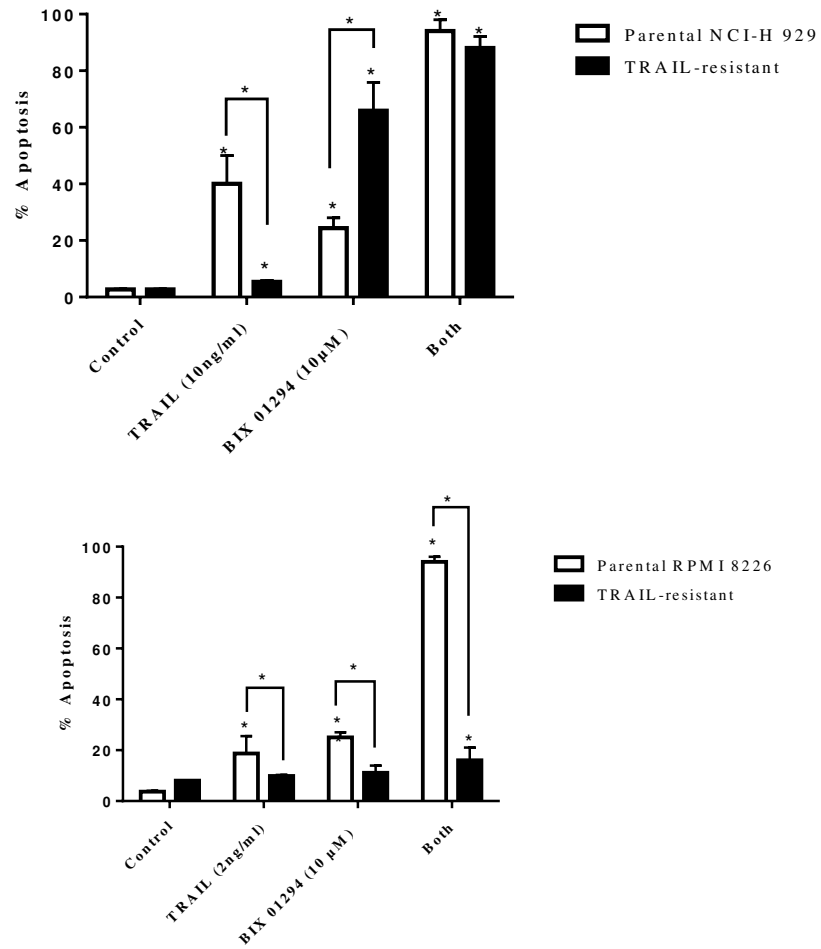
Figure 2.28 b: Morphological assessment of the effect of BIX 01294 on apoptosis in RPMI 8226 TRAIL-resistant population
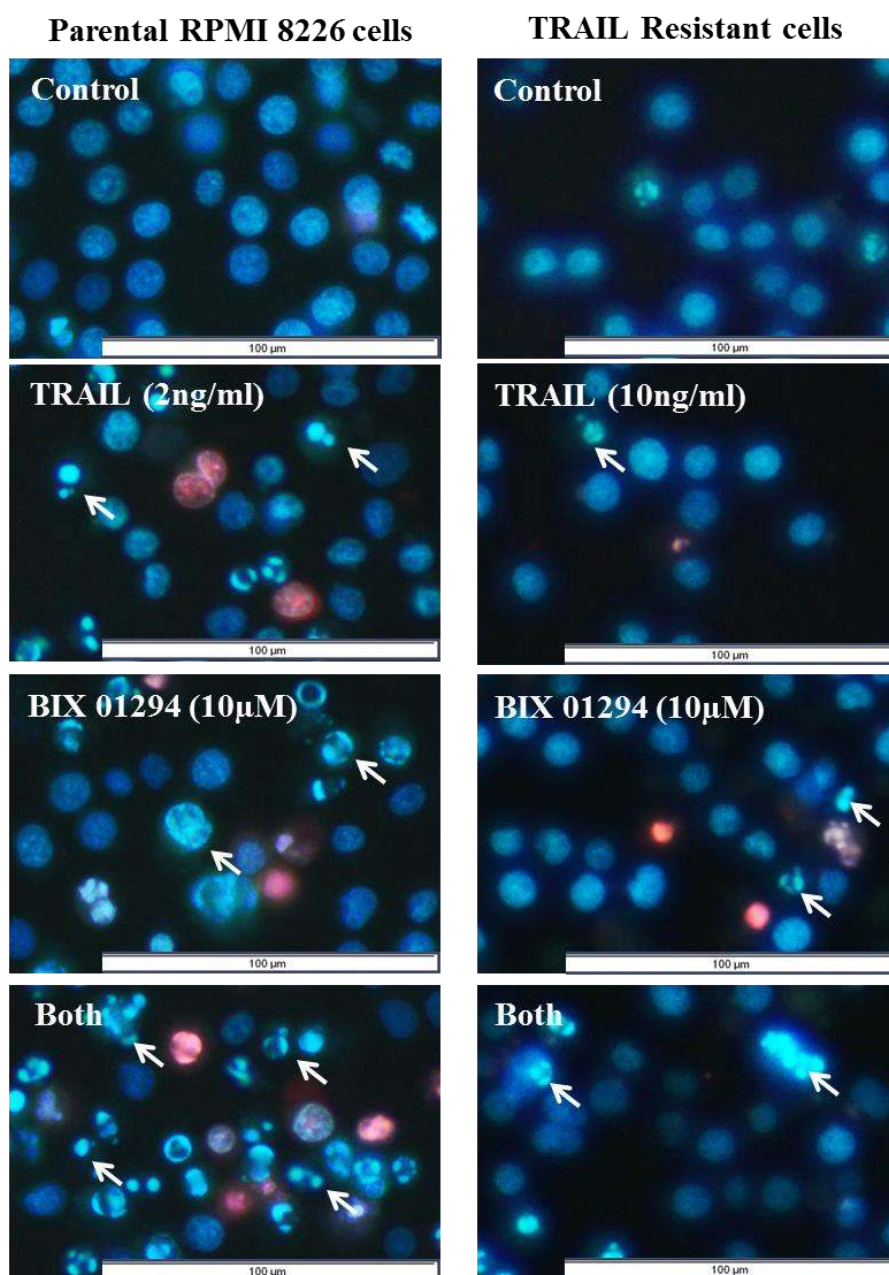
Figure 2.28: a) Effect of BIX 01294 on apoptosis in TRAIL-resistant population. Data is expressed as median with range (three independent experiments, each in triplicate). The statistical significance was determined by comparison with the vehicle control, statistical significance was set at p<0.05 by the Kruskal–Wallis test. b) Morphological assessment of apoptosis using Hoechst 33342 /PI nuclear staining, after treatment with BIX 01294 in combination with TRAIL in parental and TRAIL-resistant RPMI 8226 cell lines.

2.3.6.5 *Effect of the HMTase[i] GSK343 (EZH2[i]) in Combination with TRAIL in TRAIL-Resistant Multiple Myeloma Cells*

To determine the effect of GSK343 to induce apoptotic cell death in TRAIL resistant populations parental and TRAIL[R] were treated with GSK343+/-TRAIL for 24 h. The data are shown in Figure 2.10 which demonstrates that there was a significant reduction of the percentage of apoptosis in response to TRAIL and GSK343 in TRAIL[R] populations compared to parental cells and significant loss GSK343-induced TRAIL-sensitization in TRAIL-resistant RPMI 8226 cells ($p < 0.05$) (Figure 2.29). An example of morphological assessment of apoptosis using Hoechst 33342 nuclear staining on parental and TRAIL[R] RPMI 8226 population after treatment with GSK343 alone and in combined with TRAIL is shown in Figure 2.29 b.

Figure 2.29: Effect of GSK343 on apoptosis in TRAIL-resistant population

a)
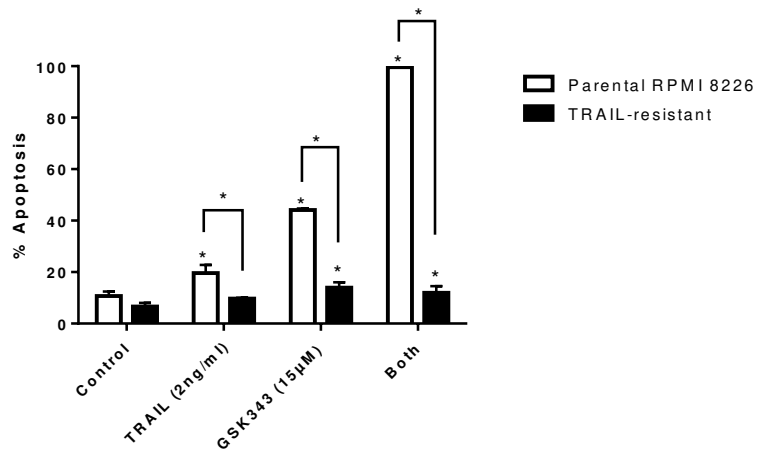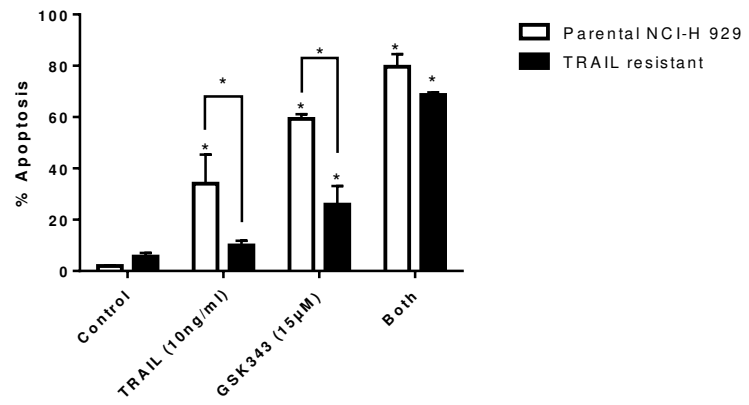
Figure 2.29 b: Morphological assessment of the effect of GSK343 on apoptosis in RPMI 8226 TRAIL-resistant population
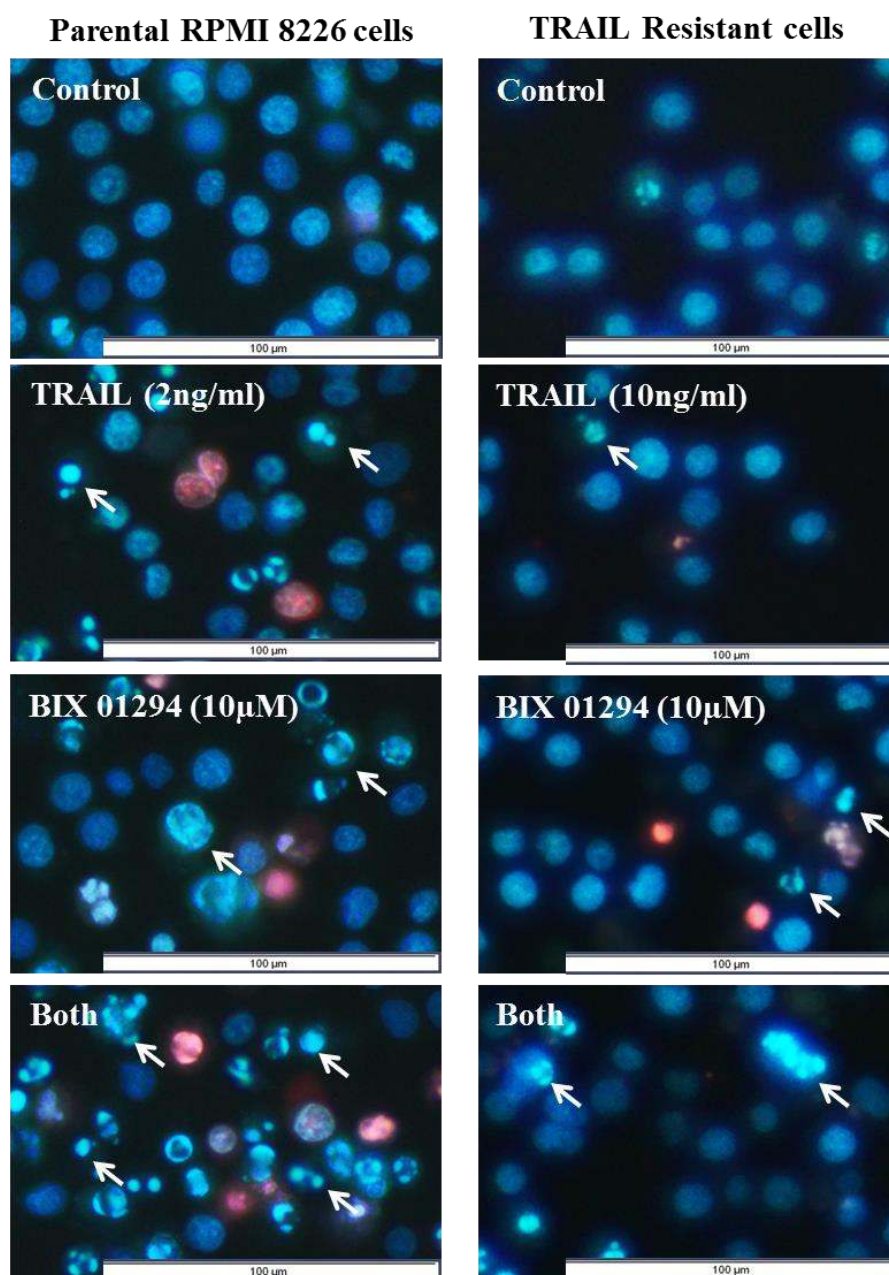
Figure 2.29: a) Effect of GSK343 on apoptosis in TRAIL-resistant population. Data is expressed as median with range (three independent experiments, each in triplicate). The statistical significance was determined by comparison with the vehicle control, statistical significance was set at p<0.05 by the Kruskal–Wallis test. b) Morphological assessment of apoptosis using Hoechst 33342 /PI nuclear staining, after treatment with GSK343 in combination with TRAIL in parental and TRAIL-resistant RPMI 8226 cell lines.

2.4   Discussion

In spite of the constant progress that has been made for available therapy, MM still remains an incurable disease and the relapse from therapy consequently occurs due to the eventual emergence of resistance to the currently used chemotherapeutic agents; therefore, an urgent need arises to find therapies that eradicate all tumour cells (Vitovski *et al*., 2012). Recently, the therapeutic potential of TRAIL-based therapy both *in vivo* and *in vitro* against various tumour cells including MM cells suggests that it may be a promising anti-myeloma therapeutic candidate. However, the susceptibility of multiple myeloma cells to TRAIL-based therapy has been established to be low in most of the myeloma cells lines, which limits its clinical applications (Kagawa *et al*., 2012). This study aimed to investigate the susceptibility and resistance of the MM cells line to apoptosis mediated by TRAIL-based therapies in addition to the combined treatment of TRAIL with other chemotherapeutic therapeutic agents in order to overcome the TRAIL resistance and target TRAIL resistance population.

These results suggest that TRAIL induces apoptosis of different myeloma cells lines with no induction of apoptosis in non-tumour cells haematopoietic stem cell CD133^{+} and normal renal cells HREC. Importantly we have illustrated that TRAIL treatment in combination with other TRAIL sensitizers including LMB, SAHA, BIX 01294 and GSK343 results in sensitising some Multiple Myeloma cell lines to TRAIL; besides, the synergistic effect of TRAIL and these anti-tumour agents varied depending on the drug concentration. A summary of the synergistic apoptotic effect in multiple myeloma cell lines in response to different drugs in combination with TRAIL is shown in Table 2.4.

Moreover, stimulation with TRAIL sensitizers reduced the proliferation of myeloma cells that increases with the co-treatment with TRAIL. This investigation has generated a TRAIL[R] population; however, TRAIL responses in cells that had been selected for

TRAIL resistance were not further enhanced by SAHA and GSK343 in both multiple myeloma cell lines. However, responses to BIX 01294 were increased in TRAIL[R] NCI-H 929 cells and to LMB in TRAIL[R] RPMI cell.

Multiple Myeloma cell line	MMSET	TRAIL Sensitivity	Apoptotic synergistic effect			
			LMB + TRAIL	SAHA + TRAIL	BIX01294 + TRAIL	GSK343 + TRAIL
OPM2	+	+	+	-	-	+
RPMI 8226	-	+	+	+	+	+
NCI-H 929	+	+	+	+	+	+
ADC-1	+	+	+	+	+	+
U266	-	-	+	+	+	+
JJN3	-	-	+	+	+	+

Table 2.3: A summary of the synergistic apoptotic effect in multiple myeloma cell lines in response to different drugs in combination with TRAIL

2.4.1 Leptomycin Restores the TRAIL Sensitivity and Inhibits Cell Proliferation of multiple myeloma Cell Lines.

TRAIL can initiate both extrinsic and intrinsic apoptotic cascades that converge on the executioner caspases-3 or -7 to trigger cell death (Testa., 2010). Of the cell lines investigated, RPMI 8226, NCI-H 929 and OPM2 as well as primary cell line ADC-1 exhibited the greatest apoptotic response following treatment with TRAIL, although the magnitude of response may differ among these cell lines, whereas the U266 and JJN3 cell lines were the least sensitive (Figure 2.5). The reason for the variation in sensitivity between MM cells lines is unclear, but it may reflect differences in the levels of the expression of TRAIL receptors (R1 and R2) and/or downstream signalling components between cell lines. Moreover, TRAIL induced apoptosis in CD34^{+} HSC with no induction of apoptosis in non-tumour cells haematopoietic stem cell CD133^{+} HSC and

renal cells HREC (Figure 2.5). However, in earlier work, TRAIL showed no apparent toxicity to hematopoietic stem cells CD34^{+} (Gazitt., 1999).

Consistent with this study, Vitovski *et al*., (2012) demonstrated that Flow cytometric analysis of Annexin V labelled myeloma cells (RPMI8226, NCI H929 and the OPM-2) after TRAIL treatment demonstrates the presence of TRAIL-induced apoptosis in all three cell lines. Additionally, TRAIL induced apoptosis in the MM cell lines apoptosis was mediated via the activation of both extrinsic and intrinsic apoptotic pathways (Vitovski *et al*., 2012).

Similar responses were observed in the previous studies that investigated the TRAIL sensitivity on the RPMI 8226 cell line. Cheriyath *et al*, (2007) displayed that treating the RPMI 8226 cell line with (25 ng/ml) TRAIL markedly increased cell death from 0.3% to 46.8% after 24 hours and from 1.2% to 11.1% after 72 hours and that the co-treatment with IFN-α2b (250 IU/ml) for 24 hours enhanced the susceptibility to TRAIL-induced apoptosis. Moreover, it has been found that the apoptotic effect of TRAIL was mediated via inducting the cleavage of molecular parameters of apoptosis PARP, MST1, and DFF-45A by 6 hours, an effect that sustained to 24 hours (Cheriyath *et al*, 2007).

The NEI LMB was shown to be a very potent anti-cancer drug against a range of cancer cell lines *in vitro* by inhibiting the export of CRM1-mediated protein from the nucleus such as a tumour suppressor protein p53 that mediates its nuclear activation (Mukta *et al*., 2009). This results in inducing the expression of pro-apoptotic p53 responsive genes including Bax and p21 in order to exhibit different cell responses e.g. apoptosis and cell cycle arrest (Mukta *et al*., 2009). Here, LMB was found to induce apoptosis in a dose-dependent manner in a panel of myeloma cell lines although with varying potency following treatment with 0-5 nM LMB for 24 h (Figure 2.6). In this study, the co-treatment of ADC-1 cells with sub-toxic doses of LMB (0-5 nM) and 2 ng/ml TRAIL significantly potentiated apoptosis to levels greater than those induced by either the

agent alone or by their additive effect (Figure 2.6). The synergistic effect of TRAIL and LMB varied on the other multiple myeloma cells line depending on the drug concentration. Moreover, LMB induced the inhibitory cell growth in the MM cell lines that further increased with the combined treatment with TRAIL. The co-treatment of TRAIL and LMB acted synergistically to inhibit cell proliferation in the MM cell lines U266, RPMI 8226, ADC-1 and additively in JJN3 and OPM2 (Figure 2.11) as well as arresting cell cycle (Figure 2.18).

In recent work, the co-treatment of a CRM1 inhibitor, selinexor and doxorubicin synergistically induced DNA damage and subsequent apoptosis in myeloma cells *in vivo*, *in vitro* and *in ex vivo* samples obtained from patients with relapsed or refractory multiple myeloma (Turner *et al.*, 2016).

This work is considered as the first study investigating the effect of co-treatment of NEI (LMB) and TRAIL in multiple myeloma cells. One previous unpublished work carried out by Haywood *et al*., (2011); working on PC3 prostate cancer cells found out that LMB induced the responses of TRAIL sensitive PC3 cells to TRAIL. This finding suggested that LM and TRAIL act in synergy and that the combination of TRAIL and LM is an effective promising therapy against prostatic cancer.

In previous work, LMB induced apoptosis in leukemia cells through cytochrome c release, caspase activation, and decrease expression of Mcl-1 and XIAP while there was no change in the expression Bcl-2 or Bax (Jang *et al.,* 2004). Other study established that LMB induces apoptosis in the prostate cell line LNCaP cell that contains wild-type p53 gene increased the transcription activity of p53 by trapping pro-apoptotic p53 responsive genes in the nucleus, includes p21, Bax and DR5 by interfering with their nucleo-cytoplasmic export and subsequent proteosomal degradation. However, the null-p53 DU-145 cells did not activate the downstream target genes (Lecane *et al*., 2003). This is consistent with later work that found out NEIs induces cytotoxic effects and

trigger apoptosis and cells cycle arrest in G_2 and/or G_1 phase in tumour cell lines by the block of nuclear export CRM1 dependent protein resultant in p53 nuclear localization and activation in cancer cells (Mutka *et al*., 2009).

2.4.2   SAHA Augmenting TRAIL-Induced Apoptosis and Cytotoxicity in Some Multiple Myeloma Cell Lines

Modification of histone acetylation status has been involved in carcinogenesis (Gillenwater *et al*., 2007). HDAC inhibitors are a class of anti-tumour agents that are able to induce apoptosis and/or cell cycle arrest in tumour cells although the underlying anti-tumour effects of molecular mechanisms are not fully understood. SAHA was developed by modifying the HDAC-inhibitory compound; it has proved to be efficient in cancer treatment both *in vivo* and *in vitro* due to its low toxicity SAHA activity is evaluated in clinical trials (Fandy *et al.*, 2005). HDAC inhibitor, SAHA can potentially re-expressed activate aberrantly silenced tumour suppressed genes via restoring histone acetylation and permitting gene transcription (Gillenwater *et al*., 2007). Inhibition of histone deacetylation mainly induces transcription of positive and negative regulators of proliferation and/or the survival of the cell and growth inhibition or cytotoxicity. (Mitsiades *et al*., 2003; Fandy *et al.,* 2005; Hideshima and Anderson, 2013)

In this study, we have evaluated the effect of HDAC inhibitor SAHA on human different multiple myeloma cell lines. The findings established that together with the SAHA induced apoptosis, inhibition growth and arresting cell cycle, the augmented apoptotic and the cytotoxic effects of TRAIL on U266 and NCI H929 (TRAIL+ 5 or 10 µM SAHA) cell lines (Figures 2.7). Additionally, the co-treatment with SAHA acted synergistically inhibiting cell proliferation in the multiple myeloma cell lines NCI-H 929, U266, OPM2, JJN3 and ADC-1 (Figure 2.11). In addition, the arrests of cell cycle at S phase in U266 when treated with SAHA (Figure 2.19). These results are consistent with a study carried out by Fandy *et al*., (2005) who found out that the two HDAC

inhibitors SAHA and TSA induced growth arrest and apoptosis in human multiple myeloma cell lines and that the augmented apoptotic and cytotoxic effects of TRAIL. However, the cell lines used were different from this study. SAHA and TSA induced the transcription and the expression of surface TRAIL DR4/DR5 death receptors, up-regulated the expression of the pro-apoptotic protein and down-regulated the expression of other anti-apoptotic proteins Bcl-2 and IAPs. Moreover, the cytotoxic effect of SAHA on MM cell lines was shown to be caspase-independent and was mediated via the release of AIF mitochondrial protein. In addition, SAHA induced G_1 phase cell cycle arrest via upregulating $p21^{WAF1}$ and $p27^{Kip1}$ expression and by reducing E2F transcriptional activity (Fandy *et al.*, 2005).

A previous study on B-cell tumour including myeloma has shown SAHA sensitized MM cells to death receptor-induced apoptosis by induction in the level of p21 and p53, and Bid cleavage suggesting a role for Bcl-2 family protein in regulation of SAHA-mediated apoptosis. Moreover, reduction expression of the anti-apoptotic proteins XIAP, flip, and cIAP2 has been reported following treatment with SAHA. However, SAHA alone did not activate caspase-3, -8, or -9 cleavages in multiple myeloma cell line (Mitsiades *et al.*, 2003).

Earlier work investigated the potential of combining HDAC[i] with TRAIL in multiple myeloma and compared the effects of combination treatment *in vitro* in MM cell lines with efficacy *in vivo* preclinical screening. *In vitro,* cell line-based studies showed synergistic induction of apoptosis in MM cell lines OPM2, RPMI 8226, JJN3, and U266 following treatment with HDAC[i] in combination with TRAIL. In addition, the HDAC[i] and TRAIL combination established dose-limiting toxicities that prohibited long term treatment (Matthews *et al.*, 2013).

More recently, co-treatment of SAHA and TRAIL have shown synergistic induction of apoptosis, inhibition of cell proliferation and change in cell cycle distribution in breast

cell cancer (Zhou *et al*., 2016). Moreover, combination therapy significantly induced the pro-apoptotic modulating molecules DR5 and caspase-3, and they also significantly suppressed the expression of anti-apoptotic molecules Bcl-2 (Zhou *et al*., 2016). Consistent with these findings Rosato., *et al* (2003) demonstrated that that co-administration of TRAIL with HDAC inhibitors SAHA or sodium butyrate synergistically induces apoptosis in human myeloid leukaemia cells by cleavage of Bid and Bcl-2, down-regulation of XIAP, moderate reduction on Bcl-XL, depletion of pro-apoptotic Bax as well as cytoplasmic release of cytochrome c, AIF and Smac/DIABLO. This provides further evidence that TRAIL/HDAC Inhibitor activate both the extrinsic and intrinsic pathways of apoptosis by activation of caspase-3 and -8. Furthermore, SAHA treatment showed a marked increase in the percentage of the cell population arrested in G_0/G_1 in addition to the modest increase in the sub-G_0 population which an apoptotic cells indicator. These events were accompanied by marked up-regulation of $p21^{WAF1/CIP1}$ (Rosato *et al*., 2003). In other study carried by Gillenwater *et al*., (2007) demonstrated that SAHA selectively inhibited growth, induced apoptosis and cell cycle change in head and neck squamous carcinoma cell lines via both intrinsic and extrinsic apoptotic pathways. SAHA–mediated apoptosis through mitochondrial pathway via increase release of cytochrome c, caspase-3 and PARP cleavage in addition to activation of extrinsic pathways signaling via up-grade the expression both Fas and Fas ligand, caspase-8 activation and Bid cleavage (Gillenwater *et al*., 2007). Furthermore, SAHA induced apoptosis in colon cancer through down-regulation of anti-apoptotic survivin (Huang and Guo., 2006).

This study examined the relation of SAHA and the activities of cellular caspase 3, in MM cell lines. It was found that HDAC inhibitors SAHA can activate caspases 3, in these cell lines (Figure 2.15). These earlier studies and with evidence shown in this

study support that the combination of SAHA and TRAIL could have promise in the cure of a number of tumours including MM.

2.4.3 The G9a HMTase[i] BIX 01294 Restores the TRAIL Sensitivity and Inhibits Cell Proliferation of MM Cell Lines.

Multiple myeloma SET domain (MMSET)/ (NSD2) is a lysine histone methyltransferase (HMTase) found abnormally expressed in many tumours, emerging as a potential target for therapeutic strategies against MM, especially t(4;14) myeloma subtype that is associated with a significantly poor prognosis (di Luccio., 2015). Loss of MMSET expression change adhesion properties, inhibits growth, and trigger apoptosis in myeloma cells by alter the genes involved in the regulation of apoptosis and the p53 pathway such Bax, Bcl-2, the cell cycle such as Cyclin E2, E2F2, and CDC25A, DNA repair genes such as ATM and GADD45A (Martinez-Garcia *et al*., 2011). Unfortunately, clinically useful HMTase inhibitors have yet to be developed.

BIX 01294 is a histone-tail mimetic inhibitor targeting the SET domain of G9a like protein HMTase and crystal structure basis of BIX 01294 illustrated that it is binding into the histone-tail cleft of the NSDs SET domain (Chang *et al*., 2009). It has been found that the selective inhibition of the NSDs may be achieved by small selective molecules targeting the histone-tail site (di Luccio., 2015). The expression of G9a is upregulated in various cancers type compared with normal tissue and G9a knockdown in cancer cell lines caused growth inhibition and apoptotic cell death with an increase in sub-G_1 population (Shankar *et al*., 2013), suggesting that BIX 01294 is potential therapeutic agent (Kim *et al*., 2013; Varier and Timmers, 2011).

In this study, BIX 01294 was found to produce significant increasing of apoptosis and decreasing the ATP levels in MMSET-positive cells (NCI-H929, OPM2 and ADC-1) (Figure 2.8 and 2.12) whereas in combination with TRAIL, BIX 01294 synergistically enhanced TRAIL responses on induction of apoptosis and reduction of ATP production

in MMSET-negative cell lines (RPMI 8226, U266 and JJN3) (Figure 2.8 and 2.12) and arresting cell cycle (Figure 2.20). G9a inhibitor BIX 01294 inhibits cell growth and apoptosis in a time-dependent manner in oral squamous cell carcinoma cell lines (Ren *et al*., 2015). Moreover, BIX 01294 inhibited the growth, induced apoptosis of bladder cancer cell lines and significantly decreased the cells proportion in the S-phase with increased in the sub-G_1 phase in a dose-dependent manner (cho *et al.,* 2011). Furthermore, a recent study demonstrated that BIX 01294 stimulated caspase-dependent apoptotic cell death in bladder cancer cells lines by up-regulated the pro-apoptotic protein PMAIP1 and down regulation the expression of the anti-apoptotic protein (Cui *et al.,* 2015). Another study has shown that BIX 01294, a specific G9a inhibitor reduced proliferation of neuroblastoma cells and promotes apoptosis by activating caspase-3 and -8 as well as increased a doxorubicin-induced inhibitory effect on cell proliferation (Lu *et al*., 2013).

However, the specific mechanism of the apoptosis mediated by G9a-mediated apoptosis in cancer cells still unclear. Lysine methylation of histone by the methyltransferase G9a is mostly linked to transcriptional repression. Transcriptional suppression of genes, including myogenin, p21, embryonic β-globin and JAK2 is dependent on G9a methyltransferase activity (Shankar *et al*., 2013). Inhibition of G9a activity with BIX 01294 re-expressed tumour suppressor genes (Shankar *et al*., 2013). Moreover, G9a was demonstrated to be present in a complex with E2F6 and other polycomb group proteins on E2F responsive promoters in G_0 stage so it will repress Ef2 responsive genes and block cell cycle progression (Ogawa *et al*., 2002). In gastric cancer, G9a is involved in repression of Runt-related transcription factor 3 (Runx3) which is inactivated in gastric cancer. In Runx3- expressing gastric cell, hypoxia induces the accumulation of G9a and H3K9me2 marks which cause silencing of Runx3 gene. G9a over-expression in gastric cancer cells grown under hypoxic conditions leads to further repression the expression

of tumour suppressor gene Runx3 (Chen *et al.*, 2006). Furthermore, knockdown of histone lysine methyltransferase in breast cancer upregulated the expression of seven in absentia homolog (SIAH1), tumour suppressor gene which induces apoptosis by activation the JNK pathway and suppresses invasion by inactivating the ERK pathway and the apoptosis stimulation following G9a siRNA treatment was recovered by knockdown of SIAH1 (Cho *et al.,* 2011).

A recent study on osteosarcoma cells has shown that G9a inhibitor agent either alone or in combination with double-strand breaks (DSBs)-inducing agents phleomycin selectively inhibited growth, induced G_2 delay and synergistically trigger apoptosis in a p53-independent manner without noticeably effect on non-tumourigenic cells. In addition, Agarwal and colleagues (2016) established that inhibition of G9a catalytic activity inhibits repair of double-strand breaks and possibly another type of DNA damage, resulting in damage persistence and ensuing inhibited proliferation and death of tumour cells (Agarwal *et al*., 2016), potentially as a cause of increase TRAIL sensitivity seen here. For the first time, this study has shown that combination treatment of TRAIL and specific G9a inhibitor BIX 01294 in any tumour type could act in a synergistic manner.

2.4.4 The EZH2 inhibitor, GSK343 Enhances TRAIL-Induced Apoptosis and Cytotoxicity in some Multiple Myeloma Cell Lines

EZH2 is an epigenetic regulatory protein which transcriptional silencing the expression of target genes. EZH2 is the catalytic subunit of PRC2, which has been involved in carcinogenesis (Verma *et al.*, 2012). EZH2 catalyzes trimethylation of lysine 27 (Lys 27) on histone H3 (H3K27) (Popovic *et al.*, 2014). Over-expression of EZH2 is found in many types of solid tumours as well as haematological malignancies (Matsukawa *et al.,* 2006; Varambally *et al*., 2002; Croonquist and Van Ness *et al*., 2005; Kleer *et al.,* 2003). High levels of EZH2 are correlated with cancer growth, metastasis, as well as the poor

outcome. A number of small molecule EZH2 inhibitors have been identified and demonstrated potent anti-cancer activity (Garapaty-Rao *et al.*, 2013). However, the exact mechanisms of apoptosis inhibition by EZH2 still poorly understood. The discovery of inhibitors of epigenetic processes leads to a reversal of epigenetic silencing by EZH2 in cancer cells (Curry *et al.*, 2015).

The two HMTases, MMSET and EZH2, that have founded genetic links to oncogenesis. EZH2, which mediates trimethylation of histone H3K27 and is linked with gene silencing, was exhibited to be coordinately expressed and function upstream of MMSET, which stimulate histone H3K36 dimethylation and is connected with active transcription. In addition, oncogenic functions of EZH2 need MMSET activity. Together, these results suggest that the EZH2-MMSET HMTase may represent an attractive therapeutic target in cancer (Asangani *et al.*, 2013). Earlier work demonstrated the interaction between MMSET and EZH2 in multiple myeloma oncogenesis and MMSET over-expression change patterns of EZH2 chromatin binding and methylation status. In addition, (4;14) translocated myeloma cells may be particularly sensitive to inhibition of EZH2 inhibitor as well as the ability of EZH2[i] stimulates miR126 expression which can then directly suppress the expression of c-MYC (Popovic *et al.*, 2014). However, in current work, EZH2 inhibitor induced apoptosis in multiple myeloma cells independently of MMSET expression.

In this work, EZH2 inhibitor, GSK343 had diverse effects when combined with TRAIL, producing either synergist or additive depending on multiple myeloma lineage and the drug dose. In this study, GSK343 alone potently induced apoptosis in U266, NCI-H 929and RPMI 8226 in high dose of drugs whereas the significant synergistic effect was observed in OPM2, RPMI 8226, NCI-H929, U266, JJN 3, and ADC-1 and however effect sizes in the latter cell line was smaller only in combined dose of 15 μM GSK 343 and 2 ng/ml TRAIL (Figure 2.9). Moreover, GSK 343 significantly reduced ATP levels

within JJN3 cells whereas the synergistic enhancement of proliferation inhibition was observed in RPMI 8226, NCI-H 929, and U266 (Figure 2.13) as well as arresting cell cycle (Figure 2.21).

Knockdown of EZH2 by short hairpin RNA suppress cell growth, invasion and stimulate apoptosis of epithelial ovarian cancer human cells in conventional 2D cultures due to the decrease of H3K27Me3 level in these cells (Li *et al*., 2010; Lu *et al*., 2010). Selective EZH2 inhibitor GSK126, EPZ005687, and EPZ-6438 show their certain effectiveness in inhibiting the growth of the EZH2-mutant cells vs. wild-type EZH2 (Wang *et al.*, 2014). Treatment with GSK343 suppresses osteosarcoma cell viability, restrained cell cycle and induction of apoptosis in osteosarcoma via suppression both the EZH2-c-Myc and EZH2-FBP1 signal pathway, suggesting that GSK343 is a potential therapeutic agent for osteosarcoma therapy (Xiong *et al.*, 2016).

Other studies have demonstrated that histone demethylase (UTX) stimulates gene expression by deleting the repressive histone mark (H3K27me3), counteracting the EZH2 activity. Loss of UTX modifies the epigenetic MM cells landscape, resulting tin changed expression of a number of genes, eventually promoting cells through induced proliferation, clonogenicity as well as adhesion. Treatment of the paired multiple myeloma cell lines *UTX* [wt] and *UTX* [-/-] with the specific EZH2 inhibitor GSK343 for a week significantly reduced the viability of ARP-1 (*UTX* wild-type), without any effect on the ARD (*UTX* null indicate that EZH2 inhibition partially reverses mutation mediated by UTX loss and may represent a potential therapy for specific type of MM (Ezponda *et al*., 2014).

In 2016, a recent study showed that inhibition of EZH2 by using UNC1999 and GSK343 decreases viability of MM cell lines in a dose- and time-dependent manner. Moreover, it stimulates apoptosis, cell cycle arrest and inhibits multiple myeloma

colony formation *in vitro* and apoptosis induction by UNC1999 was mediated by caspase-3, -8 and -9 cleavages. In addition to up-regulating the expression of Wnt and MAPK, and UNC1999 down-regulated the expression of a number of oncogenes involved in myeloma most notably CD69, JUNB and XBP1 in the INA-6 MM cell line (Agarwal *et al.,* 2016). Hernando and colleagues (2016) demonstrate that EZH2 inhibition leads to a global H3K27me3 reduction in MM cells and the EZH2 inhibitors treated cells become less proliferative and more adherent compared with EZH2 inhibitors untreated cells (Hernando *et al*., 2016). Moreover, the depletion of EZH2 in inhibiting the senescent state of melanoma cells resulting in proliferation inhibition and restoring the cellular senescence. Furthermore, the co-treatment of both EZH2 and HDAC inhibitors synergistically increase the expression p21/CDKN1A via removing histone deacetylase 1 (HDAC1) form the transcriptional start site CDKN1A as well as the downstream sites (Fan *et al.*, 2011).

Previous work on 8 multiple myeloma cell lines NCI-H 929, MM.1S, U266, KMS18, KMS11, KMS12BM, OPM 2 and RPMI 8226 in a study undertaken by Xie *et al.,* (2011) found that the EZH2[i] DZNep suppressed growth and trigger apoptosis only in NCI-H 929 and MM.1S MM cell lines. The anti-apoptotic Bcl-2 gene was up-regulated in DZNep insensitive MM cells and significant down-regulation of the arachidonate 5-lipoxygenase (*ALOX5*) gene was reported in MM sensitive cells. *ALOX5* has previously been known to have a role stimulating cancer growth and survival. Bcl-2 family inhibitor, ABT-737 synergistically suppressed growth and stimulated apoptosis of DZNep insensitive cells. These findings suggest that EZH2 inhibitor may be utilized therapeutically for a subset of multiple myeloma (Xie *et al.,* 2011).

This is the first study to link EZH2 inhibition to sensitisation of TRAIL in multiple myeloma. Only one previous work reported that EZH2 inhibitor, DZNep displayed large decrease in cell counts but no changes in apoptosis in colon cancer cells compared

to untreated cells, however, more than ten-fold increase in apoptosis was observed in colon cancer cells when these cells were challenged with combined DZNep and TRAIL therapy (Benoit *et al.,* 2013). In addition, DZNep induced transcript levels of DR5 and this was adequate to sensitize colon cancer cells to TRAIL-mediated apoptosis (Benoit *et al.,* 2013). Taken together, these results provide evidence that EZH2 inhibitors are a potential epigenetic target therapy and may senstitze MM to TRAIL-mediated apoptosis.

2.4.5 Prolonged Incubation of TRAIL Sensitive Multiple Myeloma Cells with TRAIL Reduced their Anti-Tumour Sensitivity

The anti-tumour potential of TRAIL either alone or in combination has been established in various *in vivo* models of tumour growth (Deleu *et al.*, 2009; Doi *et al* 2011; Herbst *et al.*, 2010; Von Pawel *et al.*, 2014). The hypothesis that TRAIL^R cells might be resistant to all forms of apoptosis, and that sensitization to TRAIL responses would be lost in TRAIL resistant cells vs. parental cells was tested. Interestingly TRAIL^R cells were sensitive to BIX 01294 and LMB disproving that they were generally insensitive to apoptosis (Figure 2.26 and 2.28).

Myeloma patient treatment usually involves the administration of chemotherapeutic drugs regularly for weeks or months and the initial treatment is usually successfully in that it reduces the tumour burden, but, after a period of time, the disease relapses; this is often the result of the appearance of a more resistant disease, which is increasingly more difficult to treat (Vitovski *et al.*, 2012). In the current study, TRAIL sensitive cells (NCI-H 929 or RPMI 8226) were either treated with a low dose TRAIL for 1 year or high/lethal doses of TRAIL for 6 months. The surviving cells lost their TRAIL sensitivity and become more TRAIL resistances (Figure 2.23 and 2.24). Theremore these TRAIL^R cell lines were no longer sensitized by SAHA and GSK343 (Figure 2.27 and 2.29). Consistent with these observations, Vitovski *et al.*, (2012) demonstrated that the prolonged incubation with TRAIL in myeloma cells results in the emergence of

TRAIL-resistant CD138 cells and reduce the cell toxicity in TRAIL resistant cells compared to the parental, TRAIL-sensitive culture using MTS assay. However, responses to LMB (Figure 2.26) and BIX 01294 alone (Figure 2.28) were increased in TRAIL resistant cells whilst reduced in response to SAHA (Figure 2.27) and GSK343 (Figure 2.29) in TRAIL^R population. This suggests that selection for TRAIL^R phenotype may have unpredictable effects on responses to other anti-tumour agents, but not necessarily inhibiting apoptosis.

2.5   Conclusion

This study has shown that TRAIL significantly induced apoptosis in a dose-dependent manner in multiple myeloma cell line. Moreover, anti-tumour agents LMB, SAHA, BIX 01294 and GSK343 synergistically inducing apoptosis with TRAIL in multiple myeloma cell lines, and the synergy effect of TRAIL and anti-tumour agents varied in multiple myeloma cells lines depending on drug concentration. For the first time, this study has shown that combination treatment of TRAIL and NEI (LMB), HMTase[i], (BIX 01294 or EZH2[i] (GSK343)) in multiple myeloma could act in a synergistic manner with TRAIL. The combination effect of these anti-tumour agents with TRAIL on induction of apoptosis, reduction of ATP level and cell cycle arrest indicate that using these agents could be useful in improving myeloma therapy. Importantly, these findings suggest that these anti-tumour agents may potentially enhance the action of TRAIL and the combined treatment could possibly result in reduction of the treatment doses, avoiding toxicity and using as a novel anti-cancer agent for multiple myeloma. Moreover, TRAIL sensitive cells (NCI-H 929, RPMI 8226) become more TRAIL resistant with incubation with TRAIL. However, the response of these TRAIL resistant cells demonstrated difference response with anti-tumour agents either alone or in combination with TRAIL suggests that selection for TRAIL resistant phenotype may

have unpredictable effects on responses to other anti-tumour agents, but not necessarily inhibiting apoptosis.

These observations are limited to cells grow in suspension and massive response to drugs and TRAIL on the bulk population. These results do not indicate what might happen in the solid bone lesion or address fully whether all cells are killed or whether a cancer stem cell-like population might survival therapy.

3. Comparison of TRAIL Sensitizers in Combination with TRAIL Responses in Suspension vs. 3D Cell Culture

3.1   Introduction

The study of commonly used two-dimensional (2D) and suspension *in vitro* models examining tumour progression and therapy has come under criticism, particularly in relation to the cancer stem cells hypothesis (Ricci-Vitiani *et al*., 2007). This is mostly due to the different behavior of cells when located in *in vivo* animal models. In 2D and suspension cell culture, cancer cells cannot correctly represent the function or structure of a physiological activity as compared with *in vivo* tumour condition (Friedrich *et al*., 2007). For instance, 2D culture cells exhibit uniform growth in most types of cells at the same stage of the cell cycle, and they do not have the phenotypic heterogeneity in terms of cell differentiation and gene expression in tumours (Marjanovic *et al* 2013; Meacham and Morrison., 2013).

In vivo, the cells live in three-dimensional (3D) environments consisting of fibrous networks of extracellular matrix (ECM) that delivers physical and chemical signals to the living cells. In order to understand the cell behavior, it is helpful to study the cell in 3D microenvironment; however, it is challenging to mimic the 3D environments *in vitro* (Chen *et al* 2016). Recently, numerous attempts have been made to produce a 3D cell culture system including free scaffolds for spheroid formation (Burdett *et al.*, 2010; Tung *et al.*, 2011), bioreactors (Rauh *et al*., 2011), gels (Justice *et al*., 2009) and microfluidic chips (Baker, 2011; Huh *et al*., 2011). The development of 3D culture model has many advantages; it has the potential to decrease animal testing, increases data prediction, and decreases the time and cost required in order to recognize novel candidate agents (Wang *et al.*, 2016).

Among the culture model is the alginate bead culture which is a naturally derived 3D model that relies on multi-cellular tumour spheroid formation. Spheroids models are formed from a number of normal as well as cancer cell lines and used to investigate the efficiency of anti-tumour agents and cell interaction (Wang *et al*., 2016). A significant

advantage of this 3D culture system is that the spheroid within the alginate beads can be successfully isolated for further analysis by dissolving the matrix. Also, assay is clonal and each colony derived from a single cell, studies on clonal response are difficult in suspension. These properties make the alginate bead culture system an efficient and convenient culture system for either cell or tissue culture *in vitro* (Xu *et al.,* 2014).

Although some studies illustrated that some therapeutic agents are more effective in 2D culture models (Mueller-Klieser., 1997; Friedrich *et al*., 2007), others demonstrated the superior activity of anti-tumour agents in the 3D cell culture models (Wang *et al*., 2016). Therefore, growing cells in spheroid such as the alginate bead is an efficient culture system that provides a promising alternative to the use of the monolayer systems or suspension systems for haematological cancers (Friedrich *et al*., 2007).

The development of experimental tools to facilitate the study of myeloma cell biology and susceptibility to the therapeutic agents is considerably limited due to the lack of *in vitro* model systems that permits myeloma cells reproducible growth as well as the putative cancer stem cell compartment. Multiple myeloma grow as suspension cells, and 3D cell culture may be used as a model of soft mass disseminated MM lesions that form in bone. The development of 3D model systems has recently been proposed to support *in vitro* myeloma cells expansion, facilitating modeling of *in vivo* responses, including the CD138^{-Ve} myeloma cancer stem cells and offers a physiologically relevant platform on which analyse susceptibility of myeloma cells to various classes of therapeutic agents (Jelinek., 2008).

3.1.1   Hypothesis

The current investigation has focused on the hypothesis that multiple myeloma cells were more sensitive to TRAIL sensitizers in a 3D alginate model than in suspension.

3.1.2 Aims

The aim of this study was to develop a 3D model of multiple myeloma cell lines, asses TRAIL response in 3D vs. suspension and finally asses TRAIL responses in presence and absence of TRAIL sensitizers in 3D vs. suspension.

3.2 Materials and Methods

3.2.1 Experimental Design

Six multiple myeloma cell lines were used for this study: OPM2, RPMI 8226, NCI-H929 and ADC-1 which were previously shown to have high sensitivity to TRAIL treatment and U266 and JJN3 that were the most resistant multiple myeloma cells to TRAIL (Chapter 2). In addition to TRAIL[R] cells (Chapter 2). Myeloma cells cultured as previously described (Chapter 2; Section 2.2.2 and 2.2.3) and incubated in humidified incubator at 37°C. Multiple myeloma cells were seeded into alginate culture in order to establish 3D growth. Colony formation within the alginate beads was assessed by Hoechst 33342 fluorescence microscope and Haematoxylin and Eosin staining of histological slides using an inverted microscope. Myeloma cells within the alginate were treated with the lowest doses of TRAIL +/- sensitizers which have previously been shown to synergistically enhanced apoptosis (as determined by Hoechst 33342/PI staining in suspension culture in Chapter 2).

3.2.2 Alginate Bead Culture Model

Alginate beads as a 3D culture models originally established as a model for studying the behavior of chondrocyte cell (Hauselmann *et al.*, 1992). This 3D model based on the properties of alginic acid derived from brown seaweed, which produces a viscous solution or a gel that able to polymerize in the presence of calcium or any divalent cations. These properties of alginate aid the integration of isolated cells proceeding to polymerisation as well as the formation of semi-solid support post-polymerisation. Moreover, the alginate gel can be dissolved by the addition of a chelating agent; allowing separation of cells from a large tightly cell aggregates to produce individual live cells that can be analysed (Hauselmann *et al*., 1994; Bonaventure *et al*., 1994; Lemare *et al.*, 1998).

3.2.2.1   *Induction of 3D Tumour Spheroid Formation using Alginate Bead Culture*

Multiple myeloma cells were routinely sub-cultured as described in Chapter 2. To establish 3D alginate cultures, myeloma cells at a density of 1×10^6 cells/ml were re-suspended in 1.2% (*w/v*) medium-viscosity sodium alginate in saline (Sigma). The alginate beads were then dropped through a 19-gauge needle into 200 mM $CaCl_2$ and incubated at 37°C for 15 minutes to polymerise. Following incubation, beads were washed twice with 0.15 M NaCl, and then washed in the media before the beads left in the media in the incubator to form spheroids. Alginate cultures were maintained for 10-14 days and the culture medium was changed twice a week (Le Maitre *et al*., 2005). Each 1ml of 1×10^6 cells alginate suspension was generate approximately 40 polymerized beads and each bead contained an average of 2.5×10^4 cells/bead.

3.2.3   Treatment of Multiple Myeloma cells in Alginate Beads with TRAIl+/-TRAIL Sensitisers

After 10-14 days in culture, cells were treated with TRAIL +/- TRAIL sensitizer as described in Chapter 2, using the lowest combination treatment doses that produced synergistically enhanced apoptosis in suspension. Cells were stained with Hoechst 33342/PI after 24 h as described earlier (Chapter 2).

3.2.4   Assessment of Spheroid Formation

3.2.4.1   *Fluorescence Microscopy using Hoechst 33342 and Propidium Iodide (PI) Staining*

In order to assess the colony formation in the alginate beads, beads were imaged every two or three days. Intact alginate beads containing Multiple myeloma cells were dissolved in Eppendorf tube containing 500 µl of alginate dissolving buffer (55 mM sodium citrate (Sigma), 30 mM EDITA (Fisher), 0.15M NaCl (Fisher) at pH 6) and incubated rotating for 10-15 minutes prior to centrifugation at 600g for 5 minutes. Following centrifugation, the spheroid/cell pellet of dissolved alginate beads was

carefully re-suspended in media and transferred into 96 well plates. Hoechst 33342/PI stain (10 µg/ml) was added to both dissolved and un-dissolved beads. The latter to assess apoptosis of colonies *in situ*. Viability and morphological analyses of spheroids formation were carried out on IX81 fluorescence microscope (Olympus) using Hoechst 33342/PI staining and spheroid diameters were determined from images taken.

3.2.4.2 *Histology of Cells in 3D Culture*

Alginate beads cultured for 10-14 days were fixed by immersion in 4% formaldehyde for 20 minutes at 4°C and then kept in 80% ethanol (*v/v*) in cold room. Following fixation, samples were processed into paraffin wax by using a Shandon Elliott Duplex Processor in an automated procedure of dehydration by immersion in IMS (Industrial Methylated Spirit, Fisher Scientific) followed by clearing in sub-X (Xylene Subsitute, Leica) and embedded in paraffin wax before transferred to vacuum oven (Jeio Tech OV-11) and incubated for 1 hour at 60°C and 60 cm Hg. Following incubation, cultured samples were oriented into moulds having molten wax and form a tissue block after cooling. Finally, tissue blocks removed from mould and kept at room temperature and are ready to use for histological sectioning and staining with Haematoxylin and Eosin staining (H&E).

For sectioning, tissue blocks were cut at 4 µm thickness by using a Leica SM2400 sledge microtome and placed on the surface of a 45°C water path prior to mount on glass slides (positively adhesive slide, Leica). Slides were then incubated on a 40 °C drying rack for 30 minutes in order to dry the excess of water from the section slide. Mounted section was kept at 37°C in a desiccating oven until use.

To prepare the slide for staining, section slide was de-waxed with sub-wax for 5 minutes three times prior to rehydrating in ethanol for 5 minutes, three times for each respective ethanol concentration. Sample was stained with filtered Mayer's Hematoxylin

for 5 minutes followed by rinsing with running tap water before stained with Eosin Y (Leica) for 1 minute. After staining, slides were dehydrated and clearing by immersion in ethanol and sub-X in triplicate respectively and mounted by Pertex mountant (Leica). Morphological analyses of spheroids were carried out an Olympus BX60 Microscope and optical images were taken using Q-capture III camera and Q-capture 6 software (Q-imaging-inc).

3.2.5 Statistical Analysis

Data are expressed as the median with range. Shapiro Wilke test using Stats Direct software (Stats Direct Ltd, England) was used for analysis whether data followed a normal distribution. Data which did not follow a normal distribution, Kruskal–Wallis and Connover-Inman post hoc was using to investigate significant differences. $p < 0.05$ was considered statistically significant.

3.3   Results

3.3.1   Multiple Myeloma Cells Formed Multicellular Spheroids

Five out of 6 tested Multiple myeloma cell lines namely OPM2, RPMI 8226, NCIH 929, U266 and JJN3 aggregated and had the ability to form multicellular spheroids structures within 10-14 days. In contrast, ADC-1 cell line form few loosely aggregated cells, when beads were dissolved hardly any intact spheroids were observed. However, TRAIL^R cells did not grow in 3D. Over the course of 10-14 days, the cells proliferated within the alginate beads and the average volume of cell spheroids increased as the culture day expands and the number of cell spheroids increased dramatically. Spheroid colonies range from small colonies of 2-3 cells to approximately 100 cells per spheroid by day 10-14 (Figure 3.1 and 3.2). After being seeded with the same number of cells, NCI-H 929, RPMI 8226 cells grew faster than U266 and JJN3 cells after Day 2 and maintained long term viability up to Day 14, while OPM2 cells reached a plateau after Day 10. In addition, single spheroids of approximately 100-250 μm in diameter were obtained from multiple myeloma cell lines after two weeks. An example of the 3D spheroid formation of alginate beads *in situ* for NCI-H 929 Multiple myeloma cell lines within 10-14 days is shown in Figure 3.2. Representative microscopic images of hematoxylin/eosin (H&E)–stained 4μm paraffin median sections of NCI-H 929 alginate beads which contain a number of spheroids is shown in Figure 3.3.

Figure 3.1: 3D colony formation of multiple myeloma cell lines at day 10
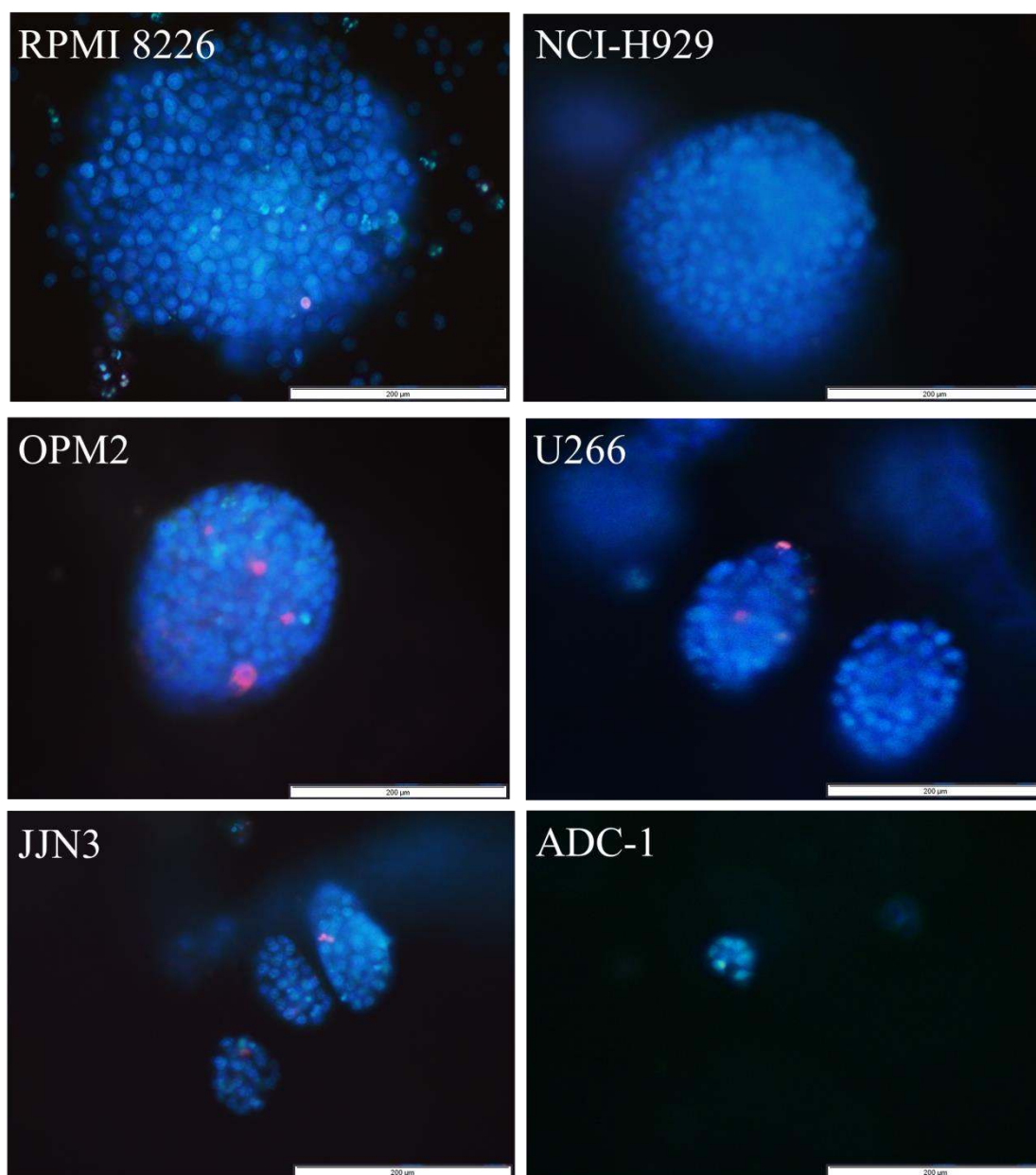
Figure 3.1: 3D colony formation of multiple myeloma cell lines at day 10. RPMI 8226, NCI-H 929, OPM2, U266, and JJN3 multiple myeloma cells proliferated within the alginate beads and form spheroid while ADC-1 cell line did not reliably form 3D colonies.

Figure 3.2: Time dependence formation of the spheroids within alginate beads *in situ* in NCI-H 929 cells
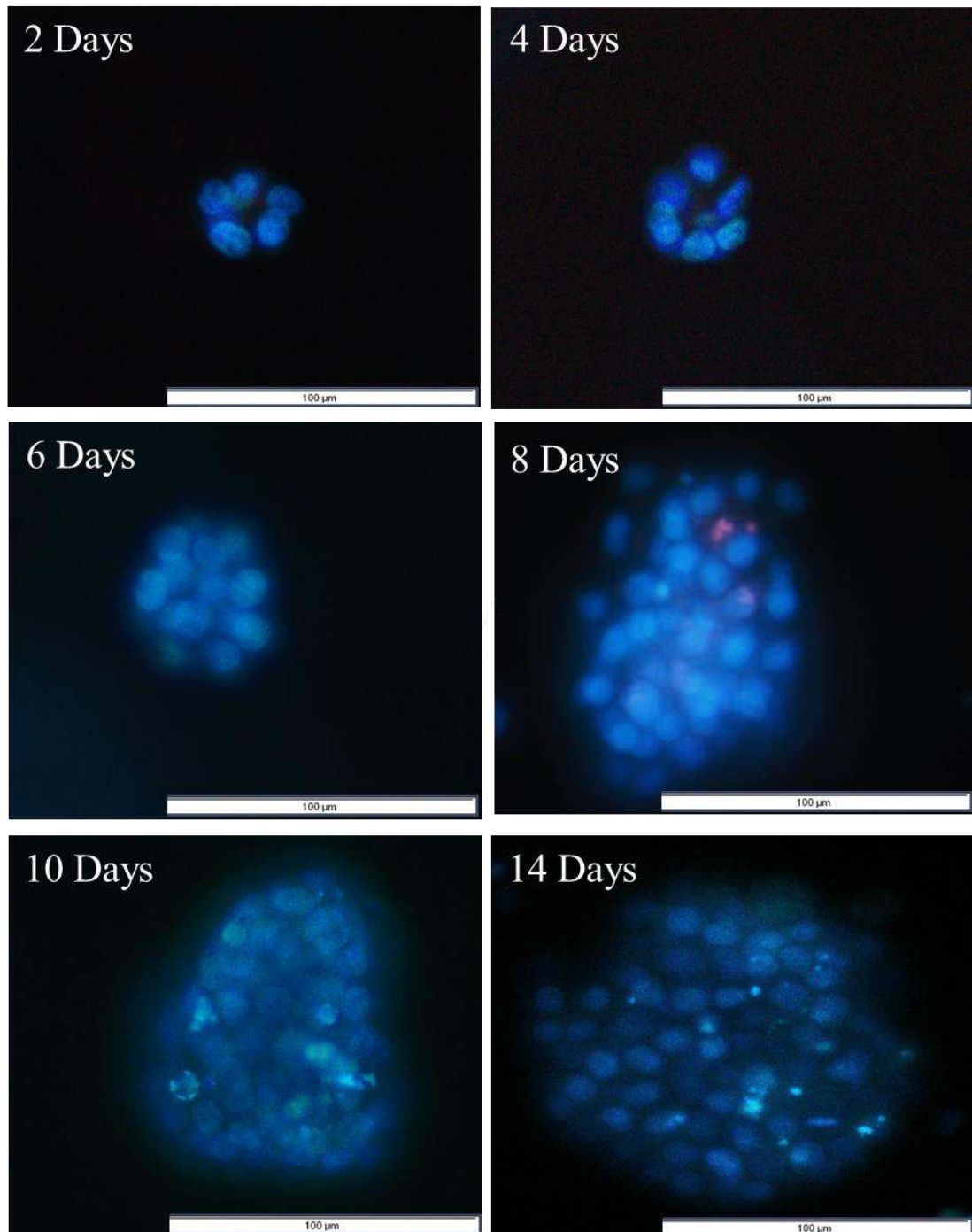
Figure 3.2: Time dependence formation of the spheroids within alginate beads in NCI-H 929 cells. a) Multiple myeloma cells had the ability to form 3D spheroids and the average volume of cell spheroids increased as the culture day expands. On day 2 small colonies of 2-3 cells could see and over course of 10 -14 days, cells proliferated within the alginate beads to form large spheroid colonies.

Figure 3.3: H&E staining of NCI-H 929 cell spheroids cultured in alginate beads on Day 14.
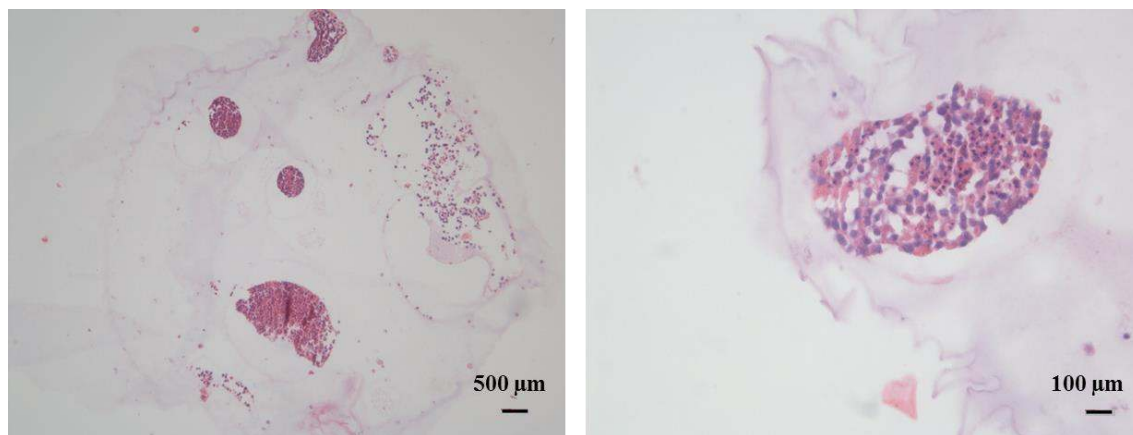
Figure 3.3: H&E staining of NCI-H 929 cell spheroids cultured in alginate beads on Day 14.

3.3.2 Effect of TRAIL Sensitizers in Combination with TRAIL on Apoptosis in Multiple Myeloma Cells Lines in 3D Alginate Cell Culture Model vs. Suspension Cell Culture

3.3.2.1 Effect of LMB in Combination with TRAIL on Apoptosis in Myeloma Cells Lines in 3D Alginate Cell Culture Model vs. Suspension Cell Culture

The effect of LMB on TRAIL-induced apoptosis in 3D cell culture vs. Suspension culture was studied using Hoechst 33342 staining of nuclear morphology. Multiple myeloma cells lines were treated with the lowest combination treatment doses which synergistically enhanced apoptosis in suspension as determined by Hoechst 33342/PI staining after 24 hours of treatment. MM cells were more sensitive to LMB in 3D culture conditions compared to suspension cultures and there was a significant increase in TRAIL-induced apoptosis by LMB treatment in NCI-H929, RPMI 8226, JJN3 and U266 cell lines ($p < 0.05$) (Figure 3.4 a). In TRAIL-sensitive cell line NCI-H 929, an apoptotic response of 16.5±4.6% and 54.2±14.5 % was measured following treatment with low dose of LMB (1nM) for 24 h in suspension and 3D cultures respectively. Whereas, the apoptotic response for combined dose of 0.5 nM LMB and 2 ng/ml TRAIL was 37.5±0.5% in suspension cultures and 99.6±0.5% when cells were grown as a 3D culture model ($p < 0.05$) (Figure 3.4 b). An example of NCI-H 929 cells on suspension and on 3D alginate culture model treated with LMB alone and in combined with TRAIL is shown in Figure 3.4 b.

Figure 3.4: Effect of LMB+/- TRAIL on apoptosis of multiple myeloma cell lines in suspension vs. 3D culture conditions.

a)
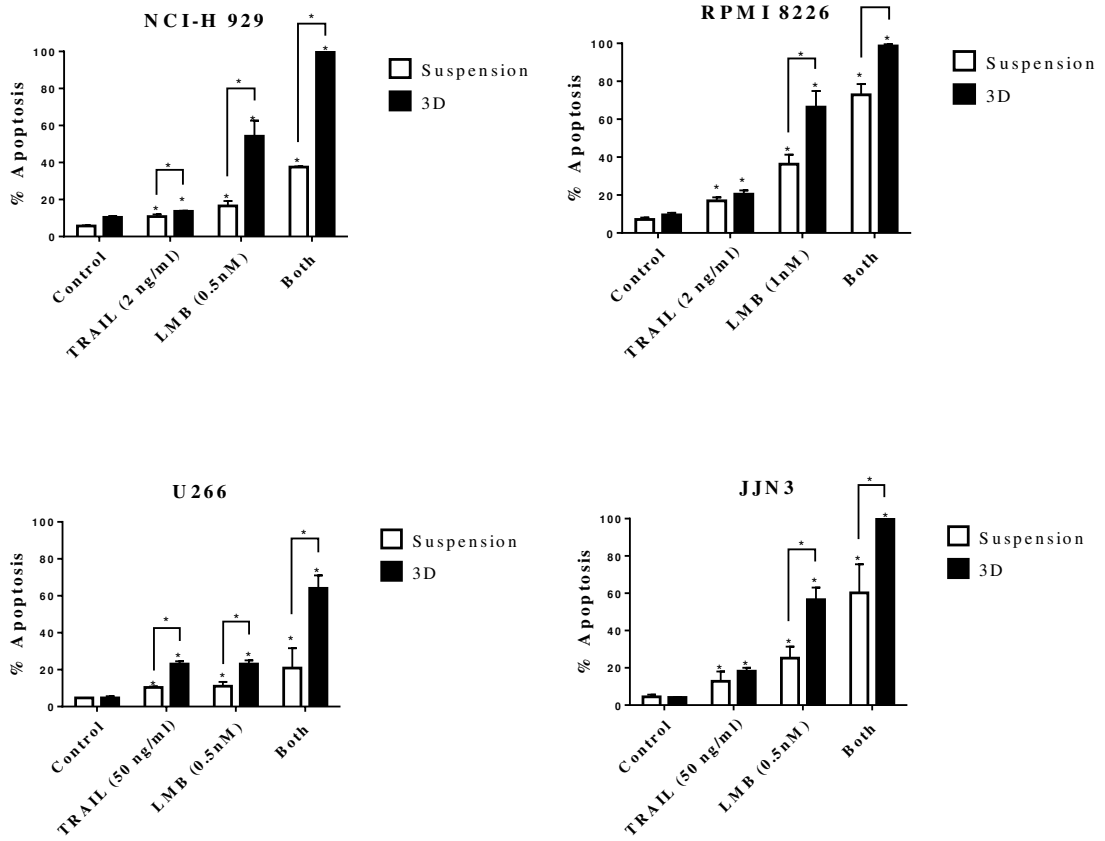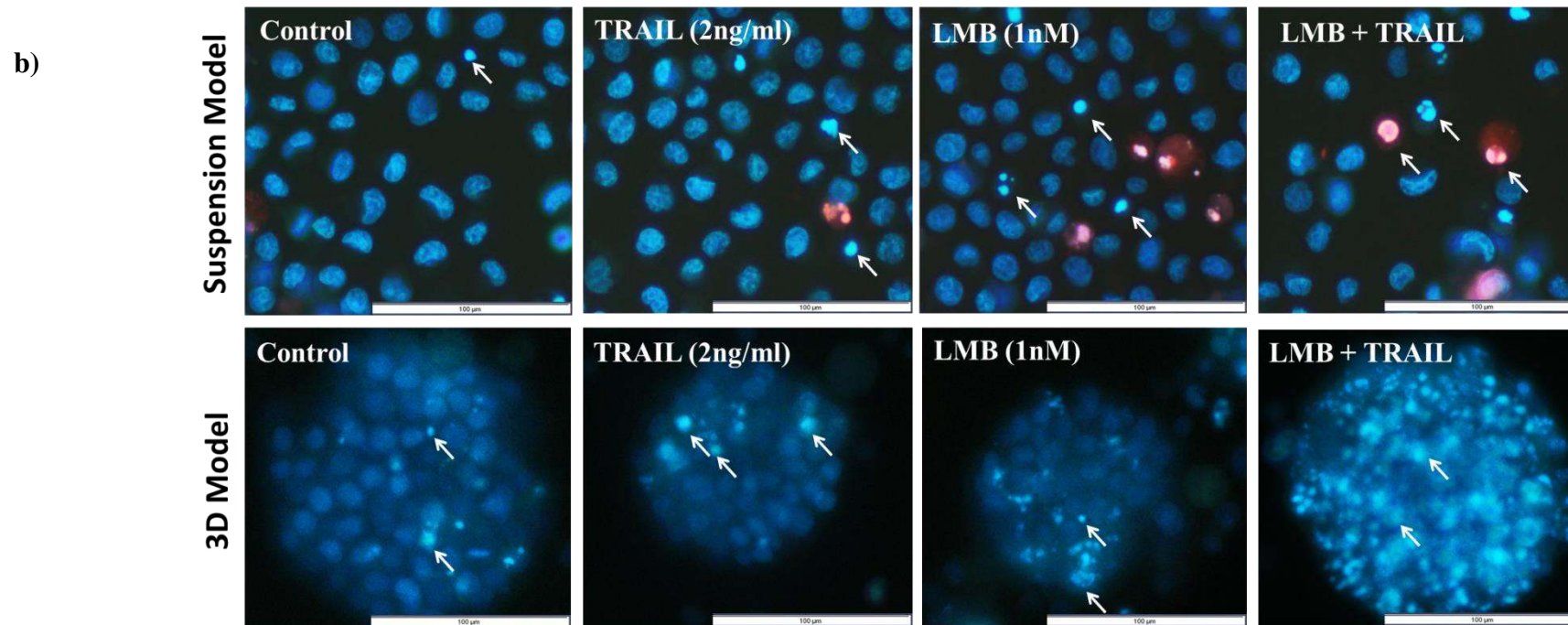
Figure 3.4: a) Effect of LMB+/- TRAIL on apoptosis of multiple myeloma cell lines in suspension vs. 3D culture conditions. Myeloma cells were treated with LMB+/- TRAIL determined by Hoechst 33342 and PI staining for 24 h. *Multiple myeloma cells were more sensitive to a low dose of LMB in 3D based alginate culture compared to suspension culture and synergistic response of LMB and TRAIL in multiple myeloma cell lines was potentiated in 3D cell culture. Data is expressed as median with range (three independent experiments, each in triplicate). p<0.05 was considered statistically significant comparing to control. The synergistic response was defined as a comparison of combination treatment group with the sum of the effects of TRAIL alone + LMB alone and significance determined by using by the Kruskal–Wallis test (p<0.05). b) An example of NCI-H 929 cells in suspension and on 3D alginate culture model treated with Nuclear Export Inhibor (LMB) alone and in combined with TRAIL.*

3.3.2.2 *Effect of SAHA in Combination with TRAIL on Apoptosis in Multiple Myeloma Cells Lines in 3D Alginate Cell Culture Model vs. Standard Cell Culture*

The effect of SAHA on TRAIL-induced apoptosis in 3D cell culture vs. suspension culture was studied using Hoechst 33342 staining of nuclear morphology. TRAIL-sensitive cells NCI-H 929 and TRAIL insensitive cells U266 multiple myeloma cells line were treated with 1 μM SAHA or 0.1% DMSO vehicle control either alone or in combination with TRAIL for 24 h. The data illustrated in Figure 3.5 demonstrated that there was a significant increase in apoptosis in responce to SAHA and TRAIL individually in NCI-H 929, and a significant increase in apoptotic response to combination therapy in suspension culture (p<0.05) (Figure 3.5). NCI-H 929 cell lines were significantly more sensitive to TRAIL, SAHA and combination therapy in 3D vs. suspension (p<0.05) (Figure 3.4). Furthermore, TRAIL insensitive cells U266 were significantly more sensitive to TRAIL and combination therapy, but not SAHA in 3D culture (p<0.05) (Figure 3.5). An example of the 3D spheroid of morphological assessment of apoptosis following SAHA treatment alone and in combined with TRAIL on MM cells *in situ* in alginate beads of NCI-H 929 MM cell lines is shown in Figure 3.5 b

Figure 3.5: Effect of SAHA+/-TRAIL on apoptosis of multiple myeloma cell lines in suspension vs. 3D culture conditions.

a)
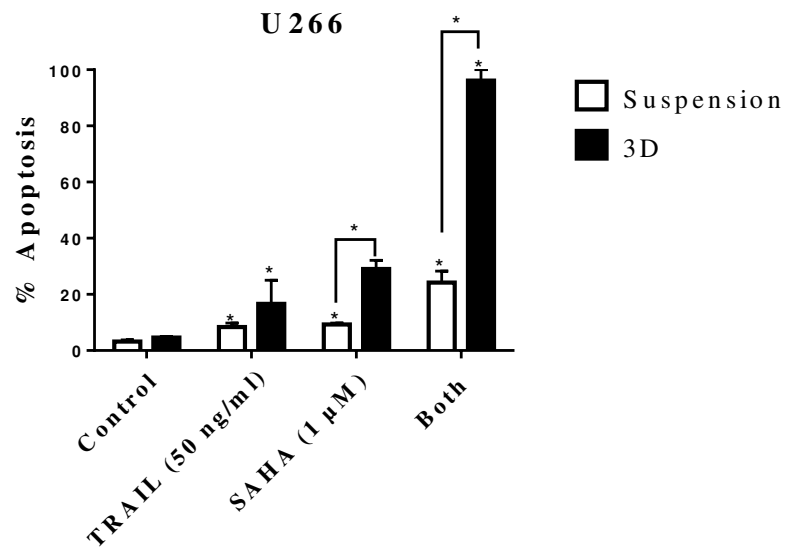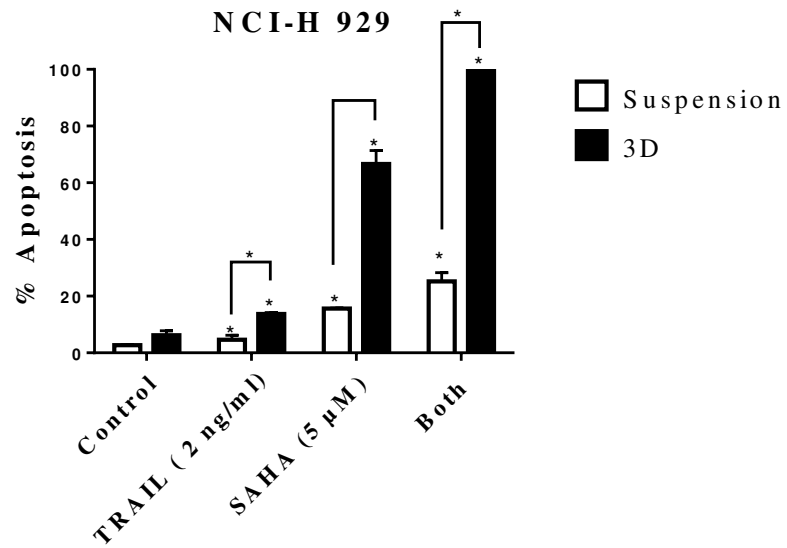
b)
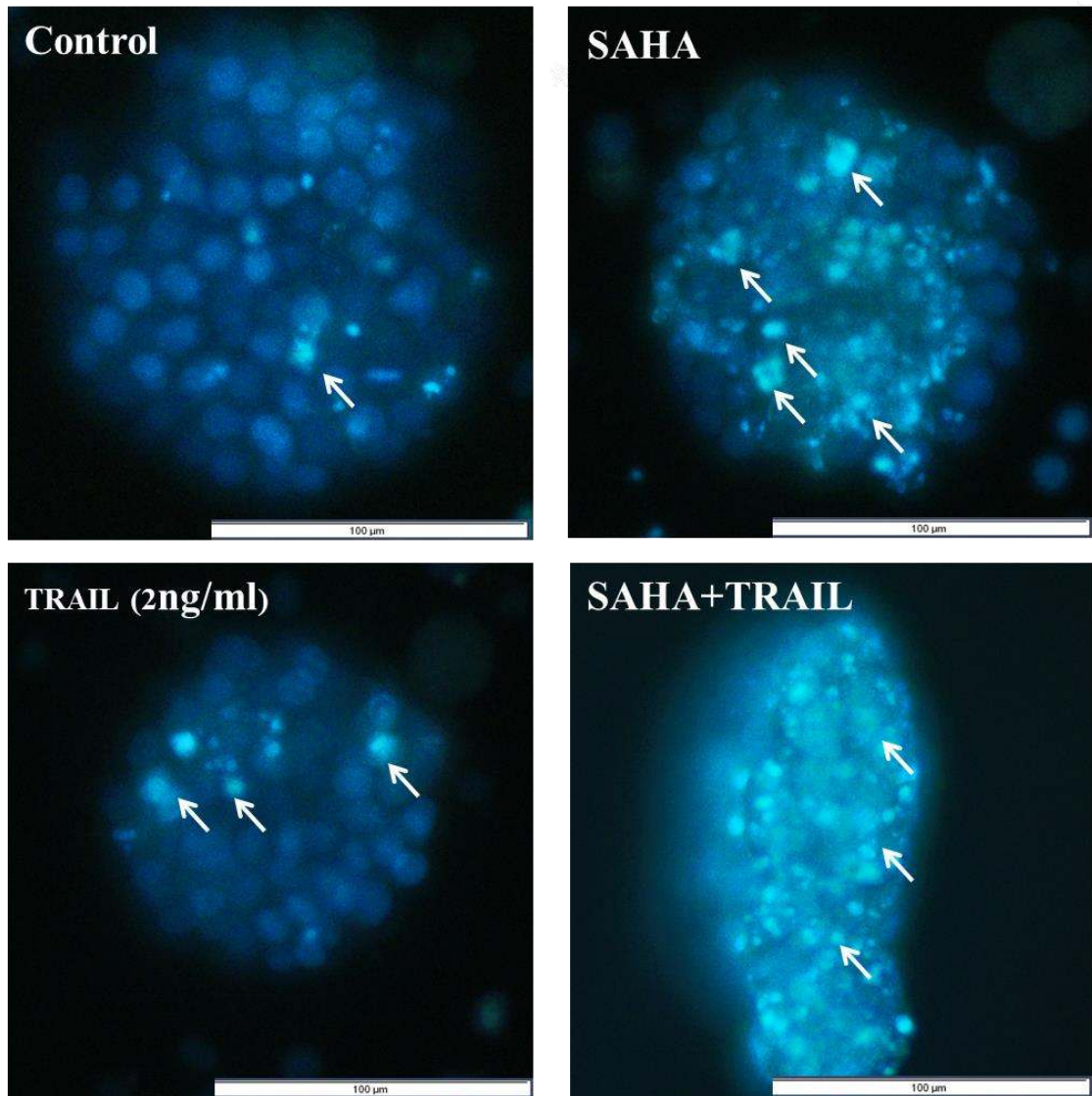
Figure 3.5: a) Effect of SAHA+/-TRAIL on apoptosis of multiple myeloma cell lines in suspension vs. 3D culture conditions. Myeloma cells were treated with SAHA+/- TRAIL determined by Hoechst 33342 and PI staining for 24 h. MM cells were more sensitive to SAHA in 3D based alginate culture compared to suspension culture and synergistic response of SAHA and TRAIL in multiple myeloma cell lines was potentiated in 3D cell culture. Data is expressed as median with range (three independent experiments, each in triplicate). p<0.05 was considered statistically significant comparing to control. b) An example of NCI-H 929 cells on suspension and in 3D alginate culture model treated with SAHA alone and in combined with TRAIL.

3.3.2.3 *Effect of BIX 01294 in Combination with TRAIL on Apoptosis in Multiple Myeloma Cells Lines in 3D Alginate Cell Culture Model vs. Standard Cell Culture*

TRAIL-sensitive cells NCI-H 929 and TRAIL insensitive cells U266 multiple myeloma cells line were treated with BIX 01294 either alone or in combination with TRAIL for 24 hours. Multiple myeloma cells were more sensitive to BIX 01294 in 3D culture conditions compared to suspension cultures and there was a significant increase in TRAIL-induced apoptosis by BIX 01294 treatment in U266 and NCI-H929 cell lines ($p < 0.05$) (Figure 3.6). At the dose of drugs used, there was a significant increase in apoptosis in TRAIL-sensitive cell lines NCI-H 929 in response to TRAIL, BIXI 01294 alone and combination therapy with TRAIL in suspension cultures ($p < 0.05$) (Figure 3.6). NCI-H 929 cell lines were significantly more sensitive to TRAIL, BIX 01294 and combination therapy in 3D vs. suspension ($p < 0.05$) (Figure 3.4). Furthermore, TRAIL resistant cells U266 were significantly more sensitive to BIX 01294, TRAIL and combination therapy in 3D culture ($p < 0.05$) (Figure 3.4). An example of the 3D spheroid of morphological assessment of apoptosis following BIX 01294 treatment alone and in combined with TRAIL on MM cells *in situ* in alginate beads of NCI-H 929 MM cell lines is shown in Figure 3.6 b.

**Figure 3.6: Effect of BIX 01294+/-TRAIL on apoptosis of multiple myeloma cell
lines in suspension vs. 3D culture conditions**

a)
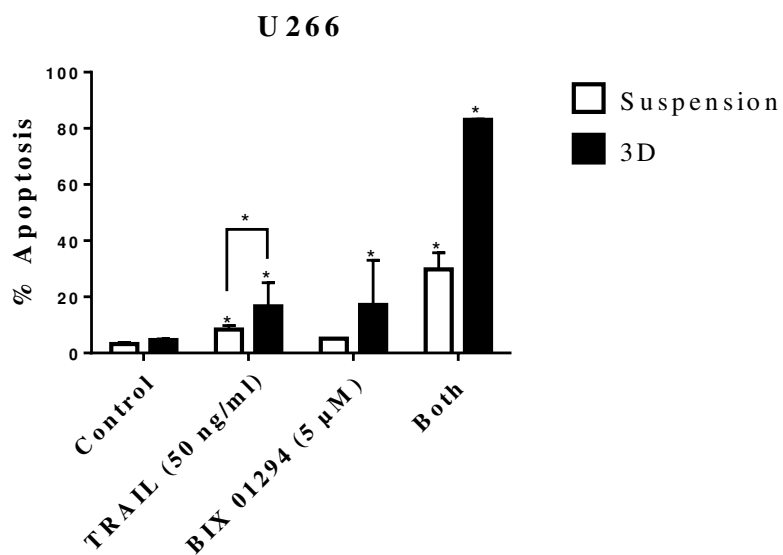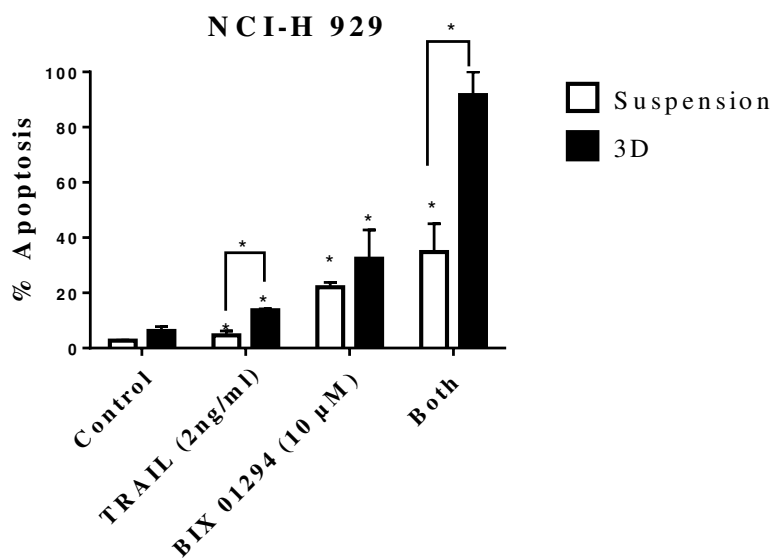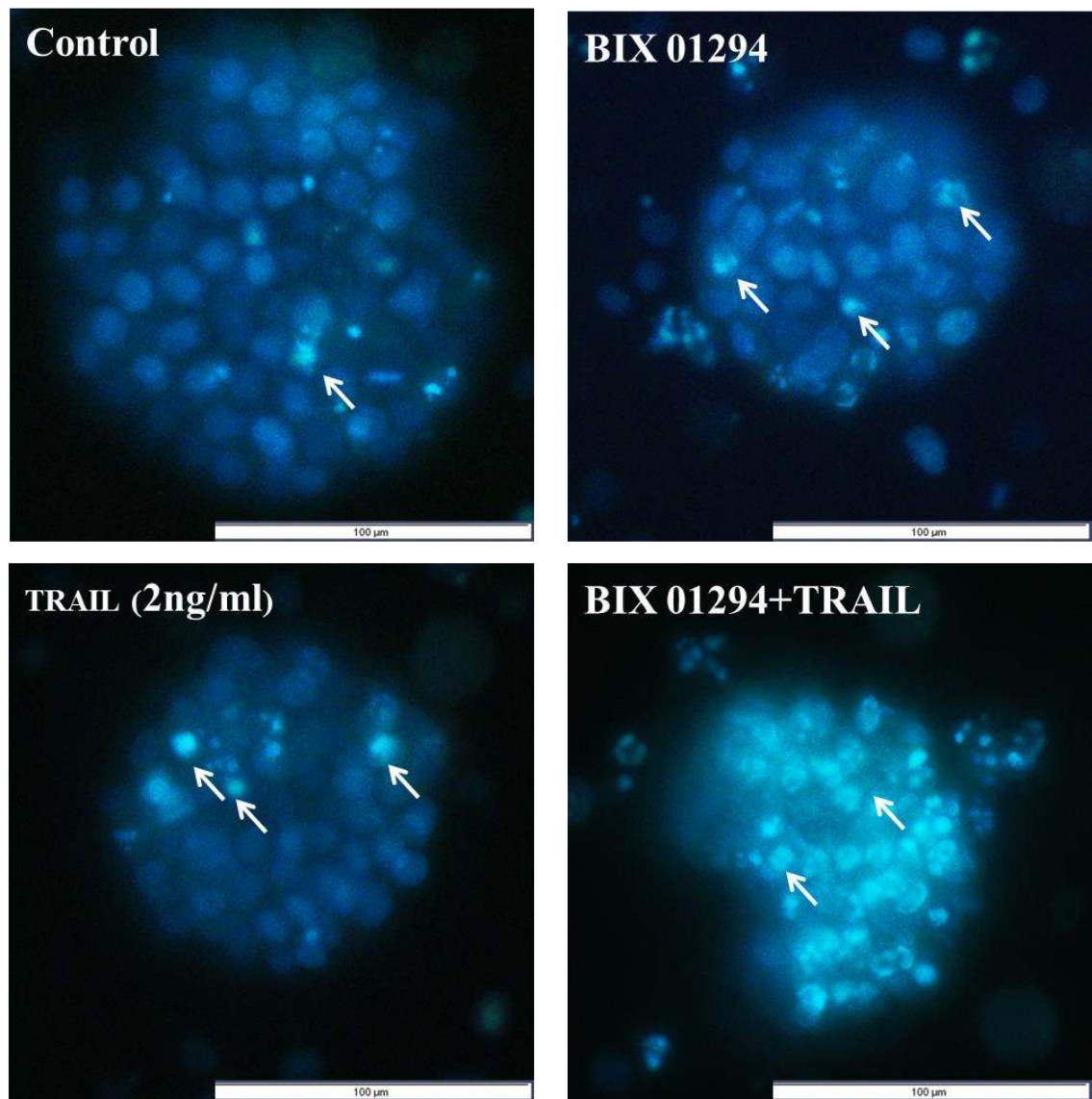
Figure 3.6: a) Effect of BIX 01294+/-TRAIL on apoptosis of multiple myeloma cell lines in 2D vs. 3D culture conditions. Myeloma cells were treated with BIX 01294+/-TRAIL determined by Hoechst 33342 and PI staining for 24 h. multiple myeloma cells were more sensitive to BIX 01294 in 3D based alginate culture compared to suspension culture and synergistic response of BIX 01294 and TRAIL in MM cell lines was potentiated in 3D cell culture. The data is expressed as median with range (three independent experiments, each in triplicate). p<0.05 was considered statistically significant comparing to control. b) An example of NCI-H 929 cells on suspension and in3D alginate culture model treated with GSK343 alone and in combined with TRAIL.

3.3.2.4 Effect of GSK343 in Combination with TRAIL on Apoptosis in Multiple Myeloma Cells Lines in 3D Alginate Cell Culture Model vs. Standard Cell Culture

3D cultures of TRAIL sensitive cells NCI-H 929 and TRAIL insensitive cells U266 multiple myeloma were subjected to treated with the EZH2[i] GSK343 treatment either alone or in combination with TRAIL for 24 hours. Myeloma cells were more sensitive to GSK343 in 3D culture conditions compared to suspension cultures and there was a significant increase in TRAIL-induced apoptosis by GSK343 treatment in multiple myeloma cell lines ($p<0.05$) (Figure 3.7). The data shows that at the dose of GSK343 used, there was no significant increase in apoptosis in U266 cell lines, but a significant increase in response to TRAIL and in combination therapy in suspension culture ($p<0.05$) (Figure 3.7). Both NCI-H 929 and U266 cell lines were significantly more sensitive to TRAIL, GSK343 and combination therapy in 3D vs. suspension ($p<0.05$) (Figure 3.7). An example of the 3D spheroid of morphological assessment of apoptosis following GSK343 treatment alone and in combined with TRAIL on multiple myeloma cells *in situ* in alginate beads of NCI-H 929 cell lines is showed in Figure 3.7 b.

Figure 3.7: Effect of GSK343+/-TRAIL on apoptosis of MM cell lines in suspension vs. 3D culture conditions.

a)
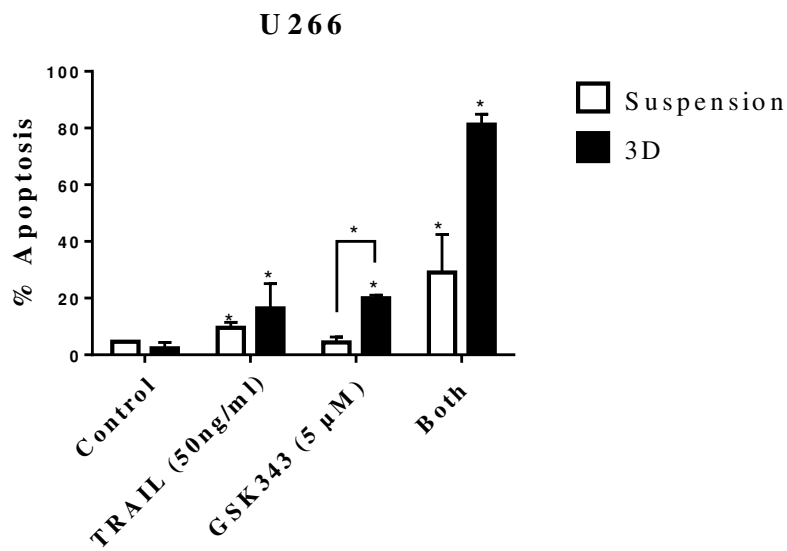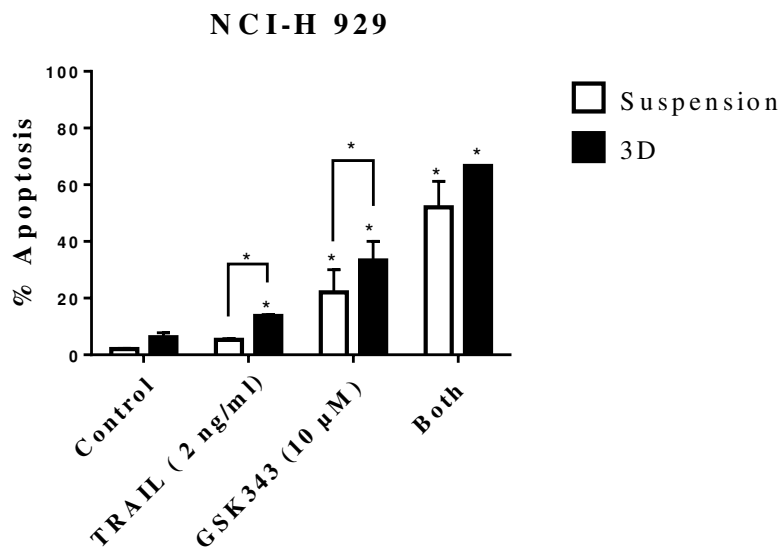
b)
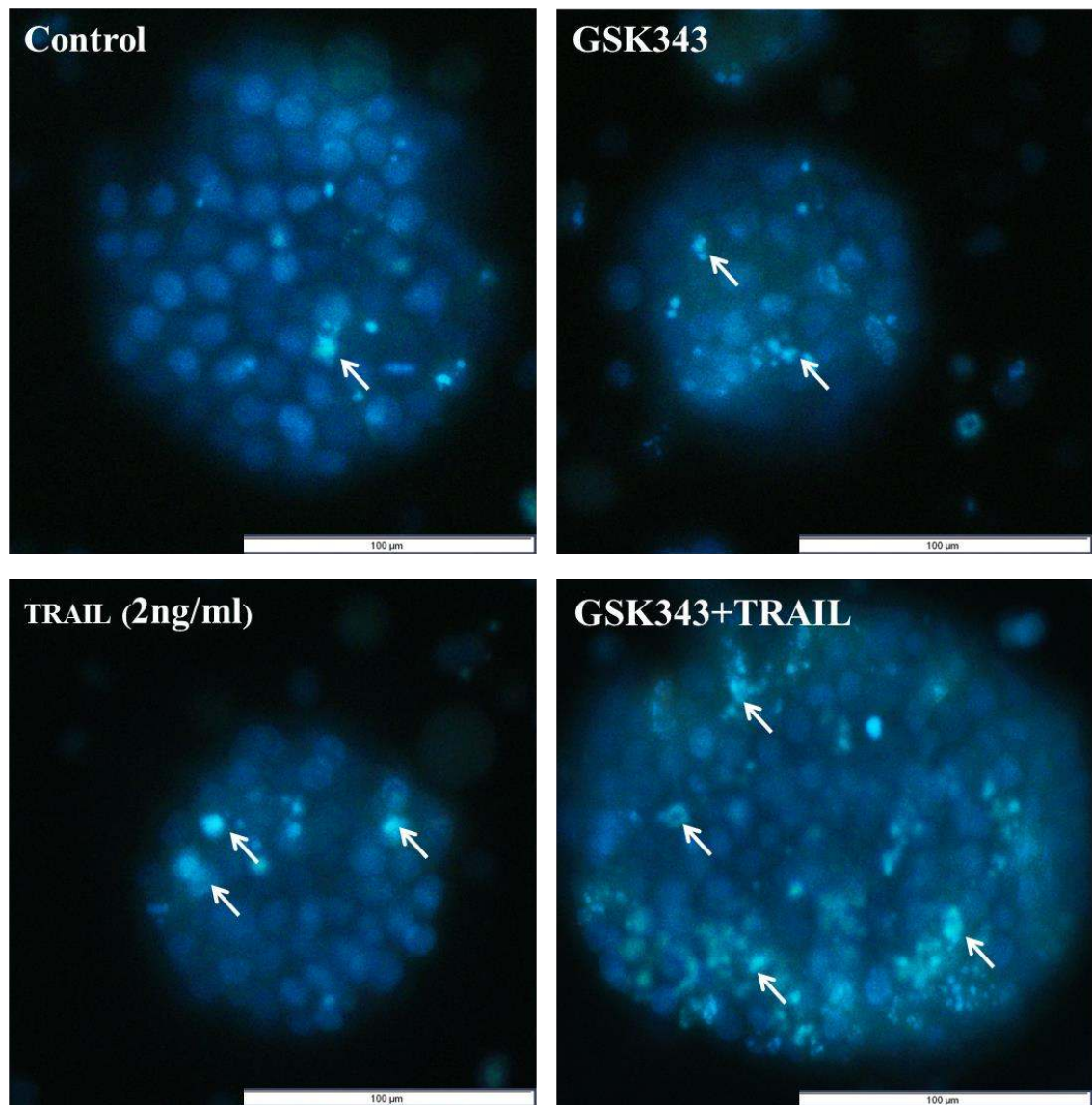
Figure 3.7: a) Effect of GSK343+/-TRAIL on apoptosis of multiple myeloma cell lines in suspension vs. 3D culture conditions. *Myeloma cells were treated with GSK343+/-TRAIL determined by Hoechst 33342 and PI staining for 24 h. MM cells were more sensitive to GSK343 in 3D based alginate culture compared to suspension culture and synergistic response of GSK343 and TRAIL in multiple myeloma cell lines was potentiated in 3D cell culture. The data is expressed as median with range (three independent experiments, each in triplicate). p<0.05 was considered statistically significant comparing to control.* ***b)*** *An example of the 3D spheroid of morphological assessment of apoptosis following GSK343 treatment alone and in combined with TRAIL on alginate beads of NCI-H 929 cell lines.*

3.4 Discussion

Micro-environmental conditions control tumorigenesis and biomimetic culture systems that allow for *in vitro* and *in vivo* tumour modeling may greatly aid studies of cancer cells' dependency on these conditions (Fischbach *et al*., 2007). Numerous attempts have efficaciously led to develop effective culture systems. In this study, alginate gel bead-3D tumour models were selected due to their ability to have representative features of the tumour microenviroment; this system was directly compared to the routine suspension culture. The data presented in this study showed that significantly higher sensitivity of cell spheroids in 3D alginate gel beads as the growth in a 3D alginate culture model sensitizes human myeloma cells to LMB, SAHA, BIX 01294 and GSK343+/-TRAIL to induce apoptosis with potent effect with TRAIL in comparing to suspension cultures.

3.4.1 Multiple Myeloma Cell Line Developed Three-Dimensional Culture *In Vitro*

Several models have been established to generate the 3D system recapitulating the specified characteristics of multiple myeloma microenvironment. These models included hydrogel systems such as collagen (Niemeyer *et al*., 2004; Yang *et al*., 2004), Matrigel (Kirshner *et al*., 2008), or synthetic polymers (Calimeri *et al*., 2011) or and specialized scaffolds like gelatin sponge collagen (Zdzisinska *et al*., 2009) or silk (Reagan *et al*., 2014); micro fluidic ossiffed tissues (Zhang *et al*., 2014; de la Puente *et al*., 2015) as well as bioreactor-based cultures. In addition to *in vitro* models, 3D *in vivo* models use fetal bone chips implanted in SCID mice; this required growth of the fetal bones in the mouse following by injected of myeloma cells into the bone (Urashima et al., 1997) as well as *in vivo* xenograft models of human myeloma cells in SCID mice. However, each has its own limitations (de la Puente *et al*., 2015). Here in this study, five out of six investigated multiple myeloma cell lines namely OPM2, RPMI 8226,

NCIH 929, U266 and JJN3 had the ability to form multicellular spheroids structures, while ADC-1 MM cell line form few loosely aggregated cells (Figure 3.1, 3.2 and 3.3). However, TRAIL^R cells did not grow in 3D.

3.4.2   TRAIL Sensitizers Induce More Apoptosis of Multiple Myeloma Cells in 3D Culture Conditions

Here, it was demonstrated for the first time that growing of human multiple myeloma cell in 3D alginate culture model significantly induced apoptosis in response to the anti-tumour agents Nuclear Export Inhibitor (LMB) (Figure 3.4), Histone Deacetylase inhibitor (HDAC) SAHA (Figure 3.5), or inhibitors of the histone methyltransferases G9a and EZH2 (BIX 01294 and GSK343) alone (Figure 3.6 and 3.7). These anti-tumour agents enhance TRAIL-induced apoptosis with potent synergistic effect in 3D cell culture and show more potent responses than suspension.

Recently, inconsistent responses were observed in studies conducted by de la Puente *et al*., (2015); they found that culturing of multiple myeloma cells in 3D tissue engineered bone marrow cultures (3DTEBM) facilitate proliferation of myeloma cells and induced drug resistance to myeloma therapy, including bortezomib and carfilzomib more than classic 2D mono-culture. Moreover, 3DTEBM cultures up-regulated cytokine secretion in the multiple myeloma environment, including pro-angiogenic molecules (VEGF, IL-8 and OPN) and pro-inflammatory cytokines (IL-1α, IL-6, TNF-α, and IL-8). In addition to recreating of the hypoxic microenvironment in the 3DTEBM culture which was confirmed by induced HIF1α and PIM hypoxia markers associated with reduced of CD138 expression and induced expression of CXCR4 in the 3D cultures (de la Puente *et al*., 2015). Co-culture of patient-derived bone marrow mononuclear cells with mesenchymal stem cells in 3D model system in previous work induced cell proliferation, expression of C-X-C chemokine receptor type 4 (CXCR4) as well as reduced the sensitivity of myeloma cells to therapeutic agents (doxorubicin,

dexamethasone, melphalan, IMiDs, bortezomib, carlzomib) compared with 2D culture (Jakubikova *et al.,* 2016).

In another study, Chandrasekaran *et al.*, 2014 demonstrated that cultured of the breast cancer cell lines as 3D tumour spheroids *in vitro* showed more TRAIL-resistant by reduced expression of death receptors DR4 and DR5 that initiate TRAIL-mediated apoptosis in comparison to cell cultured as traditional monolayer cells. In addition, 3D tumour spheroids are enriched with breast stem cell marker $CD44^{Hi}CD24^{lo}ALDH1^{Hi}$ cells. Furthermore, Chandrasekaran and colleagues attributed the reduced sensitivity to TRAIL and cancer stem cell phenotype seen in 3D tumour spheroids to the upregulation of expression of cyclooxygenase-2 (COX-2)/prostaglandin E2 (PGE_2) pathway. COX-2 is involved in the synthesis of the lipid signaling molecules named prostaglandins and has a role in cancer progression. COX-2 is one of the significant downstream targets of hypoxia inducible factors HIF-1a and HIF-1b and COX-2 knockdown sensitizes breast cell line to TRAIL-induced apoptosis (Chandrasekaran *et al*., 2014).

The epigenetic modifier EZH2 play an important role in the control of gene expression via histone hypermethylation. Over-expression of EZH2 is found in several cancer types and involved in disease progression by silencing tumour suppressor genes. EZH2 inhibitor, GSK126 in a study conducted by Tiffen *et al*., (2015) inhibited the growth, cell cycle arrest at G_2/M phase in both 2D and 3D culture melanoma cells. In addition, EZH2 inhibitor leads to reactivate of some characterized tumour suppressor genes such as stress induced gene activating transcription factor 3 (ATF3) which induced apoptosis and decreased metastatic potential (Tiffen *et al*., 2015).

The results from the current study are consistent with a study carried out by Amatangelo *et al*., (2013) that showed that EZH2 methyltransferase Inhibitors GSK343 significantly inhibited the growth and induces apoptosis of epithelial ovarian cancer cells cultured in

3D matrigel extracellular matrix, which more closely mimics the tumour microenvironment *in vivo* but not standard 2D culture model. These results propose that anti-cancer agents which display little effectiveness in conventional 2D or suspension culture models may still have therapeutic value within the solid ECM tumour microenvironment (Amatangelo *et al*., 2013).

In addition, suspension culture does not allow for clonal responses to be seen. In this investigation, multiple myeloma colonies could have variable responses to therapy, where some colonies were significantly affected by treatment, whereas other remained viable. A study carried by Cross *et al*., (2008) hypothesized that OPG mediated TRAIL resistant in PC3 cell lines was due natural distinction through acquired heterogeneity within sub-cloned cancer population, as only certain colonies originated from the similar cloned cells, where affected by TRAIL treatment whereas neighboring colonies appeared unaffected. In addition, a wide range of TRAIL response in individual colonies was observed in TRAIL-sensitive breast cancer cell line (Cross *et al*., 2008). This emphasizing the phenotypic variation of drugs sensitivity within heterogeneous cell lines.

The intracellular mechanisms of how these anti-tumour agents-induced apoptosis in 3D cultures are not entirely understood, although may relate to hypoxia and production of reactive oxygen species (ROS), glucose depletion and growth factor withdrawal that are TRAIL sensitizers. ROS has been reported to be involved in many biological processes, including programmed cell death or apoptosis (Buttke and Sandstrom., 1994; Jones *et al*., 2000). Accumulation of intercellular ROS resultant in disruption of the mitochondrial membrane potential, the release of pro-apoptotic protein cytochrome *c* into cytosol with subsequent stimulation of the caspase signals, and ultimately promotes apoptotic cell death (Woo *et al*., 2003). TRAIL has been reported to stimulate ROS generation in tumour cells (Mellier and Pervaiz., 2012). In previous work, exposure to

TRAIL induces ROS generation and activation of p38 MAP kinase, and that subsequently activation of caspases and induce apoptosis in adenocarcinoma HeLa cells (Lee *et al*., 2002). In addition, a number of anti-tumour agents sensitize TRAIL-induced apoptosis through generation of ROS in various tumour types (Chen *et al*., 2008; Kim *et al*., 2006; Lee *et al.*, 2009).

The effects of hypoxia environment on TRAIL-induced apoptosis remain to date controversial (Ehrenschwender *et al*., 2016) and there is a little information available on the apoptogenic activity of TRAIL in hypoxic conditions. Earlier work demonstrated that hypoxia induces a phenotype highly sensitive to apoptogenic effect of TRAIL in a number of cancer cell lines and hypoxia enhance TRAIL-induced apoptosis by the down-modulation of c-flip expression or by the increased expression of TRAIL-R2. In addition, the sensitive of cancer cell line to TRAIL under hypoxic environment is correlated with down-modulation of the epsilon isoform of protein kinase C (PKC) expression (Gobbi *et al*., 2010). PKC has an anti-apoptotic activity, preventing glioma cell lines from undergoing apoptosis (Okhrimenko *et al*., 2005).

However, a low oxygen environment inhibits TRAIL-induced tumour cell death in oral squamous cell carcinoma cells by blocking the translocation of lysosomal cathepsin to the cytosol (Nagaraj *et al*., 2007). Recently, growth of colorectal cancer cells under hypoxic condition induced TRAIL-resistance. Combinatorial therapy approaches of TRAIL with SMAC mimetics or XIAP-targeting drugs might constitute a reasonable therapeutic approach and overcome hypoxia-mediated cell death resistance (Ehrenschwender *et al*., 2016).

Metabolic stress by nutrient deprivation occurs commonly in cancer as well as normal tissues and triggers many potential cell death-inducing pathways (Iurlaro *et al*., 2017). Glucose depletion sensitizes tumour cells to death receptor-mediated apoptotic cell death via enhancement of DISC formation and caspase-8 activation (Munoz-Pinedo *et*

al., 2003). Glycolysis inhibition enhanced death receptor-induced apoptosis in a number of human tumour cell lines including Jurkat, HeLa, and U937 by Mcl-1 down-expression (Pradelli *et al*., 2010). Suggesting that glucose depletion in cells grow in 3D cultures enhance sensitivity of cancer cells to anti-tumour agents

3.4.3   3D Culture Enhancing Stem Cell Behavior

Culture of cancer cells in a 3D model system helps in asses the efficiency of novel therapeutic strategies. It has been established that the response behaviors of cells in 2D traditional cell cultures and 3D cultures models differ (Zschenker *et al.,* 2012; Hehlgans *et al*., 2009; Hehlgans *et al*., 2009). Some studies have been showed that 3D-grown cancer cells are chemo-resistant and radio-resistant compared with cells grown in traditional monolayers and theses cells exhibited resistance to apoptosis. However, the reason behind the difference therapy-resistance between 2D and 3D culture models still mainly unknown (Xue *et al*., 2015).

It has been found that the expression of cancer stem cells-related genes Oct3/4 and Nanog genes was significantly increased in 3D alginate-grown liver and neck squamous cell carcinoma cell lines compared with 2D cultures (Xu *et al*., 2014). Furthermore, metastatic properties of hepatocellular carcinoma cells enhanced when cultured within alginate beads via up-regulating the expression of various matrix metalloproteinases (MMPs), including MMP2, MMP9 and MT1-MMP (Xu *et al*., 2013). Other groups showed that head and neck squamous cell carcinoma cells encapsulated in alginate scaffolds had characteristics of cancer stem cell such as high tumourigenicity and drug resistance as well as an increase in the proportion of stem cell marker gene expression Nanog, Oct3/4, CD44 and ABCG2 (Liu *et al*., 2015). The expression level of stem cell marker CD133, Bmi-1, nestin, and c-kit were increased in melanoma cells cultured in soft fibrin gels (Liu *et al*., 2015).

In addition, up-regulated expression of Hypoxia-inducible factors (HIFs) genes; HIF1A and HIF2A in cancer stem cells (CSCs) and their progenies have been seen as a result in the upregulation of cancer stem cells-related genes marker in 3D culture cells (Xu *et al*., 2014). Moreover, cultured of cancer cells in a 3D matrigel microenvironment induced stem cell-like characters and significantly up-regulated the stem cell reprogramming factors expression such as Oct3, Lin28, Sox2, Nanog and miR-302a, compared with cells grown in 2D and in turn showed enhanced drug-resistance (Xue *et al*., 2015). These evidences suggested that grown of cancer cell as 3D culture model exhibit more undifferentiated characteristic in comparison to cancer cell cultured as traditional monolayer and this can be observed by an increasing in stem cell properties associated with 3D culture model.

3.5   Conclusion

Although multiple myeloma is a haematological malignancy, it forms solid bone tumours these are potentially more targeted using therapeutic agents than tumour in blood. This study showed for the first time that multiple myeloma cell lines are able to proliferate in the alginate beads and form 3D spheroid structures. Myeloma cells were more sensitive to LMB, SAHA, GSK343, and BIX 01294 alone in 3D and Nuclear Export Inhibitor and inhibitors of HDAC, EZH2 and G9a are potent sensitisers of TRAIL responses crucially in 3D cell culture, which may mimic physiological aspects of bone metastases. The development of 3D culture system is a crucial part of future of cancer research and advances in this field provide an emerging a clear picture of how 3D cancer model mimic the human microenvironment and how it could be therapeutically targeted.

4. Selection of PKH26^Hi Quiescent Populations Selects for Cells with Insensitivity to TRAIL and TRAIL Sensitizers

4.1   Introduction

For many years, a growing incidence of cancer resistance to therapeutic agents has focused research to identify the cellular phenotype responsible for drug resistance. This lead to the recognition of so-called cancer stem cells (CSCs), which have been isolated in various cancer types, including prostate, ovarian, colorectal, breast and hematopoietic tumours (Al-Hajj *et al.*, 2003; Alison *et al*., 2011; Collins *et al*., 2005; Wang and Dick., 2005). These cancer cells are thought to play a vital role in cancer progression, metastasis, self-renewal, relapse and drug resistance in many types of cancer (Yang *et al*., 2015). Quiescent Multiple Myeloma-propagating cell populations have been shown to mediate resistance to anti-tumour agents including Bortezomib, Dexamethasone and Lenadilomide (Matsui *et al.*, 2008; Vitovski *et al*., 2012). Despite recent advances in the study of pathogenesis and mechanisms of CSC-mediated disease recurrence and multi-drug resistance, it is unclear exactly what role the quiescent population plays in drug resistance (Yang *et al*., 2015).

According to the classical or stochastic CSC hypothesis which based on clonal theory of tumour initiation and progression, stem cells upon gaining a mutation gives rise to a neoplastic clone of homogenous cancer cells that have the capacity for expansion as well as cancer initiation and maintenance (Tan *et al*., 2006).   However, in the hierarchical hypothesis, the tumour sustained only by a small proportion of putative stem-like cells (Guzman-Ramirez *et al*., 2009).

One of the main characteristics of CSCs is their capability to be quiescent; cancer dormancy usually correlated with quiescent CSCs fraction that is likely to persist after cancer therapy and drive to disease relapse. This quiescence state remains the most important hurdle in achieving absolute recovery from the disease (Kusumbe and Bapat., 2009). It has been found that use of chemotherapeutic agents such as DNA modulating agents successfully kill the tumour bulk and rapidly dividing cells and tumour

regression is observed. However, the self-renewing population of CSCs is resistant and being to initiate a cancer re-growth (Zhou *et al.*, 2009; Li *et al.*, 2008). As a result, a large number of patients suffer from disease relapse, indicating the resistant character of specific cells to the initial therapy and initiate tumour progression several decades after therapy. Therefore, the supportive evidence for CSCs hypothesis suggests that targeting highly proliferative cells does not target the suspected source of the disease, and cancer could be completely eradicated if these CSCs eliminated (Hermann *et al.*, 2008).

In recent years, several *in vitro* methods have been established in order to study and isolate CSCs which include, colony formation assay, the microsphere assay, Labell-retaining assay using PKH dyes, and using some CSC markers such as the aldehyde dehydrogenase (ALDH). ALDH enzyme has recently been known with the potential to isolate CSCs in various cancer types such as hematological malignancy (Podberezin *et al.*, 2013). High enzyme levels being revealed to link to markedly increased aggressive phenotype and an indicator of poor survival rates in human breast cancer (Jiang *et al.*, 2009; Balicki., 2007). It has been found that ALDH enriched cancer cells have more clonogenic potential, re-initiate ability, self-renewal, and drug resistant and these represent a small subsite of highly tumourigenic cells. Consistent with this, the bulk of low ALDH activity cells appear to be differentiated cells with limited growth potential (Van den Hoogen *et al.*, 2010; Ginestier *et al.*, 2007). However, the ALDH activity assay has some limitations as the enzyme activity is influenced by the chemotherapy taking by the patients (Podberezin *et al.*, 2013) and may be expressed in senescent cells (Doherty *et al,* 2011).

Other surface biomarkers used to identify CSCs in a different type of cancer are CD133, CD44, and CD24 (Cojoc *et al.*, 2015) however, these markers cannot uniformly mark the CSCs (Yang *et al.*, 2015). For example, the expression of CD133 marker has demonstrated to correlate to stem cell population in oral squamous carcinoma, breast

and prostate, and many heamatological malignancies, but not in lung tumour (Felthaus *et al*., 2011). Moreover, in haematological malignancies, the expression of specific CSCs marker CD38 and CD34 have been characterized (Haase *et al*., 1995).

Membrane labelling dyes such as PKH26/67, or DiD, irreversibly bind to the lipophilic layer of cell membranes and is evenly distributed among daughter cells during cell division. As a result, cells progressively lose the dye as these non-CSC cells proliferate and divide rapidly. In contrast, quiescent CSCs cells maintain the fluorescence dye owing to lack of cell proliferation (Huang *et al.*, 1999; Lawson *et al.,* 2015; Wang *et al*., 2015; Zeuner *et al*., 2014). The decrease in fluorescence intensity over the time can be tracked using flow cytometry. In addition, it is possible to sort the cells into two populations of PKH26 positive and negative in order to study any phenotype differences and carry out further experimental analysis (Lanzkron *et al.,* 1999). Therefore, cell labelling method and using flow cytometric analysis has been widely applied for study and isolation of CSCs in different cancer types (Greve *et al.*, 2012). Isolation of cancer initiating cells by PKH26 fluorescence tracking dye have been reported in number of cancers including breast cancer (Pece *et al*., 2010), colon cancer (O'Brien *et al*., 2012), ovarian cancer (Kusumbe and Bapat., 2009) and multiple myeloma (Chen *et al*., 2014).

4.1.1 Hypothesis

It is hypothesized that PKH26^{Hi} cells are quiescent CSC-like cells and are one source of TRAIL-resistance in multiple myeloma.

4.1.2 Aims

The aims of the present study were first to determine if CSC-like cells could be identified and isolated through optimisation of the membrane labelling dye (PKH26), which is maintained in quiescent CSCs in multiple myeloma. This PKH26 is detectable by both flow cytometry and fluorescent microscopy. The small population retaining the

PKH26 dye can be physically sorting using flow cytometry (FACSAria). Secondly, the study aimed to establish whether the PKH26^{Hi} population was characteristic of CSC-like cells by assessed for proliferative potential post-sorting compared to PKH26^{Lo} cells and unsorted labelledcells. CD138 expression of sorted PKH26^{Hi} cells population was also measured by flow cytometry and compared to parental un-labelled cells.

Furthermore, the drug sensitivity of the PKH26^{Hi}, PKH26^{Lo} and unselected populations was determined by exposed to the potential anti-tumour agent TRAIL in the presence or absence of Leptomycin B (Nuclear export Inhibitor), SAHA (Histone Deacetylase inhibitor), BIX 01924 and GSK343 (Histone methyltransferase inhibitors), to determine if quiescent multiple myeloma cell populations responded differentially to the anti-tumour agent TRAIL, and also to sensitizers of TRAIL signaling. Apoptosis was assessed by Hoechst 33342 staining and assessment of nuclear morphology coupled with Annexin V-FITC staining.

4.2   Materials and Methods

4.2.1   Experimental Design

Three multiple myeloma cell lines were used in this study: two TRAIL sensitive cell lines (NCI-H 929 and RPMI 8226) and one TRAIL insensitive cell line (U266). Multiple myeloma cells cultured as previously described (Chapter 2; Section 2.2.5.1) and incubated in humidified incubator at 37ºC with 5% CO_2 atmosphere. Myloma cells were stained with the PKH26 membrane labelling kit and allowed to proliferate for 10-14 days. PKH26^{Hi} and PKH26^{Lo} cell population were separated using a FACSAria and cultured in isolation. PKH26^{Hi} and PKH^{Lo} cells were assessed for proliferative potential post-sorting, and exposed to the potential anti-tumour agent. Apoptosis was assessed by Hoechst 33342 staining and assessment of nuclear morphology coupled with Annexin V-FITC staining. The expression of CD138 in parental multiple myeloma cell lines and sorted cells was assessed using flow cytometry and analysed with FlowJo software. In addition, CD138 expression was detected in 3D growth using immunohistochemistry.

4.2.2   Optimisation of PKH26 Red Staining

Multiple myeloma cells were stained using the PKH26 membrane labelling kit (Sigma). Myeloma cells at density 1×10^6 cells/ml were centrifuged for 5 minutes at 400g and re-suspended in medium without FCS. The cells were centrifuged at 400g for 5 minutes and the supernatant was carefully aspirated and 125 μl of diluent C (PKH26 Red Fluorescent Cell linker Kits for general cell membrane labelling) was added. Then, 5 μl of PKH26 dye solution was prepared by adding 30μl of absolute ethanol to 4 μl of PKH26 Linker at 1mM. After that, the cell/dye suspension was incubated for 5 minutes at room temperature with periodic mixing. In order to stop the staining reaction, 130 μl of FCS was added and incubated for 1 minute at room temperature followed by centrifuged for 10 minutes. Finally, the cells were washed twice in 10 ml of complete

media to ensure removal of any residual dye prior to re-suspend in 2 ml of complete media and seeding into 6 well plates and media changes three times a week. Cell stain was verified by flow cytometry.

4.2.3 Assessment of PKH26 by Flow Cytometry

Multiple myeloma cell lines were stained using the optimised PKH26 staining protocol as mentioned above (Section 4.2.2) and allowed to proliferate for 10-14 days. Sample from the main cultures was taken three times a week to be assessed for stain intensity by both flow cytometry and IX81 fluorescence microscope (Olympus) and images captured using Cell-F software (Olympus) on a dual image of bright field and Texas Red Filters. Flow Cytometry was performed on a BD FACSCalibur™ (BD Biosciences) flow cytometer. Firstly, baseline measurements for the flow cytometry software template were set on day 0 by taking a sample of both unstained and stained cells at 1×10^5 cells/ml re-suspended in 1ml of complete media and this template used throughout the experiment. Flow cytometry measured the side (cell granularity) and the forward (cell size) scatter to identify the viable cell population. In addition, a histogram plot of gated population to determine the percentage of stained cells in comparison to unstained cells. Ten thousand events were acquired per sample and data analysed with FlowJo software.

4.2.4 Fluorescent Activated Cell Sorting (FACS) of PKH26 Labelling Cells

Labelled multiple myeloma cells at day 14 were sorted using Becton Dickinson FACSAria at the Sheffield University flow cytometry facility. PKH26^{Hi} and PKH26^{Lo} cell population were separated by gating around the unstained cell population from an unlabeled cell sample. Cells with a PKH26 level comparable to unstained cells were classed as PKH26^{Lo} whereas cells with a PKH26 level comparable to day 1 were classed as PKH26^{Hi}.

4.2.5 Assessment of Proliferative Potential of Post-sorted PKH26^{Hi} and PKH26^{Lo} Cells

Post-sorted PKH26^{Hi} and PKH26^{Lo} cells, in addition to unsorted cells population were cultured in isolation by seeding at 200 cells/well into 96 well plates in triplicate. Cells left to proliferate for one week in humidified incubator and the cell number assessed by a Cell Countless system (Invitrogen).

4.2.6 Effect of PKH26 Status on LMB, SAHA, BIX 01294 and GSK343-Induced TRAIL Responses on Multiple Myeloma Cell Lines

The effect of TRAIL+/-TRAIL sensitizers on apoptosis on PKH26^{Hi} and PKH26^{Lo} cells and unsorted multiple myeloma cells were assessed using double staining of Hoechst 33342 (Chapter 2) and Annexin V-FITC staining. Briefly, those cells were treated with high dose of TRAIL +/- sensitizer and analysed for analysis by Hoescht 33342 and/or Annexin V staining.

4.2.6.1 Assessment of Apoptosis in Quiescent Cells using Annexin V/ Hoechst 33342 Staining

Annexin V is a member of calcium-depending protein family that conjugates with phosphatidylserine (PS) intracellularly in order to detect apoptotic cells. In an early stage of cell death, phosphatidylserine translocates from cytoplasmic leaflet to outside leaflet of the plasma membrane creating potent charge asymmetry of the membrane. Staining with Annexin V precedes the loss of plasma membrane integrity which associated with latest stages of cell deaths due to either apoptosis or necrosis. Therefore, this technique is aimed to detect apoptosis immediately after onset of the execution stage of cell death (Balaji *et al.*, 2013). Fluorescently labelled annexin V is used to definitely target and detect apoptosis in a calcium dependent process via the establishment of phospholipid-calcium complex (Tait and Gibson., 1992; Gerke *et al*, 2005). This study used FITC-labelled Annexin V staining.

Briefly, PKH26^{Hi} and PKH26^{Lo} cells and unsorted multiple myeloma cells seeded at 10,000 cell/well in 96 well plates and stimulated with the potential anti-tumour agents LMB (5nM), SAHA (10 µM), BIX 01924 (20 µM) and GSK343 (20 µM) in the presence or absence of TRAIL (50 ng/ml) at doses known to kill most unselected cells in 24 h. In order to detect apoptosis using Hoechst 33342 staining coupled with Annexin V staining, well plates containing PKH26^{Hi} and PKH26^{Lo} cells and unsorted cells treated with anti-tumour agents was centrifuged at 400g for 5 minutes. The supernatant was removed and 100µl of Annexin V binding buffer (10 mM HEPES/NaOH, 140 mM NaCl, 2.5 mM CaCl$_2$ at pH 7.4) was added to each well. Then, 5 µl of Annexin V-FITC stain in addition to 10 µl of Hoechst 33342 staining were added/well and incubated for 20 minutes. Images were captured using Cell-F software (Olympus) using a triple filter and colour UC-30 camera on an Olympus IX-81 microscope and images analysed using Cell-F software (Olympus).

4.2.7 Identification of CD138 Expression in Multiple Myeloma Cells

CD138 expression was analysed by flow cytometry after sorting of PKH26^{Hi} cell population and compared to parental un-labelled cells. Briefly, cells plated at a density of 1 x 10^6 cell/well were transferred into FACS tubes and centrifuged at 400g for 5 minutes. 1ml of chilled 1% BSA was added to cell pellet and centrifuged again. The cell pellet was carefully re-suspend in its own volume and optimised volume of PE/Cy7 anti-human CD138 (Syndecan-1) (Mouse Monoclonal Antibody (MI15) Mouse IgG1, κ) primary antibody (2.5µl) (Biolegend) was added. 2.5 µl of PE/Cy7 Mouse IgG1, κ Isotype control Antibody (Biolegend) was added to one tube as a negative control with no fluorescence stain in addition to an unstained sample without either primary antibody or isotope which was used to set the flow cytometer gate to establish the parameters for negative staining. Cells were incubated at 4°C for 30 minutes prior to 300 µl PBS/1%

FCS was added and centrifuged. Finally, samples re-suspend in 300μl PBS/1% FCS and the stained cells analysis using flow Beckman Coulter Gallios flow cytometer instrument. Ten thousand events were acquired per sample and data analysis with FlowJo software.

4.2.8   Immunohistochemistry for CD138 Expression in 3D Alginate Culture

To prepare cells for immunohistochemistry (IHC), sections slides of MM cells cultured in alginate beads were prepared, de-waxed and rehydrated as described in Section 3.2.4.2. The slides were washing with deionized water for 5 minutes following by twice washed in TRIS-Buffered Saline (pH 7.5).

In order to detect antigen successfully by IHC techniques, the antigen must be accessible for primary antibody conjugating. The antigen may be masking by formation of cross-links to inter-, intra- or extra-cell proteins. Furthermore, the processes of tissue preparation for IHC such as chemical fixation and paraffin embedding process catalyses further establishment of cross-links that may mask tissue antigens. The process of un-masking cell antigen called Antigen Retrieval (AR) and there are a number of methods exist including, enzymatic digestion, use of heat, and treatment with protein denaturants (D'Amico *et al.*, 2009; Emoto *et al.*, 2005; Kim *et al.*, 2004). In this study applying of heat and enzymatic digestion were investigated and heat-prompted AR by Microwave was adopted. For heat applying by microwave irradiation section were immersed in antigen retrieval buffer (0.05 M Tris Buffer (6.05 g Tris in 1L dH_2O - pH 9.5) pre heated to $60^{\circ}C$ in a Sanyo microwave oven (800 watt), set to deliver 40% power for 5mins. Section slides were cooled for 1 minute at room temperature. Sections were then subjected to irritation by microwave oven at 20% power for 5 mins and cooled at room temperatures for 15 minutes in order to allow re-folding of tissue antigen.

Sections were washed twice in TBS for 5 minutes. In order to block non-specific protein interactions from the secondary antibody, 200 µL of blocking solution was applied (1% BSA in 75% TBS and 25% normal serum from the animal in which the secondary antibody was raised) per slide for 2 hours at room temperature on slow moving shaker. This study used normal Rabbit Serum (abcam).

The primary antibody (PE/Cy7 anti-human CD138 (Syndecan-1) (Biolegend) with optimised concentration were prepared and 200 µL (1:400) was added to each slide after tapping the excess of blocking solution then it incubated overnight at a humid atmosphere. Isotype control slides serve as negative control were incubated in the absence of the primary antibody but an inclusion of a control antibody of the same isotype and run alongside primary antibody section at matched protein concentration. Primary antibody binding was only considered to be specific when no binding was seen on matching isotype control slide and the lacks of immune staining confirmed that secondary antibody binding was specific to the existence of bound host species proteins either primary antibody or isotype control (True., 2008).

Following overnight incubation with primary antibody, the slides were incubated with optimized concentration of Biotinylated Rabbit Anti-Mouse IgG Fc (Abcam) Rabbit polyclonal Secondary Antibody to Mouse IgG - H&L secondary antibody (1:1500) for 30 minutes at room temperature after being washed three times in TBS washes.

After three additional washes in TBS for 5 minutes per wash, the slides were treated with avidin-biotin-peroxidase (ABC, Vecta Laboratories) for 30 minutes. Then, the slides were counter-stained with Hoechst 33342 (10 mg/ml) (Sigma-Aldrich) for 15 minutes. After that, the slides were washed with TBS for three times for 5 minutes each wash. Finally, the slides were dehydrated, cleared and mounted in 90% glycerol/TBS and kept in dark at 4°C and viewed under the fluorescence microscopy.

4.2.8.1 *Evaluation of Immunohistochemistry*

Evaluation of immuno-detection of a target protein (CD138) was by counting immuno-positive colony within the alginate beads microscopy. Qualitative analysis of immuno-fluorescence was performed on Olympus, IX81fluorescence microscope and analysed by Cell-F software.

4.2.9 Statistical Analysis

Apoptotic cells were counted manually and percent apoptosis calculated based on duplicate representative fields of view each containing at least 100 cells for three independent experiments. Median with range was calculated and the Stats Direct software was used to determine whether the data followed a normal distribution. As the data did not follow a normal distribution, significance difference determined using a Kruskal-Wallis and Connover-Inman post-hoc test with a p value of <0.05.

4.3   Results

4.3.1   Determination of PKH26 Fluorescent Intensity in Multiple Myeloma Cell Lines Over Time

NCI-H 929, RPMI 8226, and U266 cell lines were labelled with the PKH26 membrane labelling kit and allowed to proliferate for 10-14 days in order to evaluate how rapidly the dye was lost due to cell division, and whether a PKH26^{Hi} non-proliferating population remained. Assessment of PKH26 retention was through both flow cytometry and microscopy. During the first few days all cell lines remained bright red upon imaging by microscopy (Figure 4.1, 4.2 and 4.3), however, by day 14 there was a significantly reduced number of fluorescing cells as well as the intensity of dye where only a small population of red cells could be seen (Figure 4.1, 4.2 and 4.3). These results correlate with FACS data were the majority of multiple myeloma cells were positive (approximately 99%) on first days and by day 14 were an only small percentage of Myeloma cells were positive (<20%) (Figure 4.4). An example of PKH26 fluorescent positivity in NCI-H929 cell lines by flow cytometry and analysed by FlowJo is shown in Figure 4.5.

Figure 4.1: Determination of PKH26 fluorescent intensity and positivity in NCI-H 929 multiple myeloma cells over time

Figure 4.1: Determination of PKH26 fluorescent intensity and positivity in NCI-H 929 multiple myeloma cells over time by microscopy and flow cytometry. On day 1 majority of cells were positive, however, by day 14 there was a significantly reduced number of fluorescing cells. These results correlate with FACS data were the majority of multiple myeloma cells were positive (>99%) on first days and the number of PKH retained dye cells over a period of 14 days were significantly reduced (<20%). The white arrow is indicated for example of PKH26-retained dye cells.

Figure 4.2: Determination of PKH26 fluorescent intensity and positivity in RPMI 8226 multiple myeloma cells over time

Figure 4.2: Determination of PKH26 fluorescent intensity and positivity in RPMI 8226 multiple myeloma cells over time by microscopy and flow cytometry. On day 1 majority of cells were positive, however, by day 14 there was a significantly reduced number of fluorescing cells. These results correlate with FACS data were the majority of multiple myeloma cells were positive (>99%) on first days and by day 14 were only small percentage of multiple myeloma cells were positive (<20%). The white arrow is indicated for example of PKH26 retained dye cells.

Figure 4.3: Determination of PKH26 fluorescent intensity and positivity in U266 multiple myeloma cells over time

Figure 4.3: Determination of PKH26 fluorescent intensity and positivity in U266 multiple myeloma cells over time by microscopy and flow cytometry. On day 1 majority of cells were positive, however, by day 14 there was a significantly reduced number of fluorescing cells. These results correlate with FACS data were the majority of multiple myeloma cells were positive (>99%) on first days and by day 14 were only small percentage of multiple myeloma cells were positive (<20%). The white arrow is indicated for example of PKH26 retained dye cells.

Figure 4.4: PKH26 fluorescent positivity in multiple myeloma cells
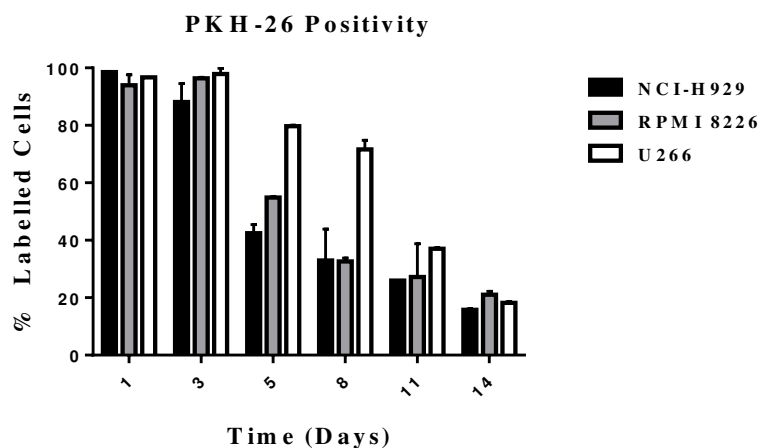
Figure 4.4: Determination of PKH26 fluorescent positivity in multiple myeloma cells over time by flow cytometry. Three multiple myeloma cell lines were assessed for decreasing in PKH26 labelling by flow cytometry every 2-3 days. Data shows the decrease of the percentage of stained cells after in comparison to unstained cells which was determined by setting a template of un-stained cells on day 0/1. The multiple myeloma cells contain a small percentage of population of dye retained cells (<20%) at day 14.

Figure 4.5: PKH-26 fluorescent positivity in NCI-H 929 cell lines analysis by flow cytometry
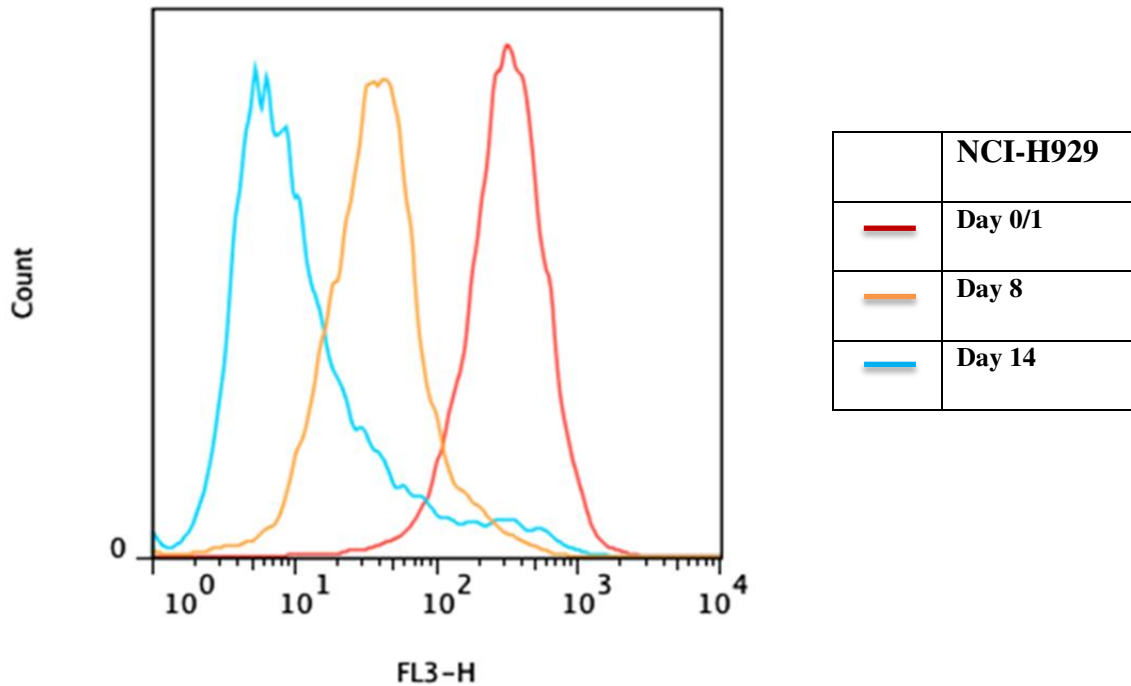
Figure 4.5: An example of histograms for PKH26 fluorescent positivity in NCI-H 929 cell lines by flow cytometry analysis by FlowJo software. FACS data showing PKH26 labelled NCI-H 929 cells at day 1, 8 and 14 days. The majority of multiple myeloma cells were positive (>99%) on first days and the number of PKH retained dye cells over a period of 14 days were significantly reduced.

4.3.2   Isolation of PKH26^{Hi}/PKH26^{Lo} Myeloma Cell by FACS

Following stained of multiple myeloma cells with PKH26 and left to proliferate, they subjected to a flow-sort isolation of two distinctive populations (PKH26^{Hi} and PKH26^{Lo}) based on gating in comparison to unstained cells. An example of selection of PKH26^{Hi} NCI-H 929 cells by cell sorting is shown in Figure 4.6. At least 50,000 cells were isolated after sorting. Immediately post-sorting, live cells counts were determined using a Cell Countless system (Invitrogen) and cell viability >80% was determined using trypan blue staining (Invitrogen) and cells were plated and assessed using microscopy and flow cytometry to confirm the purity was as indicated by the FACSaria. As shown in Figure 4.7, the PKH26^{Hi} in multiple myeloma cell lines retained the PKH26 in microscopic imaging, while there were faint few fluorescence signs in PKH26^{Lo} cells using the same exposure. Furthermore, this correlated with the PKH26 positivity using flow cytometer, which demonstrated that PKH26^{Hi} cells were >99 % positive for PKH26 fluorescence while the PKH26^{Lo} population was only approximately 2-5 % PKH26 positive (Figure 4.7).

Figure 4.6: Selection of PKH26^{Hi} NCI-H929 cells by cell sorting
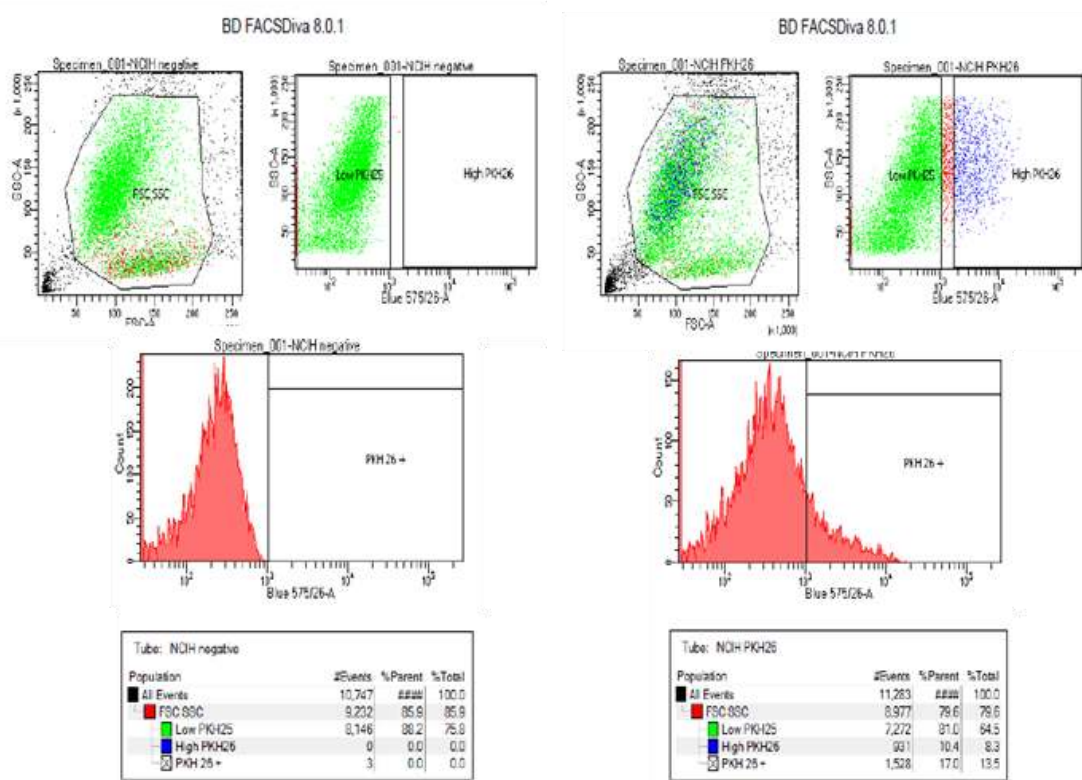
Figure 4.6: FACS Analysis of multiple myeloma unstained and PKH26 labelled cells.
The population of unlabelled multiple myeloma cells was gated in order to determine the viable population and used as a template. Then the PKH26 labelled cells analysed by flow cytometry and PKH26^{Hi} and PKH26^{Lo} cell population were separated and cultured in isolation.

Figure 4.7: Determination of PKH26 fluorescence intensity and positivity determination post-sorting
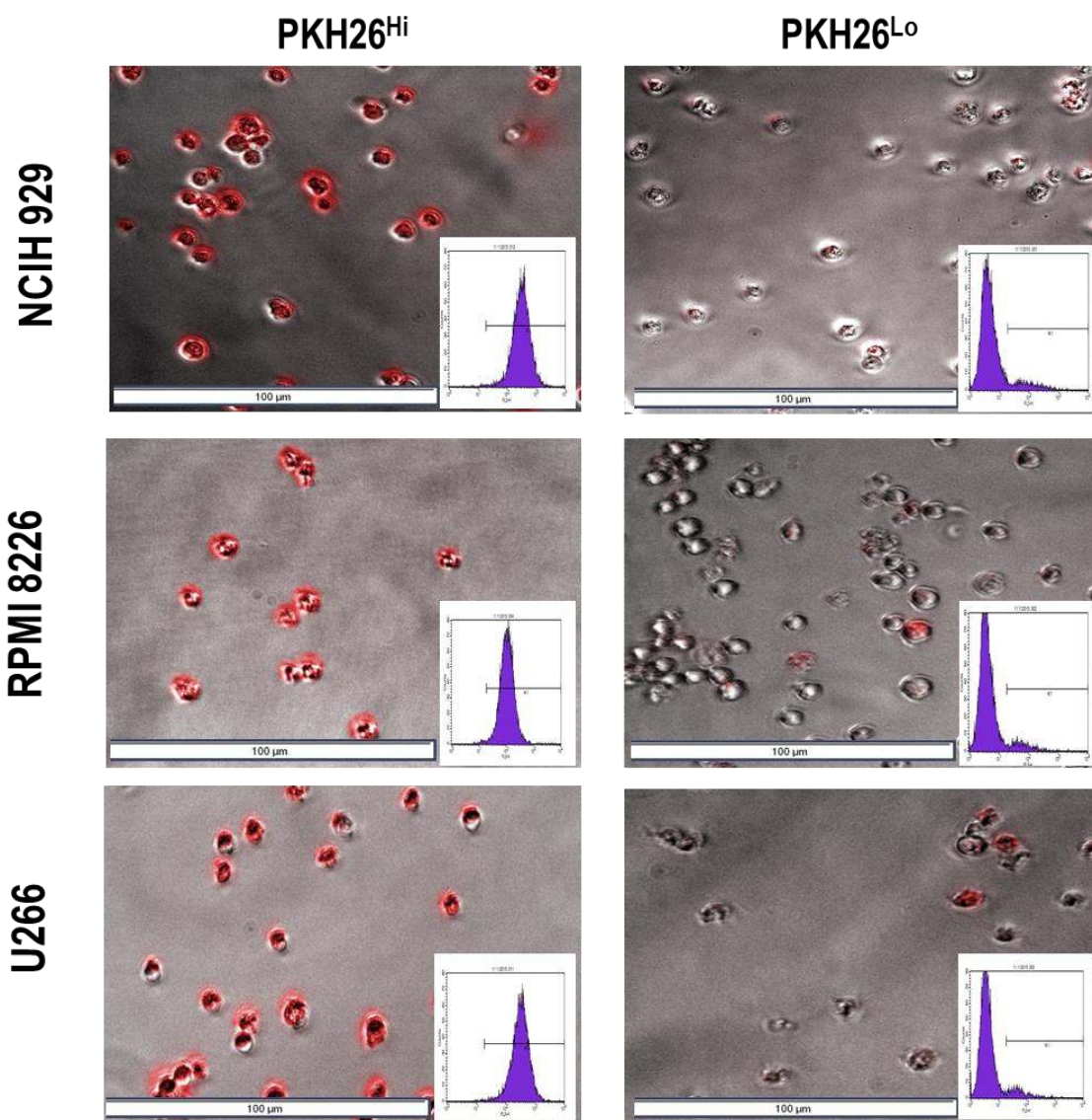
Figure 4.7: PKH26 fluorescence intensity and positivity determination post-sorting. Following FACS, PKH26^{Hi} and PKH26^{Lo} cells were cultured in isolation and fluorescence intensity was checked using fluorescence microscopy. The PKH26^{Hi} population maintained fluorescence for PKH26 and faint/absent fluorescence was seen in PKH26^{Lo} cells, or a small percent of contaminating PKH26^{Hi} cells were observed in some samples and this correlated with the PKH26 positivity using flow cytometer.

4.3.3 Proliferation Rates of PKH26^{Hi} and PKH26^{Lo} cells Compared to Unsorted Population

PKH26^{Hi}/PKH26^{Lo} cells isolated from the RPMI 8226 and NCI-H 929 multiple myeloma cell lines cells by FACSAria and post sorting analysis showed > 96% purity of cell populations with >80% cell viability. Moreover, cultured of PKH26^{Hi}/PKH26^{Lo} cells in isolation and left to proliferation displayed that PKH26-retaining cells (PKH26^{Hi}) demonstrated more proliferative potential compared to PKH26^{Lo} population in all multiple myeloma cell lines and to the unsorted population in NCI-H 929 and RPMI 8226 cell lines during the first 3 days. PKH26^{Hi} cells from multiple myeloma cell lines had higher cell count than PKH26^{Lo} populations due to these being CSCs and initiating the cell growth (Figure 4.8). Following 1 week cultured, the sorted cells did not proliferate to the same extent as the unsorted cells whereas the unsorted population revealed high proliferating following culture. However, PKH26-retaining cells (PKH26^{Hi}) demonstrated almost the same proliferative potential compared to PKH26^{Lo} populations in all multiple myeloma cell lines (Figure 4.8).

Figure 4.8: Proliferation rates of PKH26^{Hi} and PKH26^{Lo} cells compared to unsorted multiple myeloma population

Figure 4.8: Proliferation rates of PKH26^{Hi} and PKH26^{Lo} cells compared top unsorted population. PKH26^{Hi} and PKH26^{Lo} cells and unsorted population were cultured in isolation for one week following sorting and proliferation potential was assessed. Statistical significance was set at p<0.05 by the Kruskal–Wallis test.

4.3.4 Effect of PKH26 Status on LMB, SAHA, BIX 01294 and GSK343-Induced TRAIL Responses

PKH26^{Hi}, PKH26^{Lo} cell and unsorted cell population were stimulated with TRAIL+/- sensitizers at doses known to induce apoptosis in the majority of unselected cells, and apoptosis assessed by Hoechst 33342 staining and assessment of nuclear morphology coupled with Annexin V-FITC. The data shows that PKH26-retaining cells (PKH26^{Hi}) were less sensitive to TRAIL compared to unsorted parental populations in NCI-H 929 and RPMI 8226. In contrast, PKH26^{Lo} cells were similarly sensitive to TRAIL as compared to the parental cells. LMB, SAHA, BIX 01294, and GSK343 were found significantly to induce apoptosis in PKH26^{Lo} cell and unsorted cell population of myeloma cell lines NCI-H929 and RPMI 8226 following treatment for 24 h ($p < 0.0001$) (Figure 4.9, 4.10, 4.11, 4.12). However, no significant response was observed following the treatment with these TRAIL sensitizers combined with a high dose of TRAIL in PKH26^{Hi} cell population. In NCI-H 929 cells, a high apoptotic response of 74.9±6.6%, 49.06±10.3%, and 75.2±4.4% ($p < 0.0001$) were measured in unsorted population following treatment with high dose of BIX 01294, TRAIL, and combined dose of 20 µM BIX 01294 and 50 ng/ml TRAIL respectively for unsorted population (Figure 4.11a, b). The apoptotic response of PKH26^{Lo} for 20 µM BIX 01294, 50 ng/ml TRAIL, and the drug combination was 97.3±2.3%, 77.3±2.5%, and 100±0% respectively (Figure 4.11 a, b). Whereas, no significant apoptotic effect was seen in PKH26^{Hi} cell population following treatment with high dose of BIX 01294 either alone or in combination and apoptotic response of 16.6±5.6%, 15±2.7%, and 16.2±4.4% were measured in PKH26^{Hi} cell population following treatment with a high dose of BIX 01294, TRAIL, and co-treatment of both drugs respectively (Figure 4.11 a, b). The same effect was seen with a long-term culture where PKH26-retaining cells (PKH26^{Hi}) were resistant to doses of drugs that induced significantly high apoptosis in PKH26^{Lo} cells and unsorted parental populations of NCI-H 929 and RPMI 8226 cell

lines. These data suggest that PKH26[Hi] cells are much more resistant to apoptosis-inducing therapies than parental cells, or PKH26[Lo] cells, and would likely result in treatment failure (Figure 4.9, 4.10, 4.11, 4.12). An example of the morphological assessment of apoptosis for TRAIL in combination with LMB in unsorted, PKH26[Lo] and PKH26[Hi] NCI-H929 cells is shown in Figure 4.9.

Figure 4.9: Effect of PKH26 status on LMB-induced TRAIL responses in multiple myeloma cells

a)
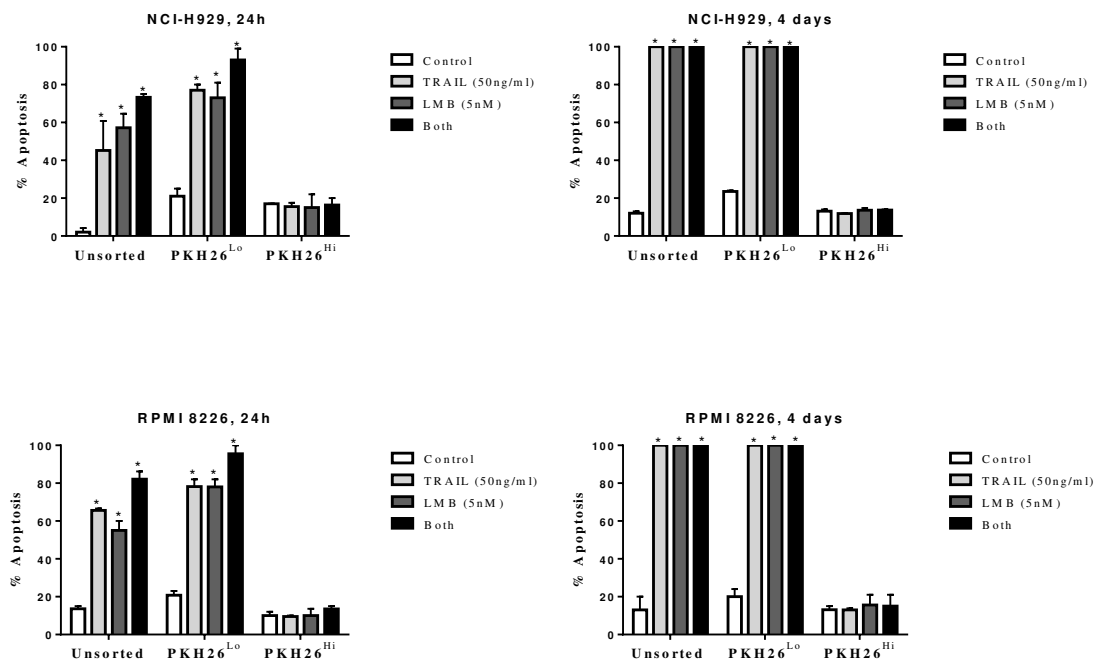
Figure 4.9 a): Effect of PKH26 status on LMB-induced TRAIL responses in NCI-H929. PKH26[Hi], PKH26[Lo] cell and unsorted cell population were stimulated with high doses of TRAIL+/-LMB and apoptosis assessed by Hoechst 33342 staining and assessment of nuclear morphology coupled with Annexin V-FITC. The data is expressed as median with range (three independent experiments, each in triplicate). The statistical significance was determined by comparison with the vehicle control, statistical significance was set at p<0.05 by the Kruskal–Wallis test.

Figure 4.9 b)
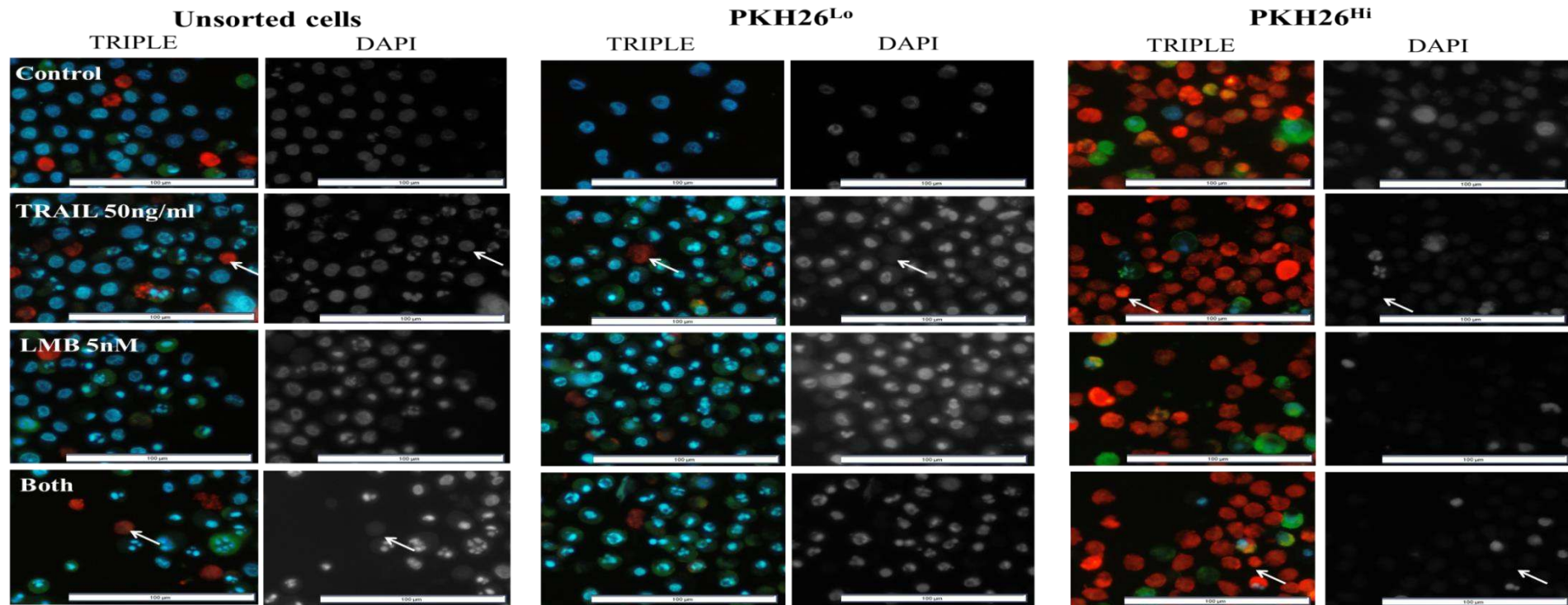
Figure 4.9 b): An example of the morphological assessment of apoptosis for TRAIL in combination with LMB in unsorted, PKH26^Lo and PKH26^HI NCI-H929 cells. *PKH26^Hi and PKH26^Lo and unsorted NCI-H929 cells with a high dose of LMB and TRAIL alone and in combined and assessment with double staining of Hoechst 33342 staining and Annexin V-FITC using fluorescence microscope. Microscopy showed the apoptosis pattern of bright condensed or fragmented chromatin, and increased signals of Annexin V (green). The white arrow indicated for example of PKH26 retained dye cells that did not undergo apoptosis.*

Figure 4.10: Effect of PKH26 status on SAHA-induced TRAIL responses in multiple myeloma cells

a)
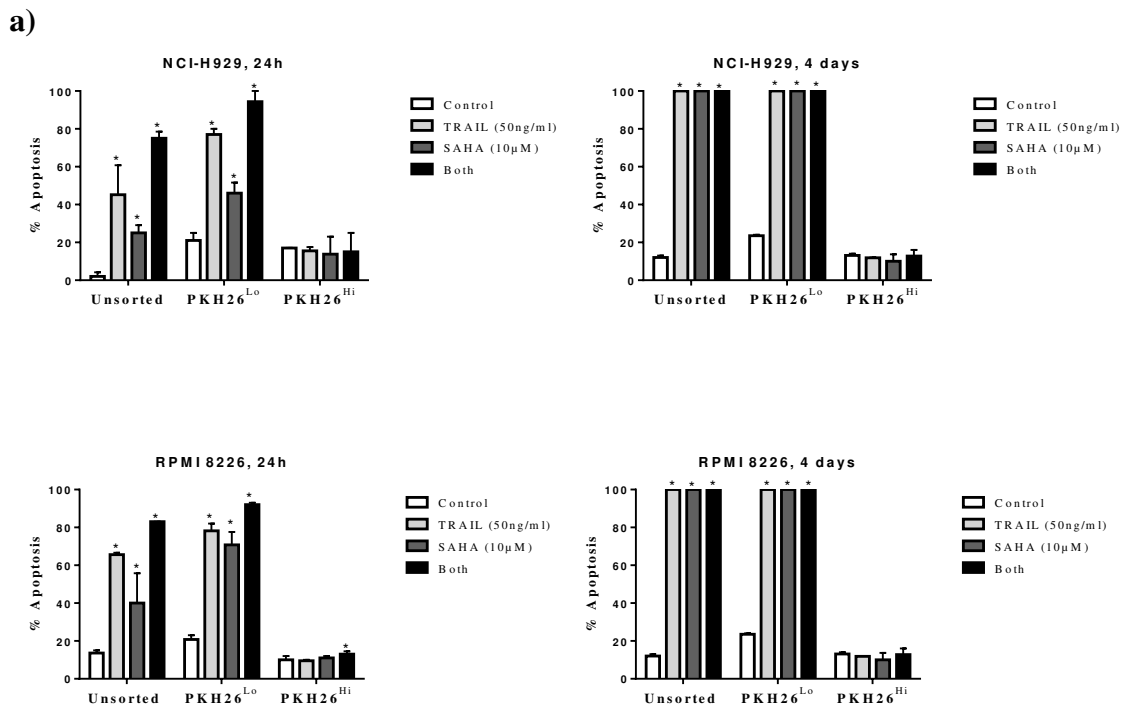
Figure 4.10 a): Effect of PKH26 status on SAHA-induced TRAIL responses in NCI-H 929. PKH26^{Hi}, PKH26^{Lo} cell and unsorted cell population were treated with high dose of SAHA and TRAIL alone and in combined for 24 h and apoptosis assessed by Hoechst 33342 staining and assessment of nuclear morphology coupled with Annexin V-FITC. The data is expressed as median with range (three independent experiments, each in triplicate). The statistical significance was determined by comparison with the vehicle control, statistical significance was set at p<0.05 by the Kruskal–Wallis test.

Figure 4.10 b)
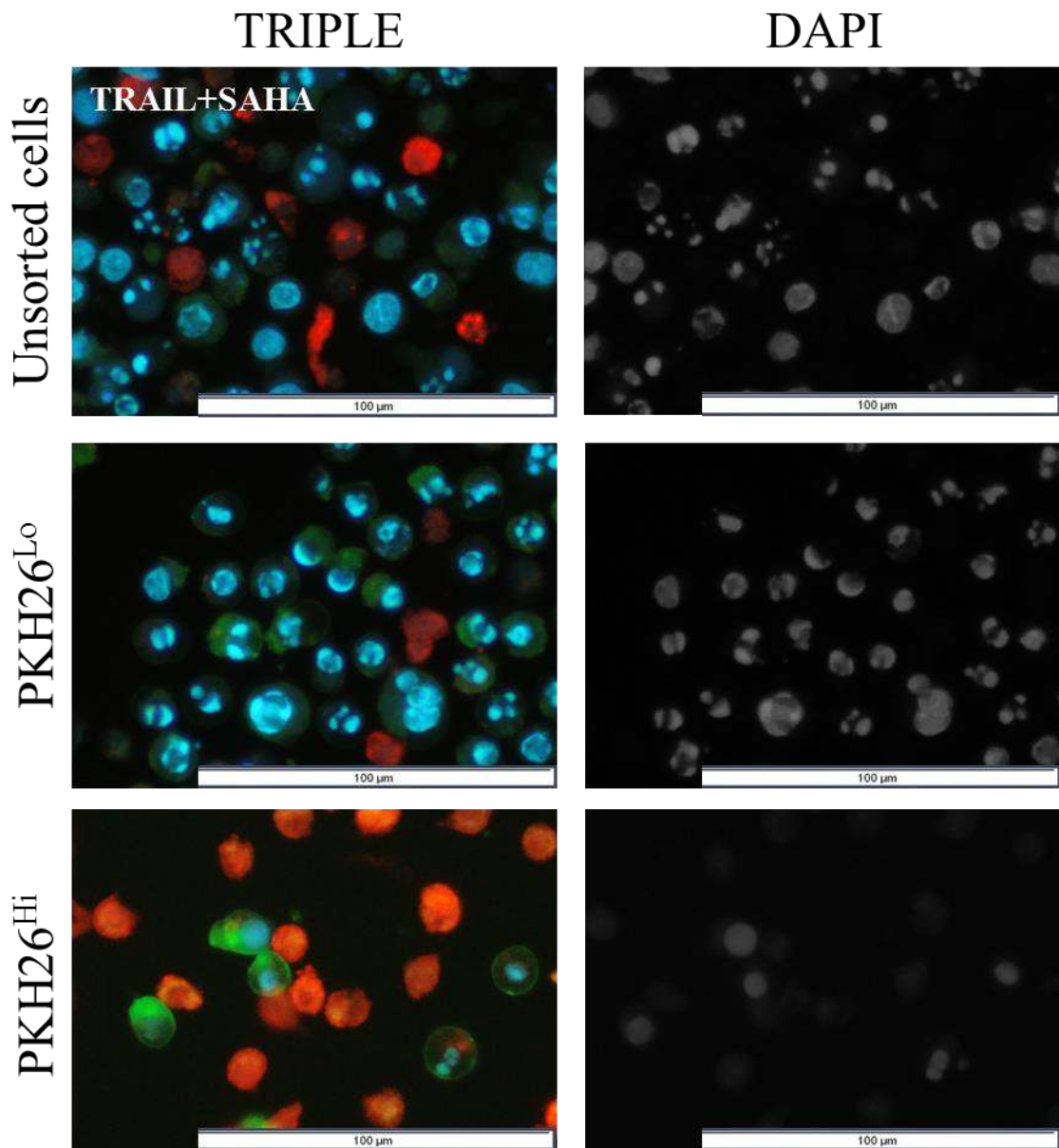
Figure 4.10 b): An example of the morphological assessment of apoptosis for TRAIL in combination with SAHA in unsorted, PKH26^{Lo} and PKH26^{HI} NCI-H929 cells. PKH26^{Hi} and PKH26^{Lo} and unsorted NCI-H929 cells with a high dose of SAHA in combination with TRAIL and assessment with double staining of Hoechst 33342 staining and Annexin V-FITC using fluorescence microscope. Microscopy showed apoptosis pattern: bright condensed or fragmented chromatin and increased signals of Annexin V (green).

Figure 4.11: Effect of PKH26 status on BIX 01294-induced TRAIL responses in multiple myeloma cells

a)
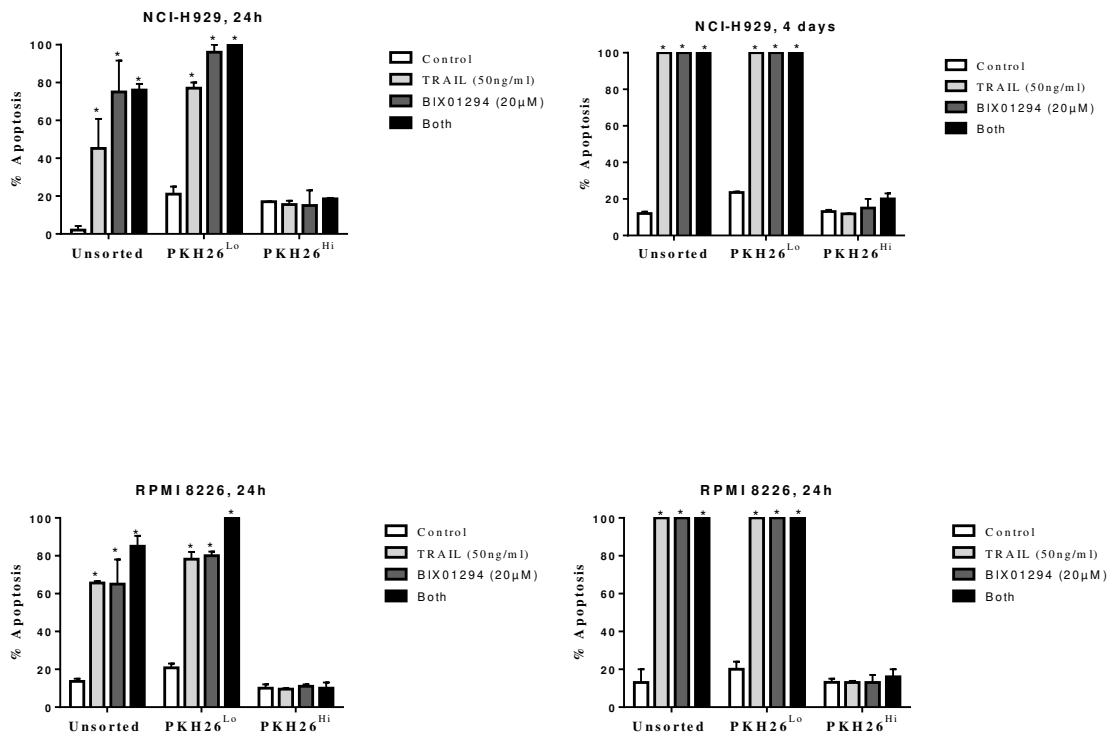
Figure 4.11 a): Effect of PKH26 status on BIX 01294-induced TRAIL responses in NCI-H929 cells. PKH26^{Hi}, PKH26^{Lo} cell isolated from MM cells and unsorted MM cell population were treated with TRAIL and BIX 01294 alone and in combined for 24h using the high dose of drugs which induced significant induction apoptosis. The data is expressed as median with range (three independent experiments, each in triplicate). The statistical significance was determined by comparison with the vehicle control, statistical significance was set at *=p<0.05 by the Kruskal–Wallis test.

Figure 4.11 b)
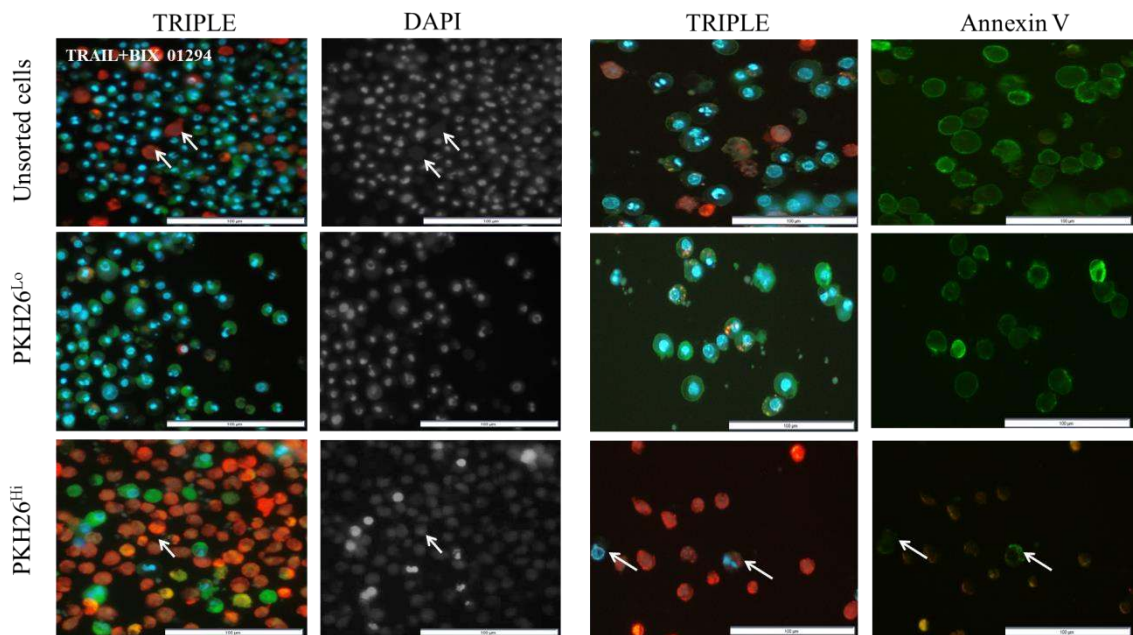
Figure 4.11 b): An example of the morphological assessment of apoptosis for TRAIL in combination with BIX 01294 in unsorted, PKH26^{Lo} and PKH26^{Hi} NCI-H929 cells. PKH26^{Hi} and PKH26^{Lo} and unsorted NCI-H929 cells with a high dose of BIX 01294 in combination with TRAIL and assessment with double staining of Hoechst 33342 staining and Annexin V-FITC using fluorescence microscope. Microscopy showed apoptosis pattern: bright condensed or fragmented chromatin and increased signals of Annexin V (green). The white arrow indicated for example of PKH26 retained dye cells.

Figure 4.12: Effect of PKH26 status on GSK343-induced TRAIL responses in multiple myeloma cells

a)
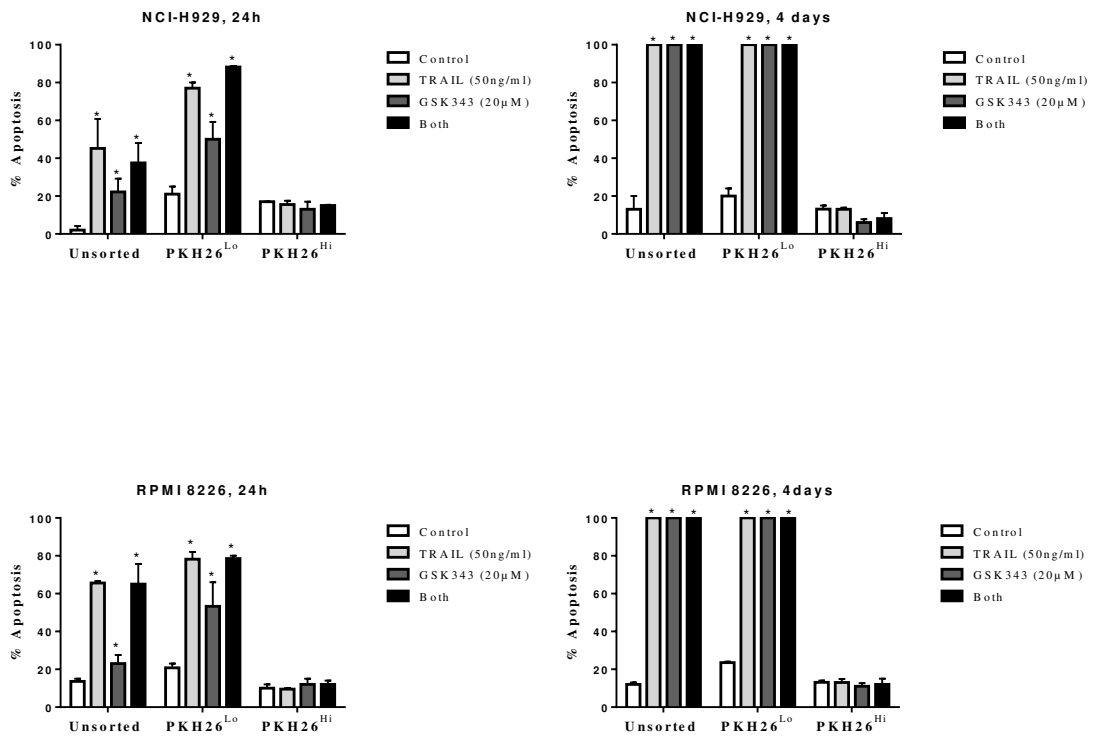
***Figure 4.12 a): Effect of PKH26 status on GSK343-induced TRAIL responses in NCI-H 929.** PKH26^{Hi}, PKH26^{Lo} cell and unsorted cell population were stimulated with high dose of TRAIL+/-GSK343 and apoptosis assessed by Hoechst 33342 staining coupled with Annexin V-FITC and examined with fluorescence microscopy. The data is expressed as median with range (three independent experiments, each in triplicate). The statistical significance was determined by comparison with the vehicle control, statistical significance was set at *=p<0.05 by the Kruskal–Wallis test.*

Figure 4.12 b)
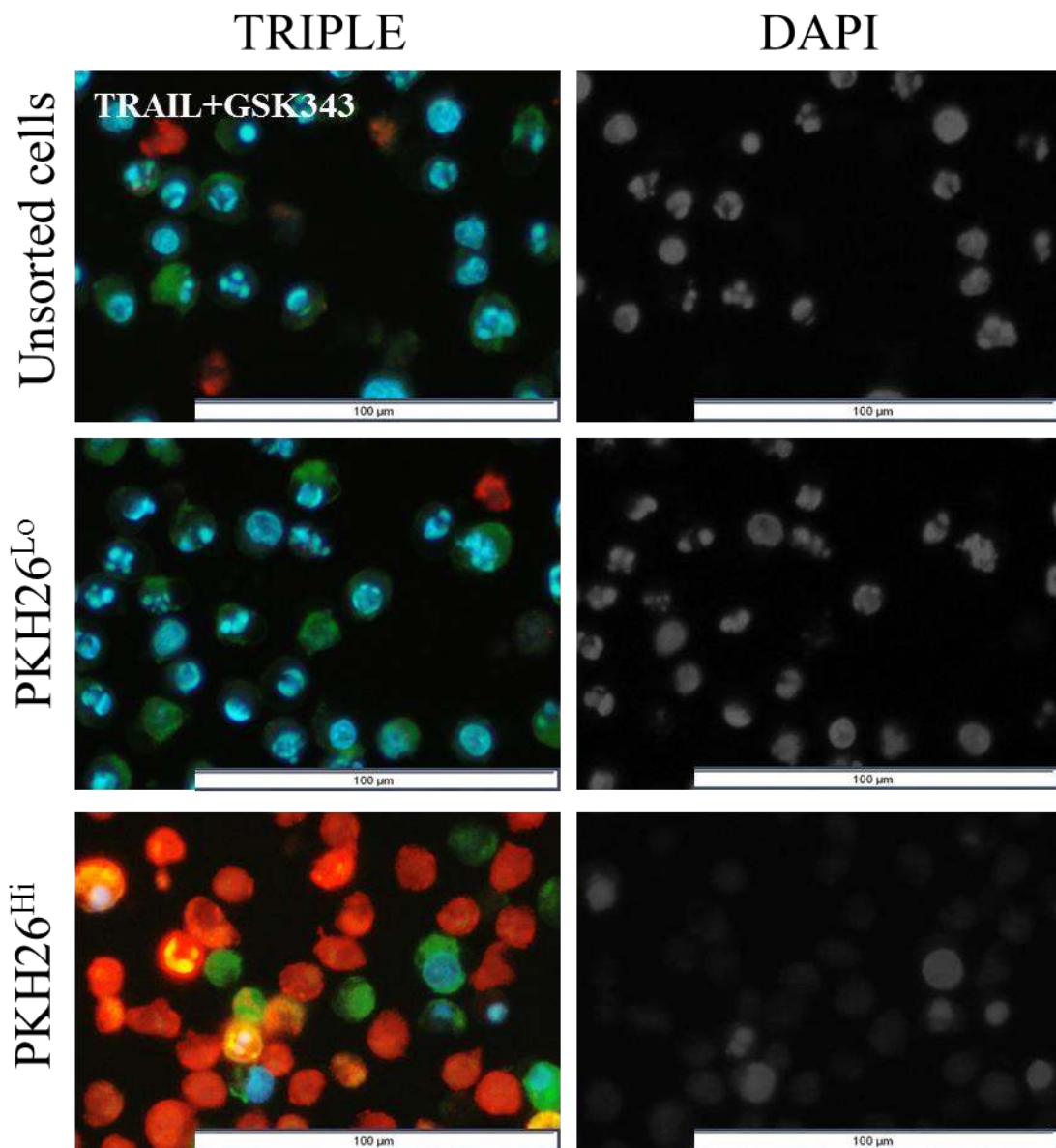
Figure 4.12 b): An example of the morphological assessment of apoptosis for TRAIL in combination with GSK343in unsorted, PKH26^Lo and PKH26^HI NCI-H929 cells. PKH26^Hi and PKH26^Lo and unsorted NCI-H929 cells with a high dose of GSK343 in combination with TRAIL and assessment with double staining of Hoechst 33342 staining and Annexin V-FITC using fluorescence microscope. Microscopy showed apoptosis pattern: bright condensed or fragmented chromatin and increased signals of Annexin V (green).

4.3.5   PKH26^{Hi} Population Contains the CD138^{-ve} Sub-population

Flow cytometric evaluation of Syndecan-1 expression by multiple myeloma cell lines showed that the majority of cells in both parental multiple myeloma cell lines RPMI 8226 and NCI-H 929 expressed a high level of cell surface antigens CD138; however, each cell line contained a distinct population of CD138^{-ve} cells that represented (Figure 4.13). Following sorting, the PKH26 ^{Hi} and PKH26 ^{Lo} cell were stained with anti-human CD138 (PE/Cy7) or isotopic control antibodies. Cells were analysed to identify the expression of percentages of CD138 in PKH26^{Hi} cells compared to unlabelled cells. Data demonstrated that the majority of the sorted PKH26^{Hi} cells did not express the surface marker CD138. Therefore, indicating that there may be small cell population with a stem cell-like phenotype within the main multiple myeloma population which also resists therapies (Figure 4.14).

To further explore the phenotype of the multi-cellular tumour spheroid model formed in the alginate beads, the expression of marker for the CD138 was detected in 3D growth using immunohistochemistry. As shown in Figure 4.15 the expression of putative cancer stem cell marker CD138 in 3D cell culture was observed in some colonies after 14 days of seeding, while it was not observed in most of the colonies within the alginate beads and some colonies with variable positivity a cross the colony. In contrast, the expression of CD138 was retained in suspension cell culture using flow cytometry (Figure 4.13).

Figure 4.13: CD138 expression on multiple myeloma cell lines as detected by flow cytometry
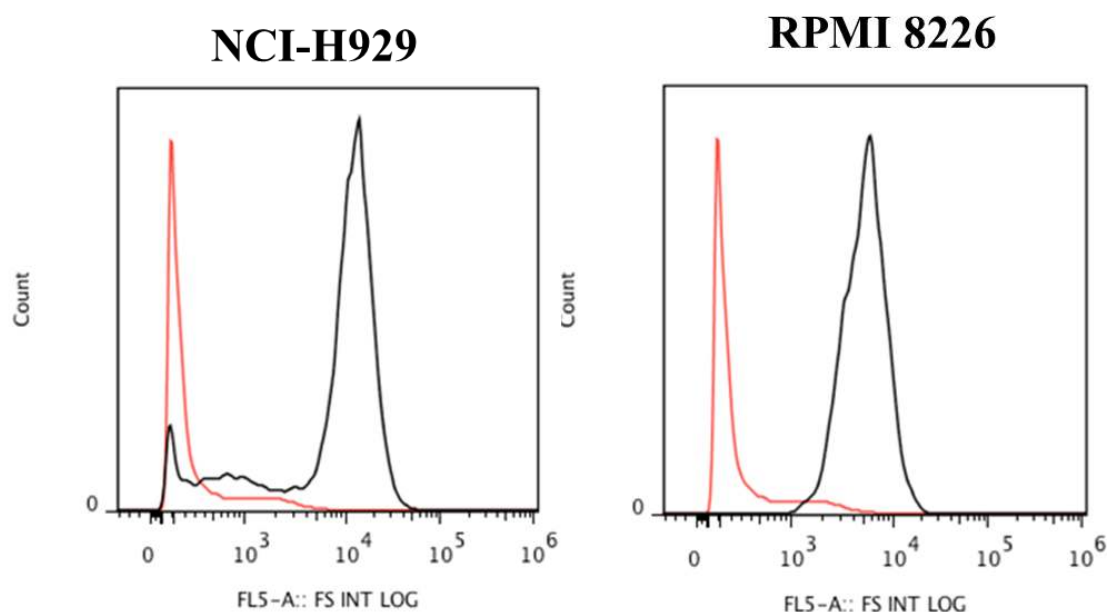
Figure 4.13: CD138 expression on myeloma cell lines as detected by flow cytometry. NCI-H 929 and RPMI 8226 multiple myeloma cell lines were incubated stained with syndecan-1(PE/Cy7). CD138 protein expression is represented as a histograms plot whereas red histograms represent staining with the isotype control antibody and black histograms represent staining with PE/Cy7 anti-human CD138 (Syndecan-1) fluorescence antibody.

Figure 4.14: CD138 activity of sorting PKH26^{Hi} cell population and compared to parental un-labelled cells by flow cytometry
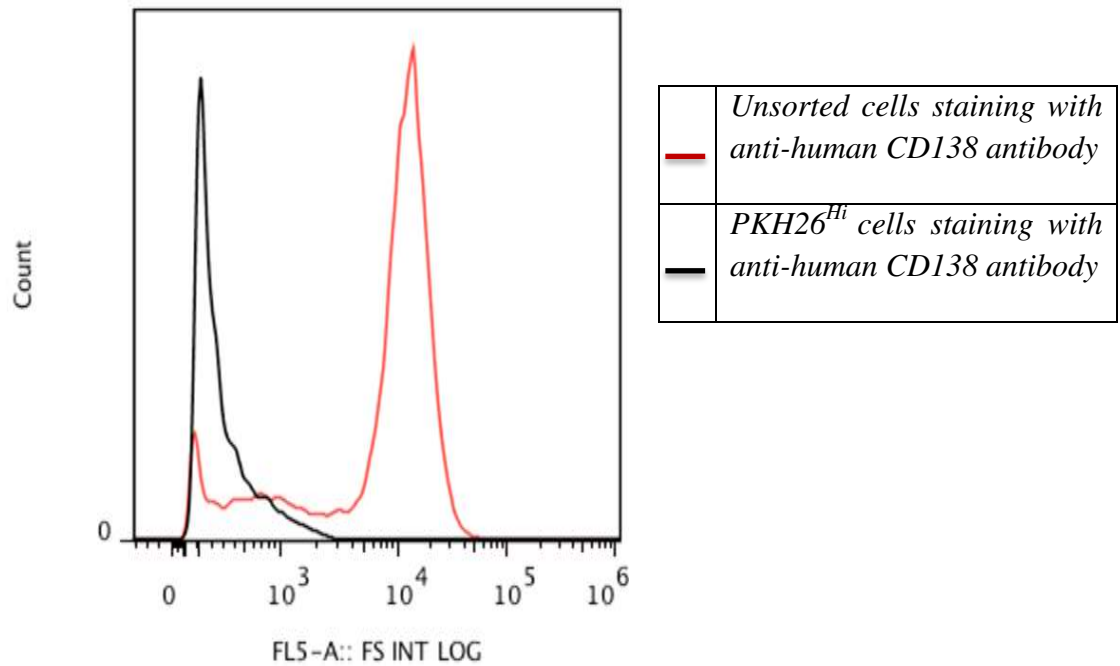
Figure 4.14: CD138 expression of sorting PKH26^{Hi} cell population and compared to parental un-labelled cells by flow cytometry. Both parental and PKH26 ^{Hi} NCI-H929 Cells at a density of 1 x 10^6/ml were stained with syndecan-1 and the level of syndecan-1 was identified using flow cytometry. Flow cytometric analysis of CD138 expression are represented as histograms plot where red histograms represent parental cells staining with PE/Cy7 anti-human CD138 (Syndecan-1) fluorescence antibody and black histograms represent PKH26 ^{Hi} cell staining with anti-syndecan-1 (PE/Cy7).

Figure 4.15: CD138 activity of NCI-H929 alginate beads immunohistochemistry
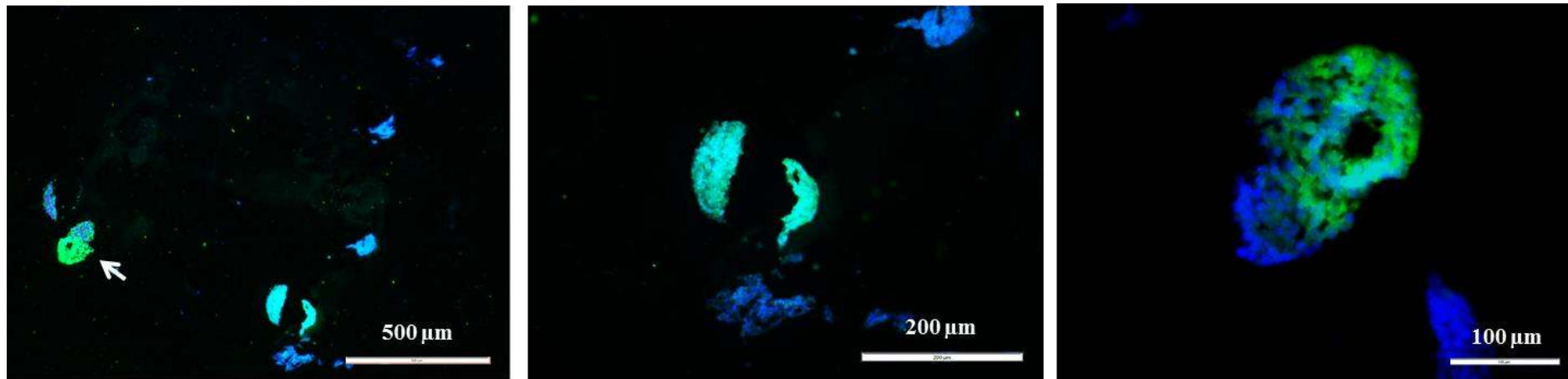
Figure 4.15: CD138 expression of NCI-H 929 alginate beads immunohistochemistry. *NCI-H 929 cells in 3D alginate beads were immuno-stained with PE/Cy7 anti-human CD138 (Syndecan-1) (green) and DAPI (blue, for nuclear stain). Some colonies stained positive; some are negative and some those that are positive, the positivity variable across the colony. The fact that most colonies in 3D are Syndecan-1 negative is counter intuitive as in 3D, CD138^{-ve} cells are very TRAIL sensitive.*

4.4   Discussion

Despite advancement in understanding of tumour mechanisms and therapy have significantly improved in recent years, cancer still one of the major health problem in many countries (Cojoc *et al*., 2015). Even though the majority of tumour bulk was eliminated by conventional therapeutic agents in some type of cancer including MM, the relapse from therapy consequently occurs. Disease relapse suggests to the existence of chemo-resistance cells population with tumour regrowth potential but the full understanding of the role of these cells in MM growth following treatment remains obscure (Matsui *et al*., 2008). Since the emergence of CSC hypothesis, evidence suggests that a curative therapy will be potential if the quiescent CSCs entirely eradicated and efficient therapy targeting all CSCs (Cojoc *et al*., 2015; Reya *et al*., 2001). The aim of this investigation was to identify and isolate CSCs-like by optimising PKH26 membrane labelling dye and if quiescent multiple myeloma cell populations responded differentially to the Death Receptor agonist TRAIL in combination with TRAIL sensitizers.

4.4.1   Isolation of CSCs using PKH26 Dye

Firstly, this study optimised the PKH26 labelling of multiple myeloma cell lines using PKH26 membrane labelling kit in order to obtain uniformly fluorescence-stained cells. The fluorescence dye integrates into the cell membrane without any toxicity and is diluted during cell division leading to dyeing of quiescent CSCs cells within a proliferating cell population. (Chen *et al*., 2014; Fisher and Mackenson., 2003). Following dye optimisation, the decrease in fluorescence intensity was monitored using both flow cytometry and microscopy. Both approaches correlated with a reduction in red fluorescence dye observed over time with only a small population of PKH26

retained cells in multiple myeloma cell lines after two weeks (Figure 4.1, 4.2, 4.3 and 4.4). Following separation of myeloma cells into PKH26^{Hi}/PKH26^{Lo} cells by FACS small number of PKH26-retaining cells (PKH26^{Hi}) was obtained due to the low percentage of cells which were still red stained compared to the whole population (Figure 4.6, 4.7). PKH26^{Hi} cell populations have been identified in many types of cancer (Kusumbe and Bapat., 2009; Pece *et al*., 2010; O'Brien *et al*., 2012; Chen *et al*., 2014). In addition, these cells displayed CSC markers such as CD44 in breast cancer besides having a self-renewing ability and drug resistance (Nakshatri., 2010).

Previous study was able to isolate near purity of human normal mammary stem cells from cultured mammospheres using PKH26 labelling dye (Pece *et al*., 2010). These cells are quiescent and possess all the stem-like characteristics. Very few cells within mammospheres retained PKH26 fluorescence dye and around one mammosphere-initiating cell is existing per mammosphere, and that this cell is likely located within the PKH26-positive cell population. By microscopically monitoring the growth of PKH positive cells cultured in methylcellulose, mammospheres were shown to be the result of the clonal expansion of single PKH-retaining cells, but not PKH26-negative cells. These PKH26^{Hi} cells displayed the quiescent state features including retention of the modulated nucleotide BrdU, absence the proliferation marker Ki-67 expression, and asymmetrically division all consistent with stem cell behavior (Pece *et al*., 2010). Moreover, analysis the panel of marker on quiescent PKH26 positive cells in Pece *et al* work by immunofluorescence revealed that quiescent PKH^{Hi} cells expressed both epithelial (CD24^{+}/EpCAM^{+}) and myoepithelial (CD49F^{+}/CK5^{+}/TP63^{+}) cells; but, they did not express terminal differentiation markers, such as E-cadherin, ASMA and MUC1. However, PKH^{Lo} cells, displayed little or none of this marker compared to PKH positive cells. The study by Pece *et al*., (2010) proposed that PKH positive cell population in breast are bipotent and the majority of colonies obtained from PKH

positive cells expressed both epithelial and myoepithelial. In contrast, PKH negative cells population develop either pure epithelial or pure myoepithelial colonies (Pece *et al*., 2010). In addition, quiescent PKH positive cells were able to grow in 3D structures and can generate mammary gland organotypic outgrowths while PKH negative cells only grew as monolayers of terminally differentiated cells and did not generate 3D structures. Taken together, these data indicating that the PKH retaining dye cells possess all the characteristics expected for stem cells (Pece *et al*., 2010).

PKH26 dye also has been used in colon cancer to isolate the quiescent cells. A study carried out by O'Brien *et al*., (2012) found a minor population of non-dividing cells within the colon cancer which can separate out and the PKH26 retained cells were able to establish spheres more quickly than the PKH26 negative cells when a sphere-forming assay was performed (O'Brien *et al*., 2012). In addition, O'Brien et al., (2012) showed that the self-renewal capacity of cancer-initiating cells is dysregulated and these cell populations possess chemotherapy and radiation resistant properties due to the expression of genes that have been involved in self-renewal properties of stem cells (O'Brien *et al*., 2012). These proteins are the inhibitor of DNA binding proteins (IDs), a family of homologous helix-loop-helix (HLH) transcriptional regulatory factors (ID1– ID4) with known functions in growth, differentiation, senescence, and migration (Fong *et al.,* 2004). According to O'Brien *et al.,* (2012) ID1 and ID3 proteins regulate self-renewal capacity of cancer initiated cells isolated from primary colon cancer samples and the knockdown of these genes resulted in a dramatic loss of tumour-initiating capacity by down-regulation of a cell-cycle inhibitor p21. p21 has a role in the prevention of exhaustion of cancer stem cells through cell-cycle restriction and protection from DNA damage (O'Brien *et al*., 2012).

4.4.2 The proliferative Potential of PKH26 Retained Cells Isolated from Multiple Myeloma Cell Lines

The PKH26^{Hi} sorted cells were evaluated for proliferation potential as this investigation hypothesized that the cells that retained the dye would proliferate faster. Results from the current study showed that the PKH26^{Hi} cell population exhibited similar proliferative potential compared to PKH26^{Lo} cell populations but they were less proliferative in compared to the unsorted population in multiple myeloma cell lines (Figure 4.8). Moreover, labelling of ovarian cancer cells with PKH26 in previous study and sorted by FACS after being left to proliferate *in vivo* demonstrated that the quiescent PKH26^{Hi} cells had highest self-renewal capabilities and higher proliferation rates as well as could initiate cancer re-growth *in vivo* even though significantly lower number of cells were injected when compared with the PKH26 negative cells population (Kusumbe and Bapat., 2009). Moreover, the isolated PKH26 negative population completely lacked the colony formation ability *in vitro* using the colony formation technique. In addition to the higher expression of stem cell marker Nanog, Oct4, Nestin, and Bmi in PKH26^{Hi} subsets while lacked expression of all four stem cell markers in the PKH26^{Lo} subset (Kusumbe and Bapat., 2009). These analyses suggested that the tumour-initiating potential of tumour lies mainly within the PKH26^{Hi}. Furthermore, two different cell populations were identified within PKH26 retained cells population; these comprised the CSCs in addition to aneuploidy cells population which seemed to have a dormant phenotype, most likely senescent cells. In the majority of cancers, cancer stem cells are thought to survive, persist and maintain functionality through therapy regimes; thus contributing to tumour dormancy and represent a difficult obstacle in limiting drug outcomes, while the genetic heterogeneity raised by quiescent or cell cycle arrested aneuploid sub-population may effect tumour therapy resistance by re-entry into the cell cycle to generate a disease progression (Kusumbe and Bapat., 2009).

The reduced cell production capacity of sorted PKH26^{Hi} and PKH26^{Lo} cells may be a consequence of a period of dormancy post-sorting. Alternatively, PKH26^{Lo} are exhausted, PKH26^{Hi} are quiescent and PKH intermediate is transit amplifying. Following a certain number of cell divisions, cells depart the stem cell pool and terminal differentiation is unavoidable, therefore PKH26^{Lo} may represent terminally differentiated cells (Young *et al.,* 1996). It has been found that isolation of hematopoietic cells CD34$^+$/Thy^{-+}1/Lin$^-$ from bone marrow or mobilized peripheral blood (MPB) by labelled with the fluorescent dye PKH26 and cultured *in vitro* in the presence of interleukin-3, interleukin-6, c-kit ligand, and leukemia inhibitory factor (LIF) resulted in retention of primitive quiescent cells. Following 14 days of the expansion period, was sorted into two population CD34$^+$/Lin$^-$/dye^{Bright} and CD34'/Lin$^-$/dye^{Dim} fractions and sub-cultured for more four weeks and single-cell proliferation assay was performed in order to identify the proliferative capacity of each cell population. A high percent of progenitors remaining dye were observed to proliferate in compare to dye dim cells which shown a lower average proliferative capacity. These results indicate that cells with a higher proliferative potential recover following culture expansion with cytokines were those that established quiescent behavior and progressive loss of production capacity of the cell seemed to be a consequence of cell division under the experimental culture conditions used in this study (Young *et al.,* 1996).

4.4.3 PKH26-retaining Cells Demonstrated Resistant Potential to Anti-tumour Agents Compared to Unsorted Parental Populations in Multiple Myeloma Cell Lines

The sorted PKH26^{Hi} cells isolated from multiple myeloma cell lines following cultured in isolation and unsorted cells were assessed for drugs sensitivity as this investigation hypothesized that the PKH26^{Hi} cells are quiescent CSC-like cells and are the source of TRAIL-resistance in Multiple Myeloma given that CD138^{-ve} cells are generally TRAIL^R

(Vitovski *et al*., 2012). Here in this study, the isolated PKH26-retaining multiple myeloma cells were less sensitive to all of the anti-tumour drugs compared to PKH26^{Lo} and unsorted parental populations (Figure 4.9, 4.10, 4.11 and 4.12). Results from the current study consistent with a work carried out by Chen *et al*., (2014) and they found that the quiescent PKH26^{Hi} multiple myeloma cells (RPMI 8226 and NCI-H 929) isolated using PKH26 dye exhibited enriched stem-like properties by the ability of forming colonies in semi-solid medium as well as more resistant to anti-tumour agents including cyclophosphamide, bortezomib, vincristine, prednisone, and rituximab *in vitro* compared with PKH26^{Lo} cell populations. In addition, the injection of PKH67^{Hi} multiple myeloma cells into NOD/SCID mice showed that quiescent PKH$^+$ cells were preferred to inhabit in the osteoblastic regions niche of the bone marrow compared with the spleen or vascular niche. These data also confirmed by immunohistochemistry analyses. Moreover, PKH$^+$ cells that expressed CD138 were generally found away from bone lining regions, however, PKH$^+$ cells that were CD138^{-ve} were also found following 48 h of *in vivo* growth. This result suggests that most quiescent multiple myeloma populations did not express the surface marker CD138. On the other hand, isolation of CD138^{+ve} and CD138^{-ve} myeloma cells followed by staining with PKH dyes and injected into irradiated mice revealed that CD138^{-ve} cells isolated from myeloma cells retained the PKH67 dye preferentially than CD138^{+ve} myeloma cells *in vivo*, demonstrating that CD138^{-ve} cells persisted as quiescent cells *in vivo* compared with the PKH$^+$ cells that expressed CD138 (Chen *et al*., 2014). Other studies showed that human prostate cancer cell lines PC3 and LNCaP and its variant C4 2B4 contain populations of cells that are slow growing/quiescent but not specifically stem like. The mitotically quiescent population was very significantly more tumourigenic *in vivo* compared to the rapidly proliferating cells and had a distinctive gene expression profile *in vitro* such as CXCR4 which has been implicated in prostate cancer cell migration (Wang *et al*.,

2015).

Other studies have shown that breast cancer initiating cells are not only the surviving sub-population of ionizing radiation but also retain the cancer stem phenotype in compare to non-tumourigenic counterparts (Nakshatri., 2010). Irradiated cancer initiating cells in breast cancer are resistant to ionizing radiation and retained their self-renewal potential, and become more aggressive compared to non-irradiated stem cell control. The radiation-resistant cells exhibit the characteristics of CICs including expression of $CD44^+/CD24^-$ marker, low proteasome activity, and retained PKH26 dye. In addition, fractionated radiation not only induces proliferation of a sub-population of PKH retained cells or cancer initiating cells but also mobilized them from a quiescent/G_0 phase to a proliferative state (G_2 phase) of the cell cycle, whereas the non-irradiated cancer stem cells are non-proliferating and are mainly in the G_0 phase of the cell cycle and the surviving non-tumourigenic cell population were driven into senescence (Lagadec *et al.,* 2010; Nakshatri., 2010).

In other studies, quiescent cells in myeloma resist proteasome inhibitors bortezomib and bortezomib-surviving MM cells characterised by upregulation of $p21^{CIP1}$ and GRP78, an unfolded protein response survival factor, and downregulated CDK6, Ki67 and pRb. Moreover, the combination treatment of bortezomib and 5-azadeoxycitidine induced apoptosis and quiescence stability and might represent a novel approach treatment of MM (Adomako *et al*., 2015). In addition, the quiescent sub-population in glioblastoma has been shown to selectively resist temozolomide therapy (Chen *et al*., 2012). Furthermore, Dormant DiD-retained myeloma cells (analogous to PKH^{Hi} cells) are resistant to melphalan (Lawson *et al*., 2015). These results suggest that target this population has the potential novel therapeutic approaches for multiple myeloma.

In contrast, quiescent or PKH^{Hi} non-small cell lung cancer were significantly more sensitive to Bcl-XL inhibition, ABT-737 than rapidly proliferating PKH^{Lo} cells,

indicating that quiescent lung cancer cells strongly depend on Bcl-XL Bcl-2 family proteins for their survival (Zeuner *et al*., 2014).

4.4.4   PKH26^{Hi} Cells are CD138^{-ve}

The data presented in this study shows that the majority of the sorted PKH26^{Hi} cells did not express the surface marker CD138 (Figure 4.14), indicating that there may be small cell population with a stem cell-like phenotype within the main multiple myeloma population. In addition, the immunofluorescence data suggested that most of the colonies within the alginate beads did not expresse CD138 in NCI-H 929 MM cell line in 3D culture (Figure 4.15).

In a study conducted by Matsui *et al*., (2004) they demonstrated that human MM cell lines RPMI 8226 and NCI-H 929 contained a high percentage of CD138^{+ve} cells with only small populations (<5%) that lacked CD138 expression. These subpopulations had significantly more clonogenic potential as well as expressed a higher level of proliferation marker Ki67 than the CD138^{+ve} cells. In addition, CD138^{-ve} expressed CD19, CD20 antigens and accordingly, none of the CD138^{+ve} of both MM cell lines expressed these antigenic markers. These data propose that stem cells of MM are CD138^{-ve} sub-population with the capability to replicate and consequently differentiate into malignant CD138^{+ve} plasma cells (Matsui *et al.,* 2004). Later, Matsui *et al.,* (2008) demonstrated that CD138^{+ve} multiple myeloma cells cannot undergo long-term proliferation but rather devolve from clonogenic CD138^{-ve} cells population. CD138^{+ve} MM plasma cells more sensitive to clinical used anti-myeloma therapy dexamethasone, lenadilomide, bortezomib, and 4-hydroxycyclophosphamide compared to CD138^{-ve} precursors *in vitro*. Moreover, CD138^{-ve} cells population possesses high drug efflux capacity and intracellular drug detoxification activity as identified by Hoechst side population analysis and Aldefluor assays. In addition to the expression of the memory

B-cell markers CD20 and CD27 that give rise to the clonogenic growth of MM cells *in vitro* (Matsui *et al.,* 2008). The week staining of PKH^{Hi} cells with Hoechst 33342 further support the notion that PKH^{Hi} cells are CSC-like cells.

These results are consistent with a study carried out by Holen *et al*., (2001). Flow cytometric analysis of CD138 expression on the surface of MM cell lines NCI-H929, RPMI 8226, U266 and JJN3 showed that multiple myeloma cell lines expressed different level the surface marker CD138 that was shed constitutively (Holen *et al*., 2001).

Findings from the current investigation are consistent with those of a previous study undertaken by Vitovski *et al*., (2012) which found out that exposure of cultured multiple myeloma cell to TRAIL results in the preferential killing of CD138^{+ve} compared to CD138^{-ve} cells population isolated from bone marrow patients with multiple myeloma. In addition, these CD138^{-ve} cells were less sensitive to doxorubicin and TRAIL alone, or the combination treatment than CD138^{+ve} cells population and have a lower level of TRAIL death receptors expression (Vitovski *et al*., 2012). Earlier work has shown that sequential exposure to the sub-toxic concentration of proteasome inhibitor bortezomib in conjunction with HDAC inhibitors SAHA potently induces mitochondrial dysfunction. Moreover, the bortezomib/HDAC inhibitor treatment significantly triggers ROS generation. In addition, co-treatment with bortezomib/HDAC inhibitors induced marked lethality in CD138^{+ve} cells, but not in the CD138^{-ve} multiple myeloma cells (Pei *et al*., 2004). Kawano *et al*., (2012) reported that CD138^{-ve} cells exhibited decreased sensitivity to lenalidomide compared with CD138^{+ve} cells fraction and high expression of genes expressed at the immature B-cell stage such as BCL6 and low expression of genes associated with mature plasma cells such as IRF4 that may explain the poor response of low expression of CD138 patients to therapy (Kawano *et al.*, 2012).

Other studies showed that CD138^{-ve} cells have high ALDH1 activity, a hallmark of

normal and cancer stem cells and the CD138^{-ve} ALDH^{+} population showed more clonogenic expansion than CD138^{+ve} ALDH^{-} population when plated into methylcellulose medium and only CD138^{-ve} cells differentiated into CD138^{+ve} population. In addition, increase expression of self-renewal and proliferation genes in the CD138^{-ve} fraction such as STAG2, RB1CC1 and Polycomb Repressor Complex (PRC) genes and their target genes including EZH2 compared to CD138^{+ve} population. Importantly, CD138^{-ve} cells were more sensitive to the EZH2 inhibitor, DZNep (Chung *et al*., 2013). In addition, CD138^{+ve} myeloma cells isolated from multiple myeloma patients in recent work responded to specific EZH2 inhibitor UNC1999 treatment, at the same dose range that was used in unsorted multiple myeloma cell lines (Agarwal *et al*., 2016).

This the first time a study has been studied the effect of the interaction between TRAIL and LMB, SAHA, BIX 01294 and GSK343 in quiescent myeloma cells PKH26^{Hi} compared to PKH26^{Lo} and unsorted parental populations. These evidences taken together, suggesting that quiescent low CD138^{-ve} expression cells are more resistant to therapy and establishment of a novel treatment strategy that target this cell population that represents miner fraction of multiple myeloma cells is necessary in order to improve their poor outcome.

4.5   Conclusion

Many therapeutic agents are effective in treatment multiple myeloma, but the majority of myeloma patients relapses. The precise mechanisms responsible for the resistance of multiple myeloma cells to chemotherapeutic agents are unknown, but chemo-resistance usually arises through multifactorial processes (Matsui *et al*., 2008). In this study, the emergence of the TRAIL-resistant population that readily arise from multiple myeloma cell lines in response to the anti-tumour agent TRAIL in presence of TRAIL sensitisers

most likely arise from the quiescent PKH26-retaining population. Therefore, PKH26^{Hi} cells may represent Myeloma-initiating population. Results from current investigation suggest that these stem-like cells contribute to the multiple myeloma drug resistance, persisting of disease and mediate it relapses in patients initially responding. Thus the development of a therapeutic approach that targets this minor sub-population within the tumour is urgently needed. Further studies are required to explore more about the mechanisms of resistant of these therapeutic resistant cells.

5. The Potential Targets of TRAIL-sensitizers in Mediating Apoptosis

5.1 Introduction

It has been demonstrated that TRAIL induces apoptosis and LMB, SAHA, BIX 01294 and GSK343 synergistically enhancing TRAIL responses in multiple myeloma cell lines (Chapters 2-3). Here, the potential mechanisms of enhancement of apoptosis were examined. Firstly, it was essential to determine whether TRAIL alone and/or in combination with TRAIL sensitizers stimulated apoptosis via extrinsic or intrinsic apoptosis pathways, as this could influence the possible apoptosis regulatory molecules that TRAIL and TRAIL sensitizers may modulate. Secondly, specific apoptotic modifiers were investigated in response to TRAIL sensitisers, and finally, preliminary experiments performed on an apoptosis protein array to identify likely targets.

5.1.1 Extrinsic and Intrinsic Apoptotic Pathways

According to Mahmood and Shukla., (2010), apoptosis or programmed cell death is an active process that plays an important role in many physiological processes; most of the chemotherapeutic and radio-therapeutic agents mediate their affect by triggering of apoptosis (Paraoan et al., 2006; Igney and Krammer., 2002) either through stimulating extrinsic and/or extrinsic apoptotic pathways (Ivanov et al., 2011). The extrinsic pathways are stimulated from outside by binding pro-apoptotic ligands such as the tumour necrosis factor (TNF) to the specific death receptors on the cell membrane (Pennarun et al., 2010) (Chapter 1). In contrast, the intrinsic pathway of the apoptosis begins from inside the cell via members of Bcl-2 protein family which prompt mitochondrial disruption resulting in pores formation in the outer-mitochondrial membrane that leads to initiating the apoptotic cascade by the caspase activating (Chapter 1) (Elmore., 2007).

Caspases as a family of cytokine proteases are crucial for the transduction cellular signal pathways that regulate the apoptosis. These caspases are usually synthesised as

inactive pro-caspase that is activated by cleavage (Elmore., 2007; Falschlehne *et al.,* 2007). In apoptotic signaling, caspase-8 and -9 are believed to be the regulative or are initiator caspases that activate downstream effector or executioner caspase-3 (Pan *et al*., 1997). Caspase-8 is activated in an extrinsic pathway of apoptosis and it is responsible for eliminating unwanted cells during development and other stimulation signals while caspase-9 is responsible for stimulating the intrinsic apoptotic pathway in response to the number of stimuli such as DNA damage, irradiation and cytotoxic therapeutic agents (Elmore., 2007). The extrinsic and the intrinsic apoptotic pathways are stimulated by the recruitment and activation of caspase-8 into the DISC or by caspase-9 into the apoptosome respectively. This will in turn stimulate the downstream apoptosis cascade by activating the executioner caspase-3, -6 and -7 (Figure 1.6) (Shankar and Srivastava, 2004; Elmore, 2007).

It is significant to know that the exact molecular mechanism for the stimulation of initiator caspases is not fully understood. Previous study by Vitovski *et al*., (2012) who showed that TRAIL induced apoptosis in the multiple myeloma cell lines; the apoptosis was mediated via the activation of both extrinsic and intrinsic apoptotic pathways through stimulating caspase-8 (the early initiator caspase of the extrinsic pathway), caspase-9 (the early initiator caspase of mitochondrial pathway) as well as caspase-3 and caspase-7 (the effector caspases of the both apoptotic pathways) (Vitovski *et al*., 2012). Moreover, the mechanisms by which HDAC[i] SAHA enhances apoptosis in myeloma cells are still largely unclear. The earlier works reported that the cytotoxic effect of SAHA on the multiple myeloma cell lines was caspase-independent (Fandy *et al.*, 2005; Mitsiades *et al.,* 2003), however since not all effects of SAHA are apoptotic, this does not address the direct apoptotic effects. Other studies illustrated that co-treatment of HDAC[i] SAHA and TRAIL on leukemic cell lines activated both the extrinsic and intrinsic pathways of apoptosis by activating caspase-3 and -8 (Rosato *et*

al., 2003). In addition, recent studies provided evidence that HMTase[i] BIX 01294 and EZH2[i] GSK343 stimulate apoptosis through both intrinsic and extrinsic pathways involving caspase-3, -8 and -9 (Cui *et al.,* 2015; Agarwal *et al.,* 2016).

5.1.2 Potential Targets of the NEI, HDAC[i] and HMTase[i] Mediated Apoptosis and Cell Cycle

5.1.2.1 Bcl-2 Family Member Proteins

Bcl-2 family proteins are the regulators of cell death and they mediate their action through intrinsic or mitochondrial apoptotic pathway by controlling the mitochondrial outer membrane permeabilization (MOMP) (Hardwick and Soane., 2013). Bcl-2 family member proteins are subdivided into pro-apoptotic or anti-apoptotic proteins (Petros *et al*., 2004). Although most of the Bcl-2 homologs suppress apoptosis, pro-apoptotic subset including Bax, Bid, and Bak are activated in response to stress or cell damage causing the loss of mitochondrial integrity and forming a channel in the mitochondrial outer membrane through which a pro-apoptotic proteins including cytochrome *c* exit mitochondria (Elmore., 2007). The release of these proteins stimulates caspase activation in the cytosol and ultimately cell death. The pro-apoptotic protein Bax plays a vital role in triggering apoptosis mediated by certain anti-tumour agents in the human cancer cells. For example, it has been shown that Bax contributes to the mitochondrial pathway of the cell death and that Bax-null colon cancer cells are resistant to apoptosis mediated by TRAIL (Deng *et al*., 2002; Leblanc *et al.,* 2002)

The role of Bcl-2- anti-apoptotic proteins such as Bcl-2, Bcl- XL, Bcl-w, A1/Bfl-1, and Mcl-1 is to block their pro-apoptotic partners and apoptosis (Martinou and Youle., 2011). Over-expression of anti-apoptotic proteins including Bcl2 and Bcl-XL inhibits apoptotic cell death (Yip and Reed., 2008). Furthermore, Wang *et al*., (2010) pointed out that a number of anti-tumour agents induced programmatic cell death through the up-regulation of pro-apoptotic genes and down up-regulating anti-apoptotic genes

(Wang *et al*., 2010).

Harakiri, BCL2 Interacting Protein (HRK) also called DP5 is a pro-apoptotic BH3 member of the Bcl2 family which involved in promoting apoptosis (Coultas *et al*., 2007). This protein activates apoptosis by selectively interacts with the anti-apoptotic Bcl-2 and Bcl-X(L) through its BH3 domain. HRK is commonly expressed in hematopoietic and cultured tissues, however, has also been found in the liver, pancreas, lung, prostate and kidney. Over-expression of HRK mediates GSK343-induced apoptosis in 3D culture epithelial ovarian cancer cells, (Amatangelo *et al*., 2013), and so was a key target in this study. Induction of apoptosis by HRK also requires the expression of pro-apoptotic Bax (Harris and Johnson., 2001). High levels of apoptosis inhibitor Bcl-2 or Bcl-xL suppress the stimulation of HRK and inhibit apoptosis following growth factor withdrawal (Sanz *et al.,* 2000). Enforced co-expression of HRK and Bcl-2 or Bcl- XL, suppress the death-inducing activity of HRK (Inohara *et al*., 1997).

5.1.2.2 Inhibitor of Apoptosis Proteins (IAP)

The inhibitor of apoptosis protein (IAP) family plays a key role in regulating cell division, apoptosis, or survival pathways. Apoptosis inhibition has a mediating role either through suppressing the executioner caspase catalytic activity or modulating the signaling pathway of the nuclear factor κB (NF-κB) (Smolewski and Robak., 2011; Zhang and Fang, 2005). Several IAP proteins have been identified, including eight members of BIRC protein (BIRC1–BIRC8) or neuronal apoptosis inhibitory protein (NAIP), cIAP2, cIAP1, X-linked inhibitor of apoptosis (XIAP), survivin (BIRC5) and ILP2. Each of the IAP protein members is characterized by the presence of one or three tandem conserved repetitions known as the baculovirus inhibitory repeat (BIR) (Zhang and Fang., 2005). The over-expression of IAPs is present in many malignancies including hematological malignancies and it can result in resistance to TRAIL-induced

apoptosis. There was a correlation between hematological disease progression and increased levels of the IAP protein XIAP. In addition, the over-expression of these anti-apoptotic proteins is an indication of poor prognostic factors (Smolewski and Robak., 2011; Zhang and Fang., 2005).

XIAP, a commonly expressed IAP protein is considered the most potent anti-apoptotic caspase inhibitor protein. Moreover, the presence of a Really Interesting New Gene (RING), the zinc finger domain gives it an ubiquitin ligase activity that facilitates the degradation of pro-apoptotic proteins such as caspases (Droin *et al*., 2013). A number of XIAP inhibitors such as embelin suppresses the proliferation of various cancer cells and induces apoptosis (Heo *et al*., 2011).

5.1.2.3   c-flip

Similar to IAP anti-apoptotic proteins, cellular FLIC inhibitory protein (c-flip) is associated with TRAIL resistance in numerous types of cancers. c-flip interacts with FADD and/or caspase-8 and death receptors (DR5) and forms an apoptosis inhibitory complex (AIC) which in turn prevents DISC formation and consequently inhibited the activation of caspase cascade signals (Sophonnithiprasert *et al*., 2015). In addition, c-flip has been reported to activate pro-survival signaling pathways such as NF-κB (portt *et al.*, 2011; Safa., 2012). High expression of c-flip has been shown in a number of cancer types such as colon cancer and lymphoma (Safa., 2012). Several natural compounds have been reported to sensitization of TRAIL-resistant cancer cells to TRAIL-mediated apoptosis through down regulation of c-flip (Sophonnithiprasert *et al*., 2015). Apoptosis induction by SAHA in cutaneous T-Cell lymphoma cells is associated with c-flip down-regulation (Al-Yacoub *et al*., 2012). Moreover, SAHA treatment sensitizes MM cells (Mitsiades *et al*., 2003) and glioblastoma cells to TRAIL-mediated apoptosis by down-regulating expression of c-flip (Bangert *et al*., 2012). Furthermore, inhibition of methyltransferases with DZNep enhanced lymphoma sensitivity to TRAIL

through c-flip degradation (Braun *et al*., 2015). Therefore c-flip is a potential modulator of TRAIL sensitive in this study.

5.1.2.4 p21

$p21^{WAF1/CIP1}$ is one of the cyclin-dependent kinase (CDK) inhibitor (CDK^i) families and it is a target of tumour suppressor; p53 plays a central role in regulating the cell cycle, in transcription regulation, cell motility as well as apoptosis. Though it is known to protect various cell types from apoptosis, its role in apoptosis is still controversial and its over-expression in tumour cells lines enhances its apoptosis (Lee *et al*., 2009). In previous studies, SAHA treatment resulted in an increase in the level of p21 in B-cell malignancies (Mitsiades *et al*., 2003) and co-treatment of SAHA and proteasome inhibitor bortezomib synergistically induced apoptosis of Burkitt's lymphoma cells by up-regulating p21 expression (Hui *et al*., 2014). LMB treatment induces apoptosis in prostate cells with increased expression of p53-responsive genes including p21 (Lecane *et al*., 2003). Moreover, G9a inhibitor BIX 01294 inhibited proliferation as well as induced cell cycle arrest in foetal pulmonary artery smooth muscle cell (PASMC) by upregulating the expression of p21 (Yang *et al*., 2012). Co-treatment of EZH2 inhibitor and HDAC inhibitor synergistically increased the expression p21 in melanoma cells (Fan *et al.*, 2011).

5.1.2.5 MMSET

The increase in the level of the histone methyltransferase (MMSET) changes the epigenetic landscape of (4; 14) translocations multiple myeloma subtype which is supposed to be the driving factor in the pathogenesis of this subtype (Asangani *et al.*, 2013). The over-expression of MMSET results in a global induction in H3K36 methylation and decreases the global levels of H3K27 methylation. Although the majority of the genome decreases the methylation of H3K27 in the presence of

MMSET; specific loci show increased the recruitment of EZH2 and increased H3K27 methylation, contributing to transcriptional suppression. The suppression of these genes likely plays an important role in the disease. It has been reported that MMSET-over-expressing cells display higher response to the inhibitors targeting EZH2-mediated methylation (Popovic *et al*., 2014). This suggests that the agents that block the enzymatic activity of MMSET and EZH2 are therapeutic potential for multiple myeloma. Unfortunately, up to now, no MMSET inhibitor agent has been identified (Popovic *et al*., 2014). Knockdown of MMSET leads to a inhibit cell proliferation, activation of caspase, decreased expression of adhesion molecules and affects the progression of cell cycle in myeloma cells harboring t(4;14) (Brito *et al*., 2009).

5.2 Introduction to Methods for Mechanistic Characterization

5.2.1 Caspase-Glo^{TM} Luminescent 8 and 9 Assays

Caspase has a key role in stimulation of cell death (Lavrik *et al*., 2005). In apoptotic pathways, caspase-3, which shown to be activated by either TRAIL or TRAIL sensitizers (Chapter 2) is activated by either initiator caspase-8 via the mitochondrial or extrinsic pathway, or caspase-9 via death receptor or intrinsic pathway (Ivanov *et al*., 2011). Caspase-Glo 8 and 9 luminescent assay were used to determine the effect of TRAIL or TRAIL sensitizers on the activation of caspase-8 and -9 to investigate whether cell death was triggered via extrinsic and/or intrinsic cascade. The addition of Caspase-Glo®-9 or-8 luminogenic substrates promotes cell lysis, followed by detection of luminescent signals due to caspase cleavage of the substrate. This generated luminescent signal is proportional to the amount of caspase 9 and 8 activity present.

5.2.2 Real Time RT-PCR

Real-time RT-PCR is a highly sensitive, precise and simple method used in the molecular diagnosis and in analysing the gene expression and it has become the most

widely used techniques for validating the data of the whole-genome microarray as well as a smaller set of genes. One of the main PCR applications is relative comparative quantification, where the target gene expression gene is displayed as a ratio to a stably expressed reference gene, known as the housekeeping gene. These internal standard genes are used for normalizing the quantification of the mRNA so it overcomes the problems related to reproducibility. Moreover, they are used as an internal standard because they display a stable expression in the various cell types of different tissues at the diverse stages of development under various extreme experimental conditions (Carraro *et al*., 2005; Jain *et al*., 2006).

5.2.3 Proteome Profiler Array

Investigating the expression of a number of apoptosis-related proteins using human proteome profiler apoptosis array is useful for understanding the roles these apoptotic molecules perform in apoptosis and disease mechanisms. It is a sensitive and rapid method to determine the relative expression level of 35 different apoptosis-related proteins involved in both intrinsic and extrinsic apoptotic cascades (Table 5.1). See appendix (Figure V) and (Table I) of Human apoptosis proteome profiler Array Coordinates.

Target	Target
Bad	HO-1/HMOX1/HSP32
Bax	HO-2/HMOX2
Bcl-2	HSP27
Bcl-x	HSP60
Pro-Caspase-3	HSP70
Cleaved Caspase-3	HTRA2/Omi
Catalase	Livin
cIAP-1	PON2
cIAP-2	p21/CIP1/CDKN1A
Claspine	p27/Kip1
Clustrine	Phospho-p53 (S15)
Cytochrome C	Phospho-p53 (S46)
TRAIL R1/DR5	Phospho-p53 (S392)
TRAIL R2/DR4	Phospho-Rad17 (S635)
FADD	SMAC/Diablo
Fas/TNF6/CD95	Survivin
HIF-1α	TNF RI/TNFRSF1A
	XIAP

Table 5.1: Apoptotic-related proteins spotted on array membrane of human proteome apoptosis profiler array

5.2.4 Hypothesis

It is hypothesized that TRAIL, NEI, HDAC^i and HMTase^i agents alter key pro- and anti-apoptotic genes in both suspension and 3D cultures models as well as in parental and TRAIL^R multiple myeloma cells and that their effects are mediated by caspase activation.

5.2.5 Aims

The aims of this study were to examine the effect of TRAIL alone and in combination with TRAIL sensitizer on the activity of initiator caspase (-8 and -9) of apoptotic cascade using Caspase-Glo-8 and -9 Luminescent Assays in multiple myeloma cell lines. Additionally, this study aimed to investigate the effect of these therapeutic agents alone on regulating key pro- and anti-apoptotic genes using Real-time PCR in parental and TRAIL^R multiple myeloma cells as well as in 3D culture. In the absence of key regulator genes identified by qRT-PCR number of apoptotic related genes was screened by proteome profiler apoptotic array. The NCI-H929 multiple myeloma cell line responded well to TRAIL and TRAIL sensitizers and was thus selected to be investigated using the proteomic array.

5.3   Materials and Methods

5.3.1   Experimental Design

Six multiple myeloma cell lines were used in this study OPM2, NCI-H 929, RPMI 8226, U266, JJN3 and ADC-1 (Chapter 2). Cells were cultured as previously described (Chapter 2) and incubated under standard cell culture conditions at 37ºC with 5% CO_2 atmosphere.

All therapeutic agents were prepared as described in Chapter 2. Multiple myeloma cell lines were treated with different concentration dose of TRAIL sensitizers -/+TRAIL including those combinations which induced synergistic induction of apoptosis as determined by Hoechst 33342/PI staining (Chapter 2) to investigate their effects on Caspase-8, and -9 activation following 24 h (Table 5.1). In addition, Real-time PCR was used for detection the expression of a number of apoptotic genes in parental multiple myeloma cells vs. TRAIL [R] cells treated with anti-tumour agents alone (Chapter 2) as well as in suspension vs. 3D culture models following treatment with concentration of drugs that induced low levels of apoptosis (Chapter 3) (Table 5.2). In this work, a small number of likely targets for RT-PCR studies was selected, including Bax, c-flip, p21, Bcl-2 and HRK. Moreover, the expression of range of pro- and anti-apoptotic proteins was tested on TRAIL sensitive cell line NCI-H929 treated with high concentration of drugs alone for 24 h using proteomic apoptotic array (Table 5.2). MM cells lines and different concentration of drugs for each technique are shown in Table 5.2.

Method	MM Cell line	Drug concentration
Caspase-Glo^{TM} Luminescent 8 and 9 Assays	All six MM cell lines: OPM2, NCI-H 929, RPMI 8226, U266, JJN3 and ADC-1	LMB: 0, 0.5, 2 and 5 nM SAHA: 0, 1, 5 and 10 μM BIX 01294: 0, 5, 10 and 15 μM GSK343: 0, 5, 10 and 15 μM Either alone and in combination with TRAIL
Real-time PCR.	NCI-H 929 vs. TRAIL^R NCI-H 929 RPMI 8226 vs. TRAIL^R RPMI 8226	**For parental and TRAIL^R cells**: LMB (1 nM), SAHA (10 μM), BIX 01294 (10 μM) and GSK343 (15 μM).
	Suspension U266 vs. 3D U266 Suspension NCI-H 929 vs. 3D NCI-H 929	**For both suspension U266 and 3D U266**: LMB (0.5 nM), SAHA (1 μM), BIX 01294 (5 μM) and GSK343 (5 μM).
Proteomic Apoptotic Profiler Array	TRAIL sensitive cell line (NCI-H 929)	SAHA (10 μM), BIX01294: (15 μM) and GSK343 (15 μM).

Table 5.2: Multiple myeloma cells lines treated with variuos concentrations of drugs for 24 h and investigated with different techniques.

5.3.2 Caspase-Glo^{TM} Luminescent 8 and 9 Assays

Caspase-8 and -9 activities in multiple myeloma cells were determined using the Caspase-Glo® 8/9 Assay (Promega, Southampton, UK) according to manufacturer's instructions. Cells were lysed as Caspase-Glo reagent added, followed by detection of luminescent signals due to caspase cleavage of the substrate. Briefly, multiple myeloma cell lines were treated with selected dose of TRAIL and chemotherapy agents (LMB, SAHA, BIX 01294 and GSK343) (Table 5.2) in white 96 well-plates (Fisher Scientific). All treatments were performed in triplicate, in three independent experiments. Following 24 h incubation, 50 µl of Caspase-Glo 8 Reagent or Caspase-Glo 9 Reagent (Promega) with the proteasome Inhibitor MG-132 to reduce nonspecific background activity were added to each well. After incubation for 90 minutes at room temperature luminescence was measured using Wallac Victor 2 1420 luminometer.

5.3.3 Real Time PCR

5.3.3.1 RNA Isolation and cDNA Synthesis

5.3.3.1.1 RNA Extraction from Monolayer Cultures

Following treatment with anti-tumour agents, TRAIL, SAHA, BIX01294, and GSK343 (Table 5.2), cells suspensions containing multiple myeloma cells from the well plate were transferred into an Eppendorf tube and centrifuged at 400g for 10 minutes. 1ml of Trizol (Invitrogen) was added to cell pellets after removing of the supernatant and incubated for 10 minutes at room temperature in order to lyse the cells. 200 µL of Chloroform (Sigma) was added per sample; samples were mixed by vortexing and incubated for 10 minutes at room temperatures prior to centrifugation at 12,000g for 15 minutes at 4°C to facilitated separation of RNA, protein and DNA layers. 500 µL of the upper aqueous phase containing the RNA was transferred to a new tube and 500 µL isopropanol (Fisher) was added to the tube sample and mixed by pipetting. Samples were incubated at room temperature for 10 minutes followed by stored at -80 °C for 1

hour in order to allow RNA precipitation. Cell pellets were re-suspended in 70% ethanol *(v/v)* (Fisher) after being centrifuged for 30 minutes at 12000g at 4°C. RNA samples were eluted in 50 μL sterile deionised water and used immediately for the synthesis of cDNA.

5.3.3.1.2 RNA Extraction from Alginate Bead Cultures

RNA was extracted using Trizol reagent (Invitrogen). Prior to Trizol extraction, alginate beads were removed from well plate and transferred into Eppendorf tubes and 500 μl alginate dissolving buffer (55 mM sodium citrate, 30 mM EDTA, 0.15 M NaCl; pH 6) were added and incubated rotating at 37°C for 15 and cells were then subsequently centrifuged at 600g for 5 minutes followed by washing in PBS twice. Then, RNA extraction by Trizol as described in Section 5.3.3.1.

RNA extracted from monolayer and alginate cultures were assessed for purity by subjected to nanodrop spectrophotometer analysis. See appendix for Figure VI. Absorbance at wave lengths of 260 and 280 nm was measured and used as an indicator of RNA integrity. The integrity of the extracted RNA was confirmed by 1% agarose gel electrophoresis and ethidium bromide staining. See appendix for Figure VII.

5.3.3.2 cDNA Synthesis

The purified RNA was quantitated and transcribed to cDNA using superscript reverse transcriptase (Bioline). RNA samples were incubated at 60°C for 5 minutes in order to denature RNA prior to Reverse Transcriptase (RT) mastermix was added. 36 μl of RT mastermix per 14μl RNA sample was added made up as shown in Table 5.3. Reactions were incubated at 42°C for 1 h followed by denaturation at 95°C for 10 minutes prior to PCR amplification. As a negative control, Reverse Transcriptase was omitted from reactions.

Master mix for 1 Reaction	14µL RNA Sample
dNTPs (40mM) (Bioline)	1.5
Random Hexamers (Applied Biosystems)	1.0
Bioscript 5x RT Buffer (Bioline)	5.0
Bioscript RT Enzyme (Bioline)	0.5
Sterile deionised PCR H$_2$O	28.0

Table 5.3 Reverse transcription mastermix used in cDNA synthesis reaction

5.3.3.3 *Quantitative Real Time-Polymerase Chain Reaction*

qRT-PCR was performed on cDNA samples using a StepOnePlus™ Real-Time PCR System (Applied Biosystems). A small number of likely HDAC and HMTase targets for RT-PCR studies were selected including Bax, p21, c-flip, Bcl-2 and HRK (Applied Biosystems) and gene expression level of these target genes was performed. TFRC Transferrin receptor (Applied Biosystems) was used as housekeeping genes to allow the comparative CT methods to calculate relative gene expression. 10 µL reactions were prepared using TaqMan Universal PCR Mastermix (Applied Biosystems), made up as shown in Table 5.4. 2 µL of cDNA sample was loaded in duplicate into a Fast PCR plate (Applied Biosystems) and 8µL of prepared TaqMan Universal PCR Mastermix was added as shown in Table 5.4. PCR Plates were sealed with adhesive film and run on the StepOnePlus Real-Time PCR machine.

Universal PCR Master Mix For 1 Reaction:	µL
Taqman Gene Expression Assay	0.5
2X Taqman Fast Mastermix	5.0
Sterilised deionised PCR H$_2$O	2.5
Cdna	2
	10.0

Table 5.4: TaqMan universal PCR mastermix

5.3.3.4   Analysis of qRT-PCR

C_T (Cycle threshold) values of the amplification plots and relative fold changes in target gene expression were analysed using the comparative method ($2^{-\Delta\Delta CT}$ method) and expressed as relative gene expression normalized to the housekeeping gene. In order to produce reliable data, threshold setting has to be maintained across the entire investigated sample as well as the selection of the most stably expressed internal reference genes are required. Mean of the two duplicated wells was calculated. Then, for each sample, ΔC_T values were determined using the equation:

$$\Delta C_T = C_T \text{(gene of interest)} - C_T \text{(mean of reference)}$$

Relative gene expression was then determined by the equation:

Relative gene expression= $2^{-\Delta CT}$

The arithmetical mean ΔC_T and standard error of mean $(\Delta C_T$ SE) were calculated using the equation:

$$\Delta\Delta C_T = \Delta C_T \text{(tested sample)} - \Delta CT \text{(untreated sample)}$$

Finally, the range for target gene relative to an internal gene sample is calculated by the equation:

$$\text{Relative gene expression= } 2^{-\Delta\Delta CT}$$

5.3.4   Proteome Profiler Array Investigating the Anti-tumour Agents Induced Apoptosis Mechanisms in Multiple Myeloma

Following treatment of NCI-H929 multiple myeloma cell line with TRAIL, SAHA, BIX 01294 and GSK343 alone (Table 5.2), cells were washed twice with PBS. Cell lysate prepared from CelLyticTM (Sigma, C2978, 10 ml/g) supplemented with protease inhibitor cocktail (Sigma, P2714, 1:100) was added in order to breakdown the cell membrane and inhibit degradation of protein by endogenous protease present in the cell extract. The total protein was quantified using Pierce™ BCA protein assay kit (Thermofisher scientific, 23225).

The proteomic profile array was performed following manufacturer's recommendations. Briefly, each antibody–coated profiler membrane was incubated with 300 μg of

prepared cell lysates and incubated for 1 hour on a rocking platform shaker and the protein extracts from control and treated sample were added to proteome membrane and incubated at 2-8 °C with shaking overnight. Antibody-coated nitrocellulose membranes were washed in triplet with IX wash buffer and 1.5 ml lyophilized biotinylated antibodies was added and incubated for 1 hour on a rocking platform shaker followed by washing with IX wash buffer for three times 10 minutes each. IRDye® 800CW Streptavidin (LI-COR, 926-32230) diluted at 1:2000 using the array buffer 5 (R&D Systems, ARY002B) was added and membrane incubated for 30 minutes on rocking platform followed by three times washing with IX wash buffer. Finally, the arrays membranes were scanned with LI-COR Odyssey® Infrared Imaging System and quantified with Image Studio™ software (LI-COR). Data was quantified by scanning the array and exploring signal values of each spot on the array membrane and the mean of two spot representing each apoptosis-related protein was calculated. Comparison of corresponding signals intensity among membrane array image was used to identify the relative difference expression level of apoptosis-related protein between control and treated samples.

5.3.5   Statistical Analysis

Median with range was calculated for CellTiter- Glo™, Caspase-8, -9 activity and PCR. To test the effect of TRAIL resistant development mRNA levels it compared in untreated cells vs. treated in both TRAIL sensitive and TRAIL resistant cells as well as compared between TRAIL sensitive cells vs. TRAIL resistant cells. Moreover, the gene expression was determined by comparison the treated cells with the vehicle control and by comparison the suspension cells with 3D cultures. Relative gene expression determined by the $2^{-\Delta\Delta CT}$ method. Stats Direct software was used to determine whether the data followed a normal distribution.   As the data did not follow a normal

distribution, significance difference determined using a Kruskal-Wallis and Connover-Inman post hoc test with a p value of <0.05.

5.4   Results

5.4.1   Effect of Anti-Tumour Agents on Caspase Activity in Multiple Myeloma Cells

5.4.1.1   *Effect of LMB on Caspase Activity in Multiple Myeloma Cells*

To determine which apoptotic pathway was responsible for LMB-mediated enhanced TRAIL-signaling, the activity of caspase-8 (early initiator caspase of the extrinsic pathway), caspase-9 (early initiator caspase of the intrinsic pathway) was measured with cell-based homogenous Caspase-Glo kit assay. Multiple myeloma cell line OPM2, RPMI 8226 NCI-H929, U266, JJN3 and ADC-1 cells treated with LMB at concentrations of 0, 0.5, 2, 5 nM alone and in combination with TRAIL for 24 hours and compared with vehicle control. TRAIL alone enhanced caspase-8 and caspase-9 activity in RPMI 8226, OPM2, and U266 cell lines ($p < 0.05$).

In response to TRAIL alone at the lowest dose that induced apoptosis, caspase-8 and -9 were induced in all cells except NCI-H929 (caspase-8 only), ADC-1 (caspase-9 only) and JJN3 no caspase induction at 50 ng/ml TRAIL (Figure 5.1). The TRAIL sensitizer LMB alone also enhanced caspase-8 and -9 activities in NCI-H929, RPMI 8226, JJN-3, and U266 ($p < 0.05$) and a significant increase was only seen in caspase-9 and caspase-8 following treatment with LMB alone in ADC-1 and OPM2 cell line respectively ($p < 0.05$), (Figure 5.1). The combination treatment further elevated caspase-8 and -9 consistent with morphological observations in all multiple myeloma cell lines (Figure 5.1). RPMI 8226 activated caspase-8 and -9 after dual treatment of 0.5 nM LMB and TRAIL whilst NCI-H929, U266, ADC-1, OPM2, and JJN3 potentially activated caspase-8 and -9 by LMB alone.

Figure 5.1: Effect of LMB+/-TRAIL on caspase-8 and caspase-9 activity of multiple myeloma cell lines

Caspase-8 Activity

Caspase-9 Activity

Figure 5.1: continued
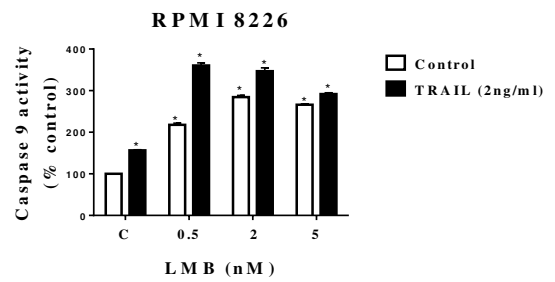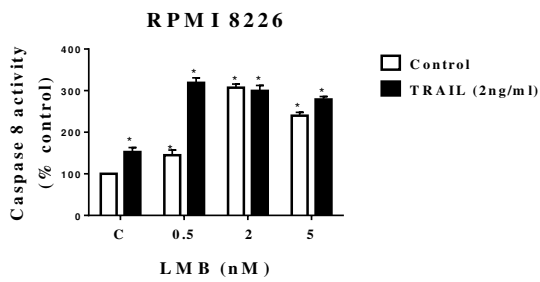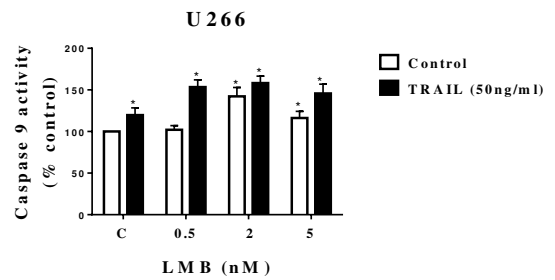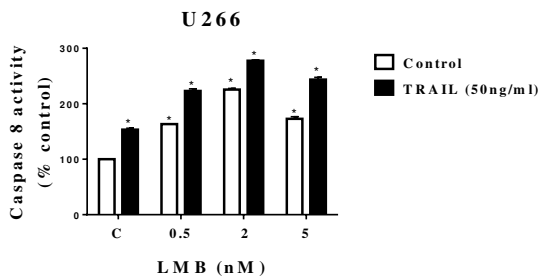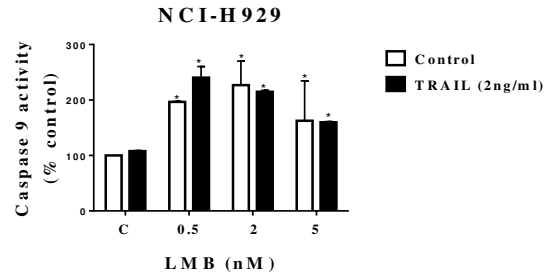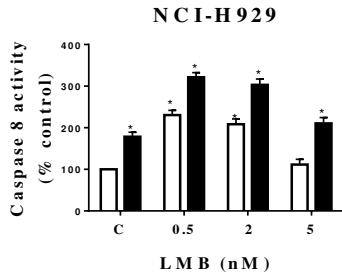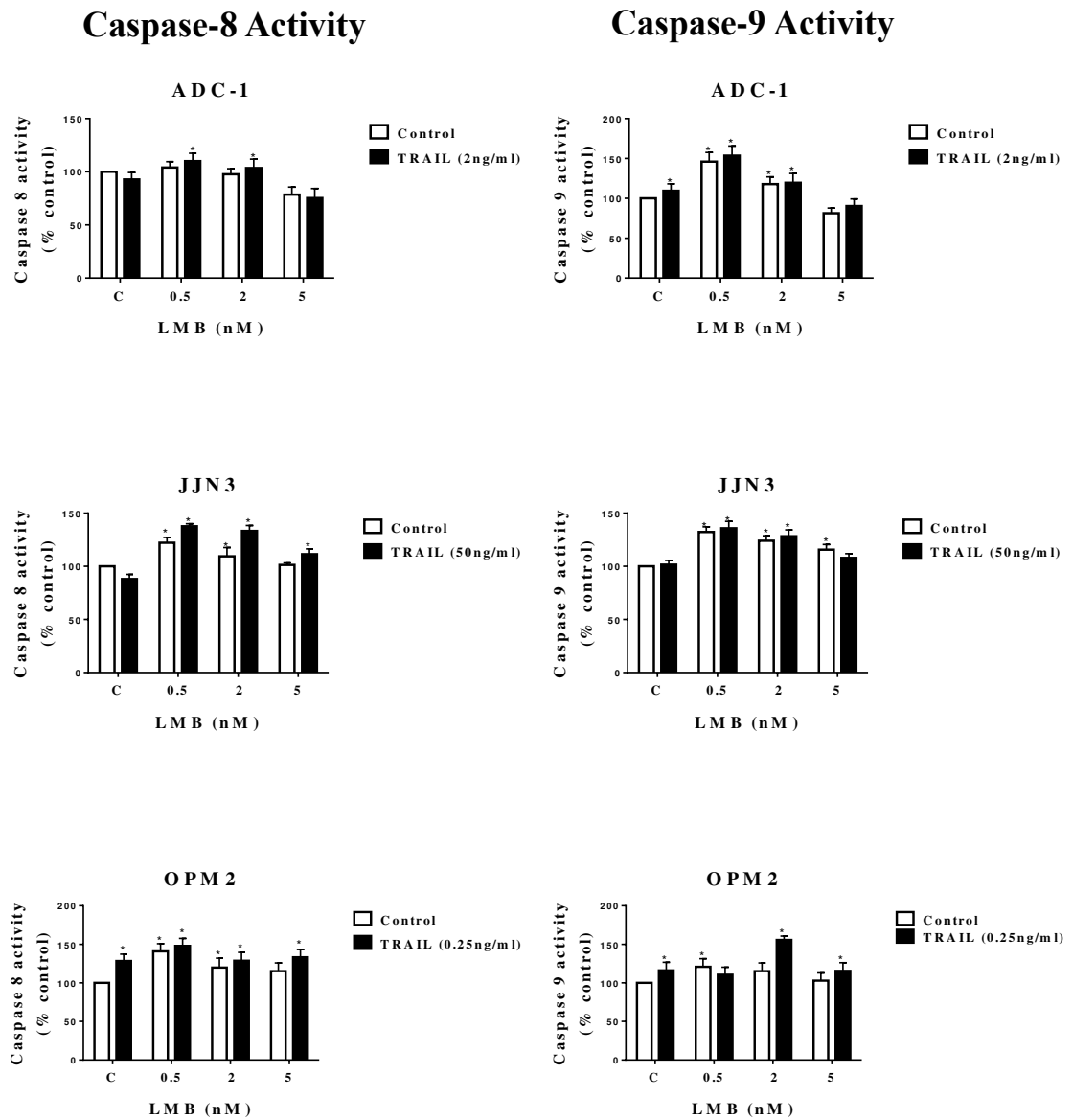
Caspase-8 Activity

Caspase-9 Activity

Figure 5.1: Effect of LMB+/-TRAIL on caspase-8 and caspase-9 activity of multiple myeloma cell lines. Multiple myeloma cells treated with LMB either alone or in combination with TRAIL for 24 h. Data was normalized to the vehicle control which was set to 100%. Caspase activation data is consistent with apoptosis induction as observed in chapter 2. The data is expressed as median with range (three independent experiments, each in triplicate). The statistical significance was determined by comparison with the vehicle control (*=p<0.05) (Kruskal–Wallis).

5.4.1.2 *Effect of the HDAC^i SAHA on Caspase Activity in Multiple Myeloma Cells*

SAHA caused a significant increase in both caspase-8 and -9 activities at 24 h in all multiple myeloma cell lines ($p < 0.05$) (Figure 5.2) and the co-treatment with TRAIL further elevated caspase-8 and -9 consistent with morphological observations in all multiple myeloma cell lines (Figure 5.2). RPMI 8226 activated caspase-8 and -9 after dual treatments of 1 µM SAHA and TRAIL and in NCI-H929 caspase-8 activation observed following combination treatment. However, U266, ADC-1, OPM2, and JJN3 activated caspase-8 and -9 by SAHA alone. The results confirm that both TRAIL and SAHA significantly increased both cellular caspase-8 and -9 activities and that enhanced apoptosis from dual treatment is in part via the intrinsic pathway.

Figure 5.2: Effect of SAHA +/-TRAIL on caspase-8 and caspase-9 activity of multiple myeloma cell lines
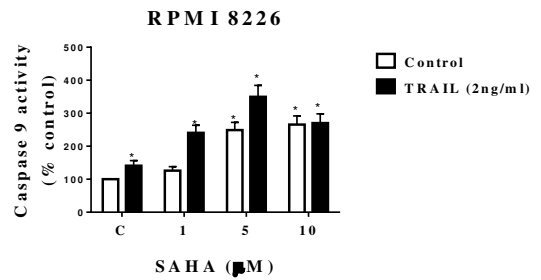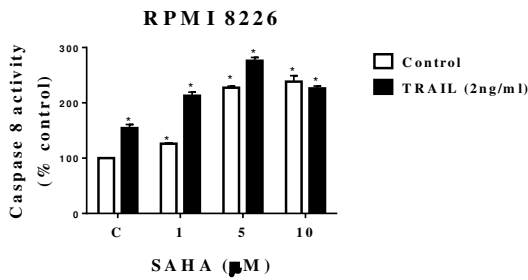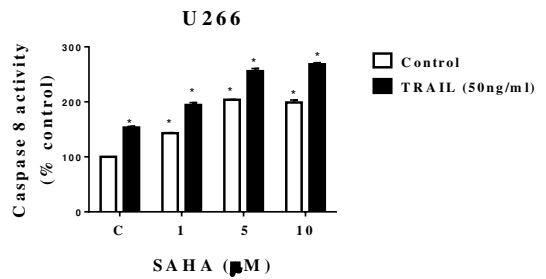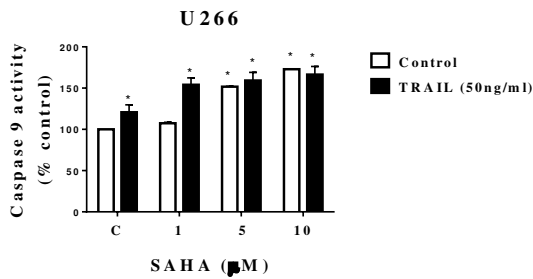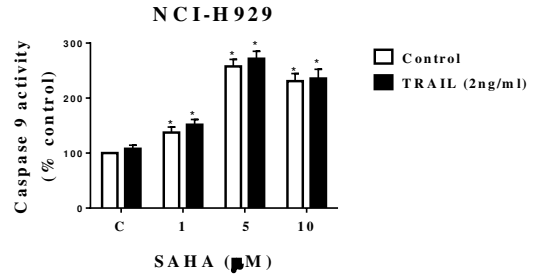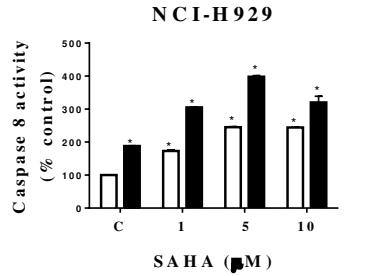
Caspase-8 Activity

Caspase-9 Activity

Caspase-8 Activity
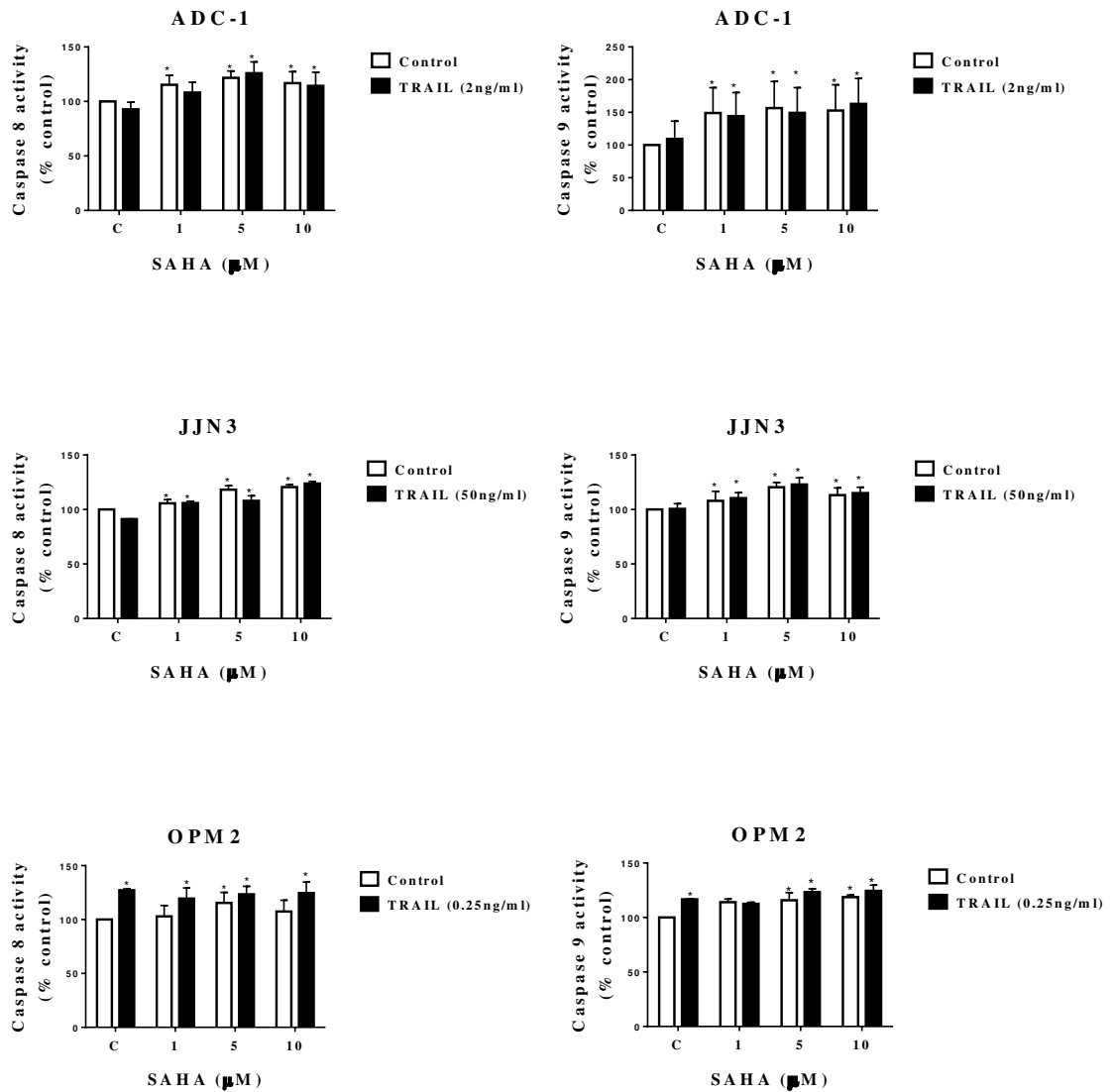
Caspase-9 Activity

Figure 5.2: Effect of SAHA +/-TRAIL on caspase-8 and caspase-9 activity of multiple myeloma cell lines. *Myeloma cells treated with SAHA either alone or in combination with TRAIL for 24 h. Data was normalized to the vehicle control which was set to 100%. The data is expressed as median with range (three independent experiments, each in triplicate). The statistical significance was determined by comparison with the vehicle control (*=p<0.05) (Kruskal–Wallis).*

5.4.1.3 *Effect of the HMTase[i] BIX01294 on Caspase Activity in Multiple Myeloma Cells*

BIX 01294 alone or in combination with TRAIL significantly increased caspase-8 and -9 activity in NCI-H929, RPMI 8226, JJN3, U266 and ADC-1 cell lines ($p < 0.05$). In OPM2 cell lines, BIX 01294 alone significantly increased caspase-8 activity while combination treatment with TRAIL significantly elevated caspase-9 activity ($p < 0.05$) (Figure 5.3). NCI-H929 activated caspase-8, after dual treatment of 5 μM BIX 01294 and TRAIL whilst in U266, ADC-1, OPM2, and JJN3 potentially activated caspase-8, -9 by BIX 01294 alone and in RPMI 8226 activated caspase-8 and -9 by TRAIL alone.

Figure 5.3: Effect of BIX 01294 +/-TRAIL on caspase-8 and caspase-9 activity of multiple myeloma cell lines

Caspase-8 Activity

Caspase-9 Activity

Figure 5.3: continued
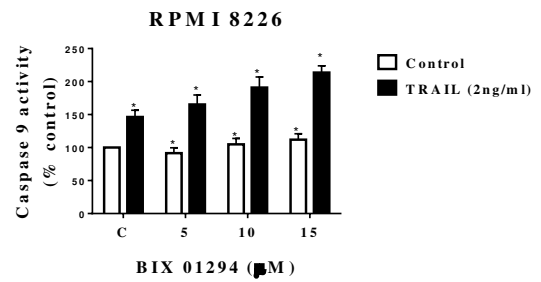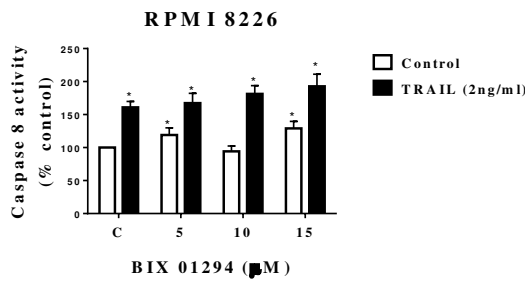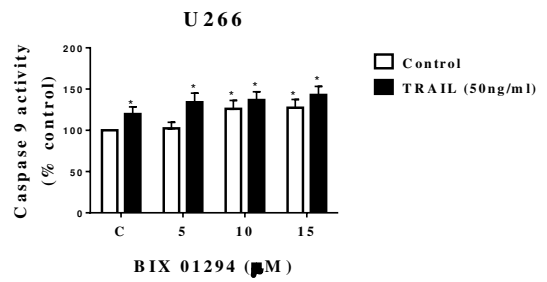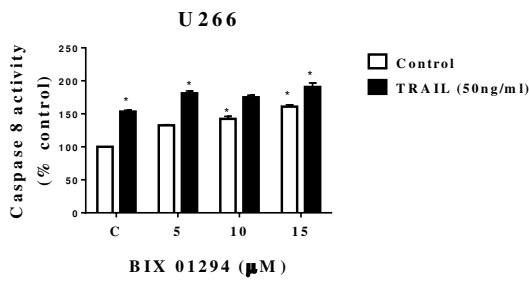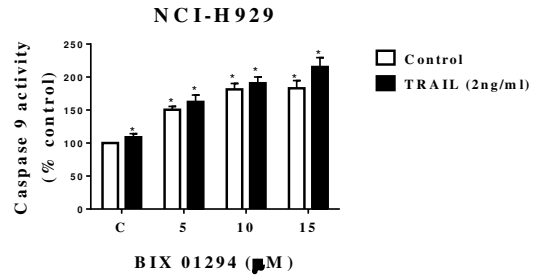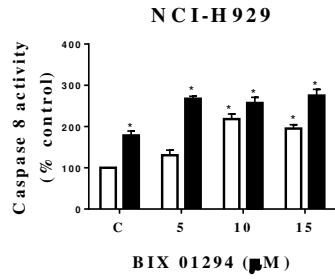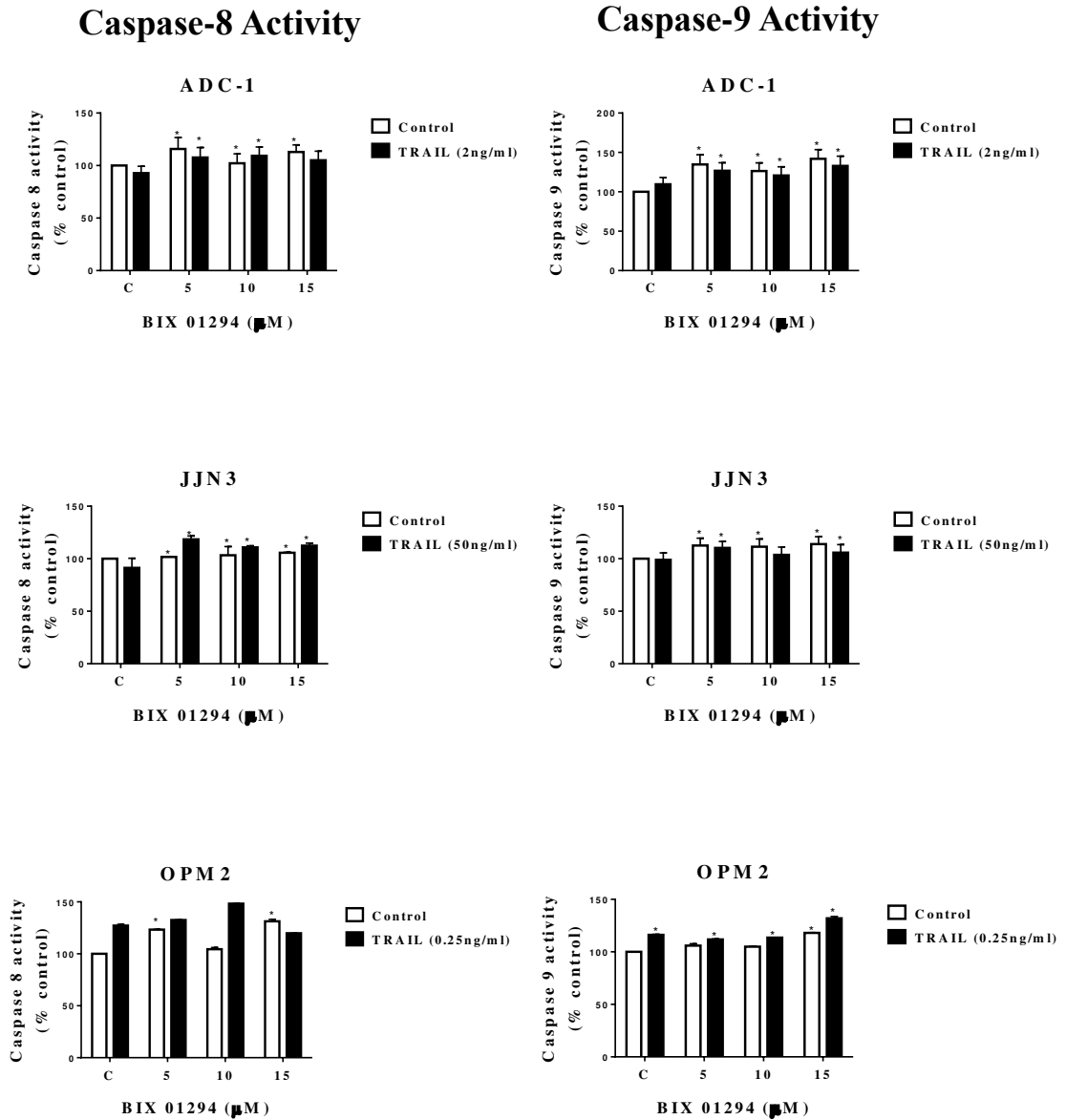
Caspase-8 Activity

Caspase-9 Activity

***Figure 5.3: Effect of BIX 01294 +/-TRAIL on caspase-8 and caspase-9 activity of multiple myeloma cell lines.** Multiple myeloma cells treated with BIX 01294 either alone or in combination with TRAIL for 24 h. Data was normalized to the vehicle control which was set to 100%. The data is expressed as median with range (three independent experiments, each in triplicate). The statistical significance was determined by comparison with the vehicle control (*=p<0.05) (Kruskal–Wallis).*

5.4.1.4 Effect of the HMTase[i] GSK343 on Caspase Activity in Multiple Myeloma Cells

Treatment with GSK343 in the presence of TRAIL resulting in significant increase of caspase-8 and -9 activity in OPM2, NCI-H929, RPMI 8226, and U266 cell line ($p < 0.05$) (Figure 5.4). While in ADC-1 cell line a significant increase was only seen in caspase-9 and no significant effect in caspase-8 following treatment with GSK343 alone and in combined with TRAIL except the highest combination dose. GSK343 did not affect caspase-9 activity, but significantly increased caspase-8 activity in JJN3 cell line (Figure 5.4). RPMI 8226 and U266 activated caspase-8 and -9 after dual treatment potentially by TRAIL as well as in NCI-H929 potentially activated caspase-8 by TRAIL.

Figure 5.4: Effect of GSK343 +/-TRAIL on caspase-8 and caspase-9 activity of multiple myeloma cell lines

Caspase-8 Activity

Caspase-9Activity
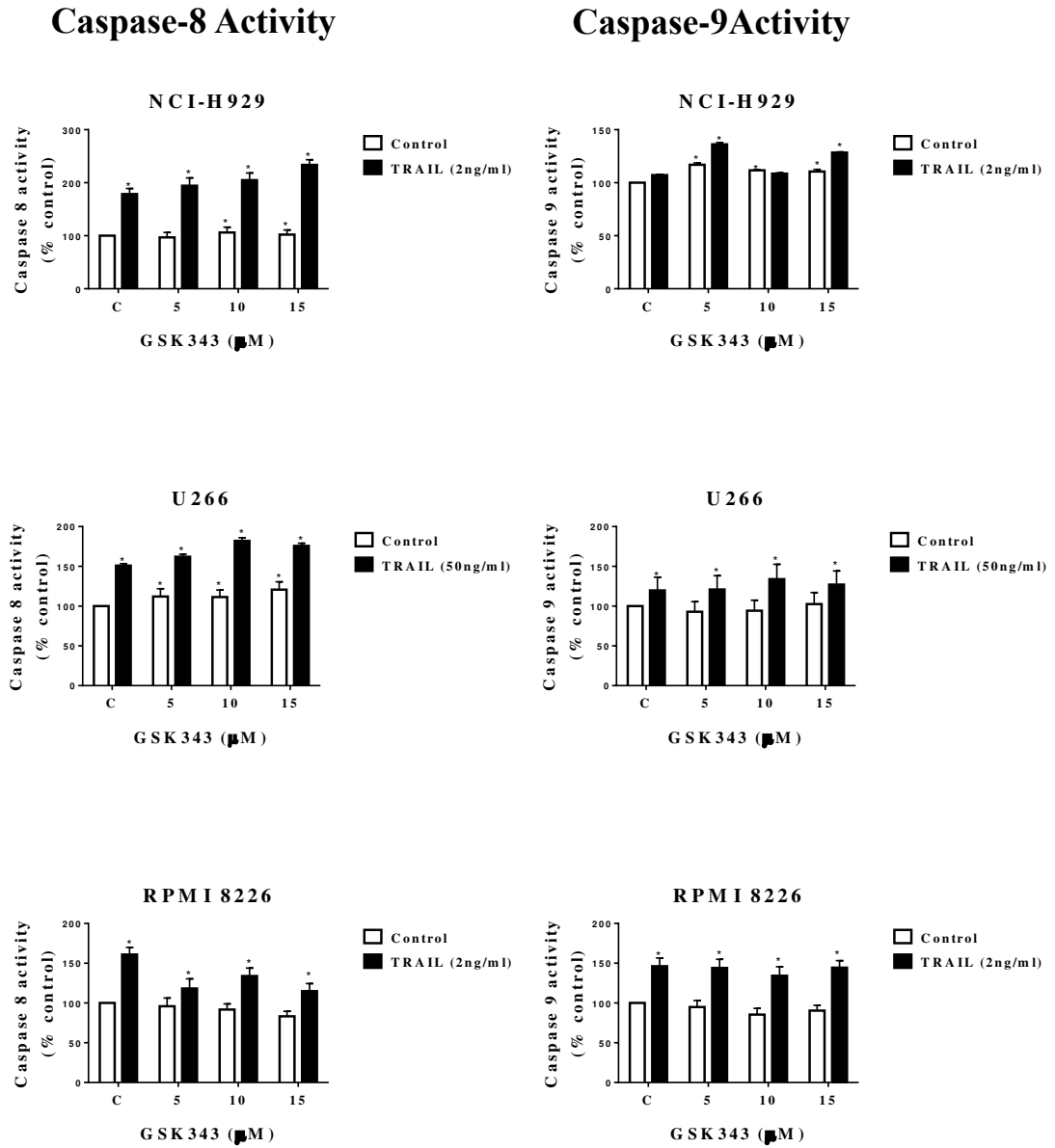
Caspase-8 Activity   Caspase-9 Activity
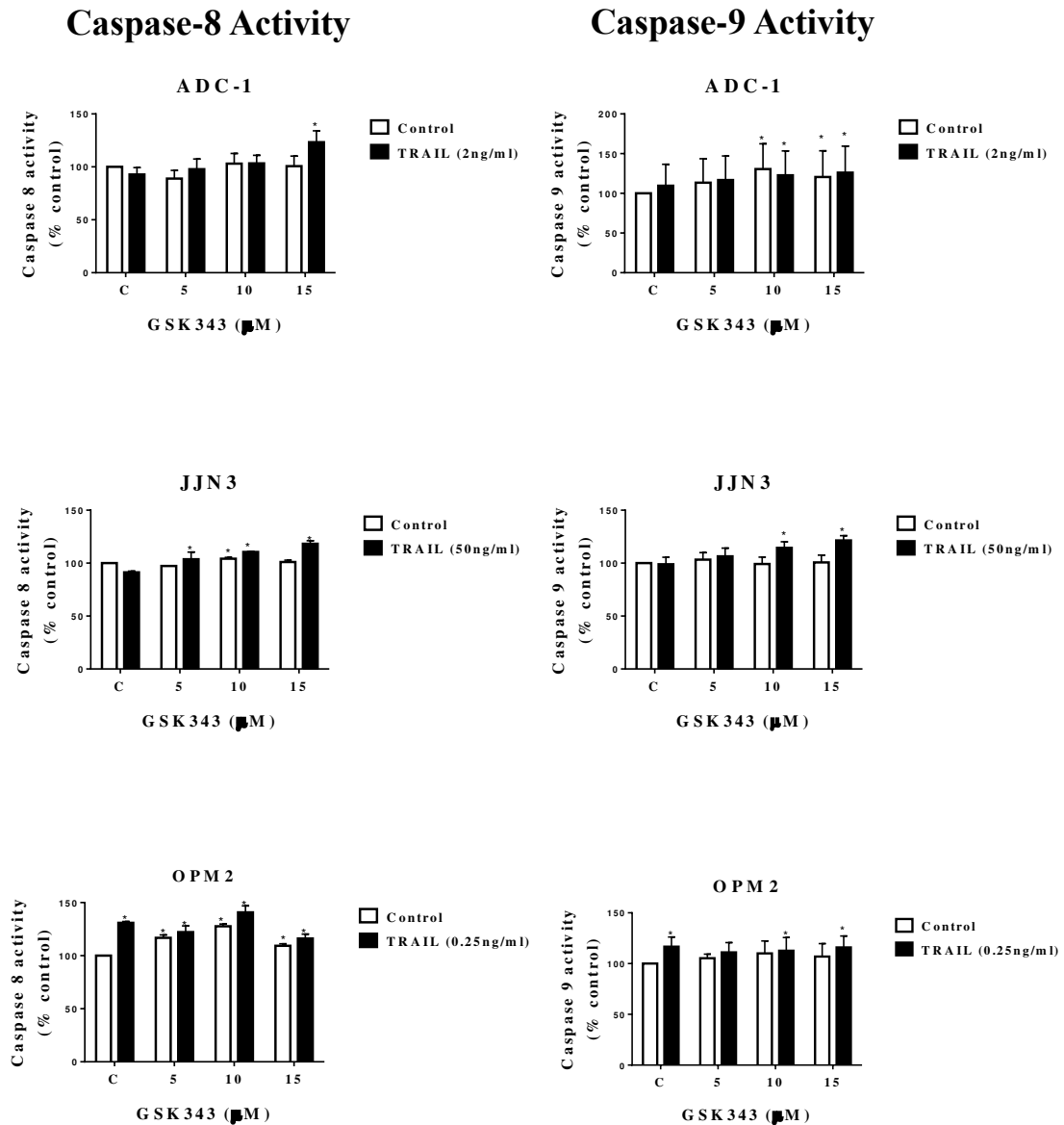
Figure 5.4: Effect of GSK343 +/-TRAIL on caspase-8 and caspase-9 activity of multiple myeloma cell lines. Multiple myeloma cells treated with GSK343 either alone or in combination with TRAIL for 24 h. Data was normalized to the vehicle control which was set to 100%. The data is expressed as median with range (three independent experiments, each in triplicate). The statistical significance was determined by comparison with the vehicle control (*=p<0.05) (Kruskal–Wallis).

5.4.2 Effect of TRAIL Treatment on Expression of Pro-Apoptotic and Anti-Apoptotic Genes in Multiple Myeloma Cells

Next, we determined the effects of TRAIL on the levels of the pro-apoptotic protein; Bax and HRK, cell cycle regulators; p21 and anti-apoptotic genes; c-flip and Bcl-2 in parental cells vs. TRAIL resistant cells. TRAIL-resistant cells were generated by acute exposure of the TRAIL sensitive cells with a high/lethal dose of TRAIL (50ng/ml) followed by a selection of TRAIL-resistant cells (Chapter 2). Treatment with TRAIL was accompanied by a significant increase in pro-apoptotic gene HRK in parental NCI-H929 and significant up regulation of c-flip and p21 in TRAIL^R NCI-H929 cells. Moreover, a significant increase in the expression of p21 and modest increase in Bcl-2 but it failed to reach significance in RPMI 8226 TRAIL-resistant cells compared to parental cells. In addition, a significant increase in expression of Bax as well as decrease but not significant in HRK expression in TRAIL-resistant cell lines compared to parental cells (Figure 5.6).

Figure 5.5: Basal gene expression in parental vs. TRAIL resistant cells
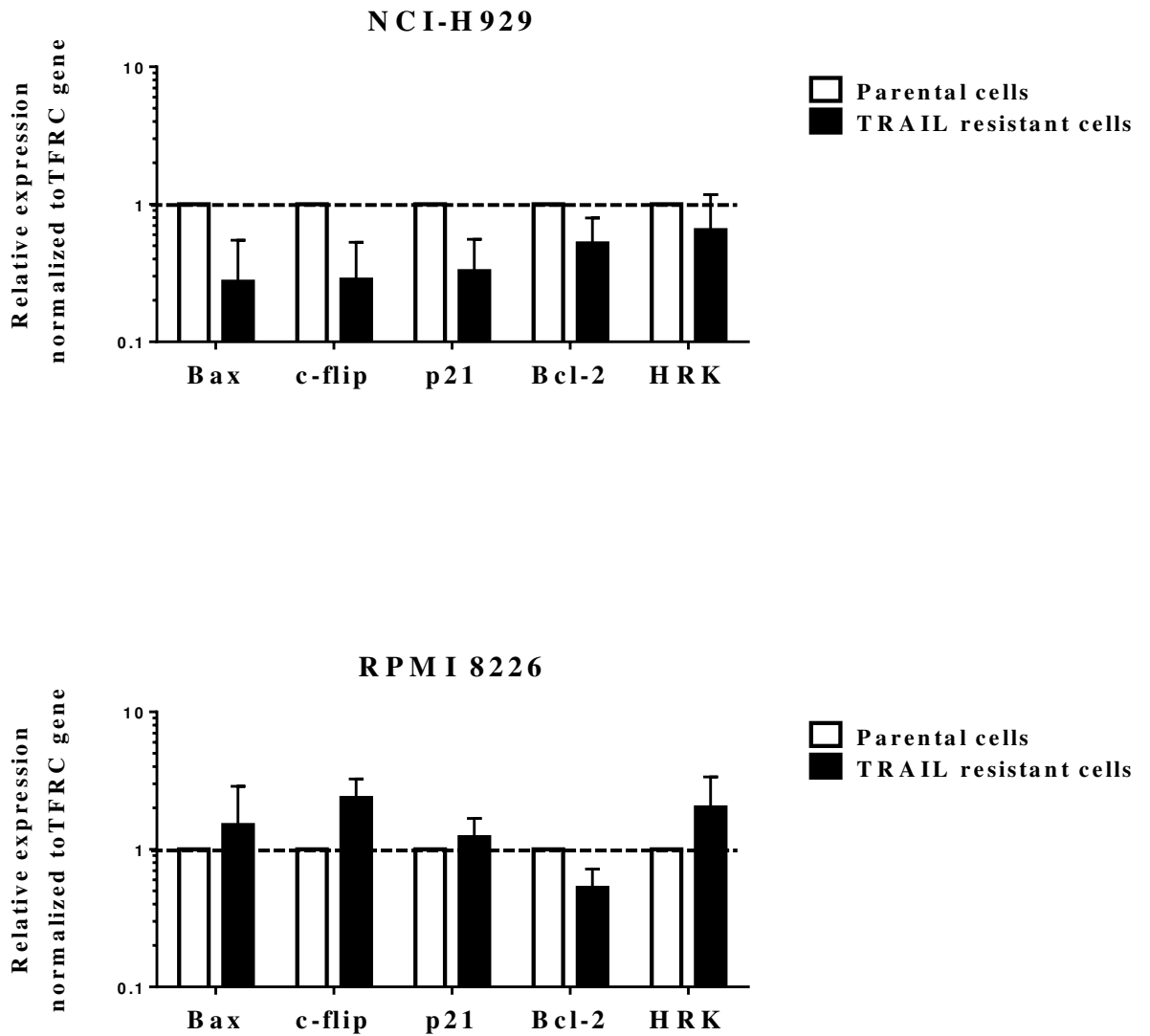
Figure 5.5: qRT-PCR demonstrates the fold changes in expression of Bax, c-flip, p21, Bcl-2 and HRK in parental vs. TRAIL resistant cells relative to the internal control gene TFRC. The graph shows that there was a small increase in expression in Bax, c-flip, p21 and HRK in TRAIL resistant RPMI 8826 cells and decrease expression of all genes in TRAIL resistant NCI-H929 cells vs. parental cells.

Figure 5.6: Effect of TRAIL on gene expression in parental vs. TRAIL resistant cells
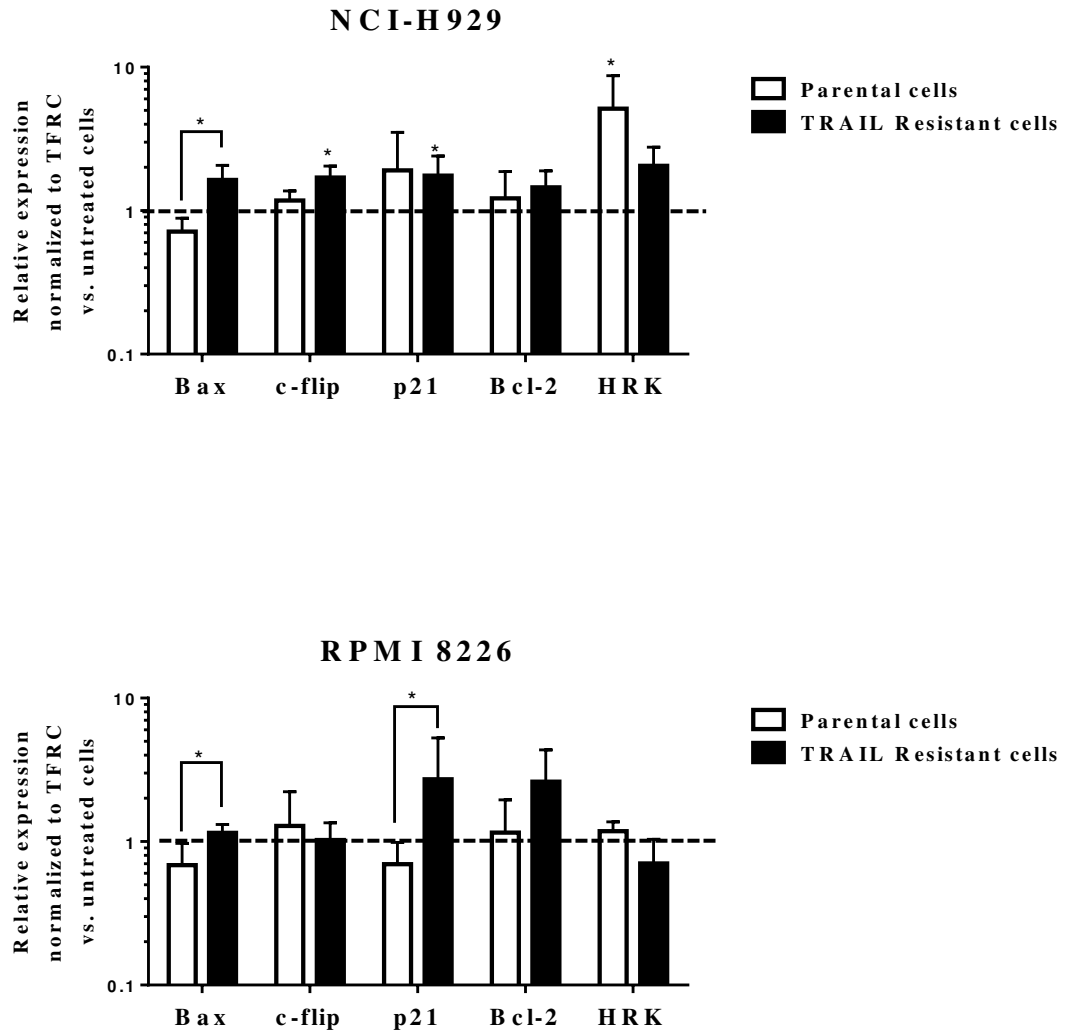
Figure 5.6: The expression of Bax, c-flip, p21, Bcl-2 and HRK in parental and TRAIL resistant cells RPMI 8226 and NCI-H929 cells stimulated with TRAIL. The anti-apoptotic genes expression Bcl-2 and c-flip was amplified by qRT-PCR in the TRAIL[R] cell lines in response to TRAIL treatment as well as decrease expression of pro-apoptotic HRK genes. The statistical significance was determined by comparison with the vehicle control and by comparison of parental with TRAIL[R] cells (*=p<0.05) (Kruskal–Wallis).

5.4.3 Effect of LMB Treatment on Expression of Pro-apoptotic and Anti-Apoptotic Genes on Parental vs. TRAIL-Resistant and in 3D Culture

This study sought to examine the potential involvement of signaling mechanisms in proliferation inhibition and apoptosis induction by LMB in TRAIL^R MM cells. qRT-PCR used to determine the expression levels of a number of pro-apoptotic and anti-apoptotic genes. The results showed increase expression of p21 in parental RPMI 8226, U266 and NCIH929 cell lines. In addition, a significant increase in Bcl-2 expression ($p < 0.05$) and a small decrease but non-significant in Bax, c-flip and MMSET as a result of treatment with LMB in RPMI 8226 TRAIL^R cells compared to parental cells (Figure 5.7).

Furthermore, the effects of LMB on the expression of apoptosis-related genes in multiple myeloma cells in 3D vs. suspension cultures condition was investigated in TRAIL-sensitive cell line NCI-H929 and TRAIL-resistant cell line U266. The data shows a significant up-regulation of pro-apoptotic gene Bax and HRK ($p < 0.05$) in 3D cultures U266 and NCI-H 929 cell line and a decrease but non-significant in p21 in 3D cultures treated with LMB (Figure 5.8)

Figure 5.7: Effect of LMB on the expression of the pro-apoptotic and anti-apoptotic genes in parental cells vs. TRAIL resistant RPMI 8226 cells
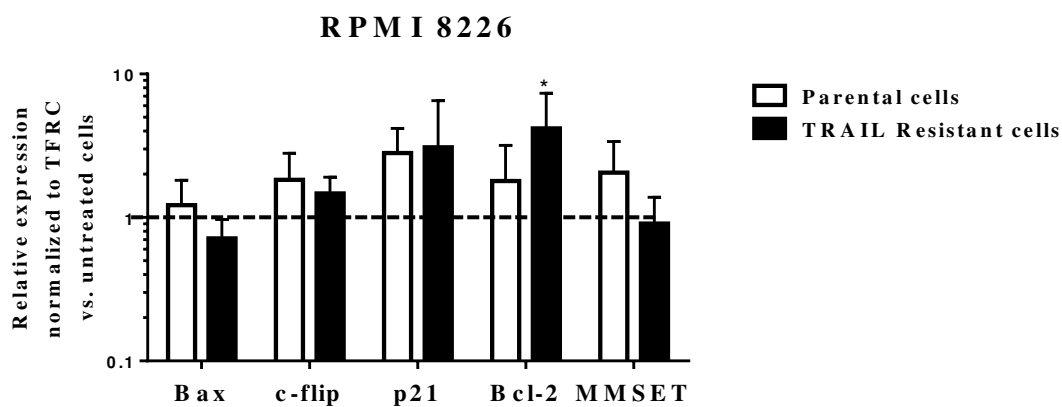
Figure 5.7: Effect of LMB on the expression of the pro-apoptotic and anti-apoptotic genes in parental cells vs. TRAIL resistant cells. TRAIL sensitive cells RPMI 8226 were treated with LMB (1nM) for 24 hours and the gene expression of Bax, c-flip, p21, Bcl-2 and MMST was determined by qR-PCR. TFRC was as an endogenous control. The statistical significance was determined by comparison with the vehicle control and by comparison of parental with TRAIL^R cells (*=p<0.05) (Kruskal–Wallis).

Figure 5.8: Effect of LMB on the expression of the pro-apoptotic and anti-apoptotic genes in suspension vs. 3D cell culture. U266 and NCIH 929 cells were treated with LMB (1 nM) for 24 hours and the gene expression of Bax, c-flip, p21, Bcl-2 and HRK was determined by qR-PCR in suspension vs. 3D. RT-PCR demonstrates that LMB significantly increases the expression of Bax and HRK genes of U266 and NCI-H929 in 3D cultures vs suspension cultures. The statistical significance was determined by comparison with the vehicle control and by comparison the suspension cells with 3D cultures (*=p<0.05) (Kruskal–Wallis).

5.4.4 Effect of SAHA Treatment on Expression of Pro-apoptotic and Anti-Apoptotic Genes in Parental vs. TRAIL-Resistant and 3D Culture Myeloma Cells

SAHA treatment (10µM) significantly up-regulation of p21 in both parental and TRAIL^R RPMI 8226 cells ($p < 0.05$) (Figure 5.14). In contrast, SAHA increased Bcl-2 in TRAIL^R cells and decrease Bcl-2 in parental cells. SAHA caused a modest decrease in c-flip in parental cells only (Figure 5.9). In U266 cell line, SAHA caused a significant up-regulation of p21 expression, and a significant decrease in c-flip expression was seen ($p < 0.05$). Moreover, significant up-regulated Bcl-2 expression ($p < 0.05$) and a non-significant increase in c-flip following treatment with SAHA in RPMI 8226 TRAIL resistant cells compared to parental cells (Figure 5.9).

In addition, the effects of SAHA on the expression of a pro-apoptotic and anti-apoptotic target genes in multiple myeloma cells in 3D vs. suspension cultures condition was investigated. A significant down-regulation of p21 in addition to significant up-regulation of HRK genes in 3D cultures NCI-H 929 cell line treated with SAHA in 3D compared with suspension cultures was seen ($p < 0.05$). In addition, increased expression of pro-apoptotic Bax was seen but, it failed to reach significance in 3D vs. suspension cultures condition (Figure 5.10)

Figure 5.9: Effect of SAHA on the expression of the pro-apoptotic and anti-apoptotic genes in parental cells vs. TRAIL-resistant RPMI8226 cells
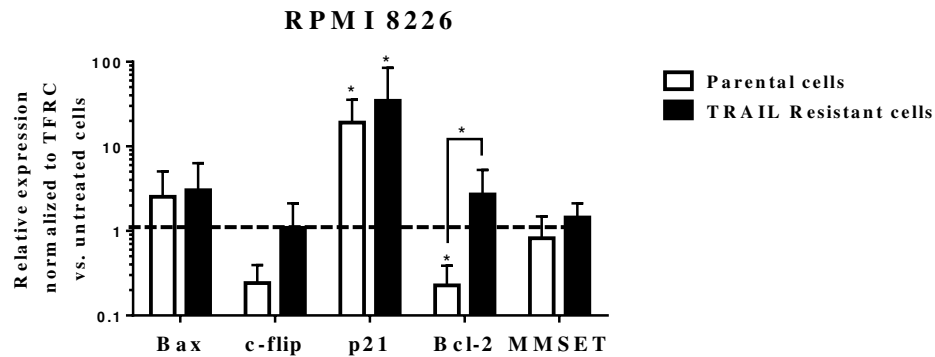
Figure 5.9: Effect of SAHA on the expression of the pro-apoptotic and anti-apoptotic genes in parental cells vs. TRAIL resistant cells. TRAIL sensitive cells RPMI 8226 were treated with SAHA (10μM) for 24 hours and the gene expression of Bax, c-flip, p21, Bcl-2 and MMSET was determined by qRT-PCR. The statistical significance was determined by comparison of the vehicle control with SAHA treated cells and by comparison of parental with TRAIL^R cells (*=p<0.05) (Kruskal–Wallis).

Figure 5.10: Effect of SAHA on the expression of the pro-apoptotic and anti-apoptotic genes in suspension vs. 3D cell culture

Figure 5.10: Effect of SAHA on the expression of the pro-apoptotic and anti-apoptotic genes in suspension vs. 3D cell culture. U266 cell line was treated with SAHA (1 μM) for 24 hours and the gene expression of Bax, c-flip, p21and HRK was determined by qR-PCR in suspension vs. 3D. The statistical significance was determined by comparison with the vehicle control and by comparison the suspension cells with 3D cultures (*=p<0.05) (Kruskal–Wallis).

5.4.5 Effect of BIX 01294 Treatment on Expression of Pro-apoptotic and Anti-Apoptotic Genes in Parental vs. TRAIL-Resistant and 3D Culture Myeloma Cells

The potential mechanism of BIX 01294 to induce apoptotic cell death in TRAIL^R population on number of pro-and anti-apoptotic genes was investigated using qRT-PCR. The data showed that significant up-regulation of p21 and down-regulation of MMSET in RPMI 8226 treated with BIX 01294 ($p < 0.05$). Moreover, BIX 01294 induced a significant up-regulation of Bcl-2, c-flip and MMSET in TRAIL^R RPMI 8226 compared to parental cells ($p < 0.05$) (Figure 5.11) that could explain the resistant behavior of this cell line to BIX 01294. However, the pro-apoptotic gene Bax significantly increased in TRAIL^R RPMI 8226 cell line compared to parental cells (Figure 5.11).

In addition, the result showed a significant up-regulation of HRK genes in 3D cultures TRAIL insensitive cell line U266 when treated with BIX 01294 ($p < 0.05$) (Figure 5.12), potentially contributing to the increase TRAIL sensitivities seen in 3D culture.

Figure 5.11: Effect of BIX 01294 on the expression of the pro-apoptotic and anti-apoptotic genes in parental cells vs. TRAIL resistant RPMI8226 cells
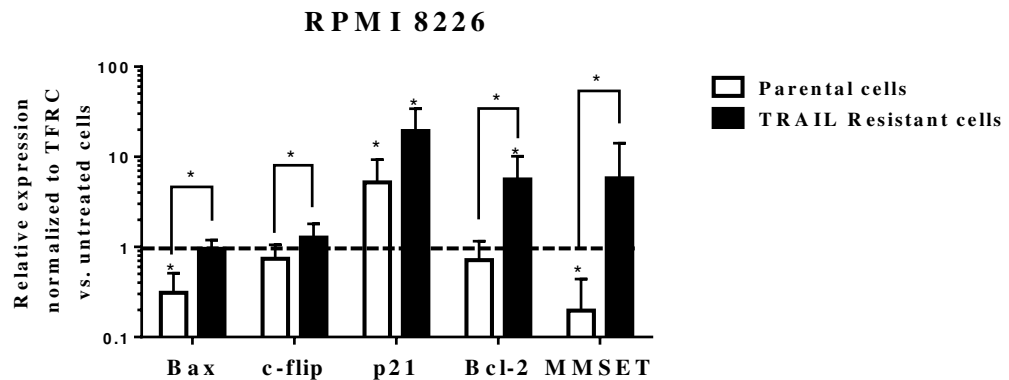
Figure 5.11: Effect of BIX 01294 on the expression of the pro-apoptotic and anti-apoptotic genes in parental cells vs. TRAIL resistant cells. TRAIL sensitive cells RPMI 8226 were treated with TRAIL or BIX 01294 (10μM) for 24 hours and the gene expression of Bax, c-flip, p21, Bcl-2 and MMSET was determined by qRT-PCR. The statistical significance was determined by comparison of the vehicle control with BIX 01294 treated cells and by comparison of parental with TRAIL[R] cells (*=p<0.05) (Kruskal–Wallis).

Figure 5.12: Effect of BIX 01294 on the expression of the pro-apoptotic and anti-apoptotic genes in suspension vs. 3D cell culture

Figure 5.12: Effect of BIX 01294 on the expression of the pro-apoptotic and anti-apoptotic genes in suspension vs. 3D cell culture. U266 cell line was treated with SAHA (1 μM) for 24 hours and the gene expression of Bax, c-flip, p21 and HRK was determined by qRT-PCR in suspension vs. 3D. The statistical significance was determined by comparison with the vehicle control and by comparison the suspension cells with 3D cultures (*=p<0.05) (Kruskal–Wallis).

5.4.6 Effect of GSK343 Treatment on Expression of Pro-apoptotic and Anti-Apoptotic Genes in Parental vs. TRAIL-Resistant and 3D Culture Myeloma Cells

Our results showed non significant up-regulation of p21 expression in parental RPMI 8226 and U266 cells treated with GSK343 as well as a non significant decrease in expression of HRK in U266 cell lines. In addition, treatment of TRAIL^R MM cell lines with GSK343 significantly increase the expression of cell cycle regulator p21, anti-apoptotic Bcl-2 genes ($p < 0.05$) in TRAIL^R RPMI 8226 cell that could explain the earlier finding in which TRAIL^R cells were less sensitive to GSK343. However, the pro-apoptotic gene Bax was also significantly increased ($p<0.05$) in TRAIL ^{R} RPMI 8226 cells upon stimulation with GSK343 compared with parental cells (Figure 5.13).

Similar to LMB, SAHA and BIX01294, GSK343 treatment exhibit a significant up-regulation ($p < 0.05$) of pro-apoptotic HRK expression in 3D culture U266 cell line compared to suspension cells (Figure 5.14).

Figure 5.13: Effect of GSK343 on the expression of the pro-apoptotic and anti-apoptotic genes in parental cells vs. TRAIL resistant RPMI8226 cells
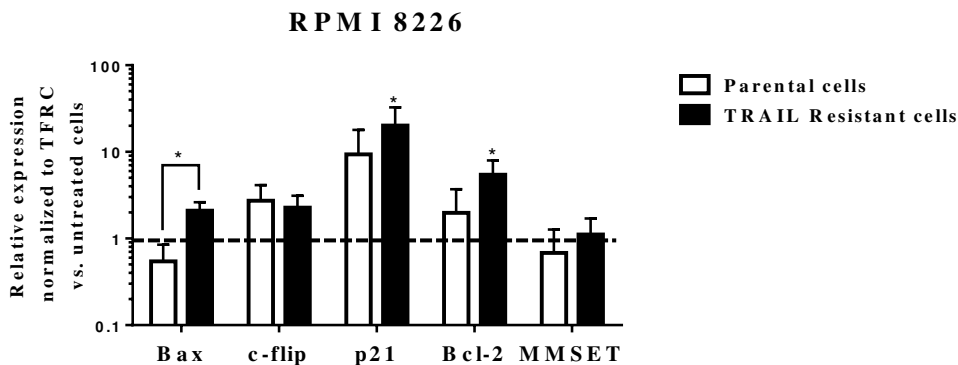
Figure 5.13: Effect of GSK343 on the expression of the pro-apoptotic and anti-apoptotic genes in parental cells vs. TRAIL resistant cells. TRAIL sensitive cells RPMI 8226 were treated with TRAIL or GSK343 (10μM) for 24 hours and the gene expression of Bax, c-flip, p21, Bcl-2 and MMSET was determined by qRT-PCR. The statistical significance was determined by comparison of the vehicle control with GSK343 treated cells and by comparison of parental with TRAIL[R] cells (*=p<0.05) (Kruskal–Wallis).

Figure 5.14: Effect of GSK343 on the expression of the pro-apoptotic and anti-apoptotic genes in suspension vs. 3D cell culture
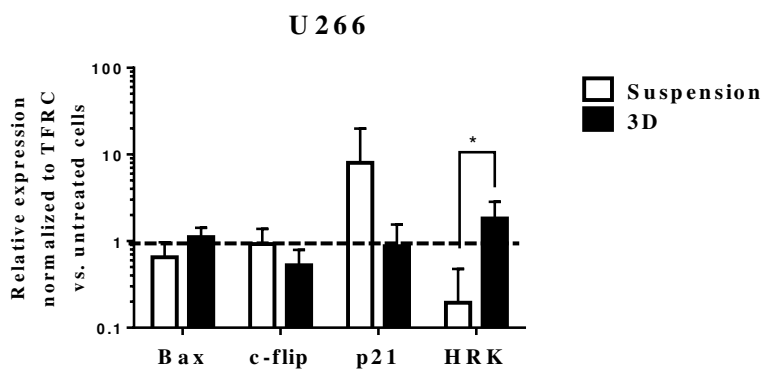
Figure 5.14: Effect of GSK343 on the expression of the pro-apoptotic and anti-apoptotic genes in suspension vs. 3D cell culture. U266 cell line was treated with GSK343 (1 μM) for 24 hours and the gene expression of Bax, c-flip, p21 and HRK was determined by qRT-PCR in suspension vs. 3D. The statistical significance was determined by comparison with the vehicle control and by comparison the suspension cells with 3D cultures (*=p<0.05) (Kruskal–Wallis).

247

5.4.7 Effects of TRAIL and TRAIL Sensitizers on the Apoptosis-Related Proteins in Multiple Myeloma cells using the Apoptotic Proteome Profiler Array

In order to determine the mechanisms of apoptosis induction by TRAIL and the epigenetic modifies, SAHA and BIX 01294 and GSK343 in multiple myeloma cells, a number of apoptosis-related protein expression was investigated in a TRAIL sensitive MM cell line NCI-H929 using apoptotic proteome profiler array. Treatment of NCI-H929 with a high dose of SAHA and BIX 01294 and GSK343 for 24 h showed some changes in apoptotic related proteins (Figures 5.15, 5.16, 5.17, 5.18 and 5.19). Epigenetic modifying agents: SAHA, and BIX 01294 and GSK343 treatment alone inhibited DR4 and anti-apoptotic protein XIAP, survivin, cIAP-1, pro-caspase 3 and Claspin expression (Figure 5.16). In addition, treatment with GSK343 caused a reduction in expression of anti-apoptotic Bcl-X (Figure 5.6). An increase in cleaved caspase-3 expression was seen following the treatment with BIX01294 (Figure 5.16). NCI-H929 cells showed a decrease in protein expression of heat shock proteins; HSP27, HSP60 and HSP70 in addition to a reduction in oxidative protein paraoxonase-2 (PON2) and heme oxygenase isoforms (HO-2) (Figure 5.17). In comparison with control treatment, a reduction of p53 isoforms phosphorylated at S15, S46 and S392 was seen in NCI-H929 cell line following treatment with SAHA, BIX 01294 and GSK343 alone for 24 h (Figure 5.18).

TRAIL alone induced Death Receptors DR5, FADD, Fas/TNFRSF6, TNFR-1 (Figure 5.16) and cleaved caspase-3 expression accompanied by decreased pro-caspase-3 and anti-apoptotic protein XIAP as well as a reduction in Survivin, and cIAP-1 expression (Figure 5.19). In addition, TRAIL treatment decreased HSP60, HSP70 and HO-2/HMOX2 expression in TRAIL sensitive cell line NCI-H929 compared to control cells (Figure 5.17). Importantly, epigenetic treatment as well as TRAIL potently decreased expression of catalase (Figure 5.15) however the basal expression was higher than the

maximum detection limit that can be accurately quantified by *LI-COR Odyssey*®.

Figure 5.15: Human Apoptosis Proteome Profiler Array
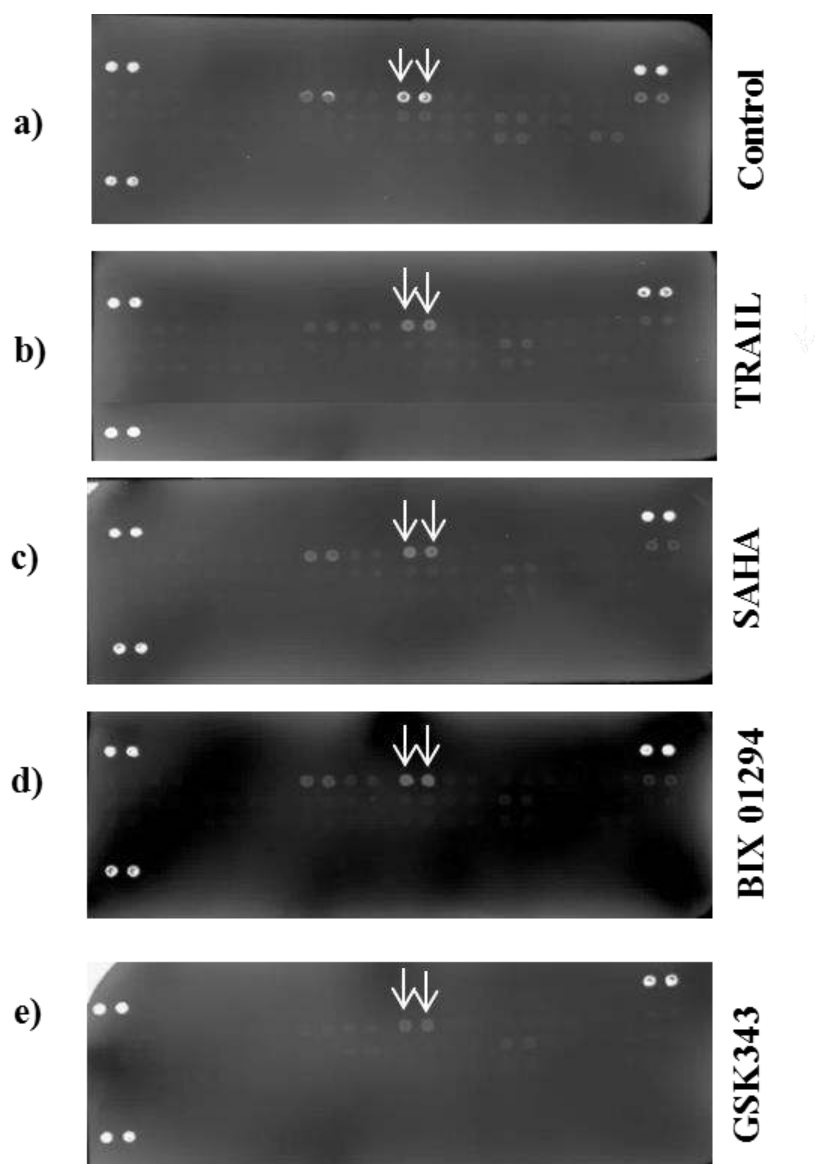
Figure 5.15: Human Apoptosis Proteome Profiler Array control membrane and treated multiple myeloma cells membrane. Approximately 1 × 10^{7} NCI-H929 cells/ml were treated with SAHA, BIX01294, GSK343 and TRAIL and apoptotic-related proteins were detected by apoptosis proteomic array. The arrays membranes were scanned with LI-COR Odyssey® Infrared Imaging System and quantified with Image Studio™ software (LI-COR). Reduction in Catalase protein expression was seen in treated cell compared to control untreated cell. The site of catalase proteins are indicated by white arrows.

Figure 5.16: Expression of pro-apoptotic Cleaved Caspase and anti-apoptotic proteins Survivin, Bcl-X, Claspin and cIAP-1 investigated with apoptotic proteomic array. NCI-H929 cells were treated with TRAIL, SAHA, BIX01294 and GSK343 alone for 24 h and the protein expression was detected by apoptotic proteome profiler. The result of untreated control was cells normalized to 1.

Figure 5.17: Expression of heat shock proteins HSP 27, HSP60, HSP70 and PON2 and HO-2 investigated with apoptotic proteomic array. NCI-H929 cells were treated with TRAIL, SAHA, BIX01294 and GSK343 alone for 24 h and the protein expression was detected by apoptotic proteome profiler. The result of untreated control was cells normalized to 1.

Figure 5.18: Expression of p53 isoforms phosphorylated at S15, S46, S392 and S635 investigated with apoptotic proteome profiler array in NCI-H929 cells
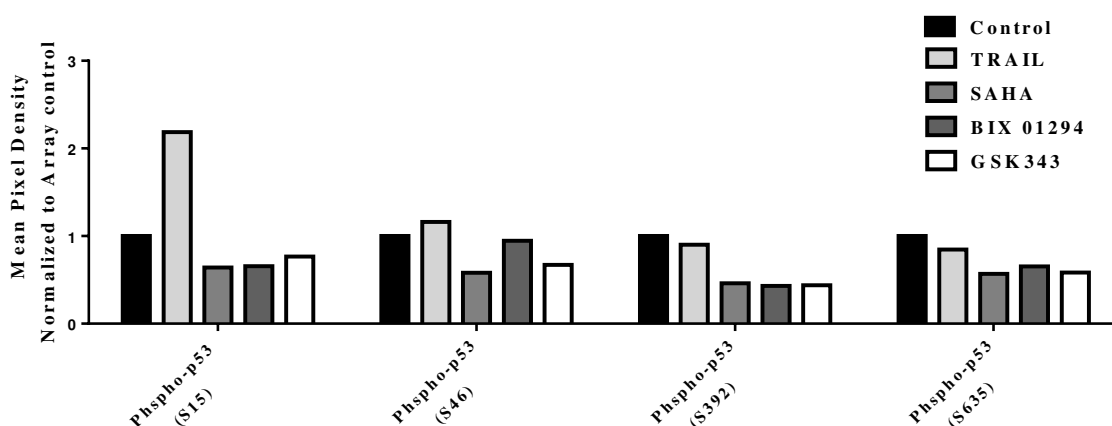
Figure 5.18: Expression of phosphorylated p53 isoforms S15, S46, S392 and S635 investigated with apoptotic proteomic array. NCI-H929 cells were treated with TRAIL, SAHA, BIX01294 and GSK343 alone for 24 h and the protein expression was detected by apoptotic proteome profiler. The result of untreated control was cells normalized to 1.

Figure 5.19: Expression of Death Receptors investigated with apoptotic proteome profiler array in NCI-H929 cells
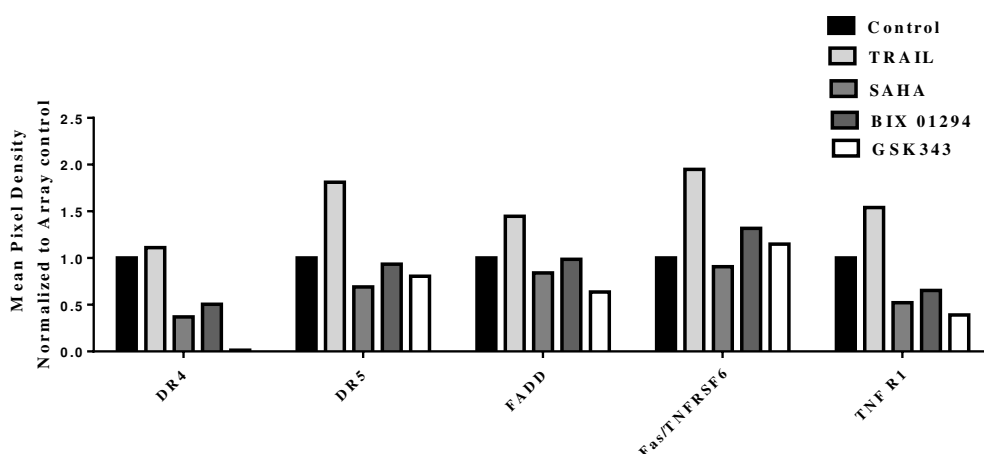
Figure 5.19: Expression of Death Receptors DR4, DR5, FADD, Fas and TNF R1 investigated with apoptotic proteome profiler array. NCI-H929 cells were treated with TRAIL, SAHA, BIX01294 and GSK343 alone for 24 h and the protein expression was detected by apoptotic proteome profiler. The result of untreated control was cells normalized to 1.

5.5 Discussion

In the TRAIL-mediated apoptosis process, initiator caspase-8 transducers trigger the apoptotic cascades either directly by means of activation of effector caspase-3/7 or via the pro-apoptotic Bid in the mitochondrial pathways. A number of involved factors have identified that influence on the TRAIL sensitivity of cancer cells; however, the exact underlying molecular mechanisms are still not fully understood. These factors include the up-regulation of pro-apoptotic genes and down up-regulation of anti-apoptotic genes (Wang *et al.*, 2010).

This investigation has previously shown that TRAIL and TRAIL sensitizers induce apoptosis in multiple myeloma cell lines (Chapter 2). Here, the potential mechanisms by which these agents mediate apoptosis were investigated. As a result, this study has demonstrated that TRAIL and TRAIL sensitizers induce both the intrinsic and extrinsic apoptotic cascades characterized by increases of initiator caspases 8/9 (Figure 5.1, 5.2, 5.3 and 5.4). qRT-PCR data reveled that upregulation of p21 expression in parental multiple myeloma cells lines as a result of treatment with LMB, SAHA, BIX 01294 and GSK343 which further increase in resistant cell lines (Figure 5.7, 5.9, 5.11, and 5.13). Moreover, SAHA treatment resulted in decreased expression of anti-apoptotic Bcl-2 and c-flip genes in myeloma cells (Figure 5.9). Furthermore, the decreased expression of MMSET was observed in RPMI 8226 cells upon treatment with BIX 01294 (Figure 5.11). In addition, increase expression of pro-apoptotic genes HRK and Bax in MM cell lines growing in 3D cultures models compared to suspension cultures as a result of treatment with these anti-tumour agents (Figure 5.8, 5.10, 5.12, and 5.14).

TRAIL treatment also shown to up-regulate pro-apoptotic Death Receptors and cleaved-caspase-3 expression (Figure 5.19 and 5.16). In addition, TRAIL and TRAIL sensitizers down-regulate anti-apoptotic protein (XIAP, survivin, cIAP-1, and claspin) (Figure 5.16) in NCI-H929 cells together with decrease in catalase (Figure 5.15), protein

expression of heat shock proteins, heme oxygenase isoforms (HO-2) and anti-oxidative protein paraoxonase-2 (PON2) (Figure 5.17).

5.5.1 Effect of the TRAIL and TRAIL Sensitizer on Intrinsic and Extrinsic Pathways: Caspase-8/-9 Activity

5.5.1.1 *The Effect TRAIL and LMB on Caspase-8/-9 Activity*

TRAIL alone enhanced caspase-8 and caspase-9 activity in RPMI 8226, OPM2, and U266. While in NCI-H929 cell line a significant increase was only seen in caspase-8 activity and in caspase-9 in ADC-1 cell line. These results are consistent with earlier study which found that TRAIL trigger multiple myeloma cell death by stimulation both extrinsic and intrinsic and extrinsic apoptotic cascades via the activation of caspase-3, -7, -8 and -9 in RPMI 8226 myeloma cell lines (Vitovski *et al*., 2012).

LMB alone also enhanced both caspase-8 and -9 activities in NCI-H929, RPMI 8226, JJN, and U266 and combination treatment further elevated caspase-8 and -9 consistent with morphological observations in all multiple myeloma cell lines. However, a significant increase was only seen in caspase-9 and caspase-8 in OPM2 cell lines following treatment with LMB alone in ADC-1 and OPM2 cell line respectively. This work is considered as the first study investigated the effect of LMB alone or in combination with TRAIL in multiple myeloma, concluding that LMB targets intrinsic and/or extrinsic pathways to trigger apoptosis in multiple myeloma, although responses differ between cell lines tested. Consistent with data in the current study, U937 leukemic cells showed that treatment with LMB induced apoptosis in leukemia cell lines via the mitochondrial pathways related to cytochrome c release and the activation of caspase-3, and -9 (Jang *et al.,* 2004). To date there are no studies investigating the effect of LMB on caspase activation on multiple myeloma. Together, these earlier studies and these results are shown in this work evidently revealed that TRAIL-and-

LMB induced apoptosis is mediated through activation of both intrinsic and extrinsic pathways.

5.5.1.2   *Effect of SAHA on Caspase-8/-9 Activity*

Epigenetic modification of gene expression has an essential role in cancer initiation and progression (Zhou *et al*., 2016). The non-selective HDAC[i] SAHA inhibits HDAC I and II class activity causes growth inhibition and death in various cancer types both *in vivo* and *in vitro* such as multiple myeloma (Marks., 2007; Hideshima and Anderson, 2013). The mechanisms of action of HDAC[i] in myeloma therapy in preclinical studies have not yet been fully understood. Inhibition of histone deacetylation mainly induces transcription of positive and negative regulators of proliferation and/or the survival of the cell and growth inhibition or cytotoxicity. (Mitsiades *et al*., 2003; Fandy *et al.,* 2005; Hildesheim and Anderson., 2013). This study examined the relation of TRAIL and TRAIL sensitizers SAHA and the activities of cellular caspase-8 and -9 in multiple myeloma cell lines. It was found that HDAC[i] SAHA can activate caspases -8 and -9 in these cell lines.

These results are consistent with the previous study in which the combination therapy of TRAIL with HDAC[i] SAHA or sodium butyrate synergistically induces apoptosis in human myeloid leukemia cells through activating both the extrinsic and intrinsic pathways of apoptosis by activation of caspase-3 and -8 (Rosato., *et al* 2015). Gillenwater *et al*., (2007) showed that SAHA selectively induced apoptosis in head and neck squamous carcinoma cell lines, through the mitochondrial pathway via increase release of cytochrome c, caspase-3 cleavage in addition to activation of and Fas death signaling via up-grade the expression both Fas and Fas ligand, caspase-8 activation and Bid cleavage (Gillenwater *et al*., 2007).

However, these results were inconsistent with two earlier studies which showed SAHA treatment in B-cell malignancy including multiple myeloma (Mitsiades *et al*., 2003) and human multiple myeloma cell lines (Fandy *et al*., 2005) induced growth arrest and triggered apoptosis in a caspase-independent without activate cleavage of caspase-8, -9, or -3 and was mediated via the release of mitochondrial apoptosis-inducing factor (AIF) (Mitsiades *et al*., 2003; Fandy *et al*., 2005).

5.5.1.3   *Effect of the HMTase[i] BIX 01294 on Caspase-8/-9 Activity*

Histone lysine methyltransferase EHMT2/G9a is a key enzyme for dimethylation of H3K9 at lysine-9 (H3K9) in euchromatin (Savickiene *et al*., 2014). Aberrant or over expressed of EHMT2/G9a has been observed in various types of human cancers including hepatocellular carcinoma (Kondo *et al*., 2007), lung cancer and bladder cancer (Cho *et al.*, 2011). BIX 01294 is a specific G9 histone lysine methyltransferase inhibitor stimulates apoptosis in human neuroblastoma cells and decrease the growth of bladder cancer cells (Lu *et al*., 2013; Cui *et al*., 2015; Kim *et al*., 2013; Varier and Timmers., 2011). G9 knockdown in aggressive lung cancer cells suppressed cell migration and invasion *in vitro* and metastasis *in vivo* (Chen *et al*., 2010), suggesting that BIX 01294 is a potential therapeutic agent (Kim *et al*., 2013; Varier and Timmers, 2011). However, the specific mechanism of the apoptosis mediated by BIX 01294-mediated apoptosis in cancer cells is still unclear. In the present study, BIX 01294 either alone or in combination with TRAIL significantly increased caspase-8 and -9 activity in NCI-H929, RPMI 8226, JJN3, U266 and ADC-1 cell lines; suggested that BIX 01294 act via both the intrinsic and extrinsic apoptotic pathways in these cell lines. However, in OPM2 cell lines BIX 01294 alone only significantly increased caspase-8 activity while combination treatment with TRAIL significantly elevated caspase-9 activity. This work is considered as the first study investigated the effect of HMTase[i] BIX 01294 alone or in combination with TRAIL on caspase in multiple myeloma; concluding that BIX 01294

target both intrinsic and extrinsic pathways to trigger apoptosis in multiple myeloma.

Similar findings were observed in the previous studies that investigated the effect of BIX 01294 on bladder cancer cell lines. Cui *et al.,* (2015) demonstrated that BIX 01294 stimulated caspase-dependent apoptosis by significantly activation of caspase-8, -9, -3 and cleaved the caspase-3, PARP1 substrate (Cui *et al.,* 2015). Another study found that treatment of neuroblastoma cell lines with BIX 01294 activating caspase-3 and -8 (Lu *et al*, 2013) as well as induced capase-3 cleavage in oral squamous cell carcinoma (Ren *et al*., 2015). In addition, BIX 01294 treatment suppressed proliferation and enhanced apoptosis of glioma cell line U251 via activation of caspase-9 and -3 (Guo *et al*., 2016). To date, there are no studies of the effect of BIX 01294 alone or in combination with TRAIL on caspase in MM. Based on earlier studies and with evidence shown in this study support that BIX 01294 is able to trigger apoptosis by activation of caspases, however, whether this lead to the stimulation of intrinsic and or extrinsic apoptotic pathways differs depending on the cell lines, and the apoptotic pathway mechanism of action may be cell lineage-specific.

5.5.1.4 *Effect of the HMTase[i] GSK343 on Caspase-8/-9 Activity*

EZH2 catalyzes trimethylation of lysine 27 (Lys 27) on histone H3 (H3K27) (Popovic *et al*., 2014) and EZH2 dysregulation has been correlated with poor cancer progression (Verma *et al*., 2012) and inhibition of EZH2 has been reported as an effective approach for the cancer treatment (Lund *et al*., 2014). GSK343 is a potent and selective inhibitor of EZH2 (Verma *et al*., 2012) that can inhibit the viability, restrained cell cycle progression as well as induce cell death of osteosarcoma cells (Xiong *et al*., 2016). However, the molecular basis of mechanisms of apoptosis inhibition by EZH2 is not fully understood (Zhang *et al*., 2014). Here, GSK343 in the presence of TRAIL resulting in significant increase of caspase-8 and -9 activity in OPM2, NCI-H929,

RPMI 8226, and U266 cell lines at 24 h; suggested that GSK343 act via both the intrinsic and extrinsic apoptotic pathways in these cell lines. However, GSK343 significantly increased only caspase-9 activity in ADC-1 cell lines and caspase-8 activity in JJN3 cell line; suggested that the apoptosis induction is via extrinsic and/or intrinsic pathways activation, however, effects are differentially modulated in different cell lines.

This work is considered as the first study investigated the effect of EZH2 inhibitor GSK343 alone or in combination with TRAIL on caspase in MM; concluding that GSK343 target both intrinsic and extrinsic pathways to trigger apoptosis in MM. However, recent work exhibited that inhibition of EZH2 by UNC1999 and GSK343 alone stimulate apoptosis in multiple myeloma cell lines INA-6, LP-1 and RPMI-8226 and the induction of apoptosis by UNC1999 was via both intrinsic and extrinsic pathways through cleavage of caspase-3, -8 and -9 (Agarwal *et al.,* 2016). These earlier studies and with evidence shown in this study support that the GSK343 is able to trigger apoptosis by activation of caspases, however, whether this leads to the stimulation of intrinsic and or extrinsic apoptotic pathways differs depending on the cell lines, the apoptotic pathway mechanism of action may be cell lineage specific and that the combination with TRAIL could have promise in the treatment of multiple myeloma.

5.5.2 Effects of TRAIL Sensitizers on Gene Expression

5.5.2.1 LMB

To investigate the apoptosis effect of TRAIL and TRAIL senstizers in myeloma cells, qRT-PCR was performed and the expression of pro-apoptotic genes Bax, anti-apoptotic genes; c-flip and Bcl-2 cell and cycle regulators p21 was determined. Results from the current study showed upregulation of p21 expression in parental multiple myeloma cell lines RPMI 8226, NCI-H929 and U266 as a result of treatment with LMB. Previous work has reported that induction of apoptosis in leukemia cells by LMB through

cytochrome c release, caspase activation, and decrease expression of Mcl-1 and XIAP while there was no change in the expression of Bcl-2 or Bax (Jang *et al.,* 2004). In another study, Lecane and colleagues demonstrated that LMB induces apoptosis in a p53-dependent manner. The treatment with LMB in the prostate cell line LNCaP cell that contains wild-type p53 gene increased the transcription activity of p53 by nuclear entrapment and the expression of p53 responsive genes includes p21, Bax and DR5 by interfering with their nucleo-cytoplasmic export and subsequent protessomal degradation. However, the null-p53 DU 145 cells did not activate the downstream target genes (Lecane *et al*., 2003). This suggests that LMB-dependent effects are in part mediated by p53, although other pro-apoptotic transcription factors are known to the trapped in the nucleus. Furthermore, unpublished work conducted in our laboratory by Haywood-Small *et al* shows LMB-mediated TRAIL enhancement apoptosis to be p53 independent in breast and prostate cells (Haywood-Small *et al*., 2011).

5.5.2.2 *SAHA*

Here, SAHA treatment resulted in a significant increase in p21 expression and decreased in anti-apoptotic genes Bcl-2, c-flip expression in multiple myeloma cells. These finding are consistent with a previous study on B-cell malignancies which showed an induction in the level of p21 and p53, and Bid cleavage after treatment with SAHA and that SAHA sensitizes myeloma cells to TRAIL-induced apoptosis with reduced expression of the anti-apoptotic proteins XIAP, c-flip, and cIAP2 (Mitsiades *et al*., 2003).

However, other studies reported that the upregulation of p21 level blocked the TRAIL-induced apoptosis, which contributed to decrease SAHA sensitivity in human leukemia cell lines by delayed cleavage of PARP, caspase-8 and silencing of p21 enhanced SAHA–mediated cell death (Wu *et al.*, 2014). Burgess *et al.,* (2001) in a previous study showed that treatment of human melanoma cell lines with HDAC[i] azelaic bis-

hydroxamic acid (ABHA) results in up-regulate expression of p21 and correlated with decreased sensitivity and inhibiting apoptosis, suggesting that p21 may provide a significant protection against SAHA-mediated apoptosis in leukaemic cells. Earlier work has shown that the expression of Bcl-2 was significantly down-regulated after treatment of cells with HDAC[i], Trichostatin A and Valproic Acid on leukaemia cells (Jasek *et al*., 2012).

Previous work has reported that majority of multiple myeloma tumour cells express high levels of c-flip and there was a correlation between c-flip over-expression and TRAIL resistance in myeloma cells (Wu *et al*., 2016). In addition, apoptosis induction by SAHA in cutaneous T-Cell lymphoma cells is associated with c-flip down regulation (Al-Yacoub *et al*., 2012) and HDAC[i] sensitize glioblastoma cells to TRAIL-mediated apoptosis by c-myc-mediated downregulation expression of anti-apoptotic genes c-flip (Bangert *et al*., 2012).

5.5.2.3   BIX 01294

In this study, increased expression of p21 as well as decreased expression of MMSET in RPMI 8226 cells upon treatment with BIX 01294. This finding are confirmed by earlier work which showed that inhibition of G9a inhibitor BIX 01294 inhibited proliferation and induced cell cycle arrest in foetal pulmonary artery smooth muscle cell (PASMC) was accompanied by upregulating p21 expression (Yang *et al*., 2012). However, the expression of p21 mRNA in other studies was not induced in neuroblastoma cell line LA1-55n treated with BIX 01294 (Lu *et al*., 2013). Other studies have reported that BIX 01294 stimulated autophagy-related cell death in colon cancer cells via selectively stimulated tumour suppressor p53 target genes, such as p21, but did not activate expression the of PUMA, a typical p53 target gene involved in apoptosis (Fan *et al*., 2015). Moreover, BIX 01294 suppressed the proliferation of glioma cells and induced apoptosis via decreased expression of Bcl-2 as well as increased expression of Bax

(Guo *et al*., 2016).

MMSET positive cells were more sensitive to BIX 01294 (Chapter 2). It is known that multiple myeloma cells are epigenetically altered as part of transformation process. 20% of cases have MMSET over-expression presumably inducing oncogene expression from transcriptionally active chromatin (H3Kme36) (Popovic *et al*., 2014). Other cases have increase EZH2 and decrease EZH2 induce myeloma-associated oncogene expression, including c-MYC, and re-express many miRNAs with TSG activity (Alzrigat *et al*., 2017). Furthermore, Zeng *et al*., (2017) showed that EZH2 decrease stem-like activity in multiple myeloma (Zeng *et al*., 2017). This suggests that targeting histone methyltransferase may useful in myeloma although most of the data suggests EZH2 and to date, no data is available on G9a.

5.5.2.4   GSK343

In the current study, treatment with GSK343 was accompanied with increase expression of cell cycle regulatory gene p21. This result is consistent with those of a study conducted by Fan, *et al.,* (2011) which showed that the depletion of EZH2 resulting in proliferation inhibition of melanoma cells and restoring the cellular senescence characteristics. Furthermore, the combination treatment of EZH2 depletion and HDAC[i] synergistically increase the expression p21/CDKN1A in melanoma cells via removing histone deacetylase 1 (HDAC1) form the transcriptional start site CDKN1A as well as the downstream sites (Fan *et al.*, 2011). Moreover, inhibition of methyltransferase activity by DZNep enhanced B-Cell lymphoma sensitivity to TRAIL-induced apoptosis through caspase-activation and accelerated c-flip degradation (Braun *et al*., 2015).

5.5.3 Effects of TRAIL and TRAIL Sensitizers on Gene Expression in TRAIL-Resistant Cells

To investigate the gene expression changes of likely apoptotic and cell cycle modulators in parental TRAIL-sensitive NCI-H-929 and RPMI 8226 cells vs. TRAIL resistant cells, qRT-PCR was performed. In the current study, prolonged incubation of TRAIL sensitive cells with TRAIL significantly increased the expression of c-flip and p21 in NCI-H 929 TRAIL resistant cells and a significant increase in p21 in RPMI 8226 TRAIL resistant cells compared to parental cells, as well as a decrease in HRK expression in TRAIL resistant cell lines in comparing to parental cells (Figure 5.6).

Moreover, LMB treatment showed a significant increase in expression of the anti-apoptotic gene Bcl-2 (Figure 5.6) in TRAIL resistant cells vs. parental cells in spite of the fact that TRAIL-resistant cells were more sensitive to LMB compared to parental cells (Chapter 2). Based on these results, it can be suggested that the expression of anti-apoptotic gene Bcl-2 is not enough to inhibit apoptosis of TRAIL resistant cells by LMB.

This investigation also showed that SAHA treatment increased expression of c-flip and Bcl-2 and p21 in TRAIL resistant cells RPMI 8226 compared to parental TRAIL sensitive (Figure 5.9)   This is consistent with earlier findings in which SAHA failed to sensitize TRAIL resistant cell lines to TRAIL (Chapter 2). The treatment with BIX 01294 resulted in a significant increase in p21. Moreover, a significant increase in anti-apoptotic Bcl-2 was observed in RPMI 8226 TRAIL RESISTANT cells (Chapter 2) (Figure 5.11) that could partly explain the resistant behavior of this cell line to BIX 01294. However, the pro-apoptotic gene Bax was significantly increased in TRAIL resistant RPMI 8226 cell line compared to parental cells.

In addition, increased expression of Bcl-2, p21 and MMSET was observed following treatment with GSK343 in RPMI 8226 TRAIL resistant cells compared to parental cells

(Figure 5.13). That may explain the earlier finding in which there was significant reduction of percentage of apoptosis in response to GSK343 in TRAIL resistant cell compared to parental cells (Chapter 2). Earlier work demonstrated an interaction between MMSET and EZH2 in MM oncogenesis and MMSET over-expression change patterns of EZH2 chromatin binding and methylation status. This work is considered as the first study investigating the possible mechanistic by which TRAIL effect on TRAIL^R MM population through examine numbers of apoptotic genes. However, the number of target genes that were tested was small making it difficult to draw a conclusion and hence a larger number of proteins were subsequently analysed using a proteome array.

5.5.4 Effects of TRAIL and TRAIL Sensitizers on Gene Expression in 3D vs. Suspension Cell Culture

In the current study, challenging the multiple myeloma cells with LMB, SAHA, BIX 01294 and GSK343 induced the expression of pro-apoptotic gene HRK and Bax in investigated multiple myeloma cell lines in 3D cultures condition compared to suspension culture, thus potentially overcoming anti-apoptotic Bcl-2 which is the HRK-interacting protein. That may explain the higher sensitivity of myeloma cells growing in 3D cultures compared to suspension cultures and these anti-tumour agents sensitize myeloma cell lines to TRAIL as this investigation has previously shown (Chapter 3).

A few investigations on HRK protein expression have been performed, and little is known about the epigenetic or post-transcriptional mechanisms that may involve in HRK inactivation (Nakamura *et al.,* 2008). HRK inactivation apparently appears in a large proportion of all cancer phenotypes and as a potential pro-apoptotic gene, HRK may participate in the growth and progression of numerous types of human tumours (Nakamura *et al.,* 2008). The HRK role in cell death has been illustrated mostly in hematopoietic and neural tissues (Harris and Johnson., 2001; Sanz *et al.,* 2000) and high

levels of HRK was found in an embryonic neuronal culture that undergoes apoptosis (Imaizumi *et al*., 1997). Only one published work has investigated the effect of GSK343 on pro-apoptotic gene HRK while working on EOC cells; it found that EZH2 inhibitor GSK343 increased the expression of the pro-apoptotic H3K27Me3 targeted gene HRK in 3D, but not in 2D cultures models consistent with this study (Amatangelo *et al*., 2013).

5.5.5 Effects of TRAIL and TRAIL Sensitizers on the Expression of Apoptosis-Related Proteins in Multiple Myeloma Cells

After investigating Bax, c-flip, p21, MMSET and HRK gene expression at qRT-PCR this investigation further clarify the potential involvement mechanisms of apoptosis induction by TRAIL and epigenetic modifiers agents: SAHA, BIX 01296 and GSK343 in a TRAIL sensitive multiple myeloma cell line NCI-H929, a number of apoptosis-related protein expression was determined using proteomic profiler array. Here, TRAIL treatment induced cleaved caspase-3, DR5, FADD, Fas/TNFRSF6 and TNF R1 proteins expression in TRAIL sensitive cell line NCI-H929 compared to control cells (Figure 5.19). In addition, TRAIL and epigenetic modifiers agents alone inhibited anti-apoptotic protein XIAP, survivin, and claspin expression (Figure 5.16), heat shock proteins (Figure 5.17), phosphorylated p53 isoforms and heme oxygenase isoforms (HO-2) (Figure 5.18). These finding consistent with a recent study by Zhou *et al*., (2016) using an apoptotic proteomic array and qRT-PCR it has been found that SAHA inhibited the expression of Bcl-2, Bcl-x and Phospho p53 (S46) and increasing DR5, CDKN1A and caspase-3 in breast cell lines. Whereas TRAIL alone significantly up-regulated the expression of Bax, caspase-3 and DR5, and down-regulated the expression of Bcl-2, Bcl-x, CDKN1A in breast MDA-MB-231 cells. Moreover, the combination therapy significantly induced the pro-apoptotic modulating proteins, and they also significantly suppressed anti-apoptotic molecules expression in breast cell lines (Zhou *et al*., 2016).

It has been reported that TRAIL treatment significantly up-regulated the Death Receptors and pro-apoptotic proteins and down-regulated the anti-apoptotic members of the Bcl-2 family in many type of cancer (LeBlanc and Ashkenazi., 2003; Zhou *et al.,*2016).

In current work, decrease expression of IAP family protein members cIAP, XIAP and survivin were accompanied with TRAIL or epigenetic modifiers agents in MM cell line compared to untreated cells (Figure 5.16). Survivin is one of important apoptosis inhibitor and it contributes to the malignant progression of lymphoma (Aoki *et al*., 2003). Previous studies linked between survivin over-expression and the resistance and sensitivity to TRAIL-mediated apoptosis in uveal melanoma (Li *et al*., 2005). A study on malignant gliomas cell lines, XIAP inhibitor embelin acted in synergy with the TRAIL and induced the TRAIL-mediated apoptosis by decrease the expression of survivin, IAP, and c-flip that conferred TRAIL resistance in glioma cells (Siegelin *et al*., 2009). Moreover, SAHA-induced apoptosis in colon cancer through down-regulation of anti-apoptotic survivin (Huang and Guo., 2006).

Here, TRAIL and epigenetic modifier agents alone inhibited heat shock proteins in multiple myeloma cell line compared to control cells (Figure 5.17). The effects of heat shock proteins including HSP27 and HSP70 have been known to have an important role in protection against apoptosis and promote cell survival (Franklin *et al*., 2005; Garrido *et al*., 2003). Over-expression of HSP27 and HSP60 was observed in many cancer types and linked to oncogenesis and therapy resistance. Inhibitions of heat shock proteins result in reduced tumour size and could constitute a novel strategy for the cancer therapy (Garrido *et al*., 2003). These findings are consistent with previous works which showed that HSP70 inhibited both caspase-dependent and -independent cell death in Jurkat T-cells. This suggests that heat shock proteins may be a key anti-apoptotic regulator at a very early stage in the cell death signaling cascades (Creagh *et al*., 2000).

5.5.5.1 *Effects of TRAIL and TRAIL Sensitizers on the Expression of Oxidative Enzyme Catalase in Multiple Myeloma Cells*

In the current work, the level of oxidative enzyme catalase was decreased in TRAIL or TRAIL senstizers treatment multiple myeloma cell line compared to control group. Generation of ROS has a key role in cell death mediated by TNF- α while Heme-oxygenase isoform HO-2 maintain cellular protection against oxidative stress and apoptosis (Basuroy *et al*., 2006). In order to protect the cell from oxidative injury and the stimulation of apoptotic pathways, ROS must be neutralized by enzymes that catalyze hydrogen peroxide, such as catalase and antioxidant metabolites like glutathione (GSH) to prevent possible cellular damage and stimulation of the apoptotic pathways (Evens *et al.,* 2005). Disruption of these enzymatic antioxidant defense systems can thus contribute to increases in ROS (Ikeda *et al*., 2004). ROS is known to induce apoptosis in tumour cells, however, the mechanisms are poorly understood (Borutaite and Brown., 2001). High ROS level has been identified in cells undergoing apoptosis. Treatment of cells with hydrogen peroxide (H_2O_2) *in vitro* alone causes either apoptosis or necrosis depending on the concentration of H_2O_2 and the cell type being investigated (Bai and Cederbaum., 2000). Importantly, cell death in multiple myeloma cells correlated with the generation of ROS and the myeloma cell sensitivity was dependent on cellular catalase activity. In addition, treatment with catalase inhibitor induced ROS-dependent apoptosis (Wang *et al*., 2006). In a clinical study investigated the role of ROS in the pathogenesis of multiple myeloma by measuring the level of enzyme activities and oxidative stress parameters such as catalase in 14 newly diagnosed multiple myeloma patients (Kuku *et al.,* 2005). It was found that all parameters of oxidative stress and enzymes activities were significantly reduced following therapy. This data propose that ROS may be participating in multiple myeloma pathogenesis (Kuku *et al.,* 2005). On the basis of the above findings, these

results indicating the important role of oxidative stress and catalase in multiple myeloma mechanism.

However, although the vast majority of studies suggest oxidative stress can stimulate apoptosis, some reports showed that it can inhibit apoptosis and stimulate survival pathways. The mechanism by which ROS inhibits apoptosis is unclear; it has been found that H_2O_2-induces inactivation of caspase-3 (Borutaite and Brown., 2001). Moreover, high level of H_2O_2 can inhibit Fas-induced apoptotic cell death in Jurkat T-cells, by reversibly inactivating caspase activity (Hampton, and Orrenius,.1997). However, over-expression of catalase in either the mitochondrial or cytosolic compartment induced sensitivity of a human liver cancer cell line (HepG2) to caspase-3 dependent-TNFα-mediated apoptosis (Bai and Cederbaum., 2000).

In summary, this work for the first time have shown some idea about the effect of LMB and G9a inhibitor, BIX 01294 and GSK343 on cell viability, cell cycle and caspase cascade and stimulated apoptosis in multiple myeloma cell lines. From this results can be concluded that the targeting of pro- and anti-apoptotic modulating molecules induce anti-tumour agents-mediated apoptosis in cancer cells and LMB, SAHA, BIX 01294 and GSK343 may be a potential novel epigenetic therapy for multiple myeloma cells.

5.6   Conclusion

TRAIL and TRAIL sensitizers (LMB, SAHA, BIX 01294, and GSK343) either alone or in combination were previously shown to activate effector caspase-3 and confirm morphological changes of apoptotic in multiple myeloma cell lines (Chapter 2). Here, TRAIL and TRAIL sensitizers induced apoptosis via both extrinsic and intrinsic pathways via activation of both caspase 8 and 9 in multiple myeloma cell lines with varies effect depending on cell lines.

TRAIL treatment increased the expression of Death Receptors DR5, FADD, Fas/TNFRSF6 and TNF R1, and decreased expression of anti-apoptotic genes XIAP, Survivin, and cIAP-1. Pro-caspase-3, anti-apoptotic protein (XIAP, survivin, cIAP-1, and claspin), heat shock proteins; HSP27, HSP60 and HSP70, heme oxygenase isoforms (HO-2), anti-oxidative protein paraoxonase-2 (PON2) and phosphorylated p53 isoforms were down-regulated following treatment with epigenetic modifiers for 24 h. Importantly, TRAIL and epigenetic modifiers were able to decrease expression of catalase in comparison with untreated cells. Providing a number of potential mechanisms by which TRAIL and TRAIL sensitizers trigger apoptosis in multiple myeloma cells. These results established that the combination treatments used in this study may target multiple signaling pathways and could act as an effective therapeutic approach against cancer. An advanced understanding of the underlying molecular mechanisms may facilitate either TRAIL or TRAIL sensitizers targeted use and the selection of appropriate combinations and determine the precise signaling of apoptosis mediated by these therapies requires further explore in future works.

6. General Discussion

The current study aimed to address the hypothesis that small molecule anti-tumour agents can enhance TRAIL sensitivity in multiple myeloma cells, both in suspension and 3D cell culture.

6.1   Key Findings

6.1.1   Effect of TRAIL and TRAIL Senstizers in Suspension multiple myeloma Cell Lines

This study has illustrated that several novel classes of agents are TRAIL sensitizers, including NEI (LMB), HMT[i] BIX01294 and EZH2[i] GSK343. These agents displayed potential anti-tumour effect through reduction of ATP level as a marker of proliferation, induction of apoptosis, and cell cycle arrest in addition to the synergistic effects observed in combination with TRAIL. This work demonstrated that these anti-tumour agents that enhanced TRAIL responses in a caspase-3-dependent manner and resulted in characteristic apoptotic morphological changes in all multiple myeloma cell lines. TRAIL sensitizers induced both caspase-8 and -9 activities in most of cell lines, confirming that apoptotic signaling used both the intrinsic and extrinsic pathways.

For the first time, the current study has shown that TRAIL displayed a synergistic induction of apoptosis by the NEI LMB and also the HMTase[i] BIX 01294 which inhibits G9a methyl transferase. None of these agents or even other agents from these classes of agents has been reported to interact with TRAIL in any cells in the published literature, although initial studies in our laboratory have shown NEIs (LMB) to enhance TRAIL in breast and prostate cancer cells (Haywood-Small *et al*., 2011). Interestingly, TRAIL alone and in combined with these agents showed a lower level of toxicity toward the non-tumours cell lines CD133^{+} haematopoeitic stem cells, and also normal renal cells (HREC). The differential sensitivity patterns observed within multiple myeloma cell lines to TRAIL are consistent with previous studies and likely reflect differential expression of apoptotic modifyers (Fandy and Srivastava., 2006).

The synergistic effect of TRAIL on induction of apoptosis and suppression of cell proliferation when combined with SAHA in ARP-1 multiple myeloma cell line have been previously reported in only one study via up-regulated transcription and the expression of surface TRAIL DR4/DR5 death receptors and pro-apoptotic protein and down-regulated expression of anti-apoptotic proteins Bcl-2 and IAPs (Fandy *et al*., 2005). In addition, earlier studies have shown that malignant mesothelioma (Neuzil *et al*., 2004), melanoma (Zhang *et al*., 2003) leukemia (Rosato *et al*., 2003), and breast cancer (Zhou *et al*., 2016) can be sensitized with HDAC[i] SAHA to undergo apoptosis by TRAIL. The sensitization of TRAIL resistant cells seems to be through up-regulation of pro apoptotic genes Bax, Bak, TRAIL-R2/DR5, and activation of caspases and down-regulation the expression of other anti-apoptotic proteins: Bcl-2, Bcl-XL and IAPs and cIAP2 and c-flip (Neuzil *et al*., 2004; Rosato *et al*., 2003; Zhang *et al*., 2003; Mitsiades *et al*., 2003; Zhou *et al*., 2016).

In this study, BIX 01294 was found to produce significant increasing of apoptosis and decreasing the ATP levels in MMSET positive cells (NCIH-929, OPM2 and ADC-1); whereas in combination with TRAIL, BIX 01294 synergistically enhanced TRAIL responses on induction of apoptosis and reduced ATP production in MMSET-negative cell lines (RPMI 8226, U266 and JJN3) and caused arresting cell cycle. Earlier work has shown that G9a inhibitor BIX01294 induced apoptosis number of cell lines: oral squamous cell carcinoma cell lines (Ren *et al*., 2015) breast cancer (Huang *et al,* 2010), neuroblastoma cells (Lu *et al.*, 2013) and bladder cancer cell lines (Cho *et al.,* 2011; Cui *et al.,* 2015). This study is the first study to investigate the effect of specific G9 inhibitor BIX01294 in multiple myeloma and to date there are no previous work to link HMTase[i] inhibition to sensitisation of TRAIL in any tumour type. Further *in vivo* work is needed to support that a small molecule G9 inhibitor, BIX 01294 enhance TRAIL-induced apoptosis and may act as a clinically useful TRAIL sensitizer.

In the current work, EZH2 inhibitor GSK343 and TRAIL displayed synergistic effect on reduction of ATP level and induction of apoptosis in multiple myeloma cell lines. Very few studies have investigated the effects of GSK343 on apoptosis induction in cancer. Only one published work has investigated the apoptotic effect of EZH2 inhibitor GSK343 in MM cell line and showed that inhibition of EZH2 by using UNC1999 and GSK343 decreases viability and induced apoptosis (Agarwal *et al.,* 2016). Recent work on osteosarcoma has shown that GSK343, a potent EZH2 inhibitor suppressed cell viability, restrained cell cycle and stimulated apoptosis (Xiong *et al.* 2016). Moreover, the combination of EZH2 (GSK343) and EHMT2 inhibitor (UNC0638) demonstrates a synergistic inhibition in growth of human breast adenocarcinoma cells (Curry *et al*., 2015). To date there are no studies of effect of the GSK343 in combination with TRAIL in any tumour types. However, only one published work reported that the interaction of other class of EZH2 inhibitor, DZNep and TRAIL displayed synergistically induced apoptosis in colon cancer cells (Benoit *et al.,* 2013).

In addition, TRAIL-resistant cells were generated by culture of RPMI 8226 and NCI-H929 by acute exposure to TRAIL, followed by selection of TRAIL-resistant cells. Our results showed that nuclear export inhibitor, and epigenetic modifiers may be a therapeutic option in combination with TRAIL and may increase TRAIL sensitivity in insensitive cells, but not in cells that have specifically been selected for acquired TRAIL-resistance. These results highlight that some TRAIL-insensitive cells are likely to be intrinsically apoptosis resistant, which may be overcome by TRAIL combined with senstisers. In contrast, when cells are selected specifically for TRAIL resistance, the mechanisms of apoptosis is likely very different in different tumours.

6.1.2 Effect of TRAIL and TRAIL Sensitizers in 3D Multiple Myeloma Cell Cultures

Although multiple myeloma is a hematological malignancy, it forms solid bone lesions and these are potentially more targeted using therapeutic agents than tumour in blood. In addition, solid tumours might respond differently. This study has shown for the first time that myeloma cell lines are able to proliferate in the alginate beads and form 3D spheroid structures. In the current work, MM cells were more sensitive to LMB, SAHA, GSK343, and BIX 01294 alone in 3D cell culture. In the 3D alginate model, all drugs synergistically induced apoptosis with TRAIL more potently than in suspension.

Consistent with these findings there is only one previous study that shows that EZH2 inhibitor, GSK126 inhibit the growth, induce apoptosis and cell cycle arrest in both 2D and 3D culture models in melanoma (Tiffen *et al.,* 2015). In contrast, results from the current study are inconsistents with in earlier observation which reported that culturing of multiple myeloma cells in 3D model system induced cell proliferation and reduced the sensitivity to myeloma therapeutic agents in comparison to cell cultured as traditional monolayer cells (Jakubikova *et al*., 2016; de la Puente *et al*., 2015). However, differential responces between anti-tumour agents are expected, especially where proliferation is required for drugs activity e.g. DNA damage agents in contrast to TRAIL. Growing of mesothelioma cell lines in multicellular spheroids contributes to acquire a chemo-resistance character to a variety of apoptotic induction agents, including TRAIL, histone deacetylase, ribotoxic stressors, and proteasome inhibitors compared to 2D cultures (Barbone *et al*., 2008). Culture of breast cancer cell lines in 3D culture models showed more TRAIL-resistance by reduced expression of death receptors DR4 and DR5 that initiate TRAIL-mediated apoptosis in comparison to cell cultured as traditional monolayer cells (Chandrasekaran *et al*., 2014). In contrast to the current studies, 3D culture of B and T cell lymphoma showed increased proliferation

potential and drug resistance to the chemotherapeutics and a new class of HDAC[i], Panobinostat (Tian *et al*., 2015).

This is the first time a study has been made of interaction between TRAIL and LMB, SAHA, GSK343, and BIX 01294 in 3D cell culture and compared with 2D cultures in any tumour types. Effective targeting of an anti-apoptotic Bcl-2 family member myeloid cell leukemia-1 (Mcl-1) in TRAIL resistant glioblastoma cells in previous work induced TRAIL sensitivity in both 2D and 3D culture (Murphy *et al*., 2014). Studies in small cell lung cancer cells reported that inhibition of the mitochondrial pyrimidine biosynthesis enzyme dihydroorotate dehydrogenase (DHODH) sensitizes small cell lung cancer cell line U1690 to TRAIL-mediated apoptosis both within cancer cells grown as monolayers 2D and in a 3D culture model accompanied by inhibited expression of apoptotic inhibitory molecules c-flip_L (He *et al.*, 2014). Recent work by Ciardiello *et al.,* (2016), showed that HDACi such as vorinostat when used in combined with anti-ErbB3 monoclonal antibody caused synergistic anti-cancer activity in non-small cell lung cancer in both 2D and 3D conditions (Ciardiello *et al*., 2016).

6.1.3   Potential Targets of TRAIL and Epigenetic Modifiers HDAC[i] and HMT[i] – Mediated Apoptosis

In response to HDAC[i] and HMTase[i], NCI-H929 cells showed a significant decrease in protein expression of anti-apoptotic proteins; XIAP, survivin, heat shock proteins, anti-oxidative protein paraoxonase-2 (PON2) and phosphorylated p53 isoforms following treatment with epigenetic modifiers for 24 h. Importantly; epigenetic treatment as well as TRAIL decreased expression of catalase in comparison with control cells. Apoptosis involves generation of reactive oxygen species and cell sensitivity is inversely related to cellular catalase activity (Wang *et al.*, 2006). Catalases protect cells against hydrogen peroxide (H_2O_2) stress by converted H_2O_2 into H_2O and O_2 (Zhao *et al*., 2005), H_2O_2 at high concentration is toxic, triggering programmed cell death (Martins and English.,

2014). Conversely, inhibition catalase by 3-amino-1, 2, 4-triazole enhance the incidence apoptosis cell death (Sancho *et al*., 2003). Recent unpuplished work from our lab confirms that decrease catalase activity with 3-amino-1, 2, 4-triazole enhances TRAIL responces, and that in NCI-H 929, SAHA decreased catalase gene expression. This new data validates the observation of decreased catalase via the proteome array and highlight catalase as a potential target of apoptotic senstizers. Furthermore, ROS are very low in quiesent cells, supporting data on PKH^{Hi} cells (Tang *et al*., 2010).

This study is considered as first work showed that TRAIL and TRAIL sensitizers down-regulate the expression of catalase in multiple myeloma cells and further *in vivo* investigation is require to performed and developing of catalase inhibitor may enhance anti-cancer activity of multiple myeloma therapeutic agents.

6.1.4 Isolation PKH26^{Hi} Quiescent Populations were Less Sensitive to TRAIL and TRAIL Sensitizers

In this study we were able to purify a minority of PKH-retained dye cells (PKH^{Hi}) by fluorescence-activated cell sorting (FACS) to TRAIL sensitive cell lines (RPMI 8226 and NCI-H929). Our results showed that the PKH26^{Hi} cell population exhibited less sensitivity to TRAIL, LMB, SAHA, BIX 01294, and GSK343 at doses known to kill most unselected cells compared to PKH26^{Lo} and unsorted parental populations in two investigated TRAIL-sensitive multiple myeloma cell lines NCI-H929 and RPMI 8226. Isolation of cancer initiating cells by PKH26 fluoresce tracking dye have been reported in number of cancers including breast cancer (Pece *et al*., 2010), colon cancer (O'Brien *et al*., 2012), ovarian cancer (Kusumbe and Bapat., 2009) and multiple myeloma (Chen *et al*., 2014). In addition, these cells displayed cancer stem cell features such as expression of stem cell markers, having self-renewing ability as well as resistant to chemotherapeutic agents (Kusumbe and Bapat., 2009; Pece *et al*., 2010; O'Brien *et al*., 2012; Chen *et al*., 2014)

These results are consistent with a previous study which found that the quiescent PKH26^{Hi} multiple myeloma cells (RPMI 8226 and NCI-H929) exhibited enriched stem-like properties by the ability of forming colonies in semi-solid medium as well as more resistant to anti-tumour agents including cyclophosphamide, bortezomib, vincristine, prednisone, and rituximab *in vitro* compared with PKH^{Lo} cell populations (Chen *et al*., 2014).

Most quiescent multiple myleoma populations could be either CD138^{+ve} and CD138^{-ve}. Those which were quiescent CD138^{-ve} cells survived *in vivo* (Chen *et al*., 2014). A previous study demonstrated that CD138^{-ve} sub-populations had significantly more clonogenic potential and expressed higher level of proliferation marker Ki67 than the CD138^{+ve} cells. This study proposed that these CD138^{-ve} sub-populations were multiple myeloma stem cells, and had the capability to replicate and consequently differentiate into malignant CD138^{+ve} plasma cells (Matsui *et al.,* 2004). Later, Matsui *et al.,* (2008) demonstrated that CD138^{+ve} multiple myeloma cells cannot undergo long-term proliferation but rather develop from clonogenic CD138^{ve} cells population (Matsui *et al.,* 2008). Other studies showed that CD138^{-ve} ALDH^{+ve} population showed more clonogenic expansion than CD138^{+ve} ALDH^{-ve} population and only CD138^{-ve} cells differentiated into CD138^{+ve} population (Chung and Chng*.,* 2013).

6.1.5   Future Directions

In order to examine the safety and efficiency of TRAIL alone and in combined with anti-tumour agents for possible human therapy, considerable in *vitro* and *in vivo* studies are required prior to any clinical intervention in humans.

The majority of anti-tumour agents used within this work are not currently used clinically for multiple myeloma. Therefore, it would be crucial to determine whether these drugs act synergistically with TRAIL this could possibly result in reducing the

treatment doses and decrease their side effect. Firstly, *in vivo* safety studies are required as nothing is known how these agents act in combination in live animals NEIs are toxic and poorly tolerated but newer agents better tolerated in mice (Mutka *at el*., 2009) and certainly no studies using NEI in combination with targetted anti-tumour agents, such as TRAIL.

6.1.6 Further Investigation on the Effect of TRAIL and Epigenetic Modifier Agents on Inhibition of Catalase

This study demonstrated that TRAIL and the epigenetic modifiers SAHA, BIX01294 and GSK343 decrease the level of catalase. The down-regulation of this protein is essential in order to inhibition of cellular growth and /or trigger apoptotic cell death. The sensitivity to anti-tumour agents on multiple myeloma cells is depend on cellular catalase activity and suppression of catalase by catalase inhibitor enhanced myeloma cell death (Wang *et al*., 2006). In addition, the level of oxidative stress parameters and enzyme activities give a preliminary idea of disease severity and evaluation of therapy response (Kuku *et al.,* 2005). Further *in vitro* study using a catalase inhibitor (3-amino-1,2,4-triazole) to enhanced therapeutic-mediated apoptosis in multiple myeloma cells, and repeating experiments but adding exogenous catalase are necessary in order to further elucidate the mechanisms by which these anti-tumour agents effect multiple myeloma cells and establish whether activities are dependent on catalase, althogh initial prelimiary studies from our laboratory are supportive of the notion that decrease catalase is a key mediator of TRAIL sensitization. Future crucial experiments will addrese whether catalase is not altered in quiesent cells, which is of particular relevance as ROS are very low in quiesent cells.

6.1.7 *ln vivo* Animal Studies

In order to confirm whether the results have the potential to be clinically useful, the effect of TRAIL alone or in combination with other chemotherapy in animal models

would require determining prior to clinical trails. Animal studies are crucial to establish whether anti-tumour agents are feasible options for human disease, and if so which are the most effective combination treatments. Previous work assessing the novel combination therapies of HDAC[i] and TRAIL in human multiple myeloma cell lines (*in vitro)* and preclinical screening using syngeneic transplanted Vk*MYC multiple myeloma (*in vivo)* showed that *in vitro* studies give some insight into activity of drug and synergistic effect of drug combination that kill myeloma cells, but, they do not always expect *in vivo* efficacy or toxicity. HDAC[i]/rhTRAIL-combination based strategies, established dose-limiting toxicities that prohibited long term treatment (Matthews *et al*., 2013).

Successive development and improvement in G9a inhibitors resulted in the discovery of more selective and potent inhibitors such as UNC0638 (Liu *et al*., 2013; Vedadi *et al.,* 2011). Unfortunately, these G9a inhibitors displayed poor pharmacokinetic properties that limited the further *in vivo* pre-clinical studies. However, the discovery of UNC0642 maintained excellent selectivity, high *in vitro* potency as well as displayed better *in vivo* pharmacokinetic properties making it appropriate target for experimental animal studies (Liu *et al*., 2013). Since G9a inhibitors are well tolerated in animal studies, combination of G9a inhibitors with TRAIL in *in vivo* studies is worthy of further investigation.

The effect of combination of LMB, epigenetic agents (BIX01294 or GSK343) with TRAIL on multiple myeloma therapy has not been investigated on multiple myeloma animal model. Therefore, testing of these drugs on pre-clinical model will be very crucial to determine non-toxic therapeutic dose as well as the maximum levels of these combination treatments that can be obtained. In particular, some death receptor agonists are known to induce liver toxicity (Lawrence *et al*., 2001) and any enhancement to off-target TRAIL responses may render the therapeutic window too small for therapeutic

benefit, however *in vivo* studies with initial dose escalation studies in healthy animals would be an initial experiment prior to any attempt to affect tumour burden.

6.2   Final Conclusions

For the first time this study clearly demonestrates that the NEI Leptomycin B, the G9a-inhibitor BIX 01294 and the EZH2-inhibitor GSK343 can enhance TRAIL-induced apoptosis and target TRAIL resistance in both suspension culture, and in a 3D cell culture as a model of solid disseminated multiple myeloma lesions and that toxicity seen was lower in non-tumour control cells. These anti-tumour agents stimulated apoptosis through extrinsic or intrinsic apoptosis pathways resulting in decrease XIAP, survivin, heat shock proteins, and decreased catalase expression. These results suggest that TRAIL in combination with TRAIL sensitizers LMB, SAHA, BIX01294 and GSK343 hold promise for MM treatment. Further *in vivo* studies are urgently required in order to develop these promising drugs as future therapy. However, studies on quiescent cells suggest that these treatments do not kill all cells. Current studies are aimed at investigating the relevance of PKH^{Hi} cells to relapse from therapy in long-term studies, both *in vitro* and *in vivo*, and the role of catalase in quiesent cells and the development of TRAIL resistance.

7. References

Abdulghani, J., Allen, J. E., Dicker, D. T., Liu, Y. Y., Goldenberg, D., Smith, C. D., Humphreys, R. & El-Deiry, W. S. 2013. Sorafenib sensitizes solid tumours to

Apo2L/TRAIL and Apo2L/TRAIL receptor agonist antibodies by the Jak2-Stat3-Mcl1 axis. PLoS One, **8**, e75414.

Adams, J. M. & Cory, S. 2002. Apoptosomes: engines for caspase activation. Current opinion in cell biology, **14**, 715-720.

Adomako, A., Calvo, V., Biran, N., Osman, K., Chari, A., Paton, J. C., Paton, A. W., Moore, K., Schewe, D. M. & Aguirre-Ghiso, J. A. 2015. Identification of markers that functionally define a quiescent multiple myeloma cell sub-population surviving bortezomib treatment. BMC cancer, **15**, 444.

Adrain, C. & Martin, S. J. 2001. The mitochondrial apoptosome: a killer unleashed by the cytochrome seas. Trends in biochemical sciences, **26**, 390-397.

Agarwal, P. & Jackson, S. P. 2016. G9a inhibition potentiates the anti-tumour activity of DNA double-strand break inducing agents by impairing DNA repair independent of p53 status. Cancer letters, **380**, 467-475.

Agarwal, P., Alzrigat, M., Parraga, A. A., Enroth, S., Singh, U., Ungerstedt, J., Osterborg, A., Brown, P. J., Ma, A., Jin, J., Nilsson, K., Oberg, F., Kalushkova, A. & Jernberg-Wiklund, H. 2016. Genome-wide profiling of histone H3 lysine 27 and lysine 4 trimethylation in multiple myeloma reveals the importance of Polycomb gene targeting and highlights EZH2 as a potential therapeutic target. Oncotarget, **7**, 6809-6823. doi: 10.18632/oncotarget.6843 [doi].

Aguirre-Ghiso, J. A. 2007. Models, mechanisms and clinical evidence for cancer dormancy. Nature Reviews Cancer, **7**, 834-846.

Alegre, M., Frauwirth, K. A. & Thompson, C. B. 2001. T-cell regulation by CD28 and CTLA-4. Nature Reviews Immunology, **1**, 220-228.

Al-Hajj, M., Wicha, M. S., Benito-Hernandez, A., Morrison, S. J. & Clarke, M. F. 2003. Prospective identification of tumourigenic breast cancer cells. Proceedings of the National Academy of Sciences of the United States of America, **100**, 3983-3988. doi: 10.1073/pnas.0530291100 [doi].

Alison, M. R., Lim, S. M. & Nicholson, L. J. 2011. Cancer stem cells: problems for therapy? The Journal of pathology, **223**, 148-162.

Alnemri, E. S., Livingston, D. J., Nicholson, D. W., Salvesen, G., Thornberry, N. A., Wong, W. W. & Yuan, J. 1996. Human ICE/CED-3 protease nomenclature. Cell, **87**, 171. doi: S0092-8674(00)81334-3 [pii].

Al-Yacoub, N., Fecker, L. F., Möbs, M., Plötz, M., Braun, F. K., Sterry, W. & Eberle, J. 2012. Apoptosis induction by SAHA in cutaneous T-cell lymphoma cells is related to downregulation of c-FLIP and enhanced TRAIL signaling. Journal of Investigative Dermatology, **132**, 2263-2274.

Alzrigat, M., Párraga, A. A., Agarwal, P., Zureigat, H., Österborg, A., Nahi, H., Ma, A., Jin, J., Nilsson, K. & Öberg, F. 2017. EZH2 inhibition in multiple myeloma

downquategulates myeloma associated oncogenes and upregulates microRNAs with potential tumour suppressor functions. OncoTarget, **8**, 10213-10224.

Amatangelo, M., Garipov, A., Li, H., Conejo-Garcia, J. R., Speicher, D. & Zhang, R. 2013. Three-dimensional culture sensitizes epithelial ovarian cancer cells to EZH2 methyltransferase inhibition. Cell Cycle, **12**, 2113-2119.

American Cancer Society. Last accessed March 2017 http://www.cancer.org.

Anderson, D. M., Maraskovsky, E., Billingsley, W. L., Dougall, W. C., Tometsko, M. E., Roux, E. R., Teepe, M. C., DuBose, R. F., Cosman, D. & Galibert, L. 1997. A homologue of the TNF receptor and its ligand enhance T-cell growth and dendritic-cell function. Nature, **390**, 175-179.

Aoki, Y., Feldman, G. M. & Tosato, G. 2003. Inhibition of STAT3 signaling induces apoptosis and decreases survivin expression in primary effusion lymphoma. Blood, **101**, 1535-1542. doi: 10.1182/blood-2002-07-2130 [doi].

Asangani, I. A., Ateeq, B., Cao, Q., Dodson, L., Pandhi, M., Kunju, L. P., Mehra, R., Lonigro, R. J., Siddiqui, J. & Palanisamy, N. 2013. Characterization of the EZH2-MMSET histone methyltransferase regulatory axis in cancer. Molecular cell, **49**, 80-93.

Ashkenazi, A. 2002. Targeting death and decoy receptors of the tumour-necrosis factor superfamily. Nature Reviews Cancer, **2**, 420-430.

Attal, M., Harousseau, J. L., Leyvraz, S., Doyen, C., Hulin, C., Benboubker, L., Yakoub Agha, I., Bourhis, J. H., Garderet, L., Pegourie, B., Dumontet, C., Renaud, M., Voillat, L., Berthou, C., Marit, G., Monconduit, M., Caillot, D., Grobois, B., Avet-Loiseau, H., Moreau, P., Facon, T. & Inter-Groupe Francophone du Myelome (IFM). 2006. Maintenance therapy with thalidomide improves survival in patients with multiple myeloma. Blood, **108**, 3289-3294. doi: blood-2006-05-022962 [pii].

Attal, M., Harousseau, J., Facon, T., Guilhot, F., Doyen, C., Fuzibet, J., Monconduit, M., Hulin, C., Caillot, D. & Bouabdallah, R. 2003. Single versus double autologous stem-cell transplantation for multiple myeloma. New England Journal of Medicine, **349**, 2495-2502.

Attal, M., Harousseau, J., Stoppa, A., Sotto, J., Fuzibet, J., Rossi, J., Casassus, P., Maisonneuve, H., Facon, T. & Ifrah, N. 1996. A prospective, randomized trial of autologous bone marrow transplantation and chemotherapy in multiple myeloma. New England Journal of Medicine, **335**, 91-97.

Bae, K., Su, Z., Frye, C., McClellan, S., Allan, R. W., Andrejewski, J. T., Kelley, V., Jorgensen, M., Steindler, D. A. & Vieweg, J. 2010. Expression of pluripotent stem cell reprogramming factors by prostate tumour initiating cells. The Journal of urology, **183**, 2045-2053.

Bai, J. & Cederbaum, A. I. 2000. Overexpression of catalase in the mitochondrial or cytosolic compartment increases sensitivity of HepG2 cells to tumour necrosis factor-alpha-induced apoptosis. The Journal of biological chemistry, **275**, 19241-19249. doi: 10.1074/jbc.M000438200 [doi].

Baker, M. 2011. Tissue models: a living system on a chip. Nature, **471**, 661-665.

Balaji, N., Devy, A. S., Sumathi, M., Vidyalakshmi, S., Kumar, G. S. & D'Silva, S. 2013. Annexin v-affinity assay-apoptosis detection system in granular cell ameloblastoma. Journal of International Oral Health, **5**, 25.

Balicki, D. 2007. Moving forward in human mammary stem cell biology and breast cancer prognostication using ALDH1. Cell Stem Cell, **1**, 485-487.

Balsas, P., López-Royuela, N., Galán-Malo, P., Anel, A., Marzo, I. & Naval, J. 2009. Cooperation between Apo2L/TRAIL and bortezomib in multiple myeloma apoptosis. Biochemical pharmacology, **77**, 804-812.

Bangert, A., Cristofanon, S., Eckhardt, I., Abhari, B. A., Kolodziej, S., Häcker, S., Vellanki, S. H. K., Lausen, J., Debatin, K. & Fulda, S. 2012. Histone deacetylase inhibitors sensitize glioblastoma cells to TRAIL-induced apoptosis by c-myc-mediated downregulation of cFLIP. Oncogene, **31**, 4677-4688.

Barbone, D., Yang, T. M., Morgan, J. R., Gaudino, G. & Broaddus, V. C. 2008. Mammalian target of rapamycin contributes to the acquired apoptotic resistance of human mesothelioma multicellular spheroids. The Journal of biological chemistry, **283**, 13021-13030. doi: 10.1074/jbc.M709698200 [doi].

Barker, N., van Es, J. H., Kuipers, J., Kujala, P., van den Born, M., Cozijnsen, M., Haegebarth, A., Korving, J., Begthel, H. & Peters, P. J. 2007. Identification of stem cells in small intestine and colon by marker gene Lgr5. Nature, **449**, 1003-1007.

Barlogie, B., Shaughnessy, J., Tricot, G., Jacobson, J., Zangari, M., Anaissie, E., Walker, R. & Crowley, J. 2004. Treatment of multiple myeloma. Blood, **103**, 20-32. doi: 10.1182/blood-2003-04-1045 [doi].

Basuroy, S., Bhattacharya, S., Tcheranova, D., Qu, Y., Regan, R. F., Leffler, C. W. & Parfenova, H. 2006. HO-2 provides endogenous protection against oxidative stress and apoptosis caused by TNF-alpha in cerebral vascular endothelial cells. American journal of physiology.Cell physiology, **291**, C897-908. doi: 00032.2006 [pii].

Baylin, S. B. & Ohm, J. E. 2006. Epigenetic gene silencing in cancer–a mechanism for early oncogenic pathway addiction? Nature Reviews Cancer, **6**, 107-116.

Benoit, Y. D., Laursen, K. B., Witherspoon, M. S., Lipkin, S. M. & Gudas, L. J. 2013. Inhibition of PRC2 histone methyltransferase activity increases TRAIL-mediated apoptosis sensitivity in human colon cancer cells. Journal of cellular physiology, **228**, 764-772.

Bergsagel, P. L. & Kuehl, W. M. 2001. Chromosome translocations in multiple myeloma. Oncogene, **20**, 5611.

Bernasconi, N. L., Traggiai, E. & Lanzavecchia, A. 2002. Maintenance of serological memory by polyclonal activation of human memory B cells. Science (New York, N.Y.), **298**, 2199-2202. doi: 10.1126/science.1076071 [doi].

Berube, C., Boucher, L. M., Ma, W., Wakeham, A., Salmena, L., Hakem, R., Yeh, W. C., Mak, T. W. & Benchimol, S. 2005. Apoptosis caused by p53-induced protein with death domain (PIDD) depends on the death adapter protein RAIDD. Proceedings of the National Academy of Sciences of the United States of America, **102**, 14314-14320. doi: 0506475102 [pii].

Bhatia, M., Wang, J. C., Kapp, U., Bonnet, D. & Dick, J. E. 1997. Purification of primitive human hematopoietic cells capable of repopulating immune-deficient mice. Proceedings of the National Academy of Sciences of the United States of America, **94**, 5320-5325.

Blade, J., Rosinol, L., Sureda, A., Ribera, J. M., Diaz-Mediavilla, J., Garcia-Larana, J., Mateos, M. V., Palomera, L., Fernandez-Calvo, J., Marti, J. M., Giraldo, P., Carbonell, F., Callis, M., Trujillo, J., Gardella, S., Moro, M. J., Barez, A., Soler, A., Font, L., Fontanillas, M., San Miguel, J. & Programa para el Estudio de la Terapeutica en Hemopatia Maligna (PETHEMA). 2005. High-dose therapy intensification compared with continued standard chemotherapy in multiple myeloma patients responding to the initial chemotherapy: long-term results from a prospective randomized trial from the Spanish cooperative group PETHEMA. Blood, **106**, 3755-3759. doi: 2005-03-1301 [pii].

Blasco, M. A. 2005. Telomeres and human disease: ageing, cancer and beyond. Nature Reviews Genetics, **6**, 611-622.

Bommert, K., Bargou, R. C. & Stühmer, T. 2006. Signalling and survival pathways in multiple myeloma. European journal of cancer, **42**, 1574-1580.

Bonaventure, J., Kadhom, N., Cohen-Solal, L., Ng, K., Bourguignon, J., Lasselin, C. & Freisinger, P. 1994. Reexpression of cartilage-specific genes by dedifferentiated human articular chondrocytes cultured in alginate beads. Experimental cell research, **212**, 97-104.

Booth, N. L., Sayers, T. J., Brooks, A. D., Thomas, C. L., Jacobsen, K., Goncharova, E. I., McMahon, J. B. & Henrich, C. J. 2009. A cell-based high-throughput screen to identify synergistic TRAIL sensitizers. Cancer immunology, immunotherapy, **58**, 1229-1244.

Borutaite, V. & Brown, G. C. 2001. Caspases are reversibly inactivated by hydrogen peroxide. FEBS letters, **500**, 114-118.

Bradner, J. E., West, N., Grachan, M. L., Greenberg, E. F., Haggarty, S. J., Warnow, T. & Mazitschek, R. 2010. Chemical phylogenetics of histone deacetylases. Nature chemical biology, **6**, 238-243.

Braun, F. K., Mathur, R., Sehgal, L., Wilkie-Grantham, R., Chandra, J., Berkova, Z. & Samaniego, F. 2015. Inhibition of methyltransferases accelerates degradation of cFLIP and sensitizes B-cell lymphoma cells to TRAIL-induced apoptosis. PloS one, **10**, e0117994.

Brito, J. L., Walker, B., Jenner, M., Dickens, N. J., Brown, N. J., Ross, F. M., Avramidou, A., Irving, J. A., Gonzalez, D., Davies, F. E. & Morgan, G. J. 2009. MMSET deregulation affects cell cycle progression and adhesion regulons in t(4;14) myeloma plasma cells. Haematologica, **94**, 78-86. doi: 10.3324/haematol.13426 [doi].

Brown, R., Fuchter, M., Curry, E., Green, I., Kandil, S., Cherblanc, F., Payne, L., Chapman-Rothe, N., Shamsaei, E. & Srimongkolpithak, N. 2014. 554 Dual EZH2 and EHMT2 histone methyltransferase inhibition increases biological efficacy in breast cancer cells. European journal of cancer, **50**, 179-180.

Brychtova, S., Fiuraskova, M., Hlobilková, A., Brychta, T. & Hirnak, J. 2007. Nestin expression in cutaneous melanomas and melanocytic nevi. Journal of cutaneous pathology, **34**, 370-375.

Burdett, E., Kasper, F. K., Mikos, A. G. & Ludwig, J. A. 2010. Engineering tumours: a tissue engineering perspective in cancer biology. Tissue Engineering Part B: Reviews, **16**, 351-359.

Burgess, A. J., Pavey, S., Warrener, R., Hunter, L. J., Piva, T. J., Musgrove, E. A., Saunders, N., Parsons, P. G. & Gabrielli, B. G. 2001. Up-regulation of p21(WAF1/CIP1) by histone deacetylase inhibitors reduces their cytotoxicity. Molecular pharmacology, **60**, 828-837.

Burgess, T. L., Qian, Y., Kaufman, S., Ring, B. D., Van, G., Capparelli, C., Kelley, M., Hsu, H., Boyle, W. J., Dunstan, C. R., Hu, S. & Lacey, D. L. 1999. The ligand for osteoprotegerin (OPGL) directly activates mature osteoclasts. The Journal of cell biology, **145**, 527-538.

Burkhart, D. L. & Sage, J. 2008. Cellular mechanisms of tumour suppression by the retinoblastoma gene. Nature Reviews Cancer, **8**, 671-682.

Buttke, T. M. & Sandstrom, P. A. 1994. Oxidative stress as a mediator of apoptosis. Immunology today, **15**, 7-10.

Calame, K. L. 2001. Plasma cells: finding new light at the end of B cell development. Nature immunology, **2**, 1103-1108.

Calimeri, T., Battista, E., Conforti, F., Neri, P., Di Martino, M., Rossi, M., Foresta, U., Piro, E., Ferrara, F. & Amorosi, A. 2011. A unique three-dimensional SCID-

polymeric scaffold (SCID-synth-hu) model for in vivo expansion of human primary multiple myeloma cells. Leukemia, **25**, 707-712.

Camidge, D., Herbst, R., Gordon, M., Eckhardt, S., Kurzroc, R., Durbin, B., Ing, J., Ling, J., Sager, J. & Mendelson, D. 2007. A phase I safety and pharmacokinetic study of apomab, a human DR5 agonist antibody, in patients with advanced cancer. Journal of Clinical Oncology, **25**, 3582-3582.

Campisi, J. 2000. Cancer, aging and cellular senescence. In vivo (Athens, Greece), **14**, 183-188.

Carnero, A. 2002. Targeting the cell cycle for cancer therapy. British journal of cancer, **87**, 129-133.

Cancer Research UK. Last accessed March 2017 http://www.cancerresearchuk.org.

Carraro, G., Albertin, G., Forneris, M. & Nussdorfer, G. G. 2005. Similar sequence-free amplification of human glyceraldehyde-3-phosphate dehydrogenase for real time RT-PCR applications. Molecular and cellular probes, **19**, 181-186.

Casciello, F., Windloch, K., Gannon, F. & Lee, J. S. 2015. Functional Role of G9a Histone Methyltransferase in Cancer. Frontiers in immunology, **6**, 487. doi: 10.3389/fimmu.2015.00487 [doi].

Cavo, M., Zamagni, E., Tosi, P., Tacchetti, P., Cellini, C., Cangini, D., de Vivo, A., Testoni, N., Nicci, C., Terragna, C., Grafone, T., Perrone, G., Ceccolini, M., Tura, S., Baccarani, M. & Bologna 2002 study. 2005. Superiority of thalidomide and dexamethasone over vincristine-doxorubicindexamethasone (VAD) as primary therapy in preparation for autologous transplantation for multiple myeloma. Blood, **106**, 35-39. doi: 2005-02-0522 [pii].

Cen, H., Mao, F., Aronchik, I, Fuentes, R. J. & Firestone, G. L. 2008. DEVD-NucView488: a novel class of enzyme substrates for real-time detection of caspase-3 activity in live cells. FASEB journal: official publication of the Federation of American Societies for Experimental Biology, **22**, 2243-2252. doi: 10.1096/fj.07-099234 [doi].

Chandrasekaran, S., Marshall, J. R., Messing, J. A., Hsu, J. & King, M. R. 2014. TRAIL-mediated apoptosis in breast cancer cells cultured as 3D spheroids. PloS one, **9**, e111487.

Chang, Y., Zhang, X., Horton, J. R., Upadhyay, A. K., Spannhoff, A., Liu, J., Snyder, J. P., Bedford, M. T. & Cheng, X. 2009. Structural basis for G9a-like protein lysine methyltransferase inhibition by BIX-01294. Nature structural & molecular biology, **16**, 312-317.

Chapman, M. A., Lawrence, M. S., Keats, J. J., Cibulskis, K., Sougnez, C., Schinzel, A. C., Harview, C. L., Brunet, J., Ahmann, G. J. & Adli, M. 2011. Initial genome sequencing and analysis of multiple myeloma. Nature, **471**, 467-472.

Chauhan, D., Uchiyama, H., Akbarali, Y., Urashima, M., Yamamoto, K., Libermann, T. A. & Anderson, K. C. 1996. Multiple myeloma cell adhesion-induced interleukin-6 expression in bone marrow stromal cells involves activation of NF-kappa B. Blood, **87**, 1104-1112.

Chen, H., Yan, Y., Davidson, T. L., Shinkai, Y. & Costa, M. 2006. Hypoxic stress induces dimethylated histone H3 lysine 9 through histone methyltransferase G9a in mammalian cells. Cancer research, **66**, 9009-9016. doi: 66/18/9009 [pii].

Chen, J. J., Chou, C. W., Chang, Y. F. & Chen, C. C. 2008. Proteasome inhibitors enhance TRAIL-induced apoptosis through the intronic regulation of DR5: involvement of NF-kappa B and reactive oxygen species-mediated p53 activation. Journal of immunology (Baltimore, Md.: 1950), **180**, 8030-8039. doi: 180/12/8030 [pii].

Chen, J., Li, Y., Yu, T., McKay, R. M., Burns, D. K., Kernie, S. G. & Parada, L. F. 2012. A restricted cell population propagates glioblastoma growth after chemotherapy. Nature, **488**, 522-526.

Chen, M. W., Hua, K. T., Kao, H. J., Chi, C. C., Wei, L. H., Johansson, G., Shiah, S. G., Chen, P. S., Jeng, Y. M., Cheng, T. Y., Lai, T. C., Chang, J. S., Jan, Y. H., Chien, M. H., Yang, C. J., Huang, M. S., Hsiao, M. & Kuo, M. L. 2010. H3K9 histone methyltransferase G9a promotes lung cancer invasion and metastasis by silencing the cell adhesion molecule Ep-CAM. Cancer research, **70**, 7830-7840. doi: 10.1158/0008-5472.CAN-10-0833 [doi].

Chen, Y., Kuo, C. W., Chueh, D. & Chen, P. 2016. Surface modified alginate microcapsules for 3D cell culture. Surface Science, **648**, 47-52.

Chen, Z., Orlowski, R. Z., Wang, M., Kwak, L. & McCarty, N. 2014. Osteoblastic niche supports the growth of quiescent multiple myeloma cells. Blood, **123**, 2204-2208. doi: 10.1182/blood-2013-07-517136 [doi].

Cheriyath, V., Glaser, K. B., Waring, J. F., Baz, R., Hussein, M. A. & Borden, E. C. 2007. G1P3, an IFN-induced survival factor, antagonizes TRAIL-induced apoptosis in human myeloma cells. The Journal of clinical investigation, **117**, 3107-3117. doi: 10.1172/JCI31122 [doi].

Chesi, M. & Bergsagel, P. L. 2013. Molecular pathogenesis of multiple myeloma: basic and clinical updates. International journal of hematology, **97**, 313-323.

Chiecchio, L., Dagrada, G. P., Ibrahim, A. H., Dachs Cabanas, E., Protheroe, R. K., Stockley, D. M., Orchard, K. H., Cross, N. C., Harrison, C. J., Ross, F. M. & UK Myeloma Forum. 2009. Timing of acquisition of deletion 13 in plasma cell dyscrasias is dependent on genetic context. Haematologica, **94**, 1708-1713. doi: 10.3324/haematol.2009.011064 [doi].

Child, J. A., Morgan, G. J., Davies, F. E., Owen, R. G., Bell, S. E., Hawkins, K., Brown, J., Drayson, M. T. & Selby, P. J. 2003. High-dose chemotherapy with

hematopoietic stem-cell rescue for multiple myeloma. New England Journal of Medicine, **348**, 1875-1883.

Chng, W., Huang, G., Chung, T., Ng, S., Gonzalez-Paz, N., Troska-Price, T., Mulligan, G., Chesi, M., Bergsagel, P. & Fonseca, R. 2011. Clinical and biological implications of MYC activation: a common difference between MGUS and newly diagnosed multiple myeloma. Leukemia, **25**, 1026-1035.

Cho, H., Kelly, J. D., Hayami, S., Toyokawa, G., Takawa, M., Yoshimatsu, M., Tsunoda, T., Field, H. I., Neal, D. E. & Ponder, B. A. 2011. Enhanced expression of EHMT2 is involved in the proliferation of cancer cells through negative regulation of SIAH1. Neoplasia, **13**, 676-IN10.

Chung, G. H. & Chng, W. J. 2013. Clonogenic multiple myeloma cells have shared stemness signature associated with patient survival.

Ciardiello, C., Roca, M. S., Noto, A., Bruzzese, F., Moccia, T., Vitagliano, C., Di Gennaro, E., Ciliberto, G., Roscilli, G., Aurisicchio, L., Marra, E., Mancini, R., Budillon, A. & Leone, A. 2016. Synergistic antitumour activity of histone deacetylase inhibitors and anti-ErbB3 antibody in NSCLC primary cultures via modulation of ErbB receptors expression. Oncotarget, **7**, 19559-19574. doi: 10.18632/oncotarget.7195 [doi].

Ciolli, S. 2012. Multiple myeloma Clinical Cases in Mineral and Bone Metabolism, **9**, 150-152.

Cojoc, M., Mäbert, K., Muders, M. H. & Dubrovska, A. 2015. A role for cancer stem cells in therapy resistance: cellular and molecular mechanisms. **31**, 16-27.

Collado, M. & Serrano, M. 2010. Senescence in tumours: evidence from mice and humans. Nature Reviews Cancer, **10**, 51-57.

Collado, M., Blasco, M. A. & Serrano, M. 2007. Cellular senescence in cancer and aging. Cell, **130**, 223-233.

Collins, A. T., Berry, P. A., Hyde, C., Stower, M. J. & Maitland, N. J. 2005. Prospective identification of tumourigenic prostate cancer stem cells. Cancer research, **65**, 10946-10951. doi: 65/23/10946 [pii].

Cook, A., Bono, F., Jinek, M. & Conti, E. 2007. Structural biology of nucleocytoplasmic transport. Annual Review of Biochemistry, **76**, 647-671.

Cook, L. & Macdonald, D. H. 2007. Management of paraproteinaemia. Postgraduate medical journal, **83**, 217-223. doi: 83/978/217 [pii].

Corbin, A. S., Agarwal, A., Loriaux, M., Cortes, J., Deininger, M. W. & Druker, B. J. 2011. Human chronic myeloid leukemia stem cells are insensitive to imatinib despite inhibition of BCR-ABL activity. The Journal of clinical investigation, **121**, 396-409. doi: 10.1172/JCI35721 [doi].

Corti, S., Locatelli, F., Papadimitriou, D., Donadoni, C., Salani, S., Del Bo, R., Strazzer, S., Bresolin, N. & Comi, G. P. 2006. Identification of a primitive brain–derived neural stem cell population based on aldehyde dehydrogenase activity. Stem cells, **24**, 975-985.

Coultas, L., Terzano, S., Thomas, T., Voss, A., Reid, K., Stanley, E. G., Scott, C. L., Bouillet, P., Bartlett, P., Ham, J., Adams, J. M. & Strasser, A. 2007. Hrk/DP5 contributes to the apoptosis of select neuronal populations but is dispensable for haematopoietic cell apoptosis. Journal of cell science, **120**, 2044-2052. doi: jcs.002063 [pii].

Creagh, E., Carmody, R. & Cotter, T. 2000. Heat shock protein 70 inhibits caspase-dependent and-independent apoptosis in Jurkat T cells. Experimental cell research, **257**, 58-66.

Croonquist, P. A. & Van Ness, B. 2005. The polycomb group protein enhancer of zeste homolog 2 (EZH2) is an oncogene that influences myeloma cell growth and the mutant ras phenotype. Oncogene, **24**, 6269-6280.

Cross, N., Waterman, E., Jokonya, N., Fowles, A., Buckle, C., Phillips, J., Holen, I., Hamdy, F. & Eaton, C. 2008. Phenotypic variations of TRAIL sensitivity in cloned populations of prostate cancer cells. Journal of cellular biochemistry, **104**, 1452-1464.

Cui, J., Sun, W., Hao, X., Wei, M., Su, X., Zhang, Y., Su, L. & Liu, X. 2015. EHMT2 inhibitor BIX-01294 induces apoptosis through PMAIP1-USP9X-MCL1 axis in human bladder cancer cells. Cancer cell international, **15**, 1.

Curry, E., Green, I., Chapman-Rothe, N., Shamsaei, E., Kandil, S., Cherblanc, F. L., Payne, L., Bell, E., Ganesh, T. & Srimongkolpithak, N. 2015. Dual EZH2 and EHMT2 histone methyltransferase inhibition increases biological efficacy in breast cancer cells. Clinical epigenetics, **7**, 84.

Dai, Y. & Grant, S. 2003. Cyclin-dependent kinase inhibitors. Current opinion in pharmacology, **3**, 362-370.

D'Amico, F., Skarmoutsou, E. & Stivala, F. 2009. State of the art in antigen retrieval for immunohistochemistry. Journal of immunological methods, **341**, 1-18.

Das, A., Wei, G., Parikh, K. & Liu, D. 2015. Selective inhibitors of nuclear export (SINE) in hematological malignancies. Experimental hematology & oncology, **4**, 7.

Davies, F. E., Rawstron, A. C., Owen, R. G. & Morgan, G. J. 2000. Controversies surrounding the clonogenic origin of multiple myeloma. British journal of haematology, **110**, 240-241.

de la Puente, P., Muz, B., Gilson, R. C., Azab, F., Luderer, M., King, J., Achilefu, S., Vij, R. & Azab, A. K. 2015. 3D tissue-engineered bone marrow as a novel model to study pathophysiology and drug resistance in multiple myeloma. Biomaterials, **73**, 70-84.

Dean, M. 2009. ABC transporters, drug resistance, and cancer stem cells. Journal of mammary gland biology and neoplasia, **14**, 3-9.

Deleu, S., Menu, E., Van Valckenborgh, E., Van Camp, B., Fraczek, J., Broek, I. V., Rogiers, V. & Vanderkerken, K. 2009. Histone deacetylase inhibitors in multiple myeloma. Hematology Reviews, **1**.

Deng, Y., Lin, Y. & Wu, X. 2002. TRAIL-induced apoptosis requires Bax-dependent mitochondrial release of Smac/DIABLO. Genes & development, **16**, 33-45. doi: 10.1101/gad.949602 [doi].

Desagher, S. & Martinou, J. 2000. Mitochondria as the central control point of apoptosis. Trends in cell biology, **10**, 369-377.

De Wilt, L., Kroon, J., Jansen, G., De Jong, S., Peters, G. & Kruyt, F. 2013. Bortezomib and TRAIL: a perfect match for apoptotic elimination of tumour cells? Critical reviews in oncology/hematology, **85**, 363-372.

di Luccio, E. 2015. Inhibition of Nuclear Receptor Binding SET Domain 2/Multiple Myeloma SET Domain by LEM-06 Implication for Epigenetic Cancer Therapies. Journal of cancer prevention, **20**, 113-120. doi: 10.15430/JCP.2015.20.2.113 [doi].

Ding, J., Li, T., Wang, X., Zhao, E., Choi, J., Yang, L., Zha, Y., Dong, Z., Huang, S. & Asara, J. M. 2013. The histone H3 methyltransferase G9A epigenetically activates the serine-glycine synthesis pathway to sustain cancer cell survival and proliferation. Cell metabolism, **18**, 896-907.

Doherty, R., Haywood-Small, S., Sisley, K. & Cross, N. 2011. Aldehyde dehydrogenase activity selects for the holoclone phenotype in prostate cancer cells. Biochemical and biophysical research communications, **414**, 801-807.

Doi, T., Murakami, H., Ohtsu, A., Fuse, N., Yoshino, T., Yamamoto, N., Boku, N., Onozawa, Y., Hsu, C. & Gorski, K. 2011. Phase 1 study of conatumumab, a pro-apoptotic death receptor 5 agonist antibody, in Japanese patients with advanced solid tumours. Cancer chemotherapy and pharmacology, **68**, 733-741.

Drewinko, B., Alexanian, R., Boyer, H., Barlogie, B. & Rubinow, S. I. 1981. The growth fraction of human myeloma cells. Blood, **57**, 333-338.

Droin, N., Guéry, L., Benikhlef, N. & Solary, E. 2013. Targeting apoptosis proteins in hematological malignancies. Cancer letters, **332**, 325-334.

Du, L., Wang, H., He, L., Zhang, J., Ni, B., Wang, X., Jin, H., Cahuzac, N., Mehrpour, M., Lu, Y. & Chen, Q. 2008. CD44 is of functional importance for colorectal cancer stem cells. Clinical cancer research: an official journal of the American Association for Cancer Research, **14**, 6751-6760. doi: 10.1158/1078-0432.CCR-08-1034 [doi].

Duiker, E., Mom, C., De Jong, S., Willemse, P., Gietema, J., van der Zee, A. & De Vries, E. 2006. The clinical trail of TRAIL. European journal of cancer, **42**, 2233-2240.

Dutta-Simmons, J., Zhang, Y., Gorgun, G., Gatt, M., Mani, M., Hideshima, T., Takada, K., Carlson, N. E., Carrasco, D. E., Tai, Y. T., Raje, N., Letai, A. G., Anderson, K. C. & Carrasco, D. R. 2009. Aurora kinase A is a target of Wnt/beta-catenin involved in multiple myeloma disease progression. Blood, **114**, 2699-2708. doi: 10.1182/blood-2008-12-194290 [doi].

Ehrenschwender, M., Knoll, G., Bittner, S., Kurz, M. & Jantsch, J. 2016. Hypoxia regulates TRAIL sensitivity of colorectal cancer cells through mitochondrial autophagy. Oncotarget, **2016**, 1-17.

Elmore, S. 2007. Apoptosis: a review of programmed cell death. Toxicologic pathology, **35**, 495-516. doi: 779478428 [pii].

Emery, J. G., McDonnell, P., Burke, M. B., Deen, K. C., Lyn, S., Silverman, C., Dul, E., Appelbaum, E. R., Eichman, C. & DiPrinzio, R. 1998. Osteoprotegerin is a receptor for the cytotoxic ligand TRAIL. Journal of Biological Chemistry, **273**, 14363-14367.

Emoto, K., Yamashita, S. & Okada, Y. 2005. Mechanisms of heat-induced antigen retrieval: does pH or ionic strength of the solution play a role for refolding antigens? The journal of histochemistry and cytochemistry: official journal of the Histochemistry Society, **53**, 1311-1321. doi: jhc.5C6627.2005 [pii].

Engels, I. H., Stepczynska, A., Stroh, C., Lauber, K., Berg, C., Schwenzer, R., Wajant, H., JaÈnicke, R. U., Porter, A. G. & Belka, C. 2000. Caspase-8/FLICE functions as an executioner caspase in anticancer drug-induced apoptosis. Oncogene, **19**, 4563.

Evens, A. M., Lecane, P., Magda, D., Prachand, S., Singhal, S., Nelson, J., Miller, R. A., Gartenhaus, R. B. & Gordon, L. I. 2005. Motexafin gadolinium generates reactive oxygen species and induces apoptosis in sensitive and highly resistant multiple myeloma cells. Blood, **105**, 1265-1273. doi: 10.1182/blood-2004-03-0964 [doi].

Ezponda, T., Popovic, R., Zheng, Y., Nabet, B., Will, C., Small, E. C., Occhionorelli, M., Tonon, G., Keats, J. J. & Kelleher, N. L. 2014. Loss of the histone demethylase UTX contributes to multiple myeloma and sensitizes cells to EZH2 inhibitors. Blood, **124**, 611-611.

Falschlehner, C., Emmerich, C. H., Gerlach, B. & Walczak, H. 2007. TRAIL signalling: decisions between life and death. The international journal of biochemistry & cell biology, **39**, 1462-1475.

Fan, C., Pan, Y., Yang, Y., Di, S., Jiang, S., Ma, Z., Li, T., Zhang, Z., Li, W. & Li, X. 2015. HDAC1 inhibition by melatonin leads to suppression of lung adenocarcinoma cells via induction of oxidative stress and activation of apoptotic pathways. Journal of pineal research, **59**, 321-333.

Fan, F., Vallet, S., Sattler, M., Tonon, G., Bashari, M. H., Bakiri, L., Goldschmidt, H., Wagner, E. F., Jaeger, D. & Podar, K. 2014. The AP-1 Transcription Factor JunB Promotes Multiple Myeloma (MM) Cell Proliferation, Survival and Drug Resistance in the Bone Marrow Microenvironment. Blood, **124**, 3446-3446.

Fan, J., Lei, P., Zheng, J., Wang, X., Li, S., Liu, H., He, Y., Wang, Z., Wei, G. & Zhang, X. 2015. The selective activation of p53 target genes regulated by SMYD2 in BIX-01294 induced autophagy-related cell death. PloS one, **10**, e0116782.

Fan, T., Jiang, S., Chung, N., Alikhan, A., Ni, C., Lee, C. C. & Hornyak, T. J. 2011. EZH2-dependent suppression of a cellular senescence phenotype in melanoma cells by inhibition of p21/CDKN1A expression. Molecular cancer research: MCR, **9**, 418-429. doi: 10.1158/1541-7786.MCR-10-0511 [doi].

Fan, Y., Liu, H., Yan, L., Luan, Y., Zhou, H., Yang, J., Yin, S. & Wang, Y. 2013. Optimized transformation of Streptomyces sp. ATCC 39366 producing leptomycin by electroporation. Journal of Microbiology, **51**, 318-322.

Fandy, T. E. & Srivastava, R. K. 2006. Trichostatin A sensitizes TRAIL-resistant myeloma cells by downregulation of the antiapoptotic Bcl-2 proteins. Cancer chemotherapy and pharmacology, **58**, 471-477.

Fandy, T. E., Shankar, S., Ross, D. D., Sausville, E. & Srivastava, R. K. 2005. Interactive effects of HDAC inhibitors and TRAIL on apoptosis are associated with changes in mitochondrial functions and expressions of cell cycle regulatory genes in multiple myeloma. Neoplasia, **7**, 646-657.

Felthaus, O., Ettl, T., Gosau, M., Driemel, O., Brockhoff, G., Reck, A., Zeitler, K., Hautmann, M., Reichert, T. & Schmalz, G. 2011. Cancer stem cell-like cells from a single cell of oral squamous carcinoma cell lines. Biochemical and biophysical research communications, **407**, 28-33.

Ferbeyre, G., de Stanchina, E., Lin, A. W., Querido, E., McCurrach, M. E., Hannon, G. J. & Lowe, S. W. 2002. Oncogenic ras and p53 cooperate to induce cellular senescence. Molecular and cellular biology, **22**, 3497-3508.

Fischbach, C., Chen, R., Matsumoto, T., Schmelzle, T., Brugge, J. S., Polverini, P. J. & Mooney, D. J. 2007. Engineering tumours with 3D scaffolds. Nature methods, **4**, 855-860.

Fischer, K. & Mackensen, A. 2003. The flow cytometric PKH-26 assay for the determination of T-cell mediated cytotoxic activity. Methods, **31**, 135-142.

Fischer, P. M. & Gianella-Borradori, A. 2003. CDK inhibitors in clinical development for the treatment of cancer. Expert opinion on investigational drugs, **12**, 955-970.

Fong, S., Debs, R. J. & Desprez, P. 2004. Id genes and proteins as promising targets in cancer therapy. Trends in molecular medicine, **10**, 387-392.

Fonseca, R., Debes-Marun, C. S., Picken, E. B., Dewald, G. W., Bryant, S. C., Winkler, J. M., Blood, E., Oken, M. M., Santana-Davila, R., Gonzalez-Paz, N., Kyle, R. A., Gertz, M. A., Dispenzieri, A., Lacy, M. Q. & Greipp, P. R. 2003. The recurrent IgH translocations are highly associated with nonhyperdiploid variant multiple myeloma. Blood, **102**, 2562-2567. doi: 10.1182/blood-2003-02-0493 [doi].

Fox, N. L., Humphreys, R., Luster, T. A., Klein, J. & Gallant, G. 2010. Tumour necrosis factor-related apoptosis-inducing ligand (TRAIL) receptor-1 and receptor-2 agonists for cancer therapy. Expert opinion on biological therapy, **10**, 1-18.

Franklin, T., Krueger-Naug, A., Clarke, D., Arrigo, A. & Currie, R. 2005. The role of heat shock proteins Hsp70 and Hsp27 in cellular protection of the central nervous system. International journal of hyperthermia, **21**, 379-392.

Friedrich, J., Ebner, R. & Kunz-Schughart, L. A. 2007. Experimental anti-tumour therapy in 3-D: spheroids–old hat or new challenge? International journal of radiation biology, **83**, 849-871.

Friedrich, J., Eder, W., Castaneda, J., Doss, M., Huber, E., Ebner, R. & Kunz-Schughart, L. A. 2007. A reliable tool to determine cell viability in complex 3-d culture: the acid phosphatase assay. Journal of biomolecular screening, **12**, 925-937. doi: 12/7/925 [pii].

Gabrea, A., Martelli, M. L., Qi, Y., Roschke, A., Barlogie, B., Shaughnessy, J. D., Sawyer, J. R. & Kuehl, W. M. 2008. Secondary genomic rearrangements involving immunoglobulin or MYC loci show similar prevalences in hyperdiploid and nonhyperdiploid myeloma tumours. Genes, Chromosomes and Cancer, **47**, 573-590.

Garapaty-Rao, S., Nasveschuk, C., Gagnon, A., Chan, E. Y., Sandy, P., Busby, J., Balasubramanian, S., Campbell, R., Zhao, F. & Bergeron, L. 2013. Identification of EZH2 and EZH1 small molecule inhibitors with selective impact on diffuse large B cell lymphoma cell growth. Chemistry & biology, **20**, 1329-1339.

Garrett, M. D. 2001. Cell cycle control and cancer. CURRENT SCIENCE-BANGALORE-, **81**, 515-522.

Garrido, C., Schmitt, E., Candé, C., Vahsen, N., Parcellier, A. & Kroemer, G. 2003. HSP27 and HSP70: potentially oncogenic apoptosis inhibitors. Cell cycle, **2**, 578-583.

Gazitt, Y. 1999. TRAIL is a potent inducer of apoptosis in myeloma cells derived from multiple myeloma patients and is not cytotoxic to hematopoietic stem cells. Leukemia, **13**, 1817-1824.

Gerke, V., Creutz, C. E. & Moss, S. E. 2005. Annexins: linking Ca2 signalling to membrane dynamics. Nature reviews Molecular cell biology, **6**, 449-461.

Ghosh, J. C., Dohi, T., Kang, B. H. & Altieri, D. C. 2008. Hsp60 regulation of tumour cell apoptosis. The Journal of biological chemistry, **283**, 5188-5194. doi: M705904200 [pii].

Gillenwater, A. M., Zhong, M. & Lotan, R. 2007. Histone deacetylase inhibitor suberoylanilide hydroxamic acid induces apoptosis through both mitochondrial and Fas (Cd95) signaling in head and neck squamous carcinoma cells. Molecular cancer therapeutics, **6**, 2967-2975. doi: 6/11/2967 [pii].

Ginestier, C., Hur, M. H., Charafe-Jauffret, E., Monville, F., Dutcher, J., Brown, M., Jacquemier, J., Viens, P., Kleer, C. G. & Liu, S. 2007. ALDH1 is a marker of normal and malignant human mammary stem cells and a predictor of poor clinical outcome. Cell stem cell, **1**, 555-567.

Gobbi, G., Masselli, E., Micheloni, C., Nouvenne, A., Russo, D., Santi, P., Matteucci, A., Cocco, L., Vitale, M. & Mirandola, P. 2010. Hypoxia-induced down-modulation of PKCε promotes TRAIL-mediated apoptosis of tumour cells. International journal of oncology, **37**, 719.

Golias, C., Charalabopoulos, A. & Charalabopoulos, K. 2004. Cell proliferation and cell cycle control: a mini review. International journal of clinical practice, **58**, 1134-1141.

Gooding, S. & Edwards, C. M. 2016. New approaches to targeting the bone marrow microenvironment in multiple myeloma. Current opinion in pharmacology, **28**, 43-49.

Gray-Schopfer, V., Wellbrock, C. & Marais, R. 2007. Melanoma biology and new targeted therapy. Nature, **445**, 851-857.

Green, D. R. & Reed, J. C. 1998. Mitochondria and apoptosis. Science, **281**, 1309.

Green, D. R. & Kroemer, G. 2009. Cytoplasmic functions of the tumour suppressor p53. Nature, **458**, 1127-1130.

Greve, B., Kelsch, R., Spaniol, K., Eich, H. T. & Götte, M. 2012. Flow cytometry in cancer stem cell analysis and separation. Cytometry Part A, **81**, 284-293.

Guo, A., Huang, Y., Ma, X. & Lin, R. 2016. Mechanism of G9a inhibitor BIX-01294 acting on U251 glioma cells. Molecular Medicine Reports, **14**, 4613-4621.

Guzmán-Ramírez, N., Völler, M., Wetterwald, A., Germann, M., Cross, N. A., Rentsch, C. A., Schalken, J., Thalmann, G. N. & Cecchini, M. G. 2009. In vitro propagation and characterization of neoplastic stem/progenitor-like cells from human prostate cancer tissue. The Prostate, **69**, 1683-1693.

Haase, D., Feuring-Buske, M., Konemann, S., Fonatsch, C., Troff, C., Verbeek, W., Pekrun, A., Hiddemann, W. & Wormann, B. 1995. Evidence for malignant transformation in acute myeloid leukemia at the level of early hematopoietic stem cells by cytogenetic analysis of CD34+ subpopulations. Blood, **86**, 2906-2912.

Hamburger, A. & Salmon, S. E. 1977. Primary bioassay of human myeloma stem cells. The Journal of clinical investigation, **60**, 846-854. doi: 10.1172/JCI108839 [doi].

Hampton, M. B. & Orrenius, S. 1997. Dual regulation of caspase activity by hydrogen peroxide: implications for apoptosis. FEBS letters, **414**, 552-556.

Hanahan, D. & Weinberg, R. A. 2011. Hallmarks of cancer: the next generation. Cell, **144**, 646-674.

Hardwick, J. M. & Soane, L. 2013. Multiple functions of BCL-2 family proteins. Cold Spring Harbor perspectives in biology, **5**, 10.1101/cshperspect.a008722. doi: 10.1101/cshperspect.a008722 [doi].

Harris, C. A. & Johnson, E. M. 2001. BH3-only Bcl-2 family members are coordinately regulated by the JNK pathway and require Bax to induce apoptosis in neurons. Journal of Biological Chemistry, **276**, 37754-37760.

Hart, A. H., Hartley, L., Parker, K., Ibrahim, M., Looijenga, L. H., Pauchnik, M., Chow, C. W. & Robb, L. 2005. The pluripotency homeobox gene NANOG is expressed in human germ cell tumours. Cancer, **104**, 2092-2098.

Hauselmann, H. J., Fernandes, R. J., Mok, S. S., Schmid, T. M., Block, J. A., Aydelotte, M. B., Kuettner, K. E. & Thonar, E. J. 1994. Phenotypic stability of bovine articular chondrocytes after long-term culture in alginate beads. Journal of cell science, **107 (Pt 1)**, 17-27.

Häuselmann, H., Aydelotte, M., Schumacher, B., Kuettner, K., Gitelis, S. & Thonar, E. 1992. Synthesis and turnover of proteoglycans by human and bovine adult articular chondrocytes cultured in alginate beads. Matrix, **12**, 116-129.

Haywood-Small. S: Welsby, N: Lewis, B: Page, D: Cross, N. (2011). Nuclear Export Inhibitors (NEIs) enhance Death Receptor 4/5-mediated apoptosis in Breast and Prostate cancer cells independently of p53. Poster presented @ Yorkshire Cancer Research Meeting, UK, June 2011.

He, T., Haapa-Paananen, S., Kaminskyy, V., Kohonen, P., Fey, V., Zhivotovsky, B., Kallioniemi, O. & Perälä, M. 2014. Inhibition of the mitochondrial pyrimidine biosynthesis enzyme dihydroorotate dehydrogenase by doxorubicin and brequinar sensitizes cancer cells to TRAIL-induced apoptosis. Oncogene, **33**, 3538-3549.

Hecht, F. 1987. On the origins of cancer genetics and cytogenetics. Cancer genetics and cytogenetics, **29**, 187-190.

Hehlgans, S., Eke, I., Storch, K., Haase, M., Baretton, G. B. & Cordes, N. 2009. Caveolin-1 mediated radioresistance of 3D grown pancreatic cancer cells. Radiotherapy and Oncology, **92**, 362-370.

Hehlgans, S., Lange, I., Eke, I. & Cordes, N. 2009. 3D cell cultures of human head and neck squamous cell carcinoma cells are radiosensitized by the focal adhesion kinase inhibitor TAE226. Radiotherapy and oncology, **92**, 371-378.

Henderson, C. & Brancolini, C. 2003. Apoptotic pathways activated by histone deacetylase inhibitors: implications for the drug-resistant phenotype. Drug resistance updates, **6**, 247-256.

Henrich, C. J., Thomas, C. L., Brooks, A. D., Booth, N. L., Lowery, E. M., Pompei, R. J., McMahon, J. B. & Sayers, T. J. 2012. Effects of cucurbitacins on cell morphology are associated with sensitization of renal carcinoma cells to TRAIL-induced apoptosis. Apoptosis, **17**, 79-89.

Heo, J. Y., Kim, H. J., Kim, S., Park, K., Park, S., Kim, S. W., Nam, D., Jang, H., Lee, S. & Ahn, K. S. 2011. Embelin suppresses STAT3 signaling, proliferation, and survival of multiple myeloma via the protein tyrosine phosphatase PTEN. Cancer letters, **308**, 71-80.

Herbst, R. S., Eckhardt, S. G., Kurzrock, R., Ebbinghaus, S., O'Dwyer, P. J., Gordon, M. S., Novotny, W., Goldwasser, M. A., Tohnya, T. M. & Lum, B. L. 2010. Phase I dose-escalation study of recombinant human Apo2L/TRAIL, a dual proapoptotic receptor agonist, in patients with advanced cancer. Journal of Clinical Oncology, **28**, 2839-2846.

Herbst, R., Mendolson, D., Ebbinghaus, S., Gordon, M., O'dwyer, P., Lieberman, G., Ing, J., Kurzrock, R., Novotny, W. & Eckhardt, G. 2006. A phase I safety and pharmacokinetic (PK) study of recombinant Apo2L/TRAIL, an apoptosis-inducing protein in patients with advanced cancer. Journal of Clinical Oncology, **24**, 3013-3013.

Hermann, P. C., Huber, S. L. & Heeschen, C. 2008. Metastatic cancer stem cells: a new target for anti-cancer therapy? Cell cycle, **7**, 188-193.

Hernando, H., Gelato, K. A., Lesche, R., Beckmann, G., Koehr, S., Otto, S., Steigemann, P. & Stresemann, C. 2016. EZH2 Inhibition Blocks Multiple Myeloma Cell Growth through Upregulation of Epithelial Tumour Suppressor Genes. Molecular cancer therapeutics, **15**, 287-298. doi: 10.1158/1535-7163.MCT-15-0486 [doi].

Hersey, P. & Zhang, X. D. 2001. How melanoma cells evade trail-induced apoptosis. Nature Reviews Cancer, **1**, 142-150.

Hervé, A., Florence, M., Philippe, M., Michel, A., Thierry, F., Kenneth, A., Jean-Luc, H., Nikhil, M. & Stéphane, M. 2011. Molecular heterogeneity of multiple myeloma: pathogenesis, prognosis, and therapeutic implications. Journal of Clinical Oncology, **29**, 1893-1897.

Hideshima, T. & Anderson, K. C. 2013. Histone deacetylase inhibitors in the treatment for multiple myeloma. International journal of hematology, **97**, 324-332.

Holen, I., Croucher, P. I., Hamdy, F. C. & Eaton, C. L. 2002. Osteoprotegerin (OPG) is a survival factor for human prostate cancer cells. Cancer research, **62**, 1619-1623.

Holen, I., Drury, N. L., Hargreaves, P. G. & Croucher, P. I. 2001. Evidence of a role for a non-matrix-type metalloproteinase activity in the shedding of syndecan-1 from human myeloma cells. British journal of haematology, **114**, 414-421.

Hotte, S., Hirte, H., Chen, E., Le, L., Corey, A., Maclean, M., Iacobucci, A., Fox, N. & Oza, A. 2005. HGS-ETR1, a fully human monoclonal antibody to the tumour necrosis factor-related apoptosis-inducing ligand death receptor 1 (TRAIL-R1) in patients with advanced solid cancer: results of a phase 1 trial. Journal of Clinical Oncology, **23**, 3052-3052.

Huang, E. H., Hynes, M. J., Zhang, T., Ginestier, C., Dontu, G., Appelman, H., Fields, J. Z., Wicha, M. S. & Boman, B. M. 2009. Aldehyde dehydrogenase 1 is a marker for normal and malignant human colonic stem cells (SC) and tracks SC overpopulation during colon tumourigenesis. Cancer research, **69**, 3382-3389. doi: 10.1158/0008-5472.CAN-08-4418 [doi].

Huang, J., Dorsey, J., Chuikov, S., Perez-Burgos, L., Zhang, X., Jenuwein, T., Reinberg, D. & Berger, S. L. 2010. G9a and Glp methylate lysine 373 in the tumour suppressor p53. The Journal of biological chemistry, **285**, 9636-9641. doi: 10.1074/jbc.M109.062588 [doi].

Huang, S., Law, P., Francis, K., Palsson, B. O. & Ho, A. D. 1999. Symmetry of initial cell divisions among primitive hematopoietic progenitors is independent of ontogenic age and regulatory molecules. Blood, **94**, 2595-2604.

Huang, X. & Guo, B. 2006. Adenomatous polyposis coli determines sensitivity to histone deacetylase inhibitor-induced apoptosis in colon cancer cells. Cancer research, **66**, 9245-9251. doi: 66/18/9245 [pii].

Huang, X., Wang, Y., Nan, X., He, S., Xu, X., Zhu, X., Tang, J., Yang, X., Yao, L. & Wang, X. 2014. The role of the orphan G protein-coupled receptor 37 (GPR37) in multiple myeloma cells. Leukemia research, **38**, 225-235.

Huang, Y. & Sheikh, M. S. 2007. TRAIL death receptors and cancer therapeutics. Toxicology and applied pharmacology, **224**, 284-289.

Huh, D., Hamilton, G. A. & Ingber, D. E. 2011. From 3D cell culture to organs-on-chips. Trends in cell biology, **21**, 745-754.

Hui, K. F., Leung, Y. Y., Yeung, P. L., Middeldorp, J. M. & Chiang, A. K. 2014. Combination of SAHA and bortezomib up-regulates CDKN2A and CDKN1A and induces apoptosis of Epstein-Barr virus-positive Wp-restricted Burkitt lymphoma and lymphoblastoid cell lines. British journal of haematology, **167**, 639-650.

Igney, F. H. & Krammer, P. H. 2002. Death and anti-death: tumour resistance to apoptosis. Nature Reviews Cancer, **2**, 277-288.

Ikeda, T., Nakata, Y., Kimura, F., Sato, K., Anderson, K., Motoyoshi, K., Sporn, M. & Kufe, D. 2004. Induction of redox imbalance and apoptosis in multiple myeloma

cells by the novel triterpenoid 2-cyano-3,12-dioxoolean-1,9-dien-28-oic acid. Molecular cancer therapeutics, **3**, 39-45.

Imaizumi, K., Tsuda, M., Imai, Y., Wanaka, A., Takagi, T. & Tohyama, M. 1997. Molecular cloning of a novel polypeptide, DP5, induced during programmed neuronal death. Journal of Biological Chemistry, **272**, 18842-18848.

Inohara, N., Ding, L., Chen, S. & Nunez, G. 1997. harakiri, a novel regulator of cell death, encodes a protein that activates apoptosis and interacts selectively with survival-promoting proteins Bcl-2 and Bcl-X(L). The EMBO journal, **16**, 1686-1694. doi: 10.1093/emboj/16.7.1686 [doi].

Iurlaro, R., Püschel, F., León-Annicchiarico, C. L., O'Connor, H., Martin, S. J., Palou-Gramón, D., Lucendo, E. & Muñoz-Pinedo, C. 2017. Glucose deprivation induces ATF4-mediated apoptosis through TRAIL death receptors. Molecular and cellular biology, MCB. 00479-16.

Ivanov, V. N., Ghandhi, S. A., Zhou, H., Huang, S. X., Chai, Y., Amundson, S. A. & Hei, T. K. 2011. Radiation response and regulation of apoptosis induced by a combination of TRAIL and CHX in cells lacking mitochondrial DNA: A role for NF-κB–STAT3-directed gene expression. Experimental cell research, **317**, 1548-1566.

J. Blade´ *, M. Teresa Cibeira, C. Ferna´ ndez de Larrea & L. Rosin˜ ol. 2010. Multiple myeloma Annals of Oncology 21 (Supplement 7): vii313–vii319, 2010, **21**.

Jagannathan-Bogdan, M. & Zon, L. I. 2013. Hematopoiesis. Development (Cambridge, England), **140**, 2463-2467. doi: 10.1242/dev.083147 [doi].

Jain, M., Nijhawan, A., Tyagi, A. K. & Khurana, J. P. 2006. Validation of housekeeping genes as internal control for studying gene expression in rice by quantitative real-time PCR. Biochemical and biophysical research communications, **345**, 646-651.

Jakubikova, J., Cholujova, D., Hideshima, T., Gronesova, P., Soltysova, A., Harada, T., Joo, J., Kong, S., Szalat, R. E. & Richardson, P. G. 2016. A novel 3D mesenchymal stem cell model of the multiple myeloma bone marrow niche: biologic and clinical applications. Oncotarget, **7**, 77326-77341.

Jang, B., Paik, J., Jeong, H., Oh, H., Park, J., Kwon, T. K., Song, D., Park, J., Kim, S. & Bae, J. 2004. Leptomycin B-induced apoptosis is mediated through caspase activation and down-regulation of Mcl-1 and XIAP expression, but not through the generation of ROS in U937 leukemia cells. Biochemical pharmacology, **68**, 263-274.

Jasek, E., Lis, G. J., Jasinska, M., Jurkowska, H. & Litwin, J. A. 2012. Effect of histone deacetylase inhibitors trichostatin A and valproic acid on etoposide-induced apoptosis in leukemia cells. Anticancer Research, **32**, 2791-2799. doi: 32/7/2791 [pii].

Jelinek, D. F. 2008. Myeloma research goes 3D. Blood, **112**, 2600-2601. doi: 10.1182/blood-2008-06-164178 [doi].

Jemal, A., Siegel, R., Ward, E., Hao, Y., Xu, J. & Thun, M. J. 2009. Cancer statistics, 2009. CA: a cancer journal for clinicians, **59**, 225-249.

Jeter, C. R., Liu, B., Liu, X., Chen, X., Liu, C., Calhoun-Davis, T., Repass, J., Zaehres, H., Shen, J. & Tang, D. G. 2011. NANOG promotes cancer stem cell characteristics and prostate cancer resistance to androgen deprivation. Oncogene, **30**, 3833-3845.

Jian, Y., Chen, Y., Geng, C., Liu, N., Yang, G., Liu, J., Li, X., Deng, H. & Chen, W. 2016. Target and resistance-related proteins of recombinant mutant human tumour necrosis factor-related apoptosis-inducing ligand on myeloma cell lines. Biomedical reports, **4**, 723-727.

Jiang, F., Qiu, Q., Khanna, A., Todd, N. W., Deepak, J., Xing, L., Wang, H., Liu, Z., Su, Y., Stass, S. A. & Katz, R. L. 2009. Aldehyde dehydrogenase 1 is a tumour stem cell-associated marker in lung cancer. Molecular cancer research : MCR, **7**, 330-338. doi: 10.1158/1541-7786.MCR-08-0393 [doi].

Johansson, C. B., Momma, S., Clarke, D. L., Risling, M., Lendahl, U. & Frisén, J. 1999. Identification of a neural stem cell in the adult mammalian central nervous system. Cell, **96**, 25-34.

Jones, D. C., Gunasekar, P. G., Borowitz, J. L. & Isom, G. E. 2000. Dopamine-Induced Apoptosis Is Mediated by Oxidative Stress and Is Enhanced by Cyanide in Differentiated PC12 Cells. Journal of neurochemistry, **74**, 2296-2304.

Jourdan, M., Reme, T., Goldschmidt, H., Fiol, G., Pantesco, V., De Vos, J., Rossi, J., Hose, D. & Klein, B. 2009. Gene expression of anti-and pro-apoptotic proteins in malignant and normal plasma cells. British journal of haematology, **145**, 45-58.

Justice, B. A., Badr, N. A. & Felder, R. A. 2009. 3D cell culture opens new dimensions in cell-based assays. Drug discovery today, **14**, 102-107.

Kagawa, K., Nakano, A., Miki, H., Oda, A., Amou, H., Takeuchi, K., Nakamura, S., Harada, T., Fujii, S. & Yata, K. 2012. Inhibition of TACE activity enhances the susceptibility of myeloma cells to TRAIL. PloS one, **7**, e31594.

Kalushkova, A., Fryknäs, M., Lemaire, M., Fristedt, C., Agarwal, P., Eriksson, M., Deleu, S., Atadja, P., Österborg, A. & Nilsson, K. 2010. Polycomb target genes are silenced in multiple myeloma. PloS one, **5**, e11483.

Kawano, M., Hirano, T., Matsuda, T., Taga, T., Horii, Y., Iwato, K., Asaoku, H., Tang, B., Tanabe, O. & Tanaka, H. 1988. Autocrine generation and requirement of BSF-2/IL-6 for human multiple myelomas. Nature, **332**, 83 - 85.

Kawano, Y., Fujiwara, S., Wada, N., Izaki, M., Yuki, H., Okuno, Y., Iyama, K., Yamasaki, H., Sakai, A. & Mitsuya, H. 2012. Multiple myeloma cells expressing low levels of CD138 have an immature phenotype and reduced sensitivity to lenalidomide. International journal of oncology, **41**, 876-884.

Khalid, H. 2016. PAD4 inhibitors: potential sensitizers of tumour cells to TRAIL-induced apoptosis. Bioscience Horizons, **9**, hzw003.

Kim, H., Kim, E. H., Eom, Y. W., Kim, W. H., Kwon, T. K., Lee, S. J. & Choi, K. S. 2006. Sulforaphane sensitizes tumour necrosis factor-related apoptosis-inducing ligand (TRAIL)-resistant hepatoma cells to TRAIL-induced apoptosis through reactive oxygen species-mediated up-regulation of DR5. Cancer research, **66**, 1740-1750. doi: 66/3/1740 [pii].

Kim, M., Turnquist, H., Jackson, J., Sgagias, M., Yan, Y., Gong, M., Dean, M., Sharp, J. G. & Cowan, K. 2002. The multidrug resistance transporter ABCG2 (breast cancer resistance protein 1) effluxes Hoechst 33342 and is overexpressed in hematopoietic stem cells. Clinical cancer research: an official journal of the American Association for Cancer Research, **8**, 22-28.

Kim, S. H., Kook, M. C., Shin, Y. K., Park, S. H. & Song, H. G. 2004. Evaluation of antigen retrieval buffer systems. Journal of molecular histology, **35**, 409-416.

Kim, Y., Kim, Y., Kim, D. E., Lee, J. S., Song, J. H., Kim, H., Cho, D., Jeong, S., Jin, D. & Jang, S. J. 2013. BIX-01294 induces autophagy-associated cell death via EHMT2/G9a dysfunction and intracellular reactive oxygen species production. Autophagy, **9**, 2126-2139.

Kimberley, F. C. & Screaton, G. R. 2004. Following a TRAIL: update on a ligand and its five receptors. Cell research, **14**, 359-372.

Kirshner, J., Thulien, K. J., Martin, L. D., Debes Marun, C., Reiman, T., Belch, A. R. & Pilarski, L. M. 2008. A unique three-dimensional model for evaluating the impact of therapy on multiple myeloma. Blood, **112**, 2935-2945. doi: 10.1182/blood-2008-02-142430 [doi].

Kleer, C. G., Cao, Q., Varambally, S., Shen, R., Ota, I., Tomlins, S. A., Ghosh, D., Sewalt, R. G., Otte, A. P., Hayes, D. F., Sabel, M. S., Livant, D., Weiss, S. J., Rubin, M. A. & Chinnaiyan, A. M. 2003. EZH2 is a marker of aggressive breast cancer and promotes neoplastic transformation of breast epithelial cells. Proceedings of the National Academy of Sciences of the United States of America, **100**, 11606-11611. doi: 10.1073/pnas.1933744100 [doi].

Kondo, M. 2010. Lymphoid and myeloid lineage commitment in multipotent hematopoietic progenitors. Immunological reviews, **238**, 37-46.

Kondo, Y., Shen, L., Ahmed, S., Boumber, Y., Sekido, Y., Haddad, B. R. & Issa, J. J. 2008. Downregulation of histone H3 lysine 9 methyltransferase G9a induces centrosome disruption and chromosome instability in cancer cells. PloS one, **3**, e2037.

Kondo, Y., Shen, L., Suzuki, S., Kurokawa, T., Masuko, K., Tanaka, Y., Kato, H., Mizuno, Y., Yokoe, M. & Sugauchi, F. 2007. Alterations of DNA methylation and histone modifications contribute to gene silencing in hepatocellular carcinomas. Hepatology Research, **37**, 974-983.

Krammer, P. H. 1998. CD95 (APO-1/Fas)-mediated apoptosis: live and let die. Advances in Immunology, **71**, 163-210.

Kruyt, F. A. 2008. TRAIL and cancer therapy. Cancer letters, **263**, 14-25.

Kubicek, S., O'Sullivan, R. J., August, E. M., Hickey, E. R., Zhang, Q., Teodoro, M. L., Rea, S., Mechtler, K., Kowalski, J. A. & Homon, C. A. 2007. Reversal of H3K9me2 by a small-molecule inhibitor for the G9a histone methyltransferase. Molecular cell, **25**, 473-481.

Kuehl, W. M. & Bergsagel, P. L. 2002. Multiple myeloma: evolving genetic events and host interactions. Nature Reviews Cancer, **2**, 175-187.

Kuehl, W. M. & Bergsagel, P. L. 2012. Molecular pathogenesis of multiple myeloma and its premalignant precursor. The Journal of clinical investigation, **122**, 3456-3463. doi: 10.1172/JCI61188 [doi].

Kuku, I., Aydogdu, I., Bayraktar, N., Kaya, E., Akyol, O. & Ali Erkurt, M. 2005. Oxidant/antioxidant parameters and their relationship with medical treatment in multiple myeloma. Cell biochemistry and function, **23**, 47-50.

Kumar, S., Fonseca, R., Ketterling, R. P., Dispenzieri, A., Lacy, M. Q., Gertz, M. A., Hayman, S. R., Buadi, F. K., Dingli, D., Knudson, R. A., Greenberg, A., Russell, S. J., Zeldenrust, S. R., Lust, J. A., Kyle, R. A., Bergsagel, L. & Rajkumar, S. V. 2012. Trisomies in multiple myeloma: impact on survival in patients with high-risk cytogenetics. Blood, **119**, 2100-2105. doi: 10.1182/blood-2011-11-390658 [doi].

Kusumbe, A. P. & Bapat, S. A. 2009. Cancer stem cells and aneuploid populations within developing tumours are the major determinants of tumour dormancy. Cancer research, **69**, 9245-9253. doi: 10.1158/0008-5472.CAN-09-2802 [doi].

Kyle, R. & Rajkumar, V. 2008. Multiple myeloma. Blood, **111**, (6), 2692-2972.

Kyrtsonis, M. C., Bartzis, V., Papanikolaou, X., Koulieris, E., Georgiou, G., Dimou, M., Tzenou, T. & Panayiotidis, P. 2010. Genetic and molecular mechanisms in multiple myeloma: a route to better understand disease pathogenesis and heterogeneity. The application of clinical genetics, **3**, 41-51.

Lacey, D., Timms, E., Tan, H., Kelley, M., Dunstan, C., Burgess, T., Elliott, R., Colombero, A., Elliott, G. & Scully, S. 1998. Osteoprotegerin ligand is a cytokine that regulates osteoclast differentiation and activation. Cell, **93**, 165-176.

Lagadec, C., Vlashi, E., Della Donna, L., Meng, Y., Dekmezian, C., Kim, K. & Pajonk, F. 2010. Survival and self-renewing capacity of breast cancer initiating cells during fractionated radiation treatment. Breast cancer research, **12**, 1.

Lange, A., Mills, R. E., Lange, C. J., Stewart, M., Devine, S. E. & Corbett, A. H. 2007. Classical nuclear localization signals: definition, function, and interaction with importin alpha. The Journal of biological chemistry, **282**, 5101-5105. doi: R600026200 [pii].

Lanzkron, S. M., Collector, M. I. & Sharkis, S. J. 1999. Hematopoietic stem cell tracking in vivo: a comparison of short-term and long-term repopulating cells. Blood, **93**, 1916-1921.

Lassus, P., Opitz-Araya, X. & Lazebnik, Y. 2002. Requirement for caspase-2 in stress-induced apoptosis before mitochondrial permeabilization. Science (New York, N.Y.), **297**, 1352-1354. doi: 10.1126/science.1074721 [doi].

Laubach, J., Richardson, P. & Anderson, K. 2011. Multiple Myeloma. Annual Review of Medicine, **62**, 249-264.

Lavrik, I. N., Golks, A. & Krammer, P. H. 2005. Caspases: pharmacological manipulation of cell death. The Journal of clinical investigation, **115**, 2665-2672. doi: 10.1172/JCI26252 [doi].

Lawrence, D., Shahrokh, Z., Marsters, S., Achilles, K., Shih, D., Mounho, B., Hillan, K., Totpal, K., DeForge, L. & Schow, P. 2001. Differential hepatocyte toxicity of recombinant Apo2L/TRAIL versions. Nature medicine, **7**, 383-385.

Lawson, M. A., McDonald, M. M., Kovacic, N., Khoo, W. H., Terry, R. L., Down, J., Kaplan, W., Paton-Hough, J., Fellows, C. & Pettitt, J. A. 2015. Osteoclasts control reactivation of dormant myeloma cells by remodelling the endosteal niche. Nature communications, **6**.

Le Maitre, C. L., Freemont, A. J. & Hoyland, J. A. 2005. The role of interleukin-1 in the pathogenesis of human intervertebral disc degeneration. Arthritis research & therapy, **7**, 1.

LeBlanc, H. & Ashkenazi, A. 2003. Apo2L/TRAIL and its death and decoy receptors. Cell Death & Differentiation, **10**, 66-75.

LeBlanc, H., Lawrence, D., Varfolomeev, E., Totpal, K., Morlan, J., Schow, P., Fong, S., Schwall, R., Sinicropi, D. & Ashkenazi, A. 2002. Tumour-cell resistance to death receptor–induced apoptosis through mutational inactivation of the proapoptotic Bcl-2 homolog Bax. Nature medicine, **8**, 274-281.

Lecane, P. S., Kiviharju, T. M., Sellers, R. G. & Peehl, D. M. 2003. Leptomycin B stabilizes and activates p53 in primary prostatic epithelial cells and induces apoptosis in the LNCaP cell line. The Prostate, **54**, 258-267.

Lee, C., Park, K., Kim, S. J., Kwon, O., Jeong, K. J., Kim, A. & Kim, Y. 2011. Generation of bivalent and bispecific kringle single domains by loop grafting as potent agonists against death receptors 4 and 5. Journal of Molecular Biology, **411**, 201-219.

Lee, J. Y., Kim, H. S., Kim, J. Y. & Sohn, J. 2009. Nuclear translocation of p21 WAF1/CIP1 protein prior to its cytosolic degradation by UV enhances DNA repair and survival. Biochemical and biophysical research communications, **390**, 1361-1366.

Lee, M., Park, S. C., Yang, Y. G., Yim, S. O., Chae, H. S., Bach, J., Lee, H. J., Kim, K. Y., Lee, W. B. & Kim, S. S. 2002. The involvement of reactive oxygen species

(ROS) and p38 mitogen-activated protein (MAP) kinase in TRAIL/Apo2L-induced apoptosis. FEBS letters, **512**, 313-318.

Lee, T., Um, H. J., Park, J., Choi, K. S. & Kwon, T. K. 2009. Withaferin A sensitizes TRAIL-induced apoptosis through reactive oxygen species-mediated up-regulation of death receptor 5 and down-regulation of c-FLIP. Free Radical Biology and Medicine, **46**, 1639-1649.

Lehnertz, B., Pabst, C., Su, L., Miller, M., Liu, F., Yi, L., Zhang, R., Krosl, J., Yung, E., Kirschner, J., Rosten, P., Underhill, T. M., Jin, J., Hebert, J., Sauvageau, G., Humphries, R. K. & Rossi, F. M. 2014. The methyltransferase G9a regulates HoxA9-dependent transcription in AML. Genes & development, **28**, 317-327. doi: 10.1101/gad.236794.113 [doi].

Lemancewicz, D., Bolkun, L., Jablonska, E., Kulczynska, A., Bolkun-Skornicka, U., Kloczko, J. & Dzieciol, J. 2013. Evaluation of TNF superfamily molecules in multiple myeloma patients: correlation with biological and clinical features. Leukemia research, **37**, 1089-1093.

Lemare, F., Steimberg, N., Le Griel, C., Demignot, S. & Adolphe, M. 1998. Dedifferentiated chondrocytes cultured in alginate beads: Restoration of the differentiated phenotype and of the metabolic responses to Interleukin-1β. Journal of cellular physiology, **176**, 303-313.

Leow, C. C., Gerondakis, S. & Spencer, A. 2013. MEK inhibitors as a chemotherapeutic intervention in multiple myeloma. Blood cancer journal, **3**, e105.

Leprêtre, C., Fleurier, Y., Martin, E. & Torriglia, A. 2008. Nuclear export of LEI/L-DNase II by Crm1 is essential for cell survival. Biochimica et Biophysica Acta (BBA)-Molecular Cell Research, **1783**, 1068-1075.

Li, H., Cai, Q., Godwin, A. K. & Zhang, R. 2010. Enhancer of zeste homolog 2 promotes the proliferation and invasion of epithelial ovarian cancer cells. Molecular cancer research: MCR, **8**, 1610-1618. doi: 10.1158/1541-7786.MCR-10-0398 [doi].

Li, H., Niederkorn, J. Y., Neelam, S. & Alizadeh, H. 2005. Resistance and susceptibility of human uveal melanoma cells to TRAIL-induced apoptosis. Archives of Ophthalmology, **123**, 654-661.

Li, J., Cao, B., Zhou, S., Zhu, J., Zhang, Z., Hou, T. & Mao, X. 2013. Cyproheptadine-induced myeloma cell apoptosis is associated with inhibition of the PI3K/AKT signaling. European journal of haematology, **91**, 514-521.

Li, K., Liu, C., Zhou, B., Bi, L., Huang, H., Lin, T. & Xu, K. 2013. Role of EZH2 in the growth of prostate cancer stem cells isolated from LNCaP cells. International journal of molecular sciences, **14**, 11981-11993.

Li, X., Lewis, M. T., Huang, J., Gutierrez, C., Osborne, C. K., Wu, M. F., Hilsenbeck, S. G., Pavlick, A., Zhang, X., Chamness, G. C., Wong, H., Rosen, J. &

Chang, J. C. 2008. Intrinsic resistance of tumourigenic breast cancer cells to chemotherapy. Journal of the National Cancer Institute, **100**, 672-679. doi: 10.1093/jnci/djn123 [doi].

Licht, J. D., Popovic, R., Min, D., Martinez-Garcia, E., Mrksch, M., Kelleher, N., Will, C. & Ezponda, T. 2011. Abstract PL05-02: MMSET: A pathogenic factor and therapeutic target in multiple Myeloma. **DOI:** 10.1158/1535-7163.TARG-11-PL05-02 Published November 2011.

Lin, T., Islam, O. & Heese, K. 2006. ABC transporters, neural stem cells and neurogenesis–a different perspective. Cell research, **16**, 857-871.

Lindenboim, L., Borner, C. & Stein, R. 2011. Nuclear proteins acting on mitochondria. Biochimica et Biophysica Acta (BBA)-Molecular Cell Research, **1813**, 584-596.

Ling, J., Herbst, R., Mendelson, D., Eckhardt, S., O'Dwyer, P., Ebbinghaus, S., Osborne, R., Cheu, M., Lieberman, G. & Lum, B. 2006. Apo2L/TRAIL pharmacokinetics in a phase 1a trial in advanced cancer and lymphoma. Journal of Clinical Oncology, **24**, 3047-3047.

Liu, C., Kelnar, K., Liu, B., Chen, X., Calhoun-Davis, T., Li, H., Patrawala, L., Yan, H., Jeter, C. & Honorio, S. 2011. The microRNA miR-34a inhibits prostate cancer stem cells and metastasis by directly repressing CD44. Nature medicine, **17**, 211-215.

Liu, F., Barsyte-Lovejoy, D., Li, F., Xiong, Y., Korboukh, V., Huang, X., Allali-Hassani, A., Janzen, W. P., Roth, B. L. & Frye, S. V. 2013. Discovery of an in vivo chemical probe of the lysine methyltransferases G9a and GLP. Journal of medicinal chemistry, **56**, 8931-8942.

Liu, T., Hong, Y., Tung, K. & Yang, P. 2016. In silico and experimental analyses predict the therapeutic value of an EZH2 inhibitor GSK343 against hepatocellular carcinoma through the induction of metallothionein genes. Oncoscience, **3**, 9.

Liu, C., Liu, Y., Xu, X., Wu, H., Xie, H., Chen, L., Lu, T., Yang, L., Guo, X. & Sun, G. 2015. Potential effect of matrix stiffness on the enrichment of tumour initiating cells under three-dimensional culture conditions. Experimental cell research, **330**, 123-134.

Liu, J., Ma, L., Li, C., Zhang, Z., Yang, G. & Zhang, W. 2013. Tumour-targeting TRAIL expression mediated by miRNA response elements suppressed growth of uveal melanoma cells. Molecular oncology, **7**, 1043-1055.

Locklin, R., Croucher, P., Russell, R. & Edwards, C. 2007. Agonists of TRAIL death receptors induce myeloma cell apoptosis that is not prevented by cells of the bone marrow microenvironment. Leukemia, **21**, 805-812.

Lode, L., Eveillard, M., Trichet, V., Soussi, T., Wuilleme, S., Richebourg, S., Magrangeas, F., Ifrah, N., Campion, L., Traulle, C., Guilhot, F., Caillot, D., Marit,

G., Mathiot, C., Facon, T., Attal, M., Harousseau, J. L., Moreau, P., Minvielle, S. & Avet-Loiseau, H. 2010. Mutations in TP53 are exclusively associated with del(17p) in multiple myeloma. Haematologica, **95**, 1973-1976. doi: 10.3324/haematol.2010.023697 [doi].

Looijenga, L. H., Stoop, H., de Leeuw, H. P., de Gouveia Brazao, C. A., Gillis, A. J., van Roozendaal, K. E., van Zoelen, E. J., Weber, R. F., Wolffenbuttel, K. P., van Dekken, H., Honecker, F., Bokemeyer, C., Perlman, E. J., Schneider, D. T., Kononen, J., Sauter, G. & Oosterhuis, J. W. 2003. POU5F1 (OCT3/4) identifies cells with pluripotent potential in human germ cell tumours. Cancer research, **63**, 2244-2250.

Lu, C., Han, H. D., Mangala, L. S., Ali-Fehmi, R., Newton, C. S., Ozbun, L., Armaiz-Pena, G. N., Hu, W., Stone, R. L. & Munkarah, A. 2010. Regulation of tumour angiogenesis by EZH2. Cancer cell, **18**, 185-197.

Lu, C., Shao, C., Cobos, E., Singh, K. P. & Gao, W. 2012. Chemotherapeutic sensitization of leptomycin B resistant lung cancer cells by pretreatment with doxorubicin. PloS one, **7**, e32895.

Lu, Z., Tian, Y., Salwen, H. R., Chlenski, A., Godley, L. A., Raj, J. U. & Yang, Q. 2013. Histone-lysine methyltransferase EHMT2 is involved in proliferation, apoptosis, cell invasion, and DNA methylation of human neuroblastoma cells. Anti-Cancer Drugs, **24**, 484-493. doi: 10.1097/CAD.0b013e32835ffdbb [doi].

Lund, A. H. & van Lohuizen, M. 2004. Epigenetics and cancer. Genes & development, **18**, 2315-2335. doi: 18/19/2315 [pii].

Lund, K., Adams, P. & Copland, M. 2014. EZH2 in normal and malignant hematopoiesis. Leukemia, **28**, 44-49.

Mahmood, Z. & Shukla, Y. 2010. Death receptors: targets for cancer therapy. Experimental cell research, **316**, 887-899.

Malumbres, M. & Barbacid, M. 2007. Cell cycle kinases in cancer. Current opinion in genetics & development, **17**, 60-65.

Mao, X., Cao, B., Wood, T. E., Hurren, R., Tong, J., Wang, X., Wang, W., Li, J., Jin, Y., Sun, W., Spagnuolo, P. A., MacLean, N., Moran, M. F., Datti, A., Wrana, J., Batey, R. A. & Schimmer, A. D. 2011. A small-molecule inhibitor of D-cyclin transactivation displays preclinical efficacy in myeloma and leukemia via phosphoinositide 3-kinase pathway. Blood, **117**, 1986-1997. doi: 10.1182/blood-2010-05-284810 [doi].

Marjanovic, N. D., Weinberg, R. A. & Chaffer, C. L. 2013. Cell plasticity and heterogeneity in cancer. Clinical chemistry, **59**, 168-179. doi: 10.1373/clinchem.2012.184655 [doi].

Marks, P. 2007. Discovery and development of SAHA as an anticancer agent. Oncogene, **26**, 1351-1356.

Martinez-Garcia, E., Popovic, R., Min, D. J., Sweet, S. M., Thomas, P. M., Zamdborg, L., Heffner, A., Will, C., Lamy, L., Staudt, L. M., Levens, D. L., Kelleher, N. L. & Licht, J. D. 2011. The MMSET histone methyl transferase switches global histone methylation and alters gene expression in t(4;14) multiple myeloma cells. Blood, **117**, 211-220. doi: 10.1182/blood-2010-07-298349 [doi].

Martinou, J. & Youle, R. J. 2011. Mitochondria in apoptosis: Bcl-2 family members and mitochondrial dynamics. Developmental cell, **21**, 92-101.

Martins, D. & English, A. M. 2014. Catalase activity is stimulated by H_2O_2 in rich culture medium and is required for H_2O_2 resistance and adaptation in yeast. Redox biology, **2**, 308-313.

Mateos, M., Ocio, E. M., Paiva, B., Rosiñol, L., Martínez-López, J., Bladé, J., Lahuerta, J., García-Sanz, R. & San Miguel, J. F. 2015. Treatment for patients with newly diagnosed multiple myeloma in 2015. Blood reviews, **29**, 387-403.

Matsui, W., Huff, C. A., Wang, Q., Malehorn, M. T., Barber, J., Tanhehco, Y., Smith, B. D., Civin, C. I. & Jones, R. J. 2004. Characterization of clonogenic multiple myeloma cells. Blood, **103**, 2332-2336. doi: 10.1182/blood-2003-09-3064 [doi].

Matsui, W., Wang, Q., Barber, J. P., Brennan, S., Smith, B. D., Borrello, I., McNiece, I., Lin, L., Ambinder, R. F., Peacock, C., Watkins, D. N., Huff, C. A. & Jones, R. J. 2008. Clonogenic multiple myeloma progenitors, stem cell properties, and drug resistance. Cancer research, **68**, 190-197. doi: 10.1158/0008-5472.CAN-07-3096 [doi].

Matsukawa, Y., Semba, S., Kato, H., Ito, A., Yanagihara, K. & Yokozaki, H. 2006. Expression of the enhancer of zeste homolog 2 is correlated with poor prognosis in human gastric cancer. Cancer science, **97**, 484-491.

Matsuo, Y. & Drexler, H. G. 1998. Establishment and characterization of human B cell precursor-leukemia cell lines. Leukemia research, **22**, 567-579.

Matthews, G., Lefebure, M., Doyle, M., Shortt, J., Ellul, J., Chesi, M., Banks, K., Vidacs, E., Faulkner, D. & Atadja, P. 2013. Preclinical screening of histone deacetylase inhibitors combined with ABT-737, rhTRAIL/MD5-1 or 5-azacytidine using syngeneic Vk* MYC multiple myeloma. Cell death & disease, **4**, e798.

McCabe, M. T., Ott, H. M., Ganji, G., Korenchuk, S., Thompson, C., Van Aller, G. S., Liu, Y., Graves, A. P., Diaz, E. & LaFrance, L. V. 2012. EZH2 inhibition as a therapeutic strategy for lymphoma with EZH2-activating mutations. Nature, **492**, 108-112.

Meacham, C. E. & Morrison, S. J. 2013. Tumour heterogeneity and cancer cell plasticity. Nature, **501**, 328-337.

Mellier, G. & Pervaiz, S. 2012. The three Rs along the TRAIL: resistance, re-sensitization and reactive oxygen species (ROS). Free radical research, **46**, 996-1003.

Menoret, E., Gomez-Bougie, P., Geffroy-Luseau, A., Daniels, S., Moreau, P., Le Gouill, S., Harousseau, J. L., Bataille, R., Amiot, M. & Pellat-Deceunynck, C. 2006. Mcl-1L cleavage is involved in TRAIL-R1- and TRAIL-R2-mediated apoptosis induced by HGS-ETR1 and HGS-ETR2 human mAbs in myeloma cells. Blood, **108**, 1346-1352. doi: blood-2005-12-007971 [pii].

Menu, E., Asosingh, K., Van Riet, I., Croucher, P., Van Camp, B. & Vanderkerken, K. 2004. Myeloma cells (5TMM) and their interactions with the marrow microenvironment. Blood Cells, Molecules, and Diseases, **33**, 111-119.

Miskolci, V., Ghosh, C. C., Rollins, J., Romero, C., Vu, H., Robinson, S., Davidson, D. & Vancurova, I. 2006. TNFα release from peripheral blood leukocytes depends on a CRM1-mediated nuclear export. Biochemical and biophysical research communications, **351**, 354-360.

Mitalipov, S. & Wolf, D. 2009. Totipotency, pluripotency and nuclear reprogramming. In: *Engineering of Stem Cells* (Ed. by Anonymous), pp. 185-199. Springer.

Mitsiades, C. S., Mitsiades, N. S., McMullan, C. J., Poulaki, V., Shringarpure, R., Hideshima, T., Akiyama, M., Chauhan, D., Munshi, N., Gu, X., Bailey, C., Joseph, M., Libermann, T. A., Richon, V. M., Marks, P. A. & Anderson, K. C. 2004. Transcriptional signature of histone deacetylase inhibition in multiple myeloma: biological and clinical implications. Proceedings of the National Academy of Sciences of the United States of America, **101**, 540-545. doi: 10.1073/pnas.2536759100 [doi].

Mitsiades, C. S., Treon, S. P., Mitsiades, N., Shima, Y., Richardson, P., Schlossman, R., Hideshima, T. & Anderson, K. C. 2001. TRAIL/Apo2L ligand selectively induces apoptosis and overcomes drug resistance in multiple myeloma: therapeutic applications. Blood, **98**, 795-804.

Mitsiades, N., Mitsiades, C. S., Poulaki, V., Anderson, K. C. & Treon, S. P. 2002. Intracellular regulation of tumour necrosis factor-related apoptosis-inducing ligand-induced apoptosis in human multiple myeloma cells. Blood, **99**, 2162-2171.

Mitsiades, N., Mitsiades, C. S., Richardson, P. G., McMullan, C., Poulaki, V., Fanourakis, G., Schlossman, R., Chauhan, D., Munshi, N. C., Hideshima, T., Richon, V. M., Marks, P. A. & Anderson, K. C. 2003. Molecular sequelae of histone deacetylase inhibition in human malignant B cells. Blood, **101**, 4055-4062. doi: 10.1182/blood-2002-11-3514 [doi].

Mitterer, M., Oduncu, F., Lanthaler, A., Drexler, E., Amaddii, G., Fabris, P., Emmerich, B., Coser, P. & Straka, C. 1999. The relationship between monoclonal myeloma precursor B cells in the peripheral blood stem cell harvests and the clinical response of multiple myeloma patients. British journal of haematology, **106**, 737-743.

Mohty, M. & Harousseau, J. L. 2014. Treatment of autologous stem cell transplant-eligible multiple myeloma patients: ten questions and answers. Haematologica, **99**, 408-416. doi: 10.3324/haematol.2013.096149 [doi].

Mueller-Klieser, W. 1997. Three-dimensional cell cultures: from molecular mechanisms to clinical applications. The American Journal of Physiology, **273**, C1109-23.

Munoz-Pinedo, C., Ruiz-Ruiz, C., Ruiz de Almodovar, C., Palacios, C. & Lopez-Rivas, A. 2003. Inhibition of glucose metabolism sensitizes tumour cells to death receptor-triggered apoptosis through enhancement of death-inducing signaling complex formation and apical procaspase-8 processing. The Journal of biological chemistry, **278**, 12759-12768. doi: 10.1074/jbc.M212392200 [doi].

Murphy, Á. C., Weyhenmeyer, B., Noonan, J., Kilbride, S. M., Schimansky, S., Loh, K. P., Kögel, D., Letai, A., Prehn, J. H. & Murphy, B. M. 2014. Modulation of Mcl-1 sensitizes glioblastoma to TRAIL-induced apoptosis. Apoptosis, **19**, 629-642.

Mutka, S. C., Yang, W. Q., Dong, S. D., Ward, S. L., Craig, D. A., Timmermans, P. B. & Murli, S. 2009. Identification of nuclear export inhibitors with potent anticancer activity in vivo. Cancer research, **69**, 510-517. doi: 10.1158/0008-5472.CAN-08-0858 [doi].

Nagaraj, N. S., Vigneswaran, N. & Zacharias, W. 2007. Hypoxia inhibits TRAIL-induced tumour cell apoptosis: involvement of lysosomal cathepsins. Apoptosis, **12**, 125-139.

Nakamura, M., Shimada, K. & Konishi, N. 2008. The role of HRK gene in human cancer. Oncogene, **27**, S105-S113.

Nakshatri, H. 2010. Radiation resistance in breast cancer: are CD44 /CD24-/proteosome low/PKH26 cells to blame? Breast Cancer Research, **12**, 1.

National Cancer institute. Last accessed March 2017 https://www.cancer.gov

Nebbioso, A., Carafa, V., Benedetti, R. & Altucci, L. 2012. Trials with 'epigenetic'drugs: an update. Molecular oncology, **6**, 657-682.

Neuzil, J., Swettenham, E. & Gellert, N. 2004. Sensitization of mesothelioma to TRAIL apoptosis by inhibition of histone deacetylase: role of Bcl-x L down-regulation. Biochemical and biophysical research communications, **314**, 186-191.

Niemeyer, P., Krause, U., Fellenberg, J., Kasten, P., Seckinger, A., Ho, A. D. & Simank, H. G. 2004. Evaluation of mineralized collagen and alpha-tricalcium phosphate as scaffolds for tissue engineering of bone using human mesenchymal stem cells. Cells, tissues, organs, **177**, 68-78. doi: 10.1159/000079182 [doi].

Niemoeller, O. M. & Belka, C. 2013. Radiotherapy and TRAIL for cancer therapy. Cancer letters, **332**, 184-193.

Nurse, P. 2000. A long twentieth century of the cell cycle and beyond. Cell, **100**, 71-78.

O'Brien, C. A., Kreso, A., Ryan, P., Hermans, K. G., Gibson, L., Wang, Y., Tsatsanis, A., Gallinger, S. & Dick, J. E. 2012. ID1 and ID3 regulate the self-renewal capacity of human colon cancer-initiating cells through p21. Cancer cell, **21**, 777-792.

Ogawa, H., Ishiguro, K., Gaubatz, S., Livingston, D. M. & Nakatani, Y. 2002. A complex with chromatin modifiers that occupies E2F- and Myc-responsive genes in G0 cells. Science (New York, N.Y.), **296**, 1132-1136. doi: 10.1126/science.1069861 [doi].

Okhrimenko, H., Lu, W., Xiang, C., Hamburger, N., Kazimirsky, G. & Brodie, C. 2005. Protein kinase C-epsilon regulates the apoptosis and survival of glioma cells. Cancer research, **65**, 7301-7309. doi: 65/16/7301 [pii].

Orkin, S. H. & Zon, L. I. 2008. Hematopoiesis: an evolving paradigm for stem cell biology. Cell, **132**, 631-644.

Palumbo, A. & Anderson, K. 2011. Multiple Myeloma. The New England Journal of Medicine, **364**, 1046-1060.

Pan, G., O'Rourke, K., Chinnaiyan, A. M., Gentz, R., Ebner, R., Ni, J. & Dixit, V. M. 1997. The receptor for the cytotoxic ligand TRAIL. Science (New York, N.Y.), **276**, 111-113.

Pan, Y., Xu, R., Peach, M., Huang, C., Branstetter, D., Durbin, B., Herbst, R., Eckhardt, G., Mendelson, D. & Holland, P. 2007. Application of pharmacodynamic assays in a phase Ia trial of Apo2L/TRAIL in patients with advanced tumours. Journal of Clinical Oncology, **25**, 3535-3535.

Paraoan, L., Gray, D., Hiscott, P., Ebrahimi, B., Damato, B. & Grierson, I. 2006. Expression of p53-induced apoptosis effector PERP in primary uveal melanomas: downregulation is associated with aggressive type. Experimental eye research, **83**, 911-919.

Passegue, E., Jamieson, C. H., Ailles, L. E. & Weissman, I. L. 2003. Normal and leukemic hematopoiesis: are leukemias a stem cell disorder or a reacquisition of stem cell characteristics? Proceedings of the National Academy of Sciences of the United States of America, **100 Suppl 1**, 11842-11849. doi: 10.1073/pnas.2034201100 [doi].

Paszekova, H., Kryukov, F., Kubiczkova, L., Hajek, R. & Sevcikova, S. 2014. High-risk multiple myeloma: different definitions, different outcomes? Clinical Lymphoma Myeloma and Leukemia, **14**, 24-30.

Patnaik, A., Wakelee, H., Mita, M., Fitzgerald, A., Hill, M., Fox, N., Howard, T., Ullrich, S., Tolcher, A. & Sikic, B. 2006. HGS-ETR2—A fully human monoclonal antibody to TRAIL-R2: results of a phase I trial in patients with advanced solid tumours. Journal of Clinical Oncology, **24**, 3012-3012.

Peacock, C. D., Wang, Q., Gesell, G. S., Corcoran-Schwartz, I. M., Jones, E., Kim, J., Devereux, W. L., Rhodes, J. T., Huff, C. A., Beachy, P. A., Watkins, D. N. & Matsui, W. 2007. Hedgehog signaling maintains a tumour stem cell compartment in

multiple myeloma. Proceedings of the National Academy of Sciences of the United States of America, **104**, 4048-4053. doi: 0611682104 [pii].

Pece, S., Tosoni, D., Confalonieri, S., Mazzarol, G., Vecchi, M., Ronzoni, S., Bernard, L., Viale, G., Pelicci, P. G. & Di Fiore, P. P. 2010. Biological and molecular heterogeneity of breast cancers correlates with their cancer stem cell content. Cell, **140**, 62-73.

Pei, X. Y., Dai, Y. & Grant, S. 2004. Synergistic induction of oxidative injury and apoptosis in human multiple myeloma cells by the proteasome inhibitor bortezomib and histone deacetylase inhibitors. Clinical cancer research : an official journal of the American Association for Cancer Research, **10**, 3839-3852. doi: 10.1158/1078-0432.CCR-03-0561 [doi].

Pennarun, B., Meijer, A., de Vries, E. G., Kleibeuker, J. H., Kruyt, F. & de Jong, S. 2010. Playing the DISC: turning on TRAIL death receptor-mediated apoptosis in cancer. Biochimica et Biophysica Acta (BBA)-Reviews on Cancer, **1805**, 123-140.

Perez, L. E., Parquet, N., Shain, K., Nimmanapalli, R., Alsina, M., Anasetti, C. & Dalton, W. 2008. Bone marrow stroma confers resistance to Apo2 ligand/TRAIL in multiple myeloma in part by regulating c-FLIP. Journal of immunology (Baltimore, Md.: 1950), **180**, 1545-1555. doi: 180/3/1545 [pii].

Perimenis, P., Galaris, A., Voulgari, A., Prassa, M. & Pintzas, A. 2016. IAP antagonists Birinapant and AT-406 efficiently synergise with either TRAIL, BRAF, or BCL-2 inhibitors to sensitise BRAFV600E colorectal tumour cells to apoptosis. BMC cancer, **16**, 624.

Peterson, C. L. & Laniel, M. 2004. Histones and histone modifications. Current Biology, **14**, R546-R551.

Petros, A. M., Olejniczak, E. T. & Fesik, S. W. 2004. Structural biology of the Bcl-2 family of proteins. Biochimica et Biophysica Acta (BBA)-Molecular Cell Research, **1644**, 83-94.

Philchenkov, A. 2012. Apoptosis-reactivating agents for targeted anticancer therapy. Biochemistry (Moscow) Supplement Series B: Biomedical Chemistry, **6**, 343-358.

Piazza, F., Manni, S. & Semenzato, G. 2013. Novel players in multiple myeloma pathogenesis: role of protein kinases CK2 and GSK3. Leukemia research, **37**, 221-227.

Plummer, R., Attard, G., Pacey, S., Li, L., Razak, A., Perrett, R., Barrett, M., Judson, I., Kaye, S., Fox, N. L., Halpern, W., Corey, A., Calvert, H. & de Bono, J. 2007. Phase 1 and pharmacokinetic study of lexatumumab in patients with advanced cancers. Clinical cancer research: an official journal of the American Association for Cancer Research, **13**, 6187-6194. doi: 13/20/6187 [pii].

Podar, K., Chauhan, D. & Anderson, K. 2009. Bone marrow microenvironment and the identification of new targets for myeloma therapy. Leukemia, **23**, 10-24.

Podberezin, M., Wen, J. & Chang, C. (. 2013. Cancer stem cells: a review of potential clinical applications. Archives of Pathology and Laboratory Medicine, **137**, 1111-1116.

Pons, D., de Vries, F. R., van den Elsen, P. J., Heijmans, B. T., Quax, P. H. & Jukema, J. W. 2009. Epigenetic histone acetylation modifiers in vascular remodelling: new targets for therapy in cardiovascular disease. European heart journal, **30**, 266-277. doi: 10.1093/eurheartj/ehn603 [doi].

Popovic, R., Martinez-Garcia, E., Giannopoulou, E. G., Zhang, Q., Zhang, Q., Ezponda, T., Shah, M. Y., Zheng, Y., Will, C. M. & Small, E. C. 2014. Histone methyltransferase MMSET/NSD2 alters EZH2 binding and reprograms the myeloma epigenome through global and focal changes in H3K36 and H3K27 methylation. PLoS Genet, **10**, e1004566.

Pore, M. M., Hiltermann, T. J. N. & Kruyt, F. A. 2013. Targeting apoptosis pathways in lung cancer. Cancer letters, **332**, 359-368.

Portt, L., Norman, G., Clapp, C., Greenwood, M. & Greenwood, M. T. 2011. Anti-apoptosis and cell survival: a review. Biochimica et Biophysica Acta (BBA)-Molecular Cell Research, **1813**, 238-259.

Pradelli, L., Beneteau, M., Chauvin, C., Jacquin, M., Marchetti, S., Munoz-Pinedo, C., Auberger, P., Pende, M. & Ricci, J. 2010. Glycolysis inhibition sensitizes tumour cells to death receptors-induced apoptosis by AMP kinase activation leading to Mcl-1 block in translation. Oncogene, **29**, 1641-1652.

Qiang, Y. W., Chen, Y., Stephens, O., Brown, N., Chen, B., Epstein, J., Barlogie, B. & Shaughnessy, J. D.,Jr. 2008. Myeloma-derived Dickkopf-1 disrupts Wnt-regulated osteoprotegerin and RANKL production by osteoblasts: a potential mechanism underlying osteolytic bone lesions in multiple myeloma. Blood, **112**, 196-207. doi: 10.1182/blood-2008-01-132134 [doi].

Qiang, Y., Endo, Y., Rubin, J. S. & Rudikoff, S. 2003. Wnt signaling in B-cell neoplasia. Oncogene, **22**, 1536-1545.

Queirolo, P. & Acquati, M. 2006. Targeted therapies in melanoma. Cancer treatment reviews, **32**, 524-531.

Quintana, E., Shackleton, M., Sabel, M. S., Fullen, D. R., Johnson, T. M. & Morrison, S. J. 2008. Efficient tumour formation by single human melanoma cells. Nature, **456**, 593-598.

Raab, M., Podar, K., Breitkreutz, I., Richardson, P. & Anderson, K. 2009. Multiple myeloma. Lancet, **374**, 324-339.

Rajkumar, S. V., Hayman, S. R., Lacy, M. Q., Dispenzieri, A., Geyer, S. M., Kabat, B., Zeldenrust, S. R., Kumar, S., Greipp, P. R., Fonseca, R., Lust, J. A., Russell, S. J., Kyle, R. A., Witzig, T. E. & Gertz, M. A. 2005. Combination therapy with

lenalidomide plus dexamethasone (Rev/Dex) for newly diagnosed myeloma. Blood, **106**, 4050-4053. doi: 2005-07-2817 [pii].

Rauh, J., Milan, F., Guenther, K. & Stiehler, M. 2011. Bioreactor systems for bone tissue engineering. Tissue Engineering Part B: Reviews, **17**, 263-280.

Reagan, M. R., Mishima, Y., Glavey, S. V., Zhang, Y., Manier, S., Lu, Z. N., Memarzadeh, M., Zhang, Y., Sacco, A., Aljawai, Y., Shi, J., Tai, Y. T., Ready, J. E., Kaplan, D. L., Roccaro, A. M. & Ghobrial, I. M. 2014. Investigating osteogenic differentiation in multiple myeloma using a novel 3D bone marrow niche model. Blood, **124**, 3250-3259. doi: 10.1182/blood-2014-02-558007 [doi].

Ren, A., Qiu, Y., Cui, H. & Fu, G. 2015. Inhibition of H3K9 methyltransferase G9a induces autophagy and apoptosis in oral squamous cell carcinoma. Biochemical and biophysical research communications, **459**, 10-17.

Reya, T., Morrison, S. J., Clarke, M. F. & Weissman, I. L. 2001. Stem cells, cancer, and cancer stem cells. Nature, **414**, 105-111.

Ricci-Vitiani, L., Lombardi, D. G., Pilozzi, E., Biffoni, M., Todaro, M., Peschle, C. & De Maria, R. 2007. Identification and expansion of human colon-cancer-initiating cells. Nature, **445**, 111-115.

Richardson, G. D., Robson, C. N., Lang, S. H., Neal, D. E., Maitland, N. J. & Collins, A. T. 2004. CD133, a novel marker for human prostatic epithelial stem cells. Journal of cell science, **117**, 3539-3545. doi: 10.1242/jcs.01222 [doi].

Rosato, R. R., Almenara, J. A., Dai, Y. & Grant, S. 2003. Simultaneous activation of the intrinsic and extrinsic pathways by histone deacetylase (HDAC) inhibitors and tumour necrosis factor-related apoptosis-inducing ligand (TRAIL) synergistically induces mitochondrial damage and apoptosis in human leukemia cells. Molecular cancer therapeutics, **2**, 1273-1284.

Ruan, J., Trotter, T. N., Nan, L., Luo, R., Javed, A., Sanderson, R. D., Suva, L. J. & Yang, Y. 2013. Heparanase inhibits osteoblastogenesis and shifts bone marrow progenitor cell fate in myeloma bone disease. Bone, **57**, 10-17.

Sachs, L. 1996. The control of hematopoiesis and leukemia: from basic biology to the clinic. Proceedings of the National Academy of Sciences of the United States of America, **93**, 4742-4749.

Safa, A. R. 2012. c-FLIP, a master anti-apoptotic regulator. Experimental oncology, **34**, 176-184. doi: 3429 [pii].

Salameh, H. J., Ahmad, A. & Kochar, T. 2013. A rare case of renal recovery in a young patient with multiple myeloma. Case reports in nephrology, **2013**, 531205. doi: 10.1155/2013/531205 [doi].

Sancho, P., Troyano, A., Fernandez, C., De Blas, E. & Aller, P. 2003. Differential effects of catalase on apoptosis induction in human promonocytic cells. Relationships with heat-shock protein expression. Molecular pharmacology, **63**, 581-589.

Santagata, S., Ligon, K. L. & Hornick, J. L. 2007. Embryonic stem cell transcription factor signatures in the diagnosis of primary and metastatic germ cell tumours. The American Journal of Surgical Pathology, **31**, 836-845. doi: 10.1097/PAS.0b013e31802e708a [doi].

Sanz, C., Benito, A., Inohara, N., Ekhterae, D., Nunez, G. & Fernandez-Luna, J. L. 2000. Specific and rapid induction of the proapoptotic protein Hrk after growth factor withdrawal in hematopoietic progenitor cells. Blood, **95**, 2742-2747.

Savickiene, J., Treigyte, G., Stirblyte, I., Valiuliene, G. & Navakauskiene, R. 2014. Euchromatic histone methyltransferase 2 inhibitor, BIX-01294, sensitizes human promyelocytic leukemia HL-60 and NB4 cells to growth inhibition and differentiation. Leukemia research, **38**, 822-829.

Sayers, T. & Cross, N. 2014. Triggering death receptors as a means of inducing tumouricial activity. Chapter 8. In:Tumour Immunology and Immunotherapy. Oxford University press, ISBN-13: 9780199676866

Sayers, T. J. & Murphy, W. J. 2006. Combining proteasome inhibition with TNF-related apoptosis-inducing ligand (Apo2L/TRAIL) for cancer therapy. Cancer Immunology, Immunotherapy, **55**, 76-84.

Schwartz, G. K. & Shah, M. A. 2005. Targeting the cell cycle: a new approach to cancer therapy. Journal of clinical oncology: official journal of the American Society of Clinical Oncology, **23**, 9408-9421. doi: 23/36/9408 [pii].

Shankar, S. & Srivastava, R. K. 2004. Enhancement of therapeutic potential of TRAIL by cancer chemotherapy and irradiation: mechanisms and clinical implications. Drug Resistance Updates, **7**, 139-156.

Shankar, S. R., Bahirvani, A. G., Rao, V. K., Bharathy, N., Ow, J. R. & Taneja, R. 2013. G9a, a multipotent regulator of gene expression. Epigenetics, **8**, 16-22.

Shao, C., Lu, C., Chen, L., Koty, P. P., Cobos, E. & Gao, W. 2011. p53-Dependent anticancer effects of leptomycin B on lung adenocarcinoma. Cancer chemotherapy and pharmacology, **67**, 1369-1380.

Shipman, C. M. & Croucher, P. I. 2003. Osteoprotegerin is a soluble decoy receptor for tumour necrosis factor-related apoptosis-inducing ligand/Apo2 ligand and can function as a paracrine survival factor for human myeloma cells. Cancer research, **63**, 912-916.

Siegel, R. L., Miller, K. D. & Jemal, A. 2016. Cancer statistics, 2016. CA: a cancer journal for clinicians, **66**, 7-30.

Siegelin, M., Gaiser, T. & Siegelin, Y. 2009. The XIAP inhibitor Embelin enhances TRAIL-mediated apoptosis in malignant glioma cells by down-regulation of the short isoform of FLIP. Neurochemistry international, **55**, 423-430.

Signore, M., Ricci-Vitiani, L. & De Maria, R. 2013. Targeting apoptosis pathways in cancer stem cells. Cancer letters, **332**, 374-382.

Simonet, W., Lacey, D., Dunstan, C., Kelley, M., Chang, M., Lüthy, R., Nguyen, H., Wooden, S., Bennett, L. & Boone, T. 1997. Osteoprotegerin: a novel secreted protein involved in the regulation of bone density. Cell, **89**, 309-319.

Singh, A. D. & Topham, A. 2003. Incidence of uveal melanoma in the United States: 1973–1997. Ophthalmology, **110**, 956-961.

Skommer, J., Darzynkiewicz, Z. & Wlodkowic, D. 2010. Cell death goes LIVE: technological advances in real-time tracking of cell death. Cell Cycle, **9**, 2330-2341.

Smith, G. S., Voyer-Grant, J. A. & Harauz, G. 2012. Monitoring cleaved caspase-3 activity and apoptosis of immortalized oligodendroglial cells using live-cell imaging and cleaveable fluorogenic-dye substrates following potassium-induced membrane depolarization. JoVE (Journal of Visualized Experiments), , e3422-e3422.

Smolewski, P. & Robak, T. 2011. Inhibitors of apoptosis proteins (IAPs) as potential molecular targets for therapy of hematological malignancies. Current Molecular Medicine, **11**, 633-649.

Sophonnithiprasert, T., Nilwarangkoon, S., Nakamura, Y. & Watanapokasin, R. 2015. Goniothalamin enhances TRAIL-induced apoptosis in colorectal cancer cells through DR5 upregulation and cFLIP downregulation. International journal of oncology, **47**, 2188-2196.

Southam, C. M. & Brunschwig, A. 1961. Quantitative studies of autotransplantation of human cancer. Preliminary report. Cancer, **14**, 971-978.

Stuckey, D. W. & Shah, K. 2013. TRAIL on trial: preclinical advances in cancer therapy. Trends in molecular medicine, **19**, 685-694.

Suliman, A., Lam, A., Datta, R. & Srivastava, R. K. 2001. Intracellular mechanisms of TRAIL: apoptosis through mitochondrial-dependent and-independent pathways. Oncogene, **20**, 2122.

Tait, J. F. & Gibson, D. 1992. Phospholipid binding of annexin V: effects of calcium and membrane phosphatidylserine content. Archives of Biochemistry and Biophysics, **298**, 187-191.

Tan, B. T., Park, C. Y., Ailles, L. E. & Weissman, I. L. 2006. The cancer stem cell hypothesis: a work in progress. Laboratory Investigation, **86**, 1203-1207.

Tang, Y., Hamburger, A. W., Wang, L., Khan, M. A. & Hussain, A. 2010. Androgen deprivation and stem cell markers in prostate cancers. Int J Clin Exp Pathol, **3**, 128-138.

Teo, H. E. & Peh, W. C. 2004. Primary bone tumours of adulthood. Cancer imaging : the official publication of the International Cancer Imaging Society, **4**, 74-83. doi: 10.1102/1470-7330.2004.0004 [doi].

Testa, U. 2010. TRAIL/TRAIL-R in hematologic malignancies. Journal of cellular biochemistry, **110**, 21-34.

Tian, Y. F., Ahn, H., Schneider, R. S., Yang, S. N., Roman-Gonzalez, L., Melnick, A. M., Cerchietti, L. & Singh, A. 2015. Integrin-specific hydrogels as adaptable tumour organoids for malignant B and T cells. Biomaterials, **73**, 110-119.

Tiffen, J. C., Gunatilake, D., Gallagher, S. J., Gowrishankar, K., Heinemann, A., Cullinane, C., Dutton-Regester, K., Pupo, G. M., Strbenac, D., Yang, J. Y., Madore, J., Mann, G. J., Hayward, N. K., McArthur, G. A., Filipp, F. V. & Hersey, P. 2015. Targeting activating mutations of EZH2 leads to potent cell growth inhibition in human melanoma by derepression of tumour suppressor genes. Oncotarget, **6**, 27023-27036. doi: 10.18632/oncotarget.4809 [doi].

True, L. D. 2008. Quality control in molecular immunohistochemistry. Histochemistry and cell biology, **130**, 473-480.

Tung, Y., Hsiao, A. Y., Allen, S. G., Torisawa, Y., Ho, M. & Takayama, S. 2011. High-throughput 3D spheroid culture and drug testing using a 384 hanging drop array. Analyst, **136**, 473-478.

Turner, J. G., Dawson, J. & Sullivan, D. M. 2012. Nuclear export of proteins and drug resistance in cancer. Biochemical pharmacology, **83**, 1021-1032.

Turner, J. G., Dawson, J. L., Grant, S., Shain, K. H., Dalton, W. S., Dai, Y., Meads, M., Baz, R., Kauffman, M. & Shacham, S. 2016. Treatment of acquired drug resistance in multiple myeloma by combination therapy with XPO1 and topoisomerase II inhibitors. Journal of Hematology & Oncology, **9**, 73.

Turner, J. G., Dawson, J., Cubitt, C. L., Baz, R. & Sullivan, D. M. 2014. Inhibition of CRM1-dependent nuclear export sensitizes malignant cells to cytotoxic and targeted agents. **27**, 62-73.

Uchida, N., Buck, D. W., He, D., Reitsma, M. J., Masek, M., Phan, T. V., Tsukamoto, A. S., Gage, F. H. & Weissman, I. L. 2000. Direct isolation of human central nervous system stem cells. Proceedings of the National Academy of Sciences of the United States of America, **97**, 14720-14725. doi: 10.1073/pnas.97.26.14720 [doi].

Uphoff, C. C. & Drexler, H. G. 2005. Eradication of mycoplasma contaminations. Basic Cell Culture Protocols, 25-34.

Urashima, M., Chen, B. P., Chen, S., Pinkus, G. S., Bronson, R. T., Dedera, D. A., Hoshi, Y., Teoh, G., Ogata, A., Treon, S. P., Chauhan, D. & Anderson, K. C. 1997. The development of a model for the homing of multiple myeloma cells to human bone marrow. Blood, **90**, 754-765.

Valentin-Opran, A., Charhon, S. A., Meunier, P. J., Edouard, C. M. & Arlot, M. E. 1982. Quantitative histology of myeloma-induced bone changes. British journal of haematology, **52**, 601-610.

Van Aller, G. S., Pappalardi, M. B., Ott, H. M., Diaz, E., Brandt, M., Schwartz, B. J., Miller, W. H., Dhanak, D., McCabe, M. T. & Verma, S. K. 2013. Long residence time inhibition of EZH2 in activated polycomb repressive complex 2. ACS chemical biology, **9**, 622-629.

van den Hoogen, C., van der Horst, G., Cheung, H., Buijs, J. T., Lippitt, J. M., Guzman-Ramirez, N., Hamdy, F. C., Eaton, C. L., Thalmann, G. N., Cecchini, M. G., Pelger, R. C. & van der Pluijm, G. 2010. High aldehyde dehydrogenase activity identifies tumour-initiating and metastasis-initiating cells in human prostate cancer. Cancer research, **70**, 5163-5173. doi: 10.1158/0008-5472.CAN-09-3806 [doi].

Varambally, S., Dhanasekaran, S. M., Zhou, M., Barrette, T. R., Kumar-Sinha, C., Sanda, M. G., Ghosh, D., Pienta, K. J., Sewalt, R. G. & Otte, A. P. 2002. The polycomb group protein EZH2 is involved in progression of prostate cancer. Nature, **419**, 624-629.

Varier, R. A. & Timmers, H. M. 2011. Histone lysine methylation and demethylation pathways in cancer. Biochimica et Biophysica Acta (BBA)-Reviews on Cancer, **1815**, 75-89.

Vedadi, M., Barsyte-Lovejoy, D., Liu, F., Rival-Gervier, S., Allali-Hassani, A., Labrie, V., Wigle, T. J., DiMaggio, P. A., Wasney, G. A. & Siarheyeva, A. 2011. A chemical probe selectively inhibits G9a and GLP methyltransferase activity in cells. Nature chemical biology, **7**, 566-574.

Verma, S. K., Tian, X., LaFrance, L. V., Duquenne, C., Suarez, D. P., Newlander, K. A., Romeril, S. P., Burgess, J. L., Grant, S. W. & Brackley, J. A. 2012. Identification of potent, selective, cell-active inhibitors of the histone lysine methyltransferase EZH2. ACS medicinal chemistry letters, **3**, 1091-1096.

Vermeulen, K., Van Bockstaele, D. R. & Berneman, Z. N. 2003. The cell cycle: a review of regulation, deregulation and therapeutic targets in cancer. Cell proliferation, **36**, 131-149.

Vitovski, S., Chantry, A. D., Lawson, M. A. & Croucher, P. I. 2012. Targeting tumour-initiating cells with TRAIL based combination therapy ensures complete and lasting eradication of multiple myeloma tumours in vivo. PloS one, **7**, e35830.

Volokhov, D. V., Graham, L. J., Brorson, K. A. & Chizhikov, V. E. 2011. Mycoplasma testing of cell substrates and biologics: review of alternative non-microbiological techniques. Molecular and cellular probes, **25**, 69-77.

von Pawel, J., Harvey, J. H., Spigel, D. R., Dediu, M., Reck, M., Cebotaru, C. L., Humphreys, R. C., Gribbin, M. J., Fox, N. L. & Camidge, D. R. 2014. Phase II Trial of Mapatumumab, a Fully Human Agonist Monoclonal Antibody to Tumour Necrosis Factor-Related Apoptosis-Inducing Ligand Receptor 1 (TRAIL-R1), in Combination With Paclitaxel and Carboplatin in Patients With Advanced Non–Small-Cell Lung Cancer. Clinical lung cancer, **15**, 188-196. e2.

Wagstaff, K. M. & Jans, D. A. 2009. Nuclear drug delivery to target tumour cells. European journal of pharmacology, **625**, 174-180.

Wang, G. G., Cai, L., Pasillas, M. P. & Kamps, M. P. 2007. NUP98–NSD1 links H3K36 methylation to Hox-A gene activation and leukaemogenesis. Nature cell biology, **9**, 804-812.

Wang, J. C. & Dick, J. E. 2005. Cancer stem cells: lessons from leukemia. Trends in cell biology, **15**, 494-501.

Wang, J., Zhu, Y., Ma, H., Chen, S., Chao, J., Ruan, W., Wang, D., Du, F. & Meng, Y. 2016. Developing multi-cellular tumour spheroid model (MCTS) in the chitosan/collagen/alginate (CCA) fibrous scaffold for anticancer drug screening. Materials Science and Engineering: C, **62**, 215-225.

Wang, N., Docherty, F., Brown, H. K., Reeves, K., Fowles, A., Lawson, M., Ottewell, P. D., Holen, I., Croucher, P. I. & Eaton, C. L. 2015. Mitotic quiescence, but not unique "stemness," marks the phenotype of bone metastasis-initiating cells in prostate cancer. FASEB journal: official publication of the Federation of American Societies for Experimental Biology, **29**, 3141-3150. doi: 10.1096/fj.14-266379 [doi].

Wang, W., Adachi, M., Kawamura, R., Sakamoto, H., Hayashi, T., Ishida, T., Imai, K. & Shinomura, Y. 2006. Parthenolide-induced apoptosis in multiple myeloma cells involves reactive oxygen species generation and cell sensitivity depends on catalase activity. Apoptosis, **11**, 2225-2235.

Wang, W., Zhao, J., Wang, H., Sun, Y., Peng, Z., Zhou, G., Fan, L., Wang, X., Yang, S. & Wang, R. 2010. Programmed cell death 4 (PDCD4) mediates the sensitivity of gastric cancer cells to TRAIL-induced apoptosis by down-regulation of FLIP expression. Experimental cell research, **316**, 2456-2464.

Wang, Y., Xiang, W., Wang, M., Huang, T., Xiao, X., Wang, L., Tao, D., Dong, L., Zeng, F. & Jiang, G. 2014. Methyl jasmonate sensitizes human bladder cancer cells to gambogic acid-induced apoptosis through down-regulation of EZH2 expression by miR-101. British journal of pharmacology, **171**, 618-635.

Wang, Z., Oron, E., Nelson, B., Razis, S. & Ivanova, N. 2012. Distinct lineage specification roles for NANOG, OCT4, and SOX2 in human embryonic stem cells. Cell stem cell, **10**, 440-454.

Wicha, M. S., Liu, S. & Dontu, G. 2006. Cancer stem cells: an old idea--a paradigm shift. Cancer research, **66**, 1883-90; discussion 1895-6. doi: 66/4/1883 [pii].

Wolf, B. B. & Green, D. R. 1999. Suicidal tendencies: apoptotic cell death by caspase family proteinases. The Journal of biological chemistry, **274**, 20049-20052.

Woo, J. H., Kim, Y. H., Choi, Y. J., Kim, D. G., Lee, K. S., Bae, J. H., Min, D. S., Chang, J. S., Jeong, Y. J., Lee, Y. H., Park, J. W. & Kwon, T. K. 2003. Molecular mechanisms of curcumin-induced cytotoxicity: induction of apoptosis through generation of reactive oxygen species, down-regulation of Bcl-XL and IAP, the release of cytochrome c and inhibition of Akt. Carcinogenesis, **24**, 1199-1208. doi: 10.1093/carcin/bgg082 [doi].

Wood, A. & Shilatifard, A. 2004. Posttranslational modifications of histones by methylation. Advances in Protein Chemistry, **67**, 201-222.

Wu, G. S. 2009. TRAIL as a target in anti-cancer therapy. Cancer letters, **285**, 1-5.

Wu, X., Yang, N., Zhou, W. H., Xu, J., Chen, J. J., Zheng, F. M., Long, Z. J., Yue, C. F., Ai, K. X., Liu, L. L., Wan, X. Y. & Liu, Q. 2014. Up-regulation of P21 inhibits TRAIL-mediated extrinsic apoptosis, contributing resistance to SAHA in acute myeloid leukemia cells. Cellular physiology and biochemistry : international journal of experimental cellular physiology, biochemistry, and pharmacology, **34**, 506-518. doi: 10.1159/000363018 [doi].

Wu, Y., Giaisi, M., Köhler, R., Chen, W., Krammer, P. H. & Li-Weber, M. 2016. Rocaglamide breaks TRAIL-resistance in human multiple myeloma and acute T-cell leukemia in vivo in a mouse xenogtraft model. Cancer letters, **389**, 70–77.

Xiao, M., Yang, S., Chen, J., Ning, X., Guo, L., Huang, K. & Sui, L. 2013. Overexpression of MMSET in endometrial cancer: a clinicopathologic study. Journal of surgical oncology, **107**, 428-432.

Xie, Z., Bi, C., Cheong, L. L., Liu, S. C., Huang, G., Zhou, J., Yu, Q., Chen, C. & Chng, W. J. 2011. Determinants of sensitivity to DZNep induced apoptosis in multiple myeloma cells. PloS one, **6**, e21583.

Xiong, X., Zhang, J., Liang, W., Cao, W., Qin, S., Dai, L., Ye, D. & Liu, Z. 2016. Fuse-binding protein 1 is a target of the EZH2 inhibitor GSK343, in osteosarcoma cells. International journal of oncology, **49**, 623-628.

Xu, X., Liu, C., Liu, Y., Li, N., Guo, X., Wang, S., Sun, G., Wang, W. & Ma, X. 2013. Encapsulated human hepatocellular carcinoma cells by alginate gel beads as an in vitro metastasis model. Experimental cell research, **319**, 2135-2144.

Xu, X., Liu, C., Liu, Y., Yang, L., Li, N., Guo, X., Sun, G. & Ma, X. 2014. Enrichment of cancer stem cell-like cells by culture in alginate gel beads. Journal of Biotechnology, **177**, 1-12.

Xue, G., Ren, Z., Grabham, P. W., Chen, Y., Zhu, J., Du, Y., Pan, D., Li, X. & Hu, B. 2015. Reprogramming mediated radio-resistance of 3D-grown cancer cells. Journal of radiation research, **56**, 656-662. doi: 10.1093/jrr/rrv018 [doi].

Yamada, H., Tada-Oikawa, S., Uchida, A. & Kawanishi, S. 1999. TRAIL causes cleavage of bid by caspase-8 and loss of mitochondrial membrane potential resulting in apoptosis in BJAB cells. Biochemical and biophysical research communications, **265**, 130-133.

Yamaguchi, H. & Hung, M. C. 2014. Regulation and Role of EZH2 in Cancer. Cancer research and treatment: official journal of Korean Cancer Association, **46**, 209-222. doi: 10.4143/crt.2014.46.3.209 [doi].

Yang, C., Jin, K., Tong, Y. & Cho, W. C. 2015. Therapeutic potential of cancer stem cells. Medical Oncology, **32**, 1-10.

Yang, H., Du, X. & Xi, Y. 2016. Effects of survivin on FVADT chemotherapy for refractory multiple myeloma. Experimental and Therapeutic Medicine, **12**, 771-776.

Yang, Q., Lu, Z., Singh, D. & Raj, J. U. 2012. BIX-01294 treatment blocks cell proliferation, migration and contractility in ovine foetal pulmonary arterial smooth muscle cells. Cell proliferation, **45**, 335-344.

Yang, X. B., Bhatnagar, R. S., Li, S. & Oreffo, R. O. 2004. Biomimetic collagen scaffolds for human bone cell growth and differentiation. Tissue engineering, **10**, 1148-1159.

Yee, L., Fanale, M., Dimick, K., Calvert, S., Robins, C., Ing, J., Ling, J., Novotny, W., Ashkenazi, A. & Burris III, H. 2007. A phase IB safety and pharmacokinetic (PK) study of recombinant human Apo2L/TRAIL in combination with rituximab in patients with low-grade non-Hodgkin lymphoma. Journal of Clinical Oncology, **25**, 8078-8078.

Yin, A. H., Miraglia, S., Zanjani, E. D., Almeida-Porada, G., Ogawa, M., Leary, A. G., Olweus, J., Kearney, J. & Buck, D. W. 1997. AC133, a novel marker for human hematopoietic stem and progenitor cells. Blood, **90**, 5002-5012.

Yip, K. & Reed, J. 2008. Bcl-2 family proteins and cancer. Oncogene, **27**, 6398-6406.

Yoo, K. H. & Hennighausen, L. 2012. EZH2 methyltransferase and H3K27 methylation in breast cancer. International journal of biological sciences, **8**, 59-65.

Younes, A., Vose, J. M., Zelenetz, A. D., Smith, M. R., Burris, H., Ansell, S., Klein, J., Kumm, E. & Czuczman, M. 2005. Results of a Phase 2 Trial of HGS-ETR1 (Agonistic Human Monoclonal Antibody to TRAIL Receptor 1) in Subjects with Relapsed/Refractory Non-Hodgkin's Lymphoma (NHL). Blood, **106**, 489-489.

Young, J. C., Varma, A., DiGiusto, D. & Backer, M. P. 1996. Retention of quiescent hematopoietic cells with high proliferative potential during ex vivo stem cell culture. Blood, **87**, 545-556.

Young, L., Sung, J., Stacey, G. & Masters, J. R. 2010. Detection of Mycoplasma in cell cultures. Nature protocols, **5**, 929-934.

Zaravinos, A., Kanellou, P., Lambrou, G. I. & Spandidos, D. A. 2014. Gene set enrichment analysis of the NF-κB/Snail/YY1/RKIP circuitry in multiple myeloma. Tumour Biology, **35**, 4987-5005.

Zdzisinska, B., Rolinski, J., Piersiak, T. & Kandefer-Szerszen, M. 2009. A comparison of cytokine production in 2-dimensional and 3-dimensional cultures of bone marrow stromal cells of multiple myeloma patients in response to RPMI8226 myeloma cells. Folia histochemica et cytobiologica, **47**, 69-74. doi: 10.2478/v10042-009-0015-1 [doi].

Zeng, D., Liu, M. & Pan, J. 2017. Blocking EZH2 methylation transferase activity by GSK126 decreases stem cell-like myeloma cells. Oncotarget, **8**, 3396-3411. doi: 10.18632/oncotarget.13773 [doi].

Zeuner, A., Francescangeli, F., Contavalli, P., Zapparelli, G., Apuzzo, T., Eramo, A., Baiocchi, M., De Angelis, M., Biffoni, M. & Sette, G. 2014. Elimination of quiescent/slow-proliferating cancer stem cells by Bcl-XL inhibition in non-small cell lung cancer. Cell Death & Differentiation, **21**, 1877-1888.

Zhang, L. & Fang, B. 2005. Mechanisms of resistance to TRAIL-induced apoptosis in cancer. Cancer gene therapy, **12**, 228-237.

Zhang, Q., Padi, S., Tindall, D. J. & Guo, B. 2014. Polycomb protein EZH2 suppresses apoptosis by silencing the proapoptotic miR-31. Cell death & disease, **5**, e1486.

Zhang, W., Lee, W. Y., Siegel, D. S., Tolias, P. & Zilberberg, J. 2014. Patient-specific 3D microfluidic tissue model for multiple myeloma. Tissue Engineering Part C: Methods, **20**, 663-670.

Zhang, X. D., Gillespie, S. K., Borrow, J. M. & Hersey, P. 2003. The histone deacetylase inhibitor suberic bishydroxamate: a potential sensitizer of melanoma to TNF-related apoptosis-inducing ligand (TRAIL) induced apoptosis. Biochemical pharmacology, **66**, 1537-1545.

Zhao, J., Chen, C. & Ma, W. 2005. Photocatalytic degradation of organic pollutants under visible light irradiation. Topics in catalysis, **35**, 269-278.

Zhou, B. S., Zhang, H., Damelin, M., Geles, K. G., Grindley, J. C. & Dirks, P. B. 2009. Tumour-initiating cells: challenges and opportunities for anticancer drug discovery. Nature reviews Drug discovery, **8**, 806-823.

Zhou, J., Bi, C., Cheong, L. L., Mahara, S., Liu, S. C., Tay, K. G., Koh, T. L., Yu, Q. & Chng, W. J. 2011. The histone methyltransferase inhibitor, DZNep, up-regulates TXNIP, increases ROS production, and targets leukemia cells in AML. Blood, **118**, 2830-2839. doi: 10.1182/blood-2010-07-294827 [doi].

Zhou, W., Feng, X., Han, H., Guo, S. & Wang, G. 2016. Synergistic effects of combined treatment with histone deacetylase inhibitor suberoylanilide hydroxamic acid and TRAIL on human breast cancer cells. Scientific reports, **6**, 28004. doi: 10.1038/srep28004 [doi].

Zilfou, J. T. & Lowe, S. W. 2009. Tumour suppressive functions of p53. Cold Spring Harbor perspectives in biology, **1**, a001883. doi: 10.1101/cshperspect.a001883 [doi].
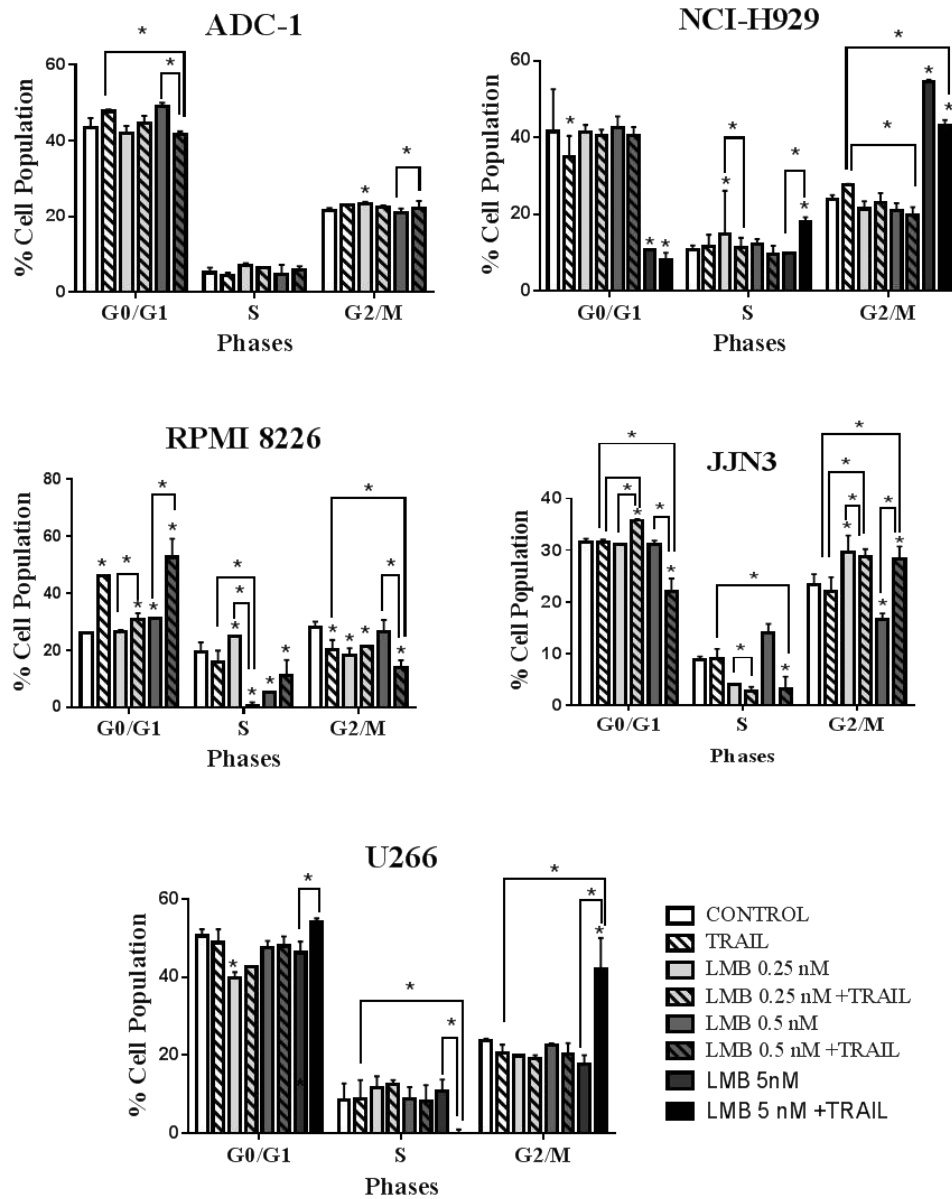
Zschenker, O., Streichert, T., Hehlgans, S. & Cordes, N. 2012. Genome-wide gene expression analysis in cancer cells reveals 3D growth to affect ECM and processes associated with cell adhesion but not DNA repair. PloS one, **7**, e34279.
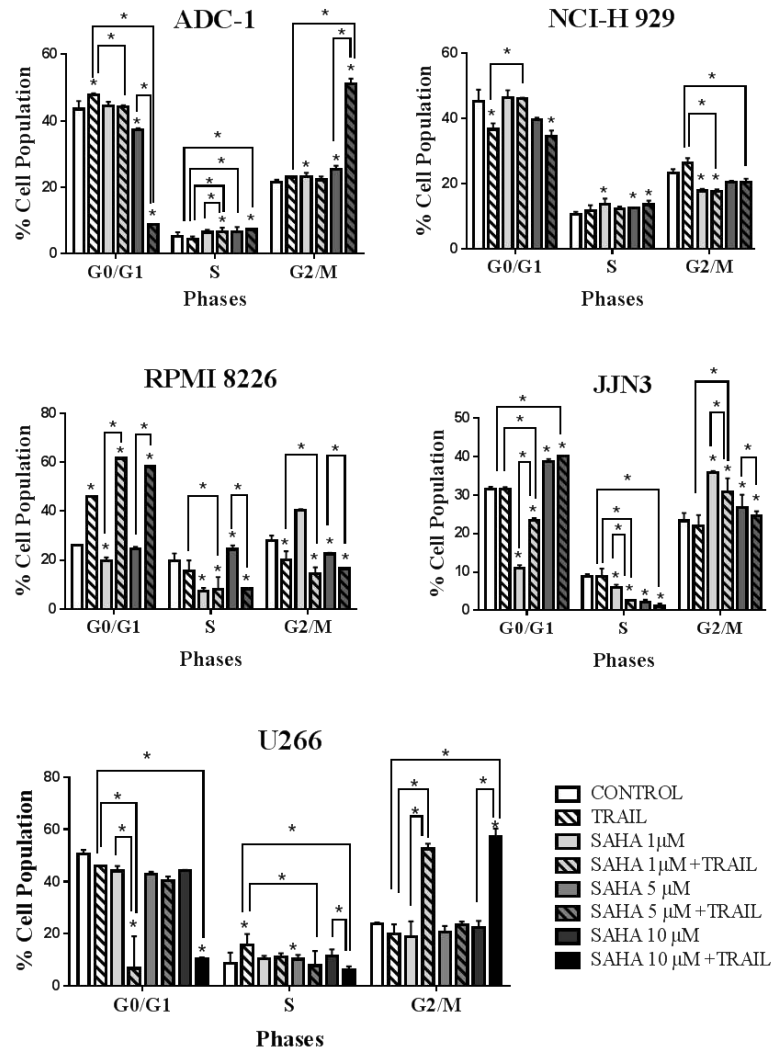
8. Appendices

Figure I: Effect of LMB in combination with TRAIL on cell cycle progression in multiple myeloma cells

Figure I: *Effect of LMB in combination with TRAIL on cell cycle progression in multiple myeloma cells. The cells were treated with LMB and TRAIL alone and in combined for 24 hours. The data is expressed as median with range (three independent experiments). The statistical significance was determined by comparison with the vehicle control and statistical significance of combined therapy was determined by comparison the percentage of treated cells in each phase to both the vehicle control and individual treatment (*=p<0.05) (Kruskal–Wallis).*
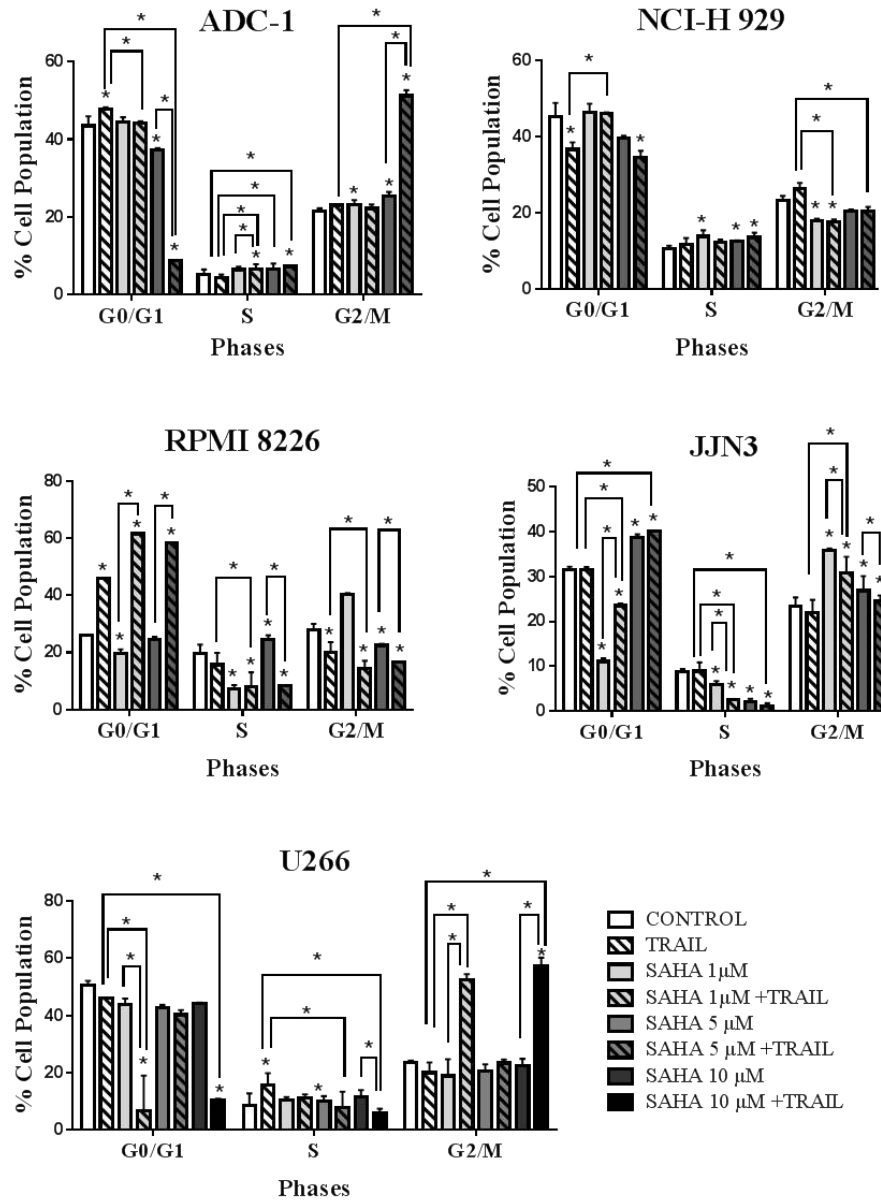
Figure II: Effect of SAHA in combination with TRAIL on cell cycle progression in multiple myeloma cells
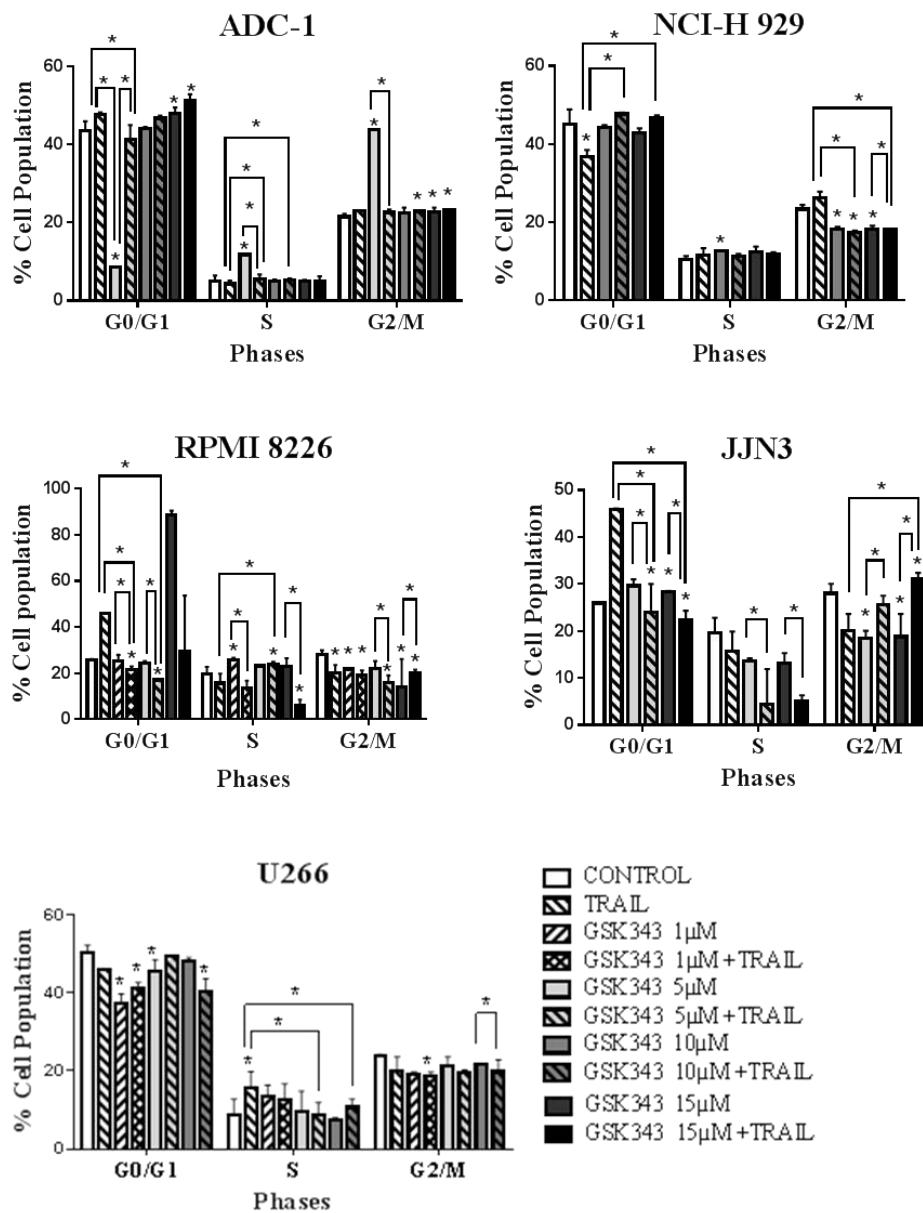

Figure II: *Effect of SAHA in combination with TRAIL on cell cycle progression in multiple myeloma cells. The cells were treated with SAHA and TRAIL alone and in combined for 24 hours. The data is expressed as median with range (three independent experiments). The statistical significance was determined by comparison with the vehicle control and statistical significance of combined therapy was determined by comparison the percentage of treated cells in each phase to both the vehicle control and individual treatment(*=p<0.05) (Kruskal–Wallis).*

Figure III: Effect of BIX 01294 in combination with TRAIL on cell cycle progression in multiple myeloma cells

Figure III: *Effect of BIX 01294 in combination with TRAIL on cell cycle progression in multiple myeloma cells. The cells were treated with BIX 0-1294 and TRAIL alone and in combined for 24 hours. The data is expressed as median with range (three independent experiments). The statistical significance was determined by comparison with the vehicle control and statistical significance of combined therapy was determined by comparison the percentage of treated cells in each phase to both the vehicle control and individual treatment(*=p<0.05) (Kruskal–Wallis). The percentage of cells in each phase was analyzed with Flow Jo software. High concentration of BIX 01294 in combination with TRAIL significantly induced accumulation in G2/M-phase (p<0.05).*

Figure IV: **Effect of GSK343 in combination with TRAIL on cell cycle progression**

in multiple myeloma cells

Figure IV: *Efect of GSK343 in combination with TRAIL on cell cycle progression in multiple myeloma cells. The cells were treated with GSK343 and TRAIL alone and in combined for 24 h. The data is expressed as median with range (three independent experiments). The statistical significance was determined by comparison with the vehicle control and statistical significance of combined therapy was determined by comparison the percentage of treated cells in each phase to both the vehicle control and individual treatment(*=p<0.05) (Kruskal–Wallis).*

| Target	Target	Target	Target
A1, A2	Reference Spots	C11, C12	HO-1/HMOX1/HSP32
A23, A24	Reference Spots	C13, C14	HO-2/HMOX2
B1, B2	Bad	C15, C16	HSP27
B3, B4	Bax	C17, C18	HSP60
B5, B6	Bcl-2	C19, C20	HSP70
B7, B8	Bcl-x	C21, C22	HTRA2/Omi
B9, B10	Pro-Caspase-3	C23, C24	Livin
B11, B12	Cleaved Caspase-3	D1, D2	PON2
B13, B44	Catalase	D3, D4	p21/CIP1/CDKN1A
B15, B16	cIAP-1	D5, D6	p27/Kip1
B17, B18	cIAP-2	D7, D8	Phospho-p53 (S15)
B19, B20	Claspine	D9, D10	Phospho-p53 (S46)
B21, B22	Clustrine	D11, D12	Phospho-p53 (S392)
B23, B24	Cytochrome C	D13, D14	Phospho-Rad17 (S635)
C1, C2	TRAIL R1/DR5	D15, D16	SMAC/Diablo
C3, C4	TRAIL R2/DR4	D17, D18	Survivin
C5, C6	FADD	D19, D20	TNF RI/TNFRSF1A
C7, C8	Fas/TNF6/CD95	D21, D22	XIAP
C9, C10	HIF-1α	D23, D24	PBS (Negative Control)
		E1, E2	Reference Spots

Table I.: Human apoptosis proteme profiler array coordinates
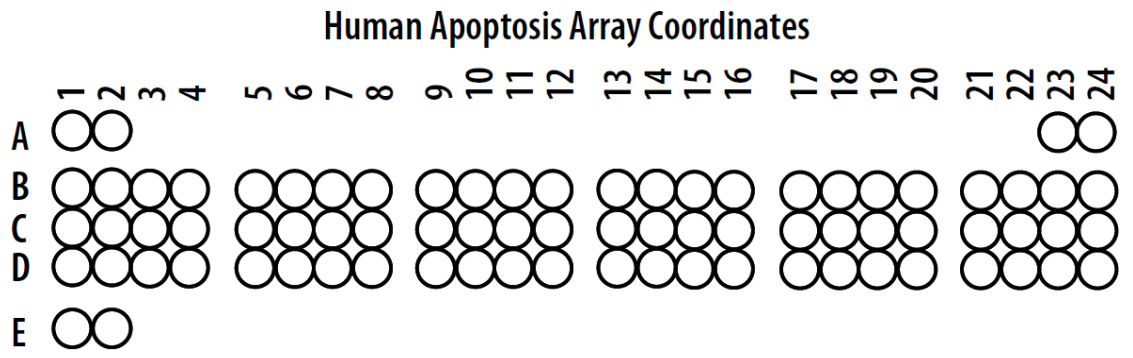
Figure V: Human apoptosis proteome profiler array coordinates.
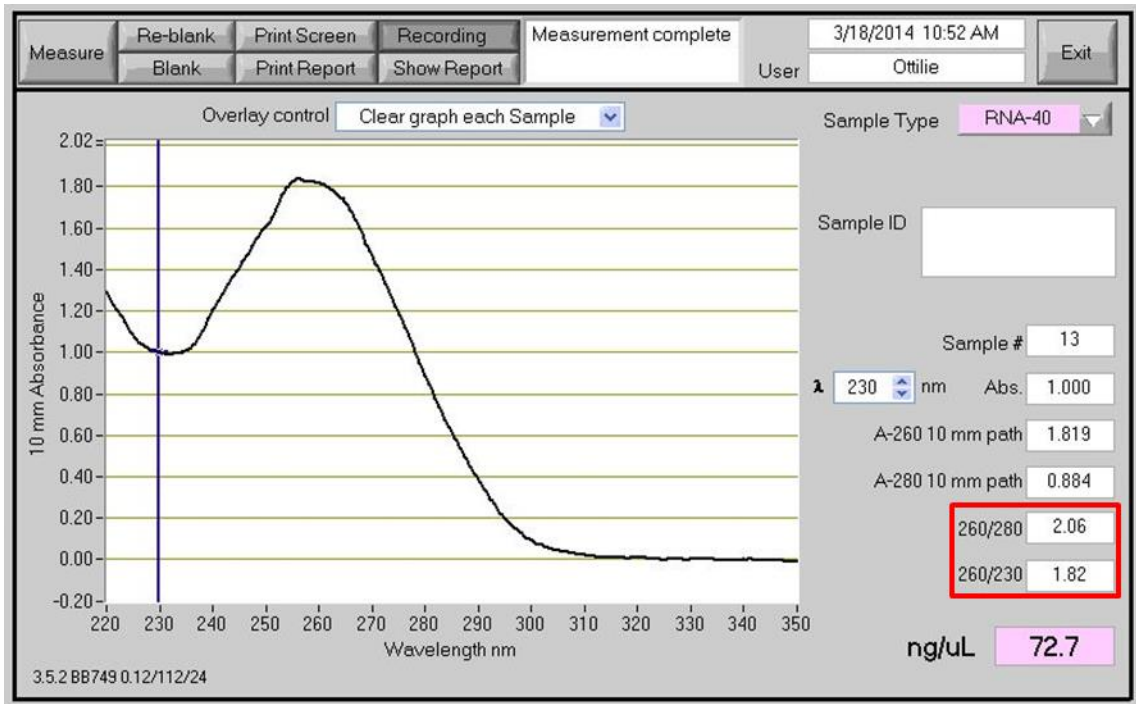
Figure VI: RNA sample purity assessment by NanoDrop-1000 spectrophotometer
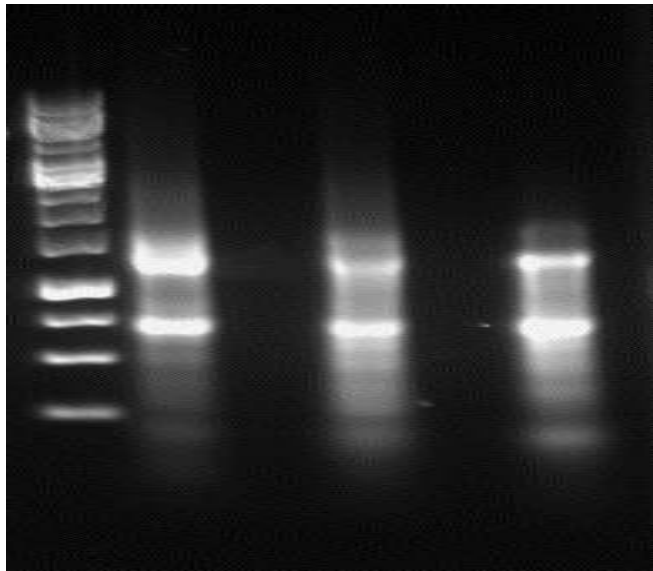
Figure VII: The integrity of the extracted RNA confirmed by 1% agarose gel electrophoresis